DESIGN AND EVALUATION OF NOVEL DIAGNOSTIC RADIOPHARMACEUTICALS BASED ON ^{99m}Tc-NITRIDO ($[^{99m}Tc{\equiv}N]^{2+}$) CORE

By

ANUPAM MATHUR

BHABHA ATOMIC RESEARCH CENTRE

A thesis submitted to the
Board of Studies in Chemical Science Discipline

In partial fulfillment of requirements
For the Degree of

DOCTOR OF PHILOSOPHY

of

HOMI BHABHA NATIONAL INSTITUTE

August, 2011

Homi Bhabha National Institute

Recommendations of the Viva Voce Board

As members of the Viva Voce Board, we certify that we have read the dissertation prepared by **Anupam Mathur** entitled **"Design and Evaluation of Novel Diagnostic Radiopharmaceuticals Based on ^{99m}Tc-Nitrido ($[^{99m}Tc{\equiv}N]^{2+}$) Core"** and recommend that it may be accepted as fulfilling the dissertation requirement for the Degree of Doctor of Philosophy.

Chairman- Dr. K.L. Ramakumar — Date: 2/11/2011

Convener- Dr. Meera Venkatesh — Date: 02 NOV 2011

External Examiner- Dr. K.R. Prabhu — Date: 2nd NOV 2011

Member 1- Dr. S. Chattopadhyay — Date: 2/11/2011

Member 2- Dr. Sharmila Banerjee — Date: 2/11/2011

Final approval and acceptance of this dissertation is contingent upon the candidate's submission of the final copies of the dissertation to HBNI.

I hereby certify that I have read this dissertation prepared under my direction and recommend that it may be accepted as fulfilling the dissertation requirement.

Date: 02 NOV 2011

Place: Mumbai

Guide - Dr. Meera Venkatesh

STATEMENT BY AUTHOR

This dissertation has been submitted in partial fulfillment of requirement for an advanced degree at Homi Bhabha National Institute (HBNI) and is deposited in the Library to be made available to borrowers under rules of the HBNI.

Brief quotations from this dissertation are allowable without special permission, provided that accurate acknowledgement of source is made. Requests for permission for extended quotation from or reproduction of this manuscript in whole or in part may be granted by the Competent Authority of HBNI when in his or her judgment the proposed use of the material is in the interests of scholarship. In all other instances, however, permission must be obtained from the author.

Anupam Mathur

DECLARATION

I, hereby declare that the investigation presented in the thesis has been carried out by me. The work is original and has not been submitted earlier as a whole or in part for a degree / diploma at this or any other Institution / University.

Anupam Mathur

Dedicated to my Parents

ACKNOWLEDGEMENTS

I wish to record my deep sense of gratitude and sincere thanks to my learned research guide Prof. Meera Venkatesh, former Head, Radiopharmaceuticals Division (RPhD), Bhabha Atomic Research Centre (BARC)] [currently Director, Division of Physical and Chemical Sciences, International Atomic Energy Agency (IAEA), Vienna] for her unstinted inspiration, guidance, encouragement, valuable suggestions and good wishes throughout my entire research tenure. Her illuminating guidance and assistance helped me to prepare this thesis. I am also grateful to her for allowing and providing facilities to me at RPhD, BARC.

It is my great privilege to acknowledge Prof. Sharmila Banerjee of RPhD, BARC who inculcated in me the interest for organic synthesis and scrutinized my entire research work and offered invaluable scientific suggestions during the course of this research work..

It is my great pleasure to thank Dr. M.R.A. Pillai, Head, RPhD, BARC and Dr. N. Ramamoorthy, Former Chief Executive, BRIT, for their constant encouragement and giving me the opportunity to work on this wonderful field of Technetium nitride chemistry.

I wish to pay my sincere thanks to Dr. A. K. Kohli, Chief Executive, Board of Radiation and Isotope Technology (BRIT) for giving me the freedom to work on the present chemistry and his constant support throughout the period of my research.

I wish to express my gratitude to Dr. N. Sivaprasad and Mr. S.S. Sachdev of Radiopharmaceuticals Programme (RPhP), BRIT, for their strong faith and support of my work.

I am very grateful to the Chairman Prof. Dr. V. Venugopal (Former Director, Radiochemistry and Isotope Group, BARC) and the members Prof. S. Chattopadhyaya, (Head, Bio-Organic Division, BARC) and Prof. Sharmila Banerjee, of the doctorial committee, for their critical reviews and suggestions all through the review of the progress of

my work and pre-synopsis viva-voce. I am grateful to them for critically reviewing this thesis.

I shall be ever grateful to Dr. K. Kothari (Retd.), Dr. G. Samuel, Mr. M. B. Mallia and Mr. S. Subramaniam of RPhD, BARC for their valuable scientific inputs, technical discussions and constant help during my experimental work which helped in finalizing the present work. I am also thankful to Dr. H. D. Sarma, RBHSD, BARC for all the help and valuable suggestions in carrying out the animal experiments.

I wish to express my sincere thanks to Prof. Adriano Duatti, Italy for providing the PNP compound and for his valuable scientific inputs and assistance during the course of my research work.

It is my pleasure to acknowledge my other colleagues of RPhD, BARC, Dr. A. Dash, Mr. P. V. Joshi, Dr. Tapas Das, Dr. Sudipta Chakraborty, Dr. Aruna Korde, Dr. Mythili Kameshwaram, Dr. Usha Pandey, Dr. Archana Mukherjee, Dr. Drishty Satpaty, Mr. Viju Chirayil, Mr. Rubel Chakraborty, Mr. Chandan Kumar and Mr. Vimal Nath Nair for their moral support and diversified help. I also gratefully acknowledge the help rendered by the technical staff Mr. A. D. Kadam, Mr. G. Gandhale, Mr. Umesh Kumar and Mr. U. Sukhale of RPhD, BARC.

Finally, I acknowledge the constant encouragement received from my colleagues Mr. G. Prabhakar, Dr. D. Padmanabhan, Mr. R. Krishna Mohan, Mr. G. Shunmugam, Mr. Tulasidhasan, Mr. N.C. Joseph, Mr. B. K. Tiwary and Mrs. Uma Sheri of RPhP, BRIT.

Last but not the least, I would like to express my deep gratitude to my daughter, wife and parents without their constant support, love and encouragement, this thesis would not have been possible.

August, 2011 Anupam Mathur

CONTENTS

CHAPTER 3

Asymmetric [2+2] Neutral Complex

SYNOPSIS

Medical imaging techniques presently play a vital role in the clinical management of the patient disorders and diseases and have witnessed enormous growth over the past few decades. While conventional imaging techniques such as X-rays, CT, MRI, etc. provide anatomical imaging, molecular imaging agents have enabled non-invasive assessment of biological and biochemical processes inside the human body with high sensitivity and specificity. Among the various molecular imaging techniques, nuclear medicine that employs radiopharmaceuticals is the most convincing, as it detects molecular and cellular changes of diseases with high precision.[1]

Radiopharmaceuticals are compounds where the molecules have radioisotope attached to it and are used as drugs routinely in nuclear medicine for diagnosis and therapy of various diseases. The choice of radioisotope determines whether the application is diagnostic or therapeutic. Diagnostic radiopharmaceuticals are labeled with either gamma emitting or positron emitting isotopes, and are used to obtain highly precise and detailed morphologic structure of organ or tissues as well as the physiological function of an organ, through the dynamic distribution of the radiotracer. These are used at very low concentrations in the range of 10^{-6} to 10^{-8} M and are not intended to have any pharmacological effect. Therapeutic radiopharmaceuticals are the molecules designed to deliver therapeutic doses of ionizing radiation at specific diseased tissue or sites.

The chemical composition of a radiopharmaceutical could be considered to consist of a target/ carrier molecule, which is generally an organic moiety with a biological role, to which a radioactive isotope of an element is chemically attached either by covalent or coordinate bond (Radiolabeling). The carrier molecule can be a biomolecule such as antibody, protein, drug, etc. or can also be a simple organic molecule, which may not have

any target specificity, but once radiolabeled, due to its overall chemical structure exhibits preferential localization in a specific target organ (metal-essential radiopharmaceuticals). The radioisotopes used for labeling are non-metals, transition metals and lanthanides. Particulate emitting isotopes such as ^{131}I, ^{32}P, ^{153}Sm, ^{90}Y, ^{177}Lu, etc. are used for therapeutic purposes whereas some of the radioisotopes most commonly used for diagnostic purposes are ^{18}F, ^{99m}Tc, ^{123}I, etc.[2]

Although during the advent of nuclear medicine, ^{131}I, ^{203}Hg, ^{198}Au which emit β-particles as well as γ–rays have been used for diagnostic purpose, the images obtained with these isotopes lack the resolution that is possible when single photon emitters such as ^{99m}Tc or ^{123}I or positron emitters such as ^{18}F are used. The technological advances over the past 3-4 decades have resulted in highly precise and well resolved images through Single Photon Emission Computed Tomography (SPECT) and Positron Emission Tomography (PET).[3]

The thesis work is aimed at preparation of novel ^{99m}Tc based SPECT agents, wherein, ^{99m}Tc is used for the radiolabeling of different carrier molecules and evaluated for biological behavior. The metal, ^{99m}Tc, exhibits ideal nuclear properties ($t_{1/2}$~ 6 h, γ-energy~140 KeV) for diagnostic imaging and several other attributes, that makes it the most widely used diagnostic radionuclide (> 80% of all nuclear medicine imaging) and hence earned it the name "Workhorse of Diagnostic Nuclear Medicine". Further the availability of ^{99m}Tc from a ^{99}Mo-^{99m}Tc generator facilitates its easy availability on a daily basis at hospital radiopharmacies.

Technetium is a transition metal and can exist in multiple oxidation states (-1 to +7) and hence is amenable for radiolabeling a variety of molecules through various strategies. The most popular labeling strategy followed for its incorporation into a carrier molecule is bi-functional chelating agent (BFCA) approach. A bi-functional chelate is a multidentate ligand (eg: Ethylene diamine tetra-acetic acid), which has appropriate ligating groups for co-

ordinating the metal and also contains a functional group for covalent attachment to the targeting molecule.

The versatile chemical nature of ^{99m}Tc has led to its existence in various core forms such as ^{99m}Tc-oxo core ($[^{99m}Tc=O]^{3+}$), ^{99m}Tc-carbonyl core ($[^{99m}Tc(CO)_3(H_2O)_3]^{+}$), ^{99m}Tc-Hydrazino nicotinamide core ([^{99m}Tc-HYNIC]) and so on. A metal core is a substitution-labile technetium complex where a few co-ordinating positions are tightly bound to the metal center while other positions are labile and exhibit a marked reactivity towards ligands having amenable co-ordinating atoms. ^{99m}Tc exists in different oxidation states in different cores and hence bind with chelates with different donor groups.[4]

The most commonly used ^{99m}Tc core is $[^{99m}Tc=O]^{3+}$ where ^{99m}Tc exists in +V oxidation state. In the recent past, there has been growing interest in ^{99m}Tc-nitrido ($[^{99m}Tc\equiv N]^{+2}$) core with ^{99m}Tc in +V oxidation state, which is isoelectronic to the conventional $[^{99m}Tc=O]^{+3}$ core. This core, unlike the oxo core, has the advantage that it is highly stable to redox conditions and pH variations. Further, owing to its excellent stability, this core also enables formation of ^{99m}Tc labeled biomolecules at high specific activity (with use of relatively lower amounts of ligand molecules in comparison with the $[^{99m}Tc=O]^{+3}$ core) which in turn is an advantage for imaging receptors or antibody binding lesions. Recently, several complexes containing this core have exhibited attractive myocardial imaging features and are in clinical evaluation for emerging as new radiopharmaceuticals.[5-7]

$[^{99m}Tc\equiv N]^{+2}$ core is reported to have affinity towards soft donor atoms such as S and P and the core forms complexes with square pyramidal geometry. However, it has been observed that ligand backbone containing four donor groups is not suitable for complexation with this core. The complexes formed with bi-dentate donor ligand are preferred with two ligand molecules involved in co-ordination with the core. The complexes formed in this way are symmetric [2+2] with ^{99m}Tc≡N occupying the apical position and the other four donors

occupying the basal plane. Dithiocarbamates and xanthates are suitable bi-dentate chelates, which are reported to form stable symmetric complexes with $[^{99m}Tc{\equiv}N]^{+2}$ core.[5, 8]

The symmetric labeling approach is well suited for metal essential radiopharmaceuticals. However, for target specific molecules such as proteins, fatty acids, etc. such a labeling approach leads to radiolabeled complexes with two targeting molecules attached to one $[^{99m}Tc{\equiv}N]^{+2}$ core. This in turn results in undesired *in-vivo* pharmacokinetics, thereby affecting the target uptake and non-target distribution pattern inside the body. To circumvent this problem, the pioneering researchers in the area introduced a long straight chain (seven membered) bi-dentate phosphorus ligand (π-acceptor), with nitrogen atom as a heteroatom in between (PNP ligand) to complex with $[^{99m}Tc{\equiv}N]^{+2}$ core. PNP ligands, due to the bulkiness and steric effects, do not form symmetric [2+2] complex and open up the possibility of preparing asymmetric [2+2] square pyramidal complexes via the formation of a new $[^{99m}TcN(PNP)]^{2+}$ intermediate. The use of long chain lipophilic PNP ligand backbone, sterically orients the two P atoms to the cis positions leaving the other two cis positions occupied by labile groups, for asymmetric [2+2] labeling. This new intermediate on reaction with bi-dentate chelating ligands carrying π-donors as co-ordinating atoms lead to novel type of mixed ligand [2+2] complexes. Complexes prepared using this $[^{99m}TcN(PNP)]^{2+}$ intermediate and bi-dentate ligands with π-donor atoms like SS or NS or SO have been reported to be stable. Cysteine, dithiols and dithiocarbamates have been found to be suitable as bi-dentate chelators for complexation with the $[^{99m}TcN(PNP)]^{2+}$ intermediate.[7, 9-14]

The amino acid, cysteine is a useful BFCA to complex with $[^{99m}TcN(PNP)]^{2+}$ intermediate, through either NH_2 and S^- or COO^- and S^-, to form stable asymmetric [2+2] ^{99m}Tc-nitrido complexes. The bioactive molecules can be linked to the cysteine moiety and then labeled with ^{99m}Tc via $[^{99m}TcN(PNP)]^{2+}$ intermediate. The nature of donor groups, decides the overall charge of the asymmetric [2+2] complexes.[9]

Aim and scope of the work

Based on the symmetric [2+2] and asymmetric [2+2] labeling approaches, an attempt has been made to prepare a significant number of ^{99m}Tc labeled preparations using $[^{99m}TcN]^{2+}$ core, for their potential use as myocardial and hypoxic imaging agents. The significance of the work is to evaluate the versatility of $[^{99m}TcN]^{2+}$ core by modifying the labeling approach and correlating the change in the *in-vivo* biological behavior. Also, the importance of this $[^{99m}TcN]^{2+}$ core for target specific radiopharmaceuticals has been explored by labeling different biomolecules for varied biological applications.

CHAPTER 1 Introduction

This chapter deals with the basic concepts of radiopharmaceutical research and its development. Right from the selection of target/ carrier molecule, choice of radionuclide and its production, to the chemistry to be followed for its incorporation in a carrier molecule is described. Apart from the chemical synthesis of radiopharmaceutical, the quality control parameters required for the evaluation of a new radiolabeled formulation are discussed. This includes all the *in-vitro* and *in-vivo* biological testing required before the clinical trial of the radiopharmaceutical for *in-vivo* patient use. The chapter ends highlighting the aim and the scope of the work carried out in the present thesis.

CHAPTER 2 Symmetric [2+2] complexes

This chapter gives an idea about the simple derivatization desired in the lead molecule for the introduction of $[^{99m}TcN]^{2+}$ core, to obtain symmetric [2+2] complexes with suitable biological characteristics. The chapter has been divided into two parts, where syntheses of

three symmetric [^{99m}TcN]-complexes suitable for myocardial imaging are presented. There are two categories of myocardial agents used for diagnostic imaging *viz. myocardial perfusion imaging and myocardial metabolic imaging*. The first part deals with symmetric [2+2] complexes prepared using dithiocarbamate ligands for perfusion imaging, whereas the next part deals with xanthate symmetric [2+2] complex for metabolic imaging.

The perfusion agents are based on the blood flow through the myocardium and the difference in uptake of the blood in the cardiac muscle is used as a measure for the detection of cardiovascular diseases. The ^{99m}Tc based perfusion agents used clinically are ^{99m}Tc-Methoxy Iso butyl Isonitrile (MIBI) and ^{99m}Tc-6,9-bis(2-ethoxyethyl)-3,12-dioxa-6,9 diphosphatetradecane (Tetrofosmin). These positively charged agents available clinically are far from ideal and get retained in the myocardium for a long time which poses logistic problems to the patient.[5] In this context, [^{99m}TcN(NOEt)$_2$], a neutral complex, has been shown to hold promise as a good myocardial perfusion imaging agent and is currently under clinical evaluation.[6] However, the results obtained using [^{99m}TcN(NOEt)$_2$] are still not as ideal as one may desire and hence the search for an improved agent forms a relevant field of research. In this respect, two new [^{99m}TcN]-dithiocarbamate complexes were synthesized and evaluated for their biological performance. The results of bio-distribution are compared with the standard agent [^{99m}TcN(NOEt)$_2$].

The work involved synthesis of two dithiocarbamate ligands *tertiary butyl dithiocarbamate* (TBDTC) and *methoxy isobutyl dithiocarbamate* (MIBDTC) followed by their radiolabeling with [^{99m}TcN]$^{2+}$ core. The rationale behind the synthesis of these two ligands is their structural similarity with the clinically used ligands for perfusion imaging, tertiary butyl isonitrile (TBI) and methoxyisobutyl isonitrile (MIBI). The bio-distribution results of the two complexes showed reasonable uptake in the myocardium. However, the

results of TBDTC and MIBDTC complexes in comparison to the standard agent NOEt were sub-optimal.

In the second part of the work, [^{99m}TcN]-fatty acid-xanthate symmetric complex was prepared and evaluated as a marker for metabolic cardiac imaging. Fatty acids are the main source of energy for the normal myocardium. A diseased myocardium undergoes a change in the fatty acid metabolism, leading to altered uptake and clearance characteristics, thereby making them useful target biomolecules for cardiac imaging. The metabolic markers currently used for myocardial imaging are ^{123}I labeled fatty acids viz. ^{123}I-Iodophenyl pentadecanoic acid and ^{123}I-beta-methyl iodo phenyl pentadecanoic acid.[15] However, the limited availability of ^{123}I via cyclotron contribute to unfavorable logistics, and hence the quest for ^{99m}Tc-labeled fatty acid for metabolic imaging continues to form a relevant field of research.

The work involved synthesis of a xanthate derivative of 15-hydroxy pentadecanoic acid, its radiolabeling with [^{99m}TcN]$^{2+}$ core and subsequently its bio-evaluation in Swiss mice. The complex showed undesirable *in-vivo* pharmacokinetic behavior due to the bulkiness of the final complex. This restricts the use of this complex for the aforementioned purpose.

CHAPTER 3 Asymmetric [2+2] neutral complex

This chapter highlights the usefulness of [^{99m}TcN]$^{2+}$ core for labeling target specific biomolecules. The symmetric [2+2] labeling approach is not suitable for target specific molecules such as proteins, fatty acids, etc. as the complexes formed are bulky with unfavorable *in-vivo* biological characteristics. This poses a problem for the labeling of target specific molecules via the base core. This problem was addressed by formation of asymmetric complexes, wherein only one biomolecule was complexed with [^{99m}TcN]$^{2+}$ core.

Biomolecules could be suitably derivatized with bi-dentate ligands containing donor atoms such as SS/ NS/ OS leading to final asymmetric [^{99m}TcN(PNP)]-complexes having single bioactive moiety per ^{99m}Tc metal centre.

The present chapter uses 16 carbon fatty acid biomolecule, as a representative example, for the present labeling strategy. The radiolabeled fatty acids, as discussed in chapter 2, are known targets for myocardial metabolic imaging. In the present case, long chain acid has been terminally linked with an amino group of cysteine (BFCA) in a four step synthetic procedure. The target ligand, 16 carbon fatty acid-cysteine conjugate, was then radiolabeled with [^{99m}TcN]$^{2+}$ core, in combination with bi-dentate PNP6 ligand (bis-phosphine ligand), leading to final asymmetric complex. The nature of BFCA cysteine donor groups involved in final complexation with [^{99m}TcN(PNP)]$^{2+}$ intermediate are (SH, COOH) which results in a neutral complex. The final complex after purification was used for carrying out the biological studies.

The biological studies involved *in-vitro* (cysteine challenge studies, serum stability studies and octanol/ water partition coefficient determination) and *in-vivo* bio-distribution studies. The results of bio-distribution have been compared with the standard agent ^{125}I-Iodophenylpentadecanoic acid (IPPA). Here, ^{125}I was used as the radiolabel instead of clinically used ^{123}I. The latter isotope is not available in India so ^{125}I was used as a rationale substitute for the present work. The results of the bio-distribution studies of the complex in Swiss mice showed low myocardial uptake alongwith rapid washout, compared with ^{125}I-IPPA, thereby, limiting its utility for the metabolic imaging. However, the initial uptake and washout kinetics as observed from non-target organs such as blood, liver and lungs are superior compared to the standard agent. Thus, the present study gives an insight into the amenable synthetic derivatization that can be carried in biomolecules, for the preparation of [^{99m}TcN] fatty acid complexes with excellent non-target clearance characteristics.

Apart from 16 carbon fatty acid-cysteine conjugate, two PNP ligands were also synthesized as a representative example of such categories of ligands. The synthesized PNP ligands were used for the preparation of $[^{99m}TcN(PNP)]^{2+}$ intermediate and characterized by HPLC.

CHAPTER 4 Asymmetric [2+2] charged complex

In this chapter, the versatility of $[^{99m}TcN]^{2+}$ core is explored by varying the charge and lipophilicity of the final asymmetric complex. The $[^{99m}TcN(PNP)]^{2+}$ intermediate is having an overall charge of +2. This intermediate leads to *in-vivo* inert complexes on complexation with bi-dentate ligands having SS/ NS/ OS donor groups. The amino acid cysteine is a useful bi-functional chelator for this intermediate, where a biomolecule can be linked to either an amino or the carboxylic acid functionality of cysteine and leaving either (SH, COOH) or (SH, NH_2) groups, respectively, available for co-ordination. The nature of bi-dentate donor groups influences the charge of the complexes. Thus, when cysteine is used as the BFCA, then structural analogues of the final $[^{99m}TcN]^{2+}$ complexes carrying different charges can be prepared by changing the mode of the conjugation of cysteine with the carrier biomolecule.

In the present work, the effect of charge has been evaluated by synthesizing a uni-positively charged structural analogue of the neutral complex reported in chapter 3. The bio-distribution results of the two complexes have been compared together with ^{125}I-IPPA to assess the effect of charge on the *in-vivo* pharmacological behavior and to evaluate the potential of charged fatty acid complex for metabolic cardiac imaging.

A 16-cysteinyl hexadecanoic acid conjugate was synthesized in a six step synthetic procedure starting with 16-bromohexadecanoic acid. The ligand on reaction with $[^{99m}TcN]^{2+}$ core together with PNP6 ligand, formed the required positively charged complex. The complex after HPLC purification was used for *in-vivo* studies in Swiss mice. In terms of

absolute uptake, the positively charged complex performed better than the neutral analogue reported earlier. The positively charged fatty acid complexes, prepared using $[^{99m}TcN(PNP)]^{2+}$ core seems to be better candidates for the development of myocardial metabolic tracers than their neutral counterparts.

The lipophilicity in an asymmetric $[^{99m}TcN]$-complex can be varied by changing the lateral alkyl groups present on the phosphorus and nitrogen atoms in PNP ligand. Also, the lipophilicity can be altered by introducing a linker between a BFCA and the biomolecule. In the present work, the latter approach was followed for the synthesis of a series of ligands with variable lipophilicities. The synthesis of ligands with different linkers was achieved by conjugating the commercially available fatty acids of different chain length (11, 12, and 15 carbons) with the acid group of cysteine in a similar fashion as that carried out for uni-positively charged 16 carbon fatty acid complex. These were then used to obtain uni-positively charged asymmetric $[^{99m}TcN]$-fatty acid complexes. The results of bio-distribution of the three positively charged 11, 12 and 15 carbon fatty acid complexes were compared with those obtained with 16 carbon complex, to see the effect of lipophilicity. The fatty acid complexes showed steady increase in the initial myocardial uptake values with increase in chain length, however, associated with slower clearance from the non-target organs.

Thus, the present study reviews the flexibility of $[^{99m}TcN]^{2+}$ core for labeling similar molecules with varied chemical nature and *in-vivo* biological characteristics.

CHAPTER 5 $[^{99m}TcN]^{2+}$ core for other imaging applications

In this chapter, $[^{99m}TcN]^{2+}$ core is used for labeling a nitro-triazole derivative, a known hypoxia marker. This chapter highlights the usefulness of $[^{99m}TcN]^{2+}$ core for labeling molecules with different *in-vivo* diagnostic applications other than the myocardial imaging discussed in previous three chapters.

The search for an ideal hypoxia-imaging agent requires high *in-vivo* stability of the labeled preparation, rapid accumulation of activity in hypoxic regions of tumors, sufficient retention times therein, and rapid clearance of activity from other non-target tissues to provide better contrast between lesion and background. However, the clearance of the activity from the blood with time must be optimum, so as to allow sufficient time for the accumulation of activity at the target hypoxic site.

Among the different $[^{99m}TcN]^{2+}$ tagging methods, the use of asymmetric approach was followed which yields complexes with high *in-vivo* inertness and excellent non-target clearance characteristics. Asymmetric [2+2] neutral complex was formed in a manner, similar to that discussed in chapter 3. Sanazole, a nitrotriazole derivative was coupled to a cysteine residue in a four step synthetic procedure, which was then radiolabeled using $[^{99m}TcN(PNP)]^{2+}$ core. The product after HPLC purification was used for carrying out the *in-vivo* bio-distribution studies in swiss mice bearing fibrosarcoma tumor. The complex showed low uptake which remained constant over the limited period of study. Though, retention of activity is observed in tumor, it could not be fully ascertained due to low uptake values. However, the rapid clearance of activity from the background organs, favors the use of this core for similar applications.

References

1. Weissleder R. *Science*, **2006**, *312*, 1168.
2. Liu S. *Chem Soc Rev*., **2004**, *33*, 445.
3. Rahmim A., Zaidi H. *Nucl Med Commun*., **2008,** *29*, 193.
4. Banerjee S., Pillai M.R.A., Ramamoorthy N. *Sem Nucl Med.*, **2001,** *32*, 260.
5. Pasqualini R., Duatti A., Bellande E., Comazzi V., Brucato V., Hoffschir D., Fagret D., Comet M. *J Nucl Med.*, **1994**, *35*, 334.

6. Fagret D., Ghezzi C., Vanzetto G. *J. Nucl. Med.*, **2001,** *42*, 1395.
7. Boschi A., Uccelli L., Bolzati C., Duatti A., Sabba N., Moretti E., Domenico G. D., Zavattini G., Refosco F., Giganti M. *J. Nucl. Med.*, **2003**, *44*, 806.
8. Baldas J., Bonnyman J., Pojer P.M., Williams G.A., Mackay M.F. *J Chem Soc Dalton Trans*, **1981**, 1798.
9. Boschi A., Bolzati C., Benini E., Malago E., Uccelli L., Duatti A., Piffanelli A., Refosco F., Tisato F. *Bioconjugate Chem.*, **2001**, *12*, 1035.
10. Bolzati C., Boschi A., Duatti A., Prakash S., Uccelli L., Refosco F., Tisato F., Bandoli G. *J. Am. Chem. Soc.*, **2000**, *122*, 4510.
11. Porchia M., Tisato F., Reffosco F., Bolzati C., Ceccato M.C., Bandoli G., Dolmella A. *Inorg Chem*, **2005**, *44*, 4766.
12. Tisato F., Reffosco F., Porchia M., Bolzati C., Bandoli G., Dolmella A., Boschi A., Jung C.M., Pietzsch H.J., Kraus W. *Inorg Chem*, **2004**, *43*, 8617.
13. Bolzati C., Mahmood A., Malago E., Uccelli L., Boschi A., Jones A.G., Refosco F., Duatti A., Tisato F. *Bioconjugate Chem.*, **2003**, *14*, 1231.
14. Cazzola E., Benini E., Pasquali M., Mirtschink P., Walther M., Pietzsch H.J., Uccelli L., Boschi A., Bolzati C., Duatti A. *Bioconjugate Chem.*, **2008**, *19*, 450.
15. Yoshinaga K., Tamaki N. *Curr. Opin. Biotech.*, **2007**, *18*, 52.

LIST OF FIGURES

LIST OF TABLES

CHAPTER 1

Introduction

The search for a man made tool or device to look inside the human body, without an operation or opening up (non-invasive approach), and to obtain clear images of different organs/ tissue and the ongoing biological processes with high delineation and clarity, is of high significance to fight the various disorders and diseases that afflict humans. Such a quest has been pursued by scientists for long, and the extraordinary discoveries and inventions witnessed during the first few decades of the last century paved way for realization of this goal. The ingenious concept of imaging penetrating radiations such as electromagnetic rays compounded with the huge technological advances that took place over the past few decades have resulted in the advent and tremendous growth in the field of diagnostic imaging.

The diagnostic imaging techniques can be broadly grouped into those in which ionizing radiation such as X-rays or gamma rays are used and the others where non-ionizing radiation such as ultrasound waves, radio-waves etc. are employed. Ultrasound imaging, fluorescence imaging and magnetic resonance imaging (MRI) are such tools which enable the physician to choose the best option for a particular situation. The need for sensitivity and clarity of image is the prime consideration while the cost is the other factor, in selecting the right modality for patient treatment.

Computed tomography (CT), MRI (with contrast agents) and ultrasound imaging are based on the differential response of the impinging waves when they strike an object, due to the physical composition of the object and hence these technologies are suitable for morphological/anatomical imaging of internal organs and are characterized by high spatial resolution. However, they have the limitation of not being able to detect diseases until structural changes are large enough to be detected by the imaging modality. For example, a

tumor cannot be imaged until the tumor reaches a size that is adequately big to cause a change in the image. But, "*in-vivo*" use of tracer molecules which emit radiations that can be detected outside the body, for imaging, is based on the localization of the tracer molecule owing to its biological behavior within the body. Thus such tracers image the functional aspects of the organ and hence technologies such as fluorescence imaging and gamma ray imaging which employ use of molecules labeled with a fluorescent or a radioactive marker have enabled the new field of "*functional imaging*" or "*molecular imaging*". These have the potential to detect diseases at the level when molecular and cellular changes occur. For example, before the tumor is large enough to cause structural changes, it can be detected with high precision, which is far earlier than when it is detectable using the anatomical imaging techniques. Such functional imaging helps the physician to identify and treat the patients at an early stage and hence has a great relevance in improving patient care and treatment. In the recent past, functional-MRI, wherein a bio-active molecule labeled with an appropriate magnetic resonance imageable moiety, has evolved as a functional imaging tool. However, among these techniques, "*Nuclear Medicine*" imaging using radiopharmaceuticals is the most popular modality used for functional and anatomical imaging, owing to the simplicity, ease as well as economical aspects.[1-3]

1.1 What are Radiopharmaceuticals?

Radiopharmaceuticals are molecules labeled with radionuclides that are used in the field of nuclear medicine, for the diagnosis or therapy of various disorders and diseases. These radioactive drugs emit radiations which are helpful in facilitating the desired medical application. Radiopharmaceuticals are most often, small organic or inorganic molecules with definite composition. The radiopharmaceutical is composed of a *target/ carrier* molecule, generally an organic moiety, to which a radioactive isotope of an element (*radioisotope*) is

chemically attached. However, ^{131}I-NaI, ^{32}P-sodium orthophosphate, etc. are few inorganic chemicals which have been used as radiopharmaceuticals over the past several decades, since the practice of nuclear medicine began. The nature and the structural activity of the radiopharmaceutical molecule directly influence its specificity for targeting the organ/ lesion of interest, while the nature of the radionuclide decides whether the intended use is for diagnosis or for therapy. Both these aspects need to be addressed when a new radiopharmaceutical is designed.[4-8]

1.1.1 Target/ Carrier molecule

The targeting carrier molecule in a radiopharmaceutical can essentially be of two kinds, *viz. target specific* and *metal essential*.[8]

The target specific molecule is a biologically active molecule such as antibody,[9-13] peptide,[14-26] etc. which has special affinity towards a specific antigen, receptor, etc. present on the cells of an organ or tissue. These specific molecules when attached to a radioisotope, form a '*target specific radiopharmaceutical*'. The Fig. 1.1 shows the structure of some target specific radiopharmaceuticals and Table 1.1 lists some of the target specific radiopharmaceuticals used in nuclear medicine.

Table 1.1 Selected target-specific diagnostic and therapeutic radiopharmaceuticals*

Radiopharmaceutical	Trade name	Primary uses
^{111}In-Capromab pendetide	ProstaScint®	Imaging of prostate cancer
^{111}In-Pentetreotide	Octreoscan®	Imaging of neuroendocrine tumors
^{111}In-Satumomab pendetide	OncoScint®	Imaging of metastatic disease associated with colorectal and ovarian cancer
^{99m}Tc-Apcitide	AcuTect®	Imaging deep vein thrombosis
^{99m}Tc-Arcitumomab	CEA-Scan®	Imaging colorectal cancer
^{99m}Tc-Depreotide	Neotect®	Imaging somatostatin receptor-positive tumors
^{90}Y-IbitumomabTiuxetan	Zevalin®	Treatment of Non-Hodgkin's Lymphoma
^{131}I-Tositumomab	Bexxar®	Treatment of Non-Hodgkin's Lymphoma

*Liu S. *Adv Drug Deliv Rev.*, **2008**, *60(12)*, 1347.

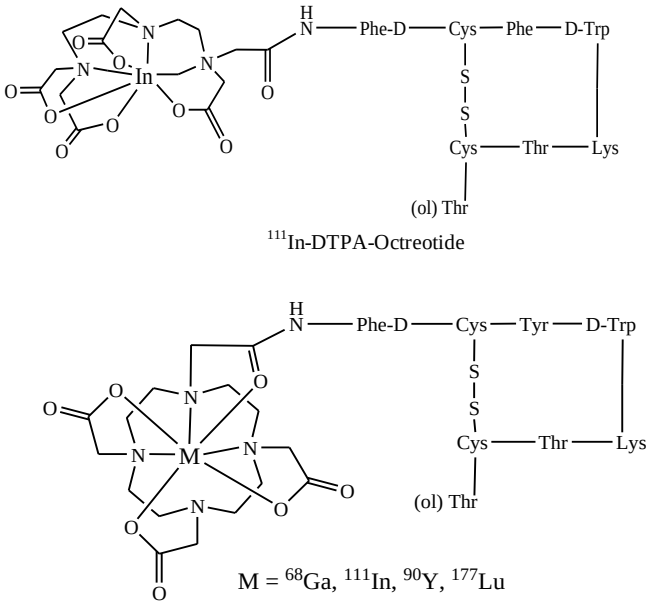

Fig. 1.1 Structures of some target specific radiopharmaceuticals used in nuclear medicine

On the other hand, a 'metal essential carrier molecule' is a simple organic molecule, which may not have any target specificity or biological activity on its own, but once radiolabeled, exhibits preferential uptake in the target site of interest, due to the unique physical and chemical properties of the radiolabeled molecule. For example, methoxy isobutyl isonitrile (MIBI), an isonitrile compound is a toxic organic chemical and does not have specificity towards the myocardium. However, once it is labeled with ^{99m}Tc metal to form $[^{99m}Tc(MIBI)_6]^+$, it shows preferential localization in the myocardium due to its overall size, charge and lipophilicity. Structures of some of the metal essential radiopharmaceuticals are shown in Fig. 1.2.

1.1.2 Radioisotopes

Discovery of the phenomenon of radioactivity and isolation of the radioactive element 'Radium' won the prestigious Nobel Prize to Madam Curie, as all of us aware. Radioisotopes, as the name suggests are radioactive isotopes of an element, with unstable nuclear

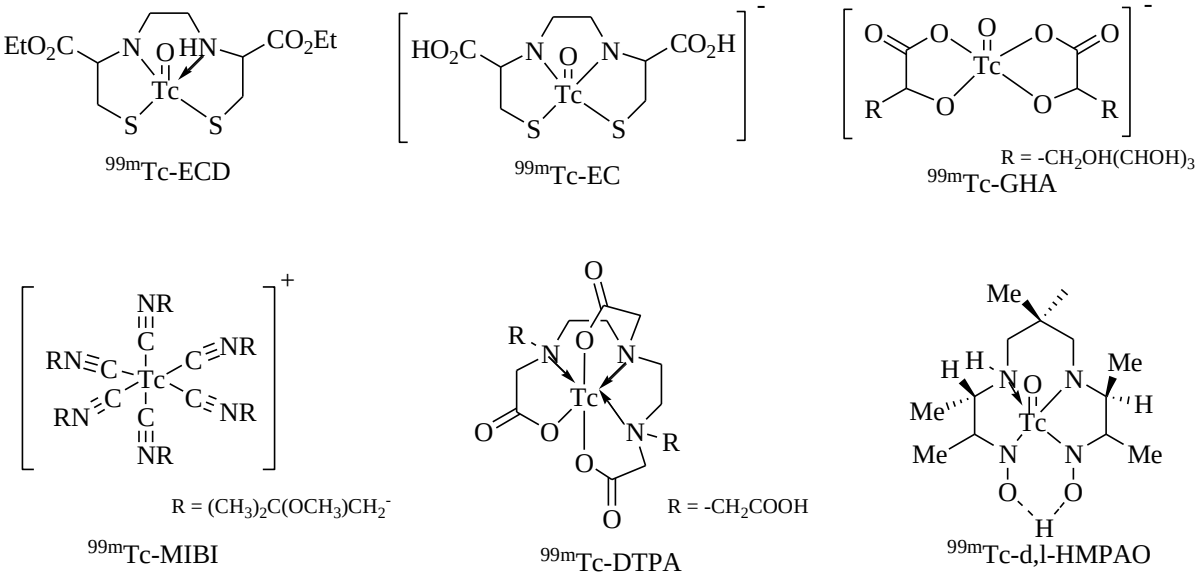

Fig. 1.2 Structures of some metal essential radiopharmaceuticals used in nuclear medicine

configuration and tend to attain stability by re-configuring the nucleus, during which process energetic radiations such as alpha (α), beta (β) or gamma (γ) rays are emitted, often resulting in an isotope of a different element. Although natural radioactivity laid the foundation to the discovery of such radiations and soon led to their applications in a variety of areas, it was with the artificial production of radioactivity (yet another "Nobel Prize" winning work by Irene-Joliot-Curie and Frederick Joliot) that the field of "applications of radioisotopes" flourished. Among the various applications of the radioisotopes, healthcare applications are very gratifying, as the energetic radiations have enabled diagnosis and treatment of several disease conditions, changing the lives of many for better.

Nuclear medicine is a medical specialty, where radiolabeled molecules, known as "Radiopharmaceuticals" are employed for the management of diseases. The choice of the radionuclide for a certain radiopharmaceutical application will depend on the nuclear emission properties, the physical half-life, the decay characteristics, the cost and

availability.[27-32] Table 1.2 and 1.3 lists some of the radionuclides used in the nuclear medicine alongwith their physical characteristics.

Radioisotopes emitting particulate radiations such as α or β or auger electron have high LET (linear energy transfer) and small energy deposition range, and are suitable for therapeutic applications (such as tumor therapy, radiation synovectomy, bone pain palliation, etc.). On the other hand, electromagnetic radiations such as γ or X-rays have low LET and deposit their energy over long range and are suitable for diagnostic applications.

Table 1.2 Important radionuclides for diagnostic radiopharmaceuticals*

1.2.1 γ-emitters and EC (electron capture) decay

Radionuclide	$t_{1/2}$ (h)	Decay mode	Main E_γ (keV) (%)	Production route
^{111}In	67.9	EC (100%)	245, 172	^{111}Cd(p,n)^{111}In
^{99m}Tc	6.1	IT (100%)	141	^{99}Mo/^{99m}Tc generator
^{201}Tl	72.0	EC (100%), Hg X-rays	135, 167	^{203}Tl(p,3n)^{201}Pb(p,n)^{201}Tl
^{123}I	13.2	EC	159 (83%)	^{124}Xe(p,2n)^{123}Cs→^{123}Xe→^{123}I ^{124}Te(p,2n) ^{123}I
^{131}I	8.0 d	β	364 (81%), 637 (7%)	^{130}Te(n,γ)^{131}Te→^{131}I ^{235}U(n,f)^{131}I

1.2.2 Positron emitting radionuclides

Radionuclide	$t_{1/2}$ (min)	Production route
^{11}C	20.3	^{14}N (p,α)
^{13}N	9.9	^{16}O (p,α)
^{15}O	2.0	^{14}N (d,n)
		^{15}N (p,n)
		^{16}O (p,pn)
^{18}F	109.8	^{18}O (p,n)
		^{20}Ne (d,α)
^{64}Cu	12.7 h	^{64}Ni (p,n)
^{68}Ga	68.3	^{68}Ge/^{68}Ga generator

*Sood D.D., Reddy A.V.R., Ramamoorthy. N. *Fundamentals of Radiochemistry*, **2004**, 298.

Table 1.3 Selected radionuclides with therapeutic potential*

Radionuclide	$t_{1/2}$ (d)	max E_β (MeV)	Main E_γ (MeV) (%)	Production route
^{32}P	14.3	1.71		$^{31}P (n,\gamma)\ ^{32}P$
				$^{32}S (n,p)\ ^{32}P$
^{89}Sr	50.5	1.46		$^{88}Sr (n,\gamma)\ ^{89}Sr$
				$^{89}Y (n,p)\ ^{89}Sr$
^{90}Y	2.7	2.27		$^{89}Y (n,\gamma)\ ^{90}Y$
				$^{235}U (n,f)\ ^{90}Sr \rightarrow\ ^{90}Y$
^{117m}Sn	13.6	0.13	0.158 (87%)	$^{116}Sn (n,\gamma)\ ^{117m}Sn$
				$^{117}Sn (n,n')\ ^{117m}Sn$
^{131}I	8.0	0.81	0.364 (81%)	$^{130}Te (n,\gamma)\ ^{131}Te \rightarrow\ ^{131}I$
				$^{235}U (n,f)\ ^{131}I$
^{153}Sm	1.9	0.80	0.103 (29%)	$^{152}Sm (n,\gamma)\ ^{153}Sm$
^{166}Ho	1.1	1.60	0.810 (6.3%)	$^{165}Ho (n,\gamma)\ ^{166}Ho$
^{177}Lu	6.7	0.50	0.113 (6.4%), 0.208 (11%)	$^{176}Lu (n,\gamma)\ ^{177}Lu$
^{186}Re	3.8	1.07	0.137 (9%)	$^{185}Re (n,\gamma)\ ^{186}Re$
^{188}Re	0.7	2.11	0.155 (15%)	$^{187}Re (n,\gamma)\ ^{188}Re$

*Sood D.D., Reddy A.V.R., Ramamoorthy. N. *Fundamentals of Radiochemistry*, **2004**, 298.

Positron emitting radioisotopes are also used for diagnostic purposes, despite being particulates, as these positively charged particles quickly combine with electrons of the surrounding medium to produce two 511 KeV gamma photons, emitted 180° apart, which can penetrate through the patient's body and can be simultaneously detected by the external detectors.

The primary consideration for the selection of the radionuclide is obviously the desired use, namely, diagnosis or therapy. Although particulate radiations are ideal for therapy, a small percentage of gamma rays of suitable energy for imaging is desired, for ensuring the localization as well as for dosimetric calculations. For diagnostic applications,

although non-particulate emitting radionuclides are preferred, nuclides such as ^{131}I which emit beta rays are also used occasionally, owing to several other logistic considerations.

The physical half-life of the radioisotope is one such critical parameter to be considered in the design of a radiopharmaceutical. The half-life of the radionuclide should match well with the *in-vivo* bio-localization and clearance properties of the radiopharmaceutical. If the time needed for the radiopharmaceutical to accumulate in the target is long, then the half-life of the radionuclide should be adequately long, so that the desired image/ therapy could be achieved. In contrast, if the radiopharmaceutical localizes in the target quickly with fast clearance from the blood and extracellular organs, then radioisotopes with shorter half-lives are more appropriate.[33-34]

One major factor that contributes to the utility of a radionuclide is its availability and cost, which in turn depend on the production possibilities and their economics.

Production of Radioisotopes

As mentioned earlier, nearly all applications use artificially produced radioisotopes. The stable nuclides can be transformed into the radioactive isotopes of the same or different element through nuclear reactions, wherein the target nuclide is impinged with a projectile such as neutron or a charged particle (proton, deuteron, etc.). Two major routes for producing artificial radioisotopes are charged particle accelerators and nuclear reactors.[35-38] Some of the production routes of radionuclides used in nuclear medicine are shown in Tables 1.2 and 1.3. Most of the radioisotopes used in varied applications are produced in nuclear reactors, as the reactor offers large volume for irradiation, and it is possible to simultaneously irradiate several samples, for economical production and possibility to produce a wide variety of radioisotopes. The accelerators are generally used to produce isotopes which cannot be produced using nuclear reactor in an economical way and constitute a smaller percentage of the total use of radioisotopes.

In nuclear reactors, radioisotopes are produced by exposing suitable target materials to the neutron flux for an appropriate period of time. So, most of the radioisotopes produced are neutron rich and mostly decay by beta emissions, often associated with gamma emission. However, there are a few exceptions where the product nuclide is neutron deficient, decaying by 'electron capture' mode or rarely by positron emission. The target nuclide on exposure to copious flow of neutrons in a nuclear reactor has a probability of absorbing the neutron in its nucleus, becoming the higher isotope of the same element. Depending upon the nuclear energy level of this nuclide, it would then take the most favorable route to attain a more stable configuration, by emission of particulates such as beta (β), proton (p), alpha (α) etc. and/ or gamma (γ) rays. Nuclear reactions such as (n,γ), (n,γβ), (n,p), (n,α) and (n,f) are used for production of radioisotopes. While the initial nuclear state and the energy of the neutron would determine the type of nuclear reaction that would take place, the rate of production of the product nuclide is determined by the neutron flux, abundance of the target nuclide and the activation cross-section for the desired reaction.

In charged particle accelerators like cyclotron, the nuclear reaction caused by bombarding target nuclide with energetic charged particles such as proton (p), deuteron (d), alpha (α), $^{3}He^{2+}$, etc. result in a different product nuclide, most often a radioactive one. Since these impinging particles are positively charged, the resulting nuclide is proton rich (or neutron deficient) and undergoes transmutation to attain better stability, by emission of positrons (β^{+}) or by electron capture (EC). In these charged particle reactions, the energy of the impinging particle is an important factor that decides the type of reaction that will occur. Radioisotopes produced through charged particle acceleration belong to a different element from their parent, and hence can be availed in very high specific activities. Although this is a great advantage, it must also be recognized that the possibility of multiple types of nuclear reactions leading to radionuclidic impurities exists and hence it is very important to tune the

energy of the impinging particles within the narrow preferred window. The need for high current and the sophisticated technology involved makes the accelerator produced isotopes more expensive than the reactor produced isotopes.

1.2 Radiopharmaceutical classification

1.2.1 Diagnostic radiopharmaceutical

Radiopharmaceuticals which aid in imaging the morphology or functioning of an internal organ or an abnormality are known as diagnostic radiopharmaceuticals, as these images are used for diagnostic purposes. Single photon emission computed tomography (SPECT) and positron emission tomography (PET) refer to the three-dimensional images reconstructed from the attenuation of single energy photons and 511 annhilation photons respectively.[39]

The early ages of diagnostic imaging during the 1950's, employed the radionuclides that were available then, such as ^{131}I, ^{198}Au, ^{51}Cr and ^{198}Hg. The pioneering work by the scientists from the Brookhaven National Laboratory in 1957 on the ^{99}Mo-^{99m}Tc generator and the quick work by the nuclear medicine physician Harper from 1961, mark the beginning of the ^{99m}Tc era.[40] Owing to the excellent attributes such as short half-life (6 h), availability in no-carrier added high specific activity form from a portable generator, emission of a single photon of 140 keV resulting from the transmutation by internal transition, amenable chemistry with multiple oxidation states for labeling a wide variety of molecules and feasible production routes from nuclear reactors at a reasonable cost, ^{99m}Tc was soon realized to have an enormous potential in imaging. The community of scientists and physicians in the nuclear medicine field achieved remarkable progress in developing ^{99m}Tc based radiopharmaceuticals, instant labeling cold kits and soon the era of ^{99m}Tc imaging matured and became very popular.

Initial periods witnessed imaging techniques that used rectilinear cameras or scanners which moved in two-dimensions to give two-dimensional pictures. The invention of gamma camera by Anger in 1957[41] was an important milestone that accelerated the growth of diagnostic nuclear medicine imaging. The advent in the computational systems and electronics during this period made it possible to build gamma cameras capable of reconstructing 3-D images from data acquired from the attenuated single energy photons and these images were termed as the "Single photon emission computed tomography". The construction of dedicated SPECT gamma cameras in 1976 gave further boost to nuclear medicine imaging. These gamma cameras were fitted with NaI (Tl) detectors which were sensitive to the photons in the range of 80-200keV range, ideally suited for detecting the 140 keV photons from the ^{99m}Tc. Although several other radionuclides such as ^{67}Ga, ^{81m}Kr, ^{82}Rb, ^{111}In, ^{123}I, ^{133}Xe and ^{201}Tl, etc. were suitable for SPECT imaging,[42-46] the commercial availability of ^{99}Mo-^{99m}Tc generators and 'kits' for instant preparation of a variety of ^{99m}Tc-radiopharmaceuticals to image nearly all the parts of body, made ^{99m}Tc the "*work-horse*" of diagnostic nuclear medicine.

Although the concept of PET imaging was already there since the 1950's, positron imaging made an entry into the clinics in the 1970's with the synthesis of ^{18}F-FDG (fluoro deoxy glucose) at the Brookhaven National Laboratory. ^{82}Rb was the other PET nuclide used then. However, PET imaging grew in leaps and bounds in the 1990's after the 3-D images of excellent quality were possible with the development of cameras with bismuth germanium oxide (BGO) scintillation detectors in a circular array with coincidence circuits designed to specifically detect the 511 keV photons emitted in opposite directions along with proper computations.

Currently, barring very few specific situations, all diagnostic imaging is either SPECT or PET done using appropriate diagnostic radiopharmaceuticals.[39] As the names suggest, the

SPECT radiopharmaceuticals have single photon emitting radionuclides tagged to the molecule while the PET radiopharmaceuticals are tagged with a positron emitter. There are several PET radionuclides, namely, ^{18}F, ^{11}C, ^{15}O, ^{13}N, ^{64}Cu, ^{68}Ga, ^{124}I, which are amenable for imaging.[47-52] But, among these, ^{18}F is the most widely used[48] both due to its half-life of 110 minutes which is longer than those of the isotopes of ^{11}C, ^{13}N and ^{15}O, as well as because of the well standardized production modality in a medical cyclotron. The PET radionuclides are nearly always produced in the cyclotron and are short lived, which makes their availability difficult and the final radiopharmaceutical preparation costly.[47-48] But, ^{18}F-FDG, the glucose analog was a great imaging tool for very sensitive detection of abnormal tissues and its application grew in a phenominal way during the 1990s in the areas of oncology, cardiology and neurology, earning it the name '*the molecule of the millennium*'.[50-51] Currently, apart from ^{18}F-FDG, several ^{18}F based radiopharmaceuticals are used regularly and ^{18}F is the most widely used PET radionuclide, although ^{11}C labeled drugs and lead molecules find a lot of applications in the drug discovery. In the recent times, ^{68}Ga has been emerging as a PET radionuclide. Despite the short half-life of 68 min, it has great potential as PET radionuclide as it is availed through a generator wherein the parent ^{68}Ge is cyclotron produced.[52]

In general, diagnostic radiopharmaceuticals are used in very low concentrations (10^{-6}-10^{-8} M), and are not intended to have any pharmacological effects. The aim of the diagnostic imaging was originally to get a detailed description of the morphologic structure of organs or tissues. In many occasions, this is achieved by using a radiopharmaceutical which accumulates in the target organ by bio-chemical means. This allowed one to test the functional aspects of the organ using the radiopharmaceutical. Further, with advent in imaging technologies and quick acquisition of images, it was possible to get a series of images in a dynamic mode, which aided in assessing the functional aspects of an organ such

as kidneys, lungs, liver etc. Thus there are two kinds of diagnostic imaging, 'static' for obtaining information on the morphology and 'dynamic' for functional parameters. Apart from these, imaging helps in follow up of therapy and in monitoring the efficacy of a specific therapeutic treatment as well as recurrence of disease. Table 1.4 lists some of the diagnostic radiopharmaceuticals used and their specific applications.

1.2.2 Therapeutic Radiopharmaceutical

Therapeutic radiopharmaceuticals are molecules designed to deliver therapeutic doses of ionizing radiation to the diseased sites. While diagnostic radiotracers rely on high target/ background ratios in a short period of time, the success of radiotherapy depends on high concentration of radionuclide in diseased target site for adequate time span to cause complete destruction of the cancerous cells.

An inherent determinant in developing any therapeutic radiopharmaceutical is the selection of appropriate radionuclides.[16,28,53-59] As mentioned earlier, particle emitting radionuclides are effective for delivering localized cytotoxic doses of ionizing radiation. Radionuclides that decay by α-particle emission, β-particle emission and auger-electron emission have been used in therapeutic radiopharmaceuticals. The effective range and linear energy transfer (LET) properties depend on the type of the particle as well as the energy. The size of the tumor, intra-tumoral distribution of the radiopharmaceutical, pharmacokinetics of the tracer are the major factors that would influence the type of radionuclide desirable for a certain therapy.[56-57] γ-ray emission may or may not accompany the particle emission process and will contribute little to the therapeutic effectiveness. However, γ-rays with energy in the diagnostically useful range are useful in imaging the localization of the therapeutic radiopharmaceutical in patients and for dosimetric purposes.[28,53,55]

Table 1.4 Selected radiopharmaceuticals used for diagnostic applications*

Organ	Function	Agents used
Brain	i) Perfusion ii) Tumors iii) Receptors	^{18}F-FDG, ^{99m}Tc-d-l-HMPAO, ^{99m}Tc-ECD ^{201}TlCl, ^{99m}Tc-d-l-HMPAO, ^{99m}Tc-GHA, ^{18}F-FDG ^{18}F-DOPA, ^{11}C-N-Methyl spiperone, ^{11}C-Carfentanil
Thyroid		NaI – $^{131/123}$I ; $^{99m}TcO_4^-$
Lungs	i) Ventilation ii) Perfusion	^{99m}Tc-aerosols, ^{133}Xe, ^{81m}Kr ^{99m}Tc-HSA microspheres / macroaggregates
Heart	i) Perfusion ii)Metabolism iii) Infarcts iv) Receptors v) Blood Pool	^{201}TlCl, ^{99m}Tc-Sestamibi, ^{99m}Tc-Tetrofosmin. ^{18}FDG, ^{123}I-FA analogs (BMIPP) ^{99m}Tc-PYP; ^{99m}Tc-glucarate ^{123}I-MIBG ^{99m}Tc-RBC; ^{99m}Tc-HSA
Bone		^{99m}Tc-phosphonate (^{99m}Tc-MDP)
Liver/ Spleen		^{99m}Tc-S colloid; ^{99m}Tc-phytate
Hepatobiliary System		^{99m}Tc-IDA derivatives
Kidneys	i) Imaging ii)Renography	^{99m}Tc-DMSA, ^{99m}Tc-GHA ^{99m}Tc-DTPA, ^{99m}Tc-MAG3, ^{99m}Tc-EC
Infection/ Inflammation	i) Infection ii)Inflammation	^{111}In / ^{99m}Tc-Leucocytes; ^{99m}Tc-Ciprofloxacin ^{99m}Tc/ ^{111}In – HIgG, ^{67}Ga-citrate
Tumors		$^{123/131}$I-MIBG, ^{111}In-Octreotide, ^{18}F-FDG, ^{11}C-Methionine, ^{111}In/^{99m}Tc/^{123}I-MoAb, ^{67}Ga-citrate

*Sood D.D., Reddy A.V.R., Ramamoorthy. N. *Fundamentals of Radiochemistry*, **2004**, 298.

1.3 Designing a new radiopharmaceutical

To design a new radiopharmaceutical, to target a specific tissue, whether for diagnostic or therapeutic purpose, a suitable carrier molecule has to be chosen based on the prior knowledge from the published literature. Quantitative structure activity relationship (QSAR) studies, help in determining the biologically active part of the biomolecule. QSAR also gives an insight into the least active part of the biomolecule which can be altered without significantly affecting the biological behavior of the molecule. This portion of the molecule is chosen for complexing or attaching the radionuclide, if required after synthetically derivatizing it suitably. After radiolabeling, the molecule is biologically evaluated both *in-vitro* and *in-vivo*. The bio-evaluation of the radiolabeled preparation in different animal models helps in deciding the utility of the radiolabeled compound for a specific application. Thus, for the development of any radiopharmaceutical for a specific target, *radiolabeling* and *biological evaluation* are very important steps.

1.3.1 Radiolabeling

The method of attaching a radioactive atom to a carrier molecule is called radiolabeling. Radiolabeling could be considered to be of two types: *isotopic and non-isotopic*.

1.3.1.1 *Isotopic labeling*

Isotopic labeling refers to replacing the existing stable atom in a biomolecule with its radioisotope. Here, the radiolabeled molecule is both structurally as well as biologically identical to the non-radioactive parent molecule. One of the common procedures followed for carrying out the isotopic labeling is via isotope exchange. Since the concentration of radioisotope is generally ~10^6 times lower than the inactive substrate, the exchange labeling method results in labeled molecules with low specific activity.

The isotope exchange labeling strategy is not suitable for receptor targeting as the large concentrations of unlabeled inactive molecules may compete with labeled molecules and saturate the target receptor sites resulting in low uptake of the radiopharmaceutical. To overcome this, isotopic labeling via a reactive intermediate is employed. Here, the labeling takes place via a reactive intermediate which leads to the desired radiolabeled compound in no-carrier added (all molecules are radiolabeled) high specific activity preparation. Since the radiolabeled product is chemically different from the inactive reactive intermediate, the two are chemically separable leading to high specific activity preparations.

The radiopharmaceutical ^{131}I-meta-iodo benzylguanidine used for diagnosis and therapy of neuroendocrine tumors is made both by isotope exchange and in no-carrier added level.[60-64] The latter preparation is extremely useful for therapeutic usage of the radiopharmaceutical and is prepared via a reactive intermediate.[63,64]

1.3.1.2 ***Non-isotopic labeling***

Labeling with a metallic radionuclide such as ^{99m}Tc is an example of non-isotopic labeling. Most often, the radionuclides used for labeling are non-metals,[48] transition metals and lanthanides.[5,6,17,28,34,65-68] The attachment of these to the carrier molecule is either through a covalent or co-ordinate bond.

1.3.1.2.1 *Non-metal labeling*

^{18}F[48,69] and $^{123/125/131}$I[70] are the most widely used non-metallic radioisotopes. These halide radioisotopes can be attached to an organic molecule by nucleophilic[48,69] or electrophilic[71-73] substitution. The former substitution method is common in ^{18}F labeling. In this, a suitable precursor of the carrier molecule is synthetically prepared. This precursor molecule has a good leaving group such as triflate, mesylate, tosylate or nosylate which can undergo nucleophilic substitution by $^{18}F^-$ in high yield.

Radioiodine labeling in aliphatic organic compounds is carried by nucleophilic substitution. However, the aliphatic radio-iodinated compounds undergo rapid de-iodination *in-vivo* as there are much more potential nucleophiles present inside the body. Thus, iodine labeling via electrophilic substitution in aromatic systems is much more favorable from *in-vivo* stability point of view. Here, the carrier molecule carrying the tyrosine moiety is an ideal substrate for the incorporation of iodine via electrophilic substitution. The electrophilic substitution is carried using mild oxidizing agents such as chloramine-T, iodogen, etc. which oxidizes the radioactive iodine (sodium iodide) present in -1 oxidation state to a uni-positive ion (+1 oxidation state). The oxidized I^+ species is an electrophile that attacks the electron rich aromatic systems. This substitution in phenyl ring is facilitated by electron releasing ortho-para directing groups such as OH, NH_2.

1.3.1.2.2 *Metal labeling*

Most of the metal radioisotopes used for radiopharmaceutical applications are transition metals (TM) and lanthanides.[5,6,17,28,34,65-68] These metals exhibit variable oxidation states and are radiolabeled to the carrier molecule via a chelate linkage. A chelate contains more than one co-ordinating donor atom (N, O, P or S) group in a suitable stereochemical orientation which co-ordinates with the radiometal in a particular oxidation state.

The preliminary affinity of a metal to a co-ordinating donor group has been explained on the basis of Hard and Soft Acid-Base theory.[74] In this theory, both metal and ligand donor groups are treated as acids and bases respectively. Hard and soft refers to the size of the acid or base respectively. The hard metal ion prefers co-ordination with hard ligand donor atom whereas soft acid prefers co-ordination with soft base. So, larger sized metal ion has affinity towards bigger non-metals such as P and S whereas smaller metal ion prefers co-ordination with N and O donors. The size of the metal ion depends on the position of the element in the periodic table and on the oxidation state of metal. It increases as we go down a group in a

periodic table and decreases with increase in the oxidation state of the metal ion. This theory empirically helps in identification of groups to be incorporated in a chelate for strongly holding a particular radiometal.

1.3.1.2.2.1 Transition metal Labeling

Transition metals (TM) are d-block elements which exhibit variable oxidation states with d-orbital electrons involved in bonding. As these exhibit variable oxidation states, the same metal will have affinity for large number of chelates with different donor groups i.e. metal in high oxidation state has preference to bind with hard donor chelate and vice-versa. The final radiolabeled complex formed will have either tetrahedral (4 co-ordination) or octahedral geometry (6 co-ordination). Transition metals used in labeling for nuclear medicine applications are $^{62/64}$Cu, ^{99m}Tc, $^{186/188}$Re, ^{111}In, etc.[5,6,17, 34,75]

A representative example of TM labeling is, ^{99m}Tc labeling with carrier molecules using three radiolabeling approaches.

i) *Direct labeling approach*: In this the radioactive metal is introduced directly to a biomolecule in presence of a reducing agent. The reducing agent reduces the Tc metal from the most stable oxidation state of +7 to a lower state and in presence of suitable donor group of biomolecule, gets attached with it. This approach is easy to carry out but the chemistry is not well defined in terms of structural characteristics and is followed mainly to label antibodies or antibody fragments labeling.[76-80]

ii) *Pre-labeling approach*: In this, the radiometal is attached to a chelate first, which is then introduced to the carrier biomolecule in a separate step. This approach has been successfully used in labeling antibodies and their fragments with ^{99m}Tc.[81-82] In this approach, the chemistry is better defined, and the targeting biomolecule is not exposed to the harsh conditions in the chelation step. However, the multiple-step radiosynthesis is too complex and time consuming for routine clinical use.

iii) *Bi-functional chelating agent (BFCA) approach*: This is the most suitable approach for receptor specific molecules. A bi-functional chelating agent is a molecule which can be linked to the carrier molecule at one end while the other end of the chelate is used for holding the metal. In this, the carrier molecule is first linked to a bi-functional chelator. If required, a linker (small organic chain) can be introduced in between the two, to modify the *in-vivo* pharmacokinetic behavior of the molecule. The radioactive metal is introduced in the end. This approach combines the ease of direct labeling with well-defined chemistry of the preformed chelate approach. This is the most practical approach for kit formulation and for development of commercial products.

1.3.1.2.2.2 Lanthanide labeling

Lanthanides are f-block elements with valence electrons being filled in the penultimate 4f-orbitals. These metals complex mostly in their +3 oxidation states since 4f-orbital electrons do not participate in the bonding. They expand their co-ordination sphere up to 9 and the geometry of the final complex is dependent upon the co-ordination number. Some of the common geometries are tri-capped prism and square anti-prism. Lanthanides such as ^{90}Y, ^{153}Sm, ^{166}Ho and ^{177}Lu have useful therapeutic applications.[16,28,34,65]

The BFCA approach is followed for the labeling of Lanthanides, with the carrier biomolecule being first attached to a BFCA followed by radiometal introduction. The BFCA most commonly used are 1,4,7,10-tetraazacyclododecane-1,4,7,10-tetraacetic acid (DOTA) and diethylenetriamine pentaacetic acid (DTPA). These BFCAs provide both thermodynamic and kinetic stability to the final complex.[16,17,27,28,34] After the labeling procedure, the chemical characterization of the radiolabeled compound is an important quality control parameter which has to be carried out before its biological evaluation *in-vitro* and *in-vivo* in animals.

1.3.1.3 *Characterization of the radiolabeled compound*

The formation of the final radiolabeled preparation can be ascertained through different chromatographic techniques such as paper chromatography, thin layer chromatography and high performance liquid chromatography, using a radioactive detector to monitor the radioactivity. Apart from this, electrophoresis is also used for determining the radiolabeling yield of the compound.

The nature of charge on the final metal complex can be ascertained using conductance measurements. The three dimensional structure of the final complex in metal labeling can be ascertained only after preparing the complex at macroscopic level using inactive isotopes or analogues and determining the final geometry using X-ray diffraction and various spectroscopic techniques such as NMR, IR and Mass spectrometry.

1.3.2 Biological evaluation

1.3.2.1 *Pharmacokinetics*

The pharmacokinetics is the bio-distribution pattern of a drug over a period of time, once it is injected inside the body. This includes absorption, distribution, metabolism and elimination of the drug. However, in context of radiopharmaceuticals it refers to distribution and elimination of the radionuclide following administration of the radiopharmaceutical. The main pharmacokinetic consideration for a radiopharmaceutical is that the radiolabeled molecule should have high target-to-background ratio in a short period of time. For this, the radiolabeled biomolecule should be cleared quickly from the blood to minimize non-target radioactivity and have a low background. But, retention time in blood should be adequately long to allow the radiolabeled biomolecule to reach the receptor or target site and achieve adequate accumulation in the desired tissue/ organ.

There are several ways to modify the pharmacokinetics of radiopharmaceuticals. These include chemical modification of the biomolecule, the use of a pharmacokinetic

modifier linker and the choice of coligands in the case of radiometal chelation. Chemical modification of the biomolecule can be achieved by introducing various hydrophilic groups or functional groups which get metabolized in the non-target organs and clears off rapidly. Also, in the case of metal complexes, the BFCA donor groups can be chosen in such a way which leads to charged complexes contributing to the reduced lipophilicity and thereby improving the clearance pattern from non-target organs. Sometimes, a linker is introduced between the biomolecule and the radiolabel. This may be a carbon chain for increasing the lipophilicity of the overall complex or an amino acid linkage for increasing the hydrophilic nature of the final radiolabeled molecule. For metal complexes containing two or more ligands for final stabilization, the choice of coligands may be used for modification and improvement of pharmacokinetics of the radiopharmaceutical.

1.3.2.2 *In-vitro studies*

1.3.2.2.1 *Stability studies*

Chemical stability is an important requirement for any pharmaceutical, especially so for radiopharmaceuticals. Thus, thermodynamic stability is an important parameter in the formation of radiopharmaceutical. Since majority of the radiopharmaceuticals are injected intravenously, they undergo distribution through the blood circulation. During this process, the trace concentrations of the radiopharmaceuticals are exposed to a large number of other potential molecules such as proteins, amino acids having suitable donor groups. Apart from organic macromolecules there are other trace elements present in the body which may challenge the integrity of the radiolabeled molecule inside the body. Thus, kinetic stability is much more significant than thermodynamic stability in the case of radiopharmaceuticals.

Radiopharmaceuticals may undergo biological interactions in the blood circulation. These include receptor binding, protein binding and chemical reactions. Receptor binding is necessary for the uptake of target specific radiopharmaceuticals. But the other two factors

affect the quality of radiopharmaceutical performance. So, these factors are evaluated *in-vitro* before injecting the radiolabeled compound *in-vivo*.

1.3.2.2.1.1 Protein binding studies

The protein binding leads to long blood retention times of the radiopharmaceutical, thereby affecting the quality of the diagnostic images. The high lipophilicity of the radiopharmaceutical may lead to high protein binding. Also, *in-vivo* degradation of the radiolabeled compound and association of the radioisotope with the macromolecules may lead to high blood pool activity. The association of the radiolabeled compound with serum proteins is determined after incubating the radiolabeled compound with the human serum and then precipitating the proteins to ascertain the degree of association.

1.3.2.2.1.2 Chemical reactions

These occur between the radiopharmaceutical and metal ions or other potential chelators present inside the body. The *in-vivo* chemical reactions such as radio de-iodination, radio de-metallation are the degradation processes leading to radiation burden to the patient. The *in-vivo* radio-de-iodination is the most common phenomenon observed with radio-iodinated aliphatic organic compounds. This arises due to the presence of potential nucleophiles present inside the body. In the case of chelated metal radiopharmaceuticals, there are several metal ions present inside the body competing for the chelated complex. The competition between the BFCA and other potential, *in-vivo* chelators, such as amino acids (cysteine, glutathione, etc.) and transferrin, results in release of metal radionuclide from the chelated complex thereby increasing non-target uptake leading to high radiation toxicity.

1.3.2.2.2 *Cell binding studies*

This involves first creating, *in-vitro,* the patho-physiological conditions present inside the body and evaluating the potential of radiolabeled compound, in terms of percentage of uptake and retention, before its evaluation *in-vivo*. For example, in the case of tumor targets,

in-vitro uptake studies are performed in different cancer cell lines to test the efficacy of the radiolabeled compound. This involves incubating the prepared radiolabeled compound with different cancer cell lines and observing the uptake after isolation of cells at different times. In case cell uptake is observed, the different parts of the cell are lysed and compound associated with a particular cell organelle is determined. Also, in case of receptor target molecules or molecules that enter the cell via active transport, the competitive cell uptake studies are carried. This involves incubating the cells together with radiolabeled compound and different concentrations of inactive target compound and observing the change in the cellular uptake pattern. These studies help in understanding the mechanism of uptake and different pathways involved in the retention of the compound inside the cell. Also, it gives an idea regarding the potentiality of the radiolabeled compound for the aforementioned radiopharmaceutical application. Once its usefulness is established *in-vitro,* it is evaluated *in-vivo* in small animals before being adjudged useful for patient use.

1.3.2.3 *In-vivo studies*

After obtaining positive *in-vitro* results, the radiolabeled preparation is evaluated for its *in-vivo* behaviour in small animal models such as mice or rats. *In-vivo* studies are carried out in normal animals initially and if deemed necessary, further studies in diease models of animals are performed. For adjudging the behavior of the radiopharmaceutical *in-vivo* in normal animals, the radiolabeled preparation is injected in the animal, and the distribution of radioactivity in various organs and blood is estimated at various time spans after the injection. In brief, animals are taken in sets of 5, injected with the radiolabeled molecule, sacrificed after the desired time span, the organs excised and counted in a radioactivity detector under a uniform geometry. If the bio-distribution results are encouraging, the radiolabeled preparation is evaluated in higher animals such as rabbit, dog, guinea pig and monkeys by external imaging using planar gamma camera or small animal SPECT camera.

The biological data obtained from the animal distribution is useful in assessing the utility of radiolabeled preparation for a specific application. If the radiopharmaceutical is intended for imaging a diseased condition such as cancerous tissue or damaged myocardium, then evaluation of the compound in small animals induced with similar disease condition is meaningful to prove the utility. In such situations, it becomes important to prove the difference in the bio-distribution of the radiopharmaceutical in the normal and the disease model.

The present work is on the development of a ^{99m}Tc based diagnostic radiopharmaceutical, using novel labeling chemistry, not yet explored in the routine established ^{99m}Tc-radiopharmaceuticals. The work comprises of the complete range of activities, right from the selection of the target and lead molecule, the latters synthetic derivatization for the incorporation of ^{99m}Tc activity and its bio-evaluation in suitable animal model. Before going to the main work, an outline of the technetium radiopharmaceuticals, its chemistry and different strategies followed for the incorporation of this metal to the different carrier molecules are discussed.

1.4 ^{99m}Tc radiopharmaceuticals

Technetium (^{99m} Tc) radiopharmaceuticals account for nearly 80% of all diagnostic studies in nuclear medicine, which amounts to nearly 30 million tests per year. These agents are available worldwide and are routinely used for imaging almost all the important organs of the body. Some of the ^{99m}Tc-based radiopharmaceuticals used in nuclear medicine are given in Table 1.5.

The credit for the discovery of this element technetium goes to Emilio Segre and Carlo Perrier after they successfully separated technetium-95m & 97m from a sample of molybdenum which had been bombarded with deuterons in Ernest Lawrence's UC Berkeley

cyclotron.[83] ^{99}Tc was the first isotope of Tc to be produced in a quantity of measurable mass, and is still the most abundant of the 22 isotopes of Tc, none of which is stable. The isotopes of Tc decay by positron emission, electron capture, or beta emission. Nine of these isotopes have excited states known as isomers. These isomers decay primarily by isomeric transformation, with the emission of γ-rays with characteristic energies. By far the most useful of these isomers and isotopes has been ^{99m}Tc.

Table 1.5 ^{99m}Tc-based diagnostic radiopharmaceuticals*

Agent	Function
^{99m}Tc - Sulphur Colloid, ^{99m}Tc-Tin Colloid, ^{99m}Tc-Phytate	Liver scanning
^{99m}Tc-Glucoheptonate, ^{99m}Tc-DTPA, ^{99m}Tc-Dimercaptosuccinate ^{99m}Tc-Mercaptoacetyl triglycine, ^{99m}Tc-Ethylene Dicysteine	Kidney function studies
^{99m}Tc-Methylene diphosphonate (MDP)	Bone scanning
^{99m}Tc-Mebrofenin	Hepatobiliary function
^{99m}Tc-HSA Microspheres / Macroaggregates, ^{99m}Tc-Aerosols	Lung Scanning
^{99m}Tc-Red blood cells; ^{99m}Tc-Pyrophosphate; ^{99m}Tc-glucarate, ^{99m}Tc-Sestamibi, ^{99m}Tc-Tetrofosmin	Cardiac studies
^{99m}Tc-d,l-HMPAO, ^{99m}Tc-L,L-ECD	Brain blood flow
^{99m}Tc-Leuocytes; ^{99m}Tc-HIgG; ^{99m}Tc-antigranulocyte antibodies; ^{99m}Tc-ciprofloxacin	Infection / Inflammation

*Sood D.D., Reddy A.V.R., Ramamoorthy. N. *Fundamentals of Radiochemistry*, 2004, 298.

1.4.1 Why ^{99m}Tc ?

^{99m}Tc is the most preferred isotope due to its suitable γ-ray energy, optimum half-life and ease of availability.[5,6,28,34] The monoenergetic photon energy (140 keV) with a γ-abundance of 88% is readily collimated to give images of high spatial resolution. Further, absence of any major particulate emission from this radioisotope, leads to reduced radiation toxicity to the patients. The 6 h half-life of ^{99m}Tc is long enough to allow a radiopharmacist to prepare the radiopharmaceutical dose, carry out the quality control tests, inject into the

patient and for nuclear medicine physicians to carry out the imaging studies. At the same time, it is short enough to permit administration of millicurie amounts of ^{99m}Tc activity without causing significant radiation dose to the patient. Furthermore, ^{99m}Tc is readily available from the ^{99}Mo-^{99m}Tc generators at low cost. Because of the above ideal characteristics, ^{99m}Tc is the '*work-horse of nuclear medicine*'. Some of the major areas of ^{99m}Tc diagnostic imaging include cerebral, myocardial, renal, liver, lung, tumor, etc.[5,6,84,85] Structures of some ^{99m}Tc radiopharmaceuticals are shown in Fig. 1.2.

1.4.2 Production of ^{99}Mo and ^{99}Mo-^{99m}Tc Generator

^{99m}Tc agents are routinely used worldwide due to the favorable logistics of transportable ^{99}Mo-^{99m}Tc generator in the hospital radiopharmacy. ^{99m}Tc is produced by β-decay of the parent radionuclide ^{99}Mo (half-life ~ 2.78 days). ^{99}Mo is produced either by fission of ^{235}U (n,f) or by neutron activation of ^{98}Mo (n, γ) in the nuclear reactor.[86] Since the parent nuclide ^{99}Mo is longer lived than the daughter ^{99m}Tc, these isotopes exist in equilibrium after a certain time after production, when the rate of growth of ^{99m}Tc becomes equal to the rate of its decay. Such parent-daughter equilibrium is a fairly common occurrence in radionuclide chains and when the parent nuclide's half-life is far longer than the daughter, the equilibrium is said to be 'secular equilibrium'. When the ratios of their half-lives is not too large, then the equilibrium is named as 'transient equilibrium' as in the case of ^{99}Mo-^{99m}Tc. ^{99m}Tc can be easily separated from the parent isotope using an appropriate technique through a gadget known as a Generator.[87]

A generator is a system where the daughter radionuclide co-existing with its longer lived parent can be preferentially separated using chemical means. A generator system is thus a means to obtain the daughter product repeatedly from the parent. The maximum activity that can be obtained is when the parent and daughter attain equilibrium (which is nearly 4 times the half-life of the daughter) and in the case of ^{99m}Tc generators, ^{99m}Tc can be availed

approximately once a day in maximum possible amount. The ^{99}Mo-^{99m}Tc generators were popularly referred to as cows, because they could be milked every morning to obtain ^{99m}Tc for preparation of radiopharmaceuticals. Different types of ^{99}Mo-^{99m}Tc generator systems are available. These are (a) column chromatography based generators, based on adsorption (e.g. column generator with alumina as sorbent) or ion-exchange, (b) column generators where the matrix is a insoluble form of the parent nuclide (eg: gel-column generator with ^{99}Mo in the form of $ZrMoO_4$), (c) solvent extraction generator and (d) sublimation generator. All these systems use different chemical methods for the separation of two isotopes.

In the alumina column generator, ^{99}Mo, in $^{99}Mo_6O_{24}^{4-}$ chemical form, is adsorbed to an acidic alumina and ^{99m}Tc formed by the decay of ^{99}Mo is preferentially eluted from the alumina column with saline. The final eluate contains ^{99m}Tc as $Na^{99m}TcO_4$ in saline. This system is suitable for supply to distant nuclear medicine centres where ^{99m}Tc can be easily eluted everyday and after subsequent labeling can be used for carrying out the *in-vivo* patient studies. The extraction efficiency of the generator is around 80%. However, for the alumina column generator, ^{99}Mo of very high specific activity, obtained through the (n,f) route is necessary, because of the limitation of the adsorbent capacity of the alumina for Mo.

In the solvent extraction generator, $^{99m}TcO_4^-$ is extracted from the alkaline sodium molybdate solution by solvent extraction using low boiling organic solvent methyl ethyl ketone (MEK). ^{99}Mo of low specific activity also can be used in this type of generators. The $^{99m}TcO_4^-$ activity after MEK removal is reformulated in saline and used for imaging studies. The solvent extraction efficiency is similar to the column generator efficiency but requires an additional processing step which may lead to some undesired impurities.

In the ‘gel generator’, ^{99}Mo is converted to a precipitate of zirconium molybdate, which is filtered, dried and used as the column matrix. ^{99m}Tc is then eluted from this by

elution with saline. Such a system is generally adopted to have a column generator when ^{99}Mo of high specific activity is unavailable.

The use of ion exchange columns to hold ^{99}Mo activity from which the ^{99m}Tc is eluted and held on to another column and finally extracted in a small volume, has elicited interest in scientists as a feasible generator system.[88] Yet, this needs reasonable amount of work before this can be a commercial generator.

1.4.3 Diverse redox chemistry

One of the characteristics of technetium is its rich and diverse redox chemistry. It exhibits various oxidation states from -1 to +7 in different compounds. The Tc (VII) is a non-reactive oxidation state. Thus, for linking the metal to a biomolecule, the Tc (VII) in $^{99m}TcO_4^-$ has to be reduced to a lower oxidation state. When $^{99m}TcO_4^-$ is reduced, the final oxidation state of ^{99m}Tc depends upon the chelator and reaction conditions. The diverse redox chemistry makes it difficult to control the oxidation state and stability of ^{99m}Tc complexes. At the same time, it also provides opportunities to modify structures and properties of ^{99m}Tc complexes by the choice of different chelators.[15,89,90]

1.4.4 Isomerism

Another aspect of technetium chemistry is isomerism, including geometric isomers, epimers, enantiomers, and diastereomers (Fig. 1.3).[15,89,91,92] Epimers are often found in square pyramidal or octahedral Tc=O and Tc≡N complexes containing chelating ligands with substituents on the ligand backbone or a tertiary amine *N*-donor atom. Formation of epimers is due to the relative orientation (*anti* and *syn*) of substituents to the $[^{99m}Tc=O]^{3+}$ core.[89,91] Enantiomers are often found in ^{99m}Tc=O complexes, such as $[^{99m}TcO(MAG_3)]$, due to asymmetrical bonding of chelator to the $[Tc=O]^{3+}$ core even though the free chelator does not have a chiral center. If a ^{99m}Tc complex contains two or more chiral centers, diastereomers may be formed, and are often separated by reversed phase HPLC methods. Isomers often

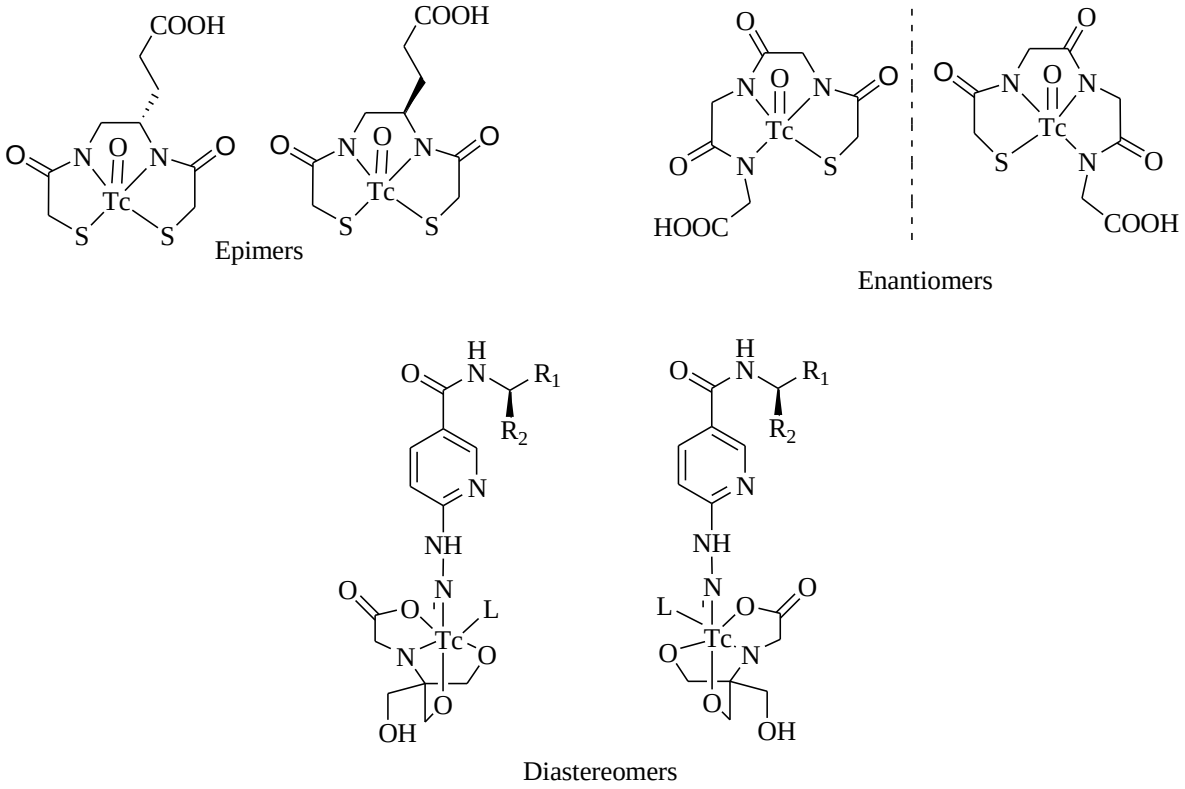

Fig. 1.3 Isomerism present in ^{99m}Tc radiopharmaceuticals

have different lipophilicity and biodistribution patterns. This is particularly true for small ^{99m}Tc complex radiopharmaceuticals as their biological properties are determined exclusively by the physical and chemical characteristics of the ^{99m}Tc complex. For example, in the case of ^{99m}Tc-HMPAO, a known radiopharmaceutical used for cerebral imaging, only the *d,l*-isomeric form shows high accumulation in the brain, whereas the *meso* form is not useful for brain imaging. For receptor-based radiopharmaceuticals, the formation of isomers for the ^{99m}Tc chelate may have significant impact on the biological properties of a radiopharmaceutical. Therefore, the choice of BFCAs should be those which form technetium complexes with minimal isomerism.

1.4.5 Technetium cores

The diverse redox chemistry of ^{99m}Tc has led to various ^{99m}Tc metal cores or synthons (Fig. 1.4)[5-7,34,58,84,85,92-99] which can be used as basic moieties for labeling molecules with ^{99m}Tc. A metal core is a substitution-labile intermediate technetium complex which shows a

marked reactivity towards ligands having some specific set of co-ordinating atoms. In these labile complexes, a few co-ordinating positions are occupied by a set of ligands that are tightly bound to the metal center. The resulting strong ligand field enables significant stabilization of the metal oxidation state preventing the complex to undergo oxidation-reduction reactions. The remaining positions of the co-ordination arrangement are usually spanned by weakly bound ligands that could be easily replaced by some other ligand carrying a specific set of donor atoms. As a result, the reaction between the intermediate labile complex and the specific ligand is expected to be kinetically favored and result in high yield of the final substituted complex. For example, ^{99m}Tc-triaquo-tricarbonyl core has ^{99m}Tc strongly bonded to three carbonyl donor groups which stabilizes the metal in +1 oxidation state and has three labile water molecules co-ordinated which get quantitatively exchanged with tri-dentate chelates having suitable donor groups. This behavior can be efficiently exploited for attaching a stable ^{99m}Tc core to a carrier molecule having the appropriate set of co-ordinating atoms. A few useful ^{99m}Tc cores which are currently used worldwide in radiopharmaceutical research are discussed below.

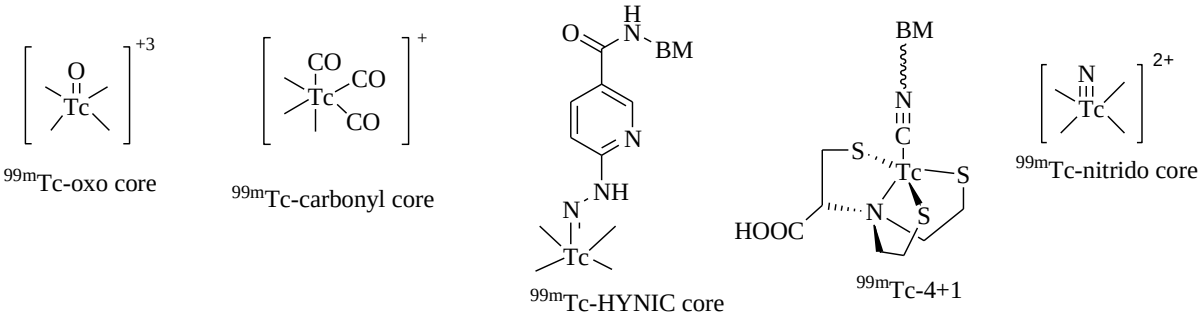

Fig. 1.4 Commonly used ^{99m}Tc-cores for radiopharmaceutical applications

1.4.5.1 *$[^{99m}Tc=O]^{3+}$ core*

This is the most commonly used ^{99m}Tc-core. The first generation ^{99m}Tc radiopharmaceuticals, presently in use, mostly contain $[^{99m}Tc=O]^{3+}$ core where ^{99m}Tc exists in

+5 oxidation state and forms complexes with ligands containing good π-donor groups such as O, N and S. The $[^{99m}Tc=O]^{3+}$ core forms square pyramidal complexes with tetra-dentate chelators such as N_2S_2 diamidedithiols, N_3S triamidethiols, N_2S_2 monoamide monoamine dithiols and N_2S_2 diaminedithiols.[59,100-124] The $[^{99m}Tc=O]^{3+}$ core is unstable under redox conditions and pH variations. Under these conditions, it gets converted to a non-reactive species, hydrolyzed technetium, $^{99m}TcO_2.H_2O$. To prevent its formation, large amount of chelating ligand is required to obtain the final radiolabeled complex in high labeling yield > 90%. However, this latter approach of labeling is not suitable for target specific radiopharmaceuticals as the antigen or receptor present on the target site have low concentrations. The presence of excess cold ligand will saturate the target thus reducing the uptake of the radioactive drug. But reducing the ligand amount slows down the overall reaction kinetics thereby increasing the formation of hydrolyzed technetium and in effect lowering the overall labeling yields. To circumvent this problem, a transchelation method was introduced where a large amount of secondary ligand is taken which stabilizes the $[^{99m}Tc=O]^{3+}$ core and is then kinetically replaced by the desired ligand in a quantitative yield.

In the recent past, there has been tremendous growth in the ^{99m}Tc-chemistry and a number of other metal cores have been introduced. These include ^{99m}Tc-carbonyl core ($[^{99m}Tc(CO)_3(H_2O)_3]^+$), ^{99m}Tc-hydrazino nicotinamide core ([^{99m}Tc-HYNIC]), ^{99m}Tc (III) core and ^{99m}Tc-nitrido ($[^{99m}Tc\equiv N]^{+2}$) core. Unlike $[^{99m}Tc=O]^{3+}$ core, these cores are highly stable towards redox conditions and pH variations and have high affinity for ligands containing a specific donor atom groups. Since the core prefers specific donor groups, the required amount of carrier molecule, tethered with these specific donors, used for radiolabeling is very less, resulting in high specific activity complexes. Some of these cores require a coligand for stabilization. As one of the advantages of all the new cores is ligand flexibility, the chelators can here be varied to a large extent, enabling a systematic screening of biological properties

and receptor binding. For the $[^{99m}TcN]^{2+}$ and $[^{99m}Tc(CO)_3]^{+}$ precursors, kits are available that make routine studies on a reproducible basis possible. The stability of the formed complexes is high but they still differ in their properties and hence, the potential biomolecules and radiopharmaceuticals derived from these complexes could also have different properties. A brief overview of these novel cores and their chemistry is given below. Since the present thesis work is based on $[^{99m}TcN]^{2+}$ core, a detailed description of the core is presented.

1.4.5.2 *$[^{99m}Tc(CO)_3(H_2O)_3]^{+}$ core*

This metal core is of low molecular weight as compared to other new cores. The ^{99m}Tc here is in +1 oxidation state and is stabilized by the presence of three CO donor groups. The low oxidation state of the metal contributes to the stability of the intermediate core due to π-back-bonding from the filled d-orbitals of the metal to the empty anti-bonding orbital of CO ligand. The three water molecules bonded to the metal center are labile in nature and can be replaced by suitable tri-dentate π-donor ligands. Hydro- and lipo-philicity can be varied over a broad range and a combination of mono-, bi- and tri-dentate ligands is possible. However, mono-dentate and bi-dentate chelators often form ^{99m}Tc (I)-tricarbonyl complexes with low solution stability, which results in high protein binding and high background activity in the blood stream. In contrast, tri-dentate chelators form ^{99m}Tc (I)-tricarbonyl complexes with high stability and rapid clearance from blood and other major organs. The charge on the final complex depends on the tri-dentate system used for the formation of the final complex leading to either uni-positively charged, neutral or negatively charged complexes. The use of different chelates can be introduced to fine tune the biological properties. Some of the useful tri-dentate systems for this core is iminodiacetate, diethylenetriamine, etc. The basic nature of the core is lipophilic in nature and complexes prepared using this core show clearance via the hepatobiliary pathway.[125-136]

1.4.5.3 *[^{99m}Tc-HYNIC] core*

This core has been found to be extremely useful for the labeling of small peptides, antibody fragments and other biomolecules.[137-157] Here, two different ligands are used for the final stabilization of the metal complex. One of the ligand is a hydrazino-nicotinamide (HYNIC) BFCA to which the biomolecule is linked and the other is a coligand which stabilizes the final metal complex with ^{99m}Tc in +5 oxidation state. Since HYNIC can only occupy one or two co-ordination sites, a coligand, such as tricine, is often needed to complete the co-ordination sphere of technetium. The hydrazine *N* co-ordination to the ^{99m}Tc metal has a partial double bond character with both the hydrazine protons de-protonated to achieve stabilization in presence of other coligand. The advantage of using HYNIC as the BFCA is its high ^{99m}Tc-labeling efficiency and the choice of coligands such as tricine, glucoheptonate, ethylene diamine diacetic acetic acid (EDDA), which allow easy modification of hydrophilicity and pharmacokinetics of the ^{99m}Tc-labeled biomolecules (BM). However, the use of tricine as coligand often results in complexes with solution instability and leads to multiple species.[158-159] To overcome this problem, several versatile ternary ligand systems (HYNIC, tricine and water-soluble phosphine) that form ternary ligand technetium complexes [^{99m}Tc(HYNIC-BM)(tricine)(phosphine)] were introduced.[159-161] These ternary ligand ^{99m}Tc complexes have very high solution stability and form diastereomers if the biomolecule contains one or more chiral centers.

1.4.5.4 *^{99m}Tc (III) core*

^{99m}Tc in (III) state is found to form stable complexes when a tetra-dentate ligand and a mono-dentate ligand co-ordinate the metal centre.[162-167] In this '4+1' labeling approach, the tetra-dentate ligand is a less flexible NS_3 (tetra-dentate umbrella) ligand which stabilizes ^{99m}Tc in +3 oxidation state in combination with a mono-dentate ligand usually a soft donor such as an isocyanide or a phosphine. The biomolecule is mostly attached as the mono-

dentate donor which leads to minimum distortion and no special care in respect of stereochemistry has to be taken into account.[168-170] A big advantage of the ^{99m}Tc (III) approach is that the ^{99m}Tc building block is small. However, it is still less flexible since the chemistry is more or less fixed. Besides molecular weight, the topology of the ^{99m}Tc (III) precursor is a strong advantage, since it is small and highly symmetric, without active groups pointing out of the topology of the overall complex.

1.4.5.5 *[^{99m}Tc≡N]$^{+2}$core*

1.4.5.5.1 *Historical Background*

This core was introduced by Baldas and Bonnyman in 1981. It was prepared by refluxing sodium pertechnetate with sodium azide and hydrochloric acid.[171-172] The harsh reaction conditions used for the preparation of this core restricted its use for limited complexation studies[173-175] and thus affected the growth of [^{99m}Tc≡N]-based radiopharmaceutical. However, the core gained popularity in the 1990s when Duatti and co-workers introduced a mild reaction condition for the preparation of this core.[175] The pharmaceutical safety of the reaction substrates employing hydrazine derivative, *N*-methyl, *S*-methyl dithiocarbazate as nitride (N^{3-}) donor in presence of $SnCl_2$ as reducing agent, and other reaction conditions allowed its exploration for radiopharmaceutical applications.

1.4.5.5.2 *Chemistry*

Among the new cores, ^{99m}Tc-nitrido ([^{99m}Tc≡N]$^{+2}$) core is iso-electronic to the conventional [^{99m}Tc=O]$^{+3}$ core and exists in +V oxidation state. However, this core is more stable under redox conditions and pH variations compared to the conventional [^{99m}Tc=O]$^{+3}$ core.[176] This facilitates complexation with small amounts of ligand, leading to high specific activity complexes. It has been observed that a ligand backbone containing tetra-dentate donor groups[177] is not suitable for complexation with this core. The complexes formed with bi-dentate donor ligand are preferred with two ligand molecules involved in co-ordination

with the core.[178-181] ^{99m}Tc-nitrido core is reported to have affinity towards soft donor atoms such as S and the core forms complexes with square pyramidal geometry.[171] Dithiocarbamates and xanthates have two S donor atoms making them suitable bi-dentate chelates which are reported to form stable symmetric complexes with ^{99m}Tc-nitrido core.[178-181] The complexes formed in this way are symmetric [2+2] with ^{99m}Tc≡N occupying the apical position and the other four donors occupying the basal plane. Several myocardial perfusion agents using this core have been prepared[181] and the most promising ones are in clinical trials. ^{99m}TcN-NOEt (NOEt = *N*-ethoxy, *N*-ethyl dithiocarbamate)[178,182] (Fig. 1.5) is one of the complex based on this core which is presently under phase III clinical trial. Similarly, many neutral dithiocarbamate complexes have shown potential as brain perfusion agent.[183-184]

Apart from symmetric [2+2] complexes prepared using $[^{99m}Tc{\equiv}N]^{+2}$ core, a large number of asymmetric [2+2] complexes have been prepared,[185-196] with a long chain bi-dentate phosphorus (PNP) lipophilic backbone occupying two *cis* positions in the basal plane of the square pyramidal geometry and leaving the other two *cis* positions occupied by bi-dentate π-donor ligands such as NS/ OS/ SS donors.[186,193,195] The bi-dentate PNP donor ligand can be varied for tuning the *in-vivo* biological characteristics of the final complex. Dithiocarbamate,[188,191] dithiols[196] and cysteine [with either (SH, NH_2) or (SH, COOH)][187,190,192] are suitable bi-dentate chelates containing good π-donor groups to yield final asymmetric complexes in high yield. The target molecule or the biomolecule is generally derivatized with a π-donor group for linking it to ^{99m}Tc metal core. Thus, $[^{99m}TcN]^{2+}$ core is very flexible with respect to the labeling chemistry and can have complexes with the same target molecule, yet differing in *in-vivo* biological characteristics. The asymmetric [2+2] labeling approach is suitable for target specific radiopharmaceuticals[185] and has been evaluated for a large number of biological targets.

These include brain receptor imaging,[190,192] myocardial imaging,[196] peptide receptor imaging,[197,198] etc. Several radiolabeled preparations containing asymmetric ^{99m}Tc-nitrido core have exhibited attractive features and hence hold promise for emerging as new radiopharmaceuticals. Some of the complexes of this class such as ^{99m}TcN-DBODC [DBODC = bis(*N*-ethoxyethyl) dithiocarbamate],[194,199] ^{99m}TcN-15-crown-5[92,200] and ^{99m}TcN-MPO (2-mercaptopyridine *N*-oxide)[201] (Fig. 1.5) have shown excellent characteristics of a myocardial agent and are currently under exploration. These complexes give better myocardial diagnostic images than the presently clinically used ^{99m}Tc radiopharmaceuticals.

Based on this core, in the present work, an attempt has been made to prepare a number of ^{99m}Tc labeled complexes and have been bio-evaluated in small animal model. Major part of the thesis work is aimed at exploring such complexes for myocardial imaging. Thus, before going to the outline of the work carried in the different chapters of the thesis, a brief description about radiopharmaceuticals for myocardial imaging is discussed.

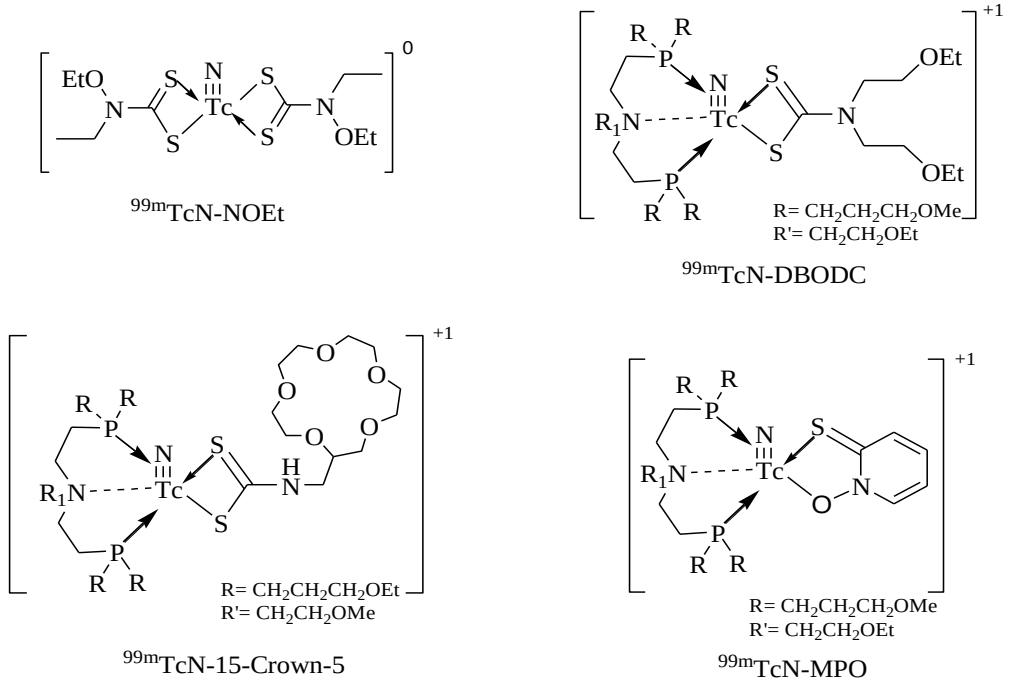

Fig. 1.5 ^{99m}TcN-based symmetric and asymmetric complexes for myocardial perfusion imaging

1.5 Myocardial Imaging

Diagnostic radiopharmaceuticals are used to obtain both static and dynamic images of a target site or organ which gives anatomical and functional information about the target. The latter information is unique for the radiopharmaceuticals as it quantitatively defines the patho-physiological condition of the target. Thus, diagnostic radiopharmaceuticals used for myocardial imaging help in detection of various cardiac abnormalities.

A radiolabeled myocardial agent injected intravenously in patient differentiates the *normal* state of the myocardium from the diseased state i.e. *ischemic* and *infarcted*.[202,203] In the *normal myocardium*, the myocardial cells have normal blood flow (perfusion). Since the cells are perfused normally, the oxygen and nutrient supply is adequate and myocardial functioning is normal. However, in diseased *ischemic state,* the arteries are partially blocked leading to the narrowing of the vessels which in turn results in reduced blood flow to some parts of the myocardium. The metabolic activity of these cells decreases due to reduced oxygen concentrations. However, under stress conditions such as in the case of a physical exercise, the increase in the whole body oxygen demands and increase in blood flow rates, lead to ischemic cells devoid of complete blood supply. But, on restoring the rest condition the reduced perfusion or blood flow in the cells is restored. However, if the ischemic state is prolonged, it may permanently damage the myocardial cells (*infarction)*. Once the cells are dead, even restoring the blood perfusion to these cells, the myocyte function is not restored.

A radiopharmaceutical, as a non-invasive tool, helps in differentiating and quantitative assessing the three different states of the myocardium and helps nuclear medicine clinicians in assessing the healthy state of the heart. There are two classes of radiopharmaceutical agents used for the detection of myocardial abnormalities *viz. perfusion and metabolic agents*.[204-207]

1.5.1 Myocardial Perfusion Imaging

Perfusion imaging is based on blood flow, where the radiopharmaceutical travels with the blood flow and the gamma rays emitted from the isotope is detected externally using a radioactive detector. Since the radiolabeled drug moves with blood, reduced or altered perfusion in the myocardium is easily detected differentiating abnormal from the normal myocardium. It plays a key role in detecting any ischemia or infarction in terms of site, severity and extent. Apart from this, certain other myocardial functional parameters such as myocardial viability and left ventricular function using wall motion, wall thickening, ejection fraction and ejection volume values can be detected using a perfusion agent.[208]

Some of the desired characteristics of myocardial perfusion imaging agent[207,209] are

- ✓ high first pass myocardial extraction
- ✓ favorable myocardial uptake and retention with minimal wash out allowing appropriate time for external detection
- ✓ fast blood clearance with high heart to background ratio for early imaging
- ✓ fast lung and liver clearance and minimal residual abdominal activity interfering with image acquisition
- ✓ myocardial uptake proportional to blood flow with linear relationship at both low and high flow
- ✓ *in-vitro* and *in-vivo* stability

A number of perfusion tracers based on PET and SPECT are available in the nuclear medicine centers for myocardial imaging.[204,205] PET tracers used worldwide for perfusion studies are ^{15}O-H_2O and ^{13}N-NH_3. However, the production logistics and short half-lives of PET based perfusion tracers makes the SPECT based agents popular for the aforementioned purpose. SPECT agents used for routine perfusion studies are either ^{99m}Tc based or non-technetium radiopharmaceuticals, which are used following a *single* or *double* injection

protocol for detecting the myocardial abnormalities.[206,207,209] Some of the SPECT agents used regularly in nuclear medicine department for myocardial perfusion imaging are discussed below.

1.5.1.1 *^{201}TlCl*

^{201}Tl-Thallous chloride is the gold standard used for carrying out the perfusion studies.[203-207] It shows a high first pass myocardial extraction ~85%, which is the standard for determining the myocardial viability. It is a cyclotron produced radionuclide, however, its half-life of 73 h allows the transportation of the radionuclide to centers which do not have inbuilt cyclotron facility. ^{201}Tl has the same hydration radius as that of K^+ and accumulates in the myocardium to an extent of approximately 60% via sodium-potassium ATP-ase pump. ^{201}TlCl exhibits redistribution phenomenon. This means that the activity which has got distributed in the myocardium at the time of stress, gets redistributed once the rest condition is restored to other low perfused viable myocardial tissues, if any observed in the stress image. This in turn means that if the first injection of the radiopharmaceutical is made under the stress condition, the activity will distribute to the healthy muscles, and not to the infarcted and ischemic tissues. But, once the patient come back to the rest stage, the activity within the myocardium will redistribute itself into the other viable muscles (namely the ischemic portions) also, which were not perfused during stress. Such a phenomenon allows imaging the heart at 2 stages, stress and then rest, with one injection of the radiopharmaceutical. Since ^{201}Tl undergoes such redistribution, single injection is adequate for carrying out both the stress and rest studies. The drawbacks of ^{201}Tl imaging relates to unfavorable radiation dosimetry (total absorbed dose 0.72 rad/ 111 kBq) and the high cost of production. Also, the physical characteristics of this isotope are suboptimal. ^{201}Tl emits predominantly mercury X-rays at 69 to 83 KeV, an energy level that is marginally suitable for imaging with

conventional gamma cameras. This relatively low energy causes some problems because of attenuation within the body.

1.5.1.2 *^{99m}Tc-labeled agents*

A number of technetium based agents have shown suitability as perfusion markers. The ^{99m}Tc-based agents provide varied advantages over the ^{201}Tl imaging.[207,209] The 140 keV photon energy of ^{99m}Tc provides improved resolution due to less scatter and less tissue attenuation. The short half-life (6 h) and better radiation dosimetry permit administration of a ten-fold higher dose of a ^{99m}Tc labeled radiopharmaceutical yielding better image quality and images in a shorter time period. The ease of availability from a ^{99}Mo-^{99m}Tc generator permits the use of ^{99m}Tc-labeled perfusion tracers in a nuclear medicine laboratory at any time whenever needed.

The ^{99m}Tc based perfusion agents commercially available and used clinically are uni-positively charged complexes *viz.* ^{99m}Tc-methoxy isobutylisonitrile (MIBI) and ^{99m}Tc-6,9-bis(2-ethoxyethyl)-3,12-dioxa-6,9 diphosphatetradecane (tetrofosmin).[203-207,209] These are lipophilic complexes that cross and enter myocardial cell membranes via passive diffusion. However, cellular retention occurs specifically within the mitochondria as a result of an electrostatic interaction of the positive charge of the compound and negative membrane potential of the mitochondria. The myocardial extraction of these agents is lower than that of ^{201}Tl, but adequate. However, these agents exhibit minimal redistribution with prolonged retention in the myocardium and hence a double injection protocol involving separate injections of the ^{99m}Tc-agents, once during stress and then at rest is followed. The imaging protocol for ^{99m}Tc-agents is a complete one-day protocol, where the stress imaging is carried out initially with the ^{99m}Tc agent followed by an image at rest with the same agent injected at higher amounts after 4-6 h. One of the undesired features of these agents is the long imaging time protocol which is inconvenient for the patients. But, the radiation dosimetry is favorable

with a total absorbed dose of 0.5 rad to the patient. In the present work, an attempt has been made to prepare neutral ^{99m}Tc complexes based on $[^{99m}TcN]^{2+}$ core for myocardial perfusion imaging and evaluated in mice.

1.5.2 Metabolic agents

Metabolic markers are used for the detection of coronary artery diseases and are much more sensitive than the perfusion agents in detecting cardiac abnormalities. These include the radiolabeled biological molecules such as fatty acid and glucose which are prime source of energy for the myocardium. Thus, radiolabeled fatty acids and glucose analogues can serve as useful candidates for the identification of myocardial disease. The metabolic markers currently used for myocardial imaging are ^{123}I labeled fatty acids and ^{18}F-fluoro deoxy glucose.[205,208,210]

1.5.2.1 *^{123}I labeled fatty acids*

The basic knowledge of fatty acid metabolism in the myocardium is necessary to understand the usefulness of radiolabeled fatty acids for myocardial imaging. In brief, fatty acids are the main source of energy for the normal myocardium.[210,211] They are taken up in the cell either by passive diffusion or via protein mediated active transport.[212] Once inside the cell, fatty acids are metabolized by β-oxidation in the myocardium producing acetyl co-enzyme A which through Kreb's cycle releases energy in the form of ATP responsible for the functioning of cardiac muscle.[210] A small portion of fatty acids is stored in the form of triglycerides and lipids. An ischemic myocardium which has low oxygen content switches from fats to glucose for its energy and the fatty acid metabolism is lower than the normal myocardium. Thus, this change in fatty acid metabolism is useful in differentiating the diseased myocardium from the normal which can help decision making for therapy. Another feature of the fatty acid metabolism in the myocardium is a phenomenon called *metabolic stunning*. This is a process observed in the myocardium after post-ischemic event. Here, the

myocardial blood flow returns to baseline after ischemic event but the ischemia induced metabolic shift from fatty acid to glucose persists for prolonged period. This reversible process of prolonged metabolic alteration is referred to as metabolic stunning. Thus, this phenomenon is of high clinical utility for identification of previous ischemic episode or early stage of myocardial damage in high risk patients.[211,213,214]

The desired characteristics of a radiolabeled fatty acid for myocardial imaging are high myocardial uptake, slow myocardial catabolism, adequately long retention for imaging, clearance from non-target organs such as lungs, liver and blood, stability of the compound and the ready availability.[214] It has been observed that fatty acids having carbon chain lengths between 15-21 show maximum extraction in the myocardium[215] and the carboxylic acid group of the radiolabeled long chain fatty acid should be free for its uptake in the heart.[216]

Uptake of the radiolabeled fatty acid in the myocardium indicates normal heart while the ischemic/ infarcted cells are seen as cold spot region in the radiolabeled fatty acid imaging. The ischemic region after revascularization and prolonged metabolic stunning returns to normal fatty acid metabolism and can be evaluated using fatty acid imaging.[210,211]

The fatty acid β-oxidation metabolism in the myocardium is rapid. To quantitate the fatty acid metabolism, PET agents ^{11}C-acetate and ^{11}C-palmitic acid are used.[204,208,210] The early clearance rate in the myocardium of ^{11}C-acetate is indicative of oxidative metabolism. In this, the activity clears off rapidly in the form of $^{11}CO_2$. However, for SPECT studies to be feasible, the radiolabeled fatty acids require extended myocardial retention so as to obtain suitable SPECT images. In this regard, several long chain fatty acids have been labeled with ^{123}I and evaluated as metabolic tracer for myocardial imaging. But, all of them suffered from *in-vivo* instability arising from de-iodination.[210] Also, they did not get retained in the heart thereby making it difficult for SPECT imaging. To circumvent these problems, a pentadecanoic acid with an aromatic phenyl ring substituted at 15 carbon was introduced and

labeled with ^{123}I. The labeled compound para-^{123}I-iodophenylpentadecanoic acid (IPPA)[210,211,217] showed prolonged retention in the myocardium with reduced *in-vivo* de-iodination. The presence of phenyl ring altered the straight chain β-oxidation metabolic activity and thereby extended the retention of the radioactivity in the myocardium long enough for SPECT imaging. Thus, it has been shown that radiolabeled fats serve as useful tool for myocardial imaging.

Although ^{123}I-IPPA exhibited myocardial retention, it was not adequately long, and hence a modified agent ^{123}I-beta-methyl-iodophenylpentadecanoic acid (BMIPP) was introduced.[210,211,218] The latter radiolabeled compound has a methyl group at the β-carbon of IPPA. The methyl group halts β-oxidation pathway in the very first step, as the oxidative process cuts off straight chain 2 carbon fractions, thereby increasing the retention of activity in the myocardium.

Both IPPA and BMIPP are metabolic substrates but ^{123}I-IPPA is rapidly metabolized resulting in rapid clearance from the heart whereas ^{123}I-BMIPP being a branched chain fatty acid does not readily undergo β-oxidation and is retained. Thus, ^{123}I-IPPA imaging involves study of washout kinetics which reflect fatty acid metabolism. The ischemic areas have low initial uptake but prolonged retention whereas ^{123}I-BMIPP does not show uptake in ischemic areas which is seen as a cold spot.

1.5.2.2 *^{18}F-Fluorodeoxyglucose (FDG)*

The viability of the myocardial cell can be determined using ^{18}F-FDG. Apart from the normal cells, a viable cell also refers to the ischemic cell which is not dead and slow blood perfusion is present. The ischemic myocardial cell depends on glucose for cell survival. Thus, ^{18}F-FDG is a useful agent for clinicians in assessing the cell viability and helping them in deciding the therapeutic treatment strategy.[204, 205,208,219,220]

^{18}F-FDG, a mimic of glucose, is transported across the lipid plasma membrane through active transport of membrane proteins. Substitution of hydroxyl group on C-2 of glucose with ^{18}F does not interfere with the ability of the molecule to be transported into tissue and to serve as substrate for the enzyme hexo-kinase to enter the glcolytic cycle.[221-222] However, absence of hydroxyl group on C-2 prevents the product 2-deoxy-2-fluoro-D-glucose-6-phosphate after enzyme action from undergoing the next step in the glycolysis pathway of isomerization into a keto form. The enzyme catalyzed phosphorylated product is predominantly in ionized form at physiological pH and is intracellularly trapped at its site of formation. This leads to retention of this ^{18}F labeled product in viable ischemic cells and is imaged externally.

From the above deliberations it can be seen that there are two different classes of metabolic markers for cardiac imaging in use, both of which are based on cyclotron produced radioisotopes ^{123}I and ^{18}F. The inherent drawbacks in the use of cyclotron produced radionuclides such as limited availability and high cost of isotope production lead to unfavorable logistics for the widescale production and use of these radiopharmaceuticals. Hence, there is a great interest in the research community for the development of ^{99m}Tc-based agents for this purpose and it continues to form a relevant field of research. Thus, in the present work an attempt has been made to prepare a series of ^{99m}Tc-fatty acid complexes employing $[^{99m}Tc{\equiv}N]^{2+}$ core which have been evaluated in mice.

1.6 Outline of the thesis work

The present thesis comprises of five chapters. Apart from *Introduction*, the subsequent three chapters give an insight to the flexibility of $[^{99m}TcN]^{2+}$ core, by radiolabeling molecules through different methods for myocardial imaging. The last chapter highlights the versatility of this core for different radiopharmaceutical applications, by picking up a relevant target of tumor hypoxia imaging.

In the chapter 2 entitled *symmetric [2+2] complexes*, $[^{99m}TcN]^{2+}$ core has been used for the preparation of three symmetric neutral complexes. All the three complexes prepared have the potential for myocardial imaging and have been bio-evaluated accordingly. The three complexes have been classified in two different parts. The first part relates to molecules suitable for perfusion imaging whereas the second part relates to molecule for metabolic imaging.

In the first part, two different bidentate dithiocarbamate derivatives, tertiary butyl dithiocarbamate and methoxy isobutyl dithiocarbamate, have been synthesized and radiolabeled with $[^{99m}TcN]^{2+}$ core to give the final complexes which have been subsequently bio-evaluated in swiss mice. In the second part, a symmetric $[^{99m}TcN]^{2+}$ xanthate complex of 15 carbon chain fatty acid has been synthesized and evaluated in swiss mice as a metabolic marker.

In the chapter 3 entitled *asymmetric [2+2] neutral complex*, the usefulness of $[^{99m}TcN]^{2+}$ core for labeling target specific biomolecules is discussed. Here, a new asymmetric fatty acid complex using $[^{99m}TcN]^{2+}$ core was synthesized and evaluated for myocardial imaging. Since two different bi-dentate ligands (π-acceptor and π-donor) are required for the formation of such complexes, the initial part of the chapter relates to the synthesis of both categories of bi-dentate ligands. In this regard, two long chain π-acceptor bis(phosphine) ligands (PNP) were synthesized and in the other π-donor category, a 16

carbon fatty acid-cysteine conjugate was prepared. The choice of fatty acid-cysteine conjugation was carried in such a way that the cysteine donors available for final complex formation finally yield neutral complex. The latter part of the chapter relates to the radiolabeling of the synthesized PNP ligands. Also, an asymmetric complex has been prepared with a PNP ligand and synthesized fatty acid derivative. The final complex was evaluated in swiss mice for metabolic cardiac imaging and the results were compared with the ^{125}I labeled standard agent IPPA.

In the chapter 4, *asymmetric [2+2] charged complex*, the versatility of $[^{99m}TcN]^{2+}$ core is explored by varying the charge and lipophilicity of the final asymmetric complex. In this regard, a series of four positively charged fatty acid complexes of varying chain lengths 11, 12, 15 and 16 carbons have been synthesized and bio-evaluated in swiss mice. The effect of charge has been evaluated by comparing a uni-positively charged 16-carbon ^{99m}Tc fatty acid complex with its neutral structural analogue reported in chapter 3.

The biological results of the four synthesized fatty acid complexes of different chain lengths were compared to evaluate the effect of lipophilicity on the target uptake and non-target clearance characteristics.

In the chapter 5, *$[^{99m}TcN]^{2+}$ core for other imaging applications*, the present core has been used for labeling a nitrotriazole derivative, sanazole, which is a known hypoxia marker. This chapter highlights the usefulness of $[^{99m}TcN]^{2+}$ core for labeling molecules with potential for different *in-vivo* diagnostic applications. The nitrotriazole was synthetically modified and labeled with $[^{99m}TcN]^{2+}$ core along with PNP ligand to give the final asymmetric neutral complex. The final complex has been evaluated in a suitable tumor model and the results discussed.

CHAPTER 2

Symmetric [2+2] Complexes

2.1 Introduction

As detailed in the previous chapter, radiopharmaceutical preparations with enhanced specific activity and stability are the key requirements when specific binding to the receptor or antigen on the targeted tissues is the mechanism of action. In the case of ^{99m}Tc based radiopharmaceuticals, this has led to the development of novel technetium cores such as $[^{99m}TcN]^{2+}$, capable of labeling various molecules and forming high specific activity complexes.[7] This core has high affinity for bi-dentate ligands having groups such as dithiocarbamates and xanthates (S donors) forming square pyramidal complexes of type $[^{99m}TcNL_2]$ [L = bi-dentate ligand] where Tc≡N occupies the apical position and the four S atoms span the basal plane. Since two molecules of the same ligand (L) are bound to the $[^{99m}TcN]^{2+}$ core and the complexes formed are symmetric along a plane passing through Tc≡N moiety, such class of complexes are termed '*symmetric [2+2] complexes'* (Fig. 2.1).

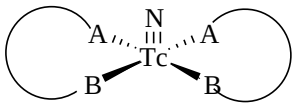

$\left[^{99m}TcNL_2\right]$

L = Bi-dentate ligand (AB donor)

Fig. 2.1 General structure of symmetric [2+2] complexes

The $[^{99m}TcN]^{2+}$ intermediate core has an overall charge of +2, which on complexation with two molecules of uni-negative anion (dithiocarbamate/ xanthate sodium salts) forms neutral symmetric [2+2] complexes. Also, the lateral alkyl groups present on

dithiocarbamates/ xanthates provide lipophilic nature to the complexes. The neutral and lipophilic properties are necessary attributes of radiopharmaceutical preparations intended for myocardial perfusion imaging.[223]

The present chapter has been divided into two parts where the first part deals with symmetric [2+2] complexes prepared using dithiocarbamate ligands and the latter with a xanthate ligand. The work involves synthesis of suitable ligands, radiolabeling with $[^{99m}TcN]^{2+}$ core and subsequent evaluation as a myocardial agent in suitable small animal.

2.2 [^{99m}TcN]-Dithiocarbamate symmetric [2+2] complexes as myocardial perfusion tracers

2.2.1 Introduction

The search for a new ^{99m}Tc based myocardial imaging agent with optimum characteristics is a continuing and relevant field of research till date. ^{201}TlCl, the currently used gold standard for myocardial perfusion imaging is produced in a cyclotron and hence less accessible. In addition, it has other limitations due to its long half-life (73 h) and large radiation dose to the patient.[224] The characteristics of ^{99m}Tc-labeled myocardial imaging agents currently available *viz.* ^{99m}Tc-methoxyisobutyl isonitrile (MIBI) and ^{99m}Tc-tetrofosmin, are also far from being ideal.[191] Unlike ^{201}TlCl, the aforementioned agents do not undergo redistribution in the myocardium[225] warranting the unavoidable double injection protocol that imposes logistic problems. Moreover, these uni-positively charged complexes are taken up and retained in the heart for a longer time due to the negative membrane potential of the myocytes.[226] This hinders the possibility of rest and stress studies, needed to distinguish between ischemic and infarcted regions of the myocardium, to be performed on the same day. Hence, currently these agents are injected at a small dose (typically 185 MBq or 5 mCi) initially for stress studies followed by a large dose (typically 740 MBq or 20 mCi) after a gap of 4-6 h. A logical approach therefore, constitutes the search for an agent that is neutral and sufficiently lipophilic to be taken up and retained in the heart for sufficient time, but not too long. In this direction, ^{99m}Tc-teboroxime was the first of a class of neutral complexes that showed myocardial extraction, but had the serious limitation of being rapidly washed out from the target tissue.[227] ^{99m}TcN(NOEt)$_2$ complex, which makes use of the [^{99m}Tc≡N]$^{+2}$ core is one of the latest in this category, showing considerable promise as a myocardial perfusion imaging agent, and is currently in phase III clinical trials.[182] This agent

shows good redistribution in heart like ^{201}Tl, and can be administered at a higher activity in a single injection, leading to better image quality at a lower radiation dose to the patient, compared to that with ^{201}TlCl. However, its use is limited owing to high lung and liver uptake, warranting a better formulation.

1-isocyano-2-methoxy-2-methylpropane (MIBI) labeled with ^{99m}Tc is one of the predominant ^{99m}Tc-labeled myocardial imaging agents in clinical use today. ^{99m}Tc labeled 2-isocyano-2-methylpropane (TBI) has also shown good myocardial uptake, although high accumulation of activity in the liver and lung make it unattractive for regular clinical use.[7] In an effort to develop a ^{99m}Tc-based neutral agent that could strike a perfect balance between redistribution and hence optimum residence time to enable rest-stress study on the same day as well as achieving good target to non-target ratio, two dithiocarbamate ligands were synthesized in the present study, using t-butylamine and methoxyisobutyl amine as the respective precursors. These compounds structurally resemble TBI and MIBI ligands except for the co-ordinating group (Fig. 2.2), where a dithiocarbamate group has replaced the isonitrile group. Labeling was carried out using a $[^{99m}TcN]^{2+}$ core and the complexes prepared were studied with respect to

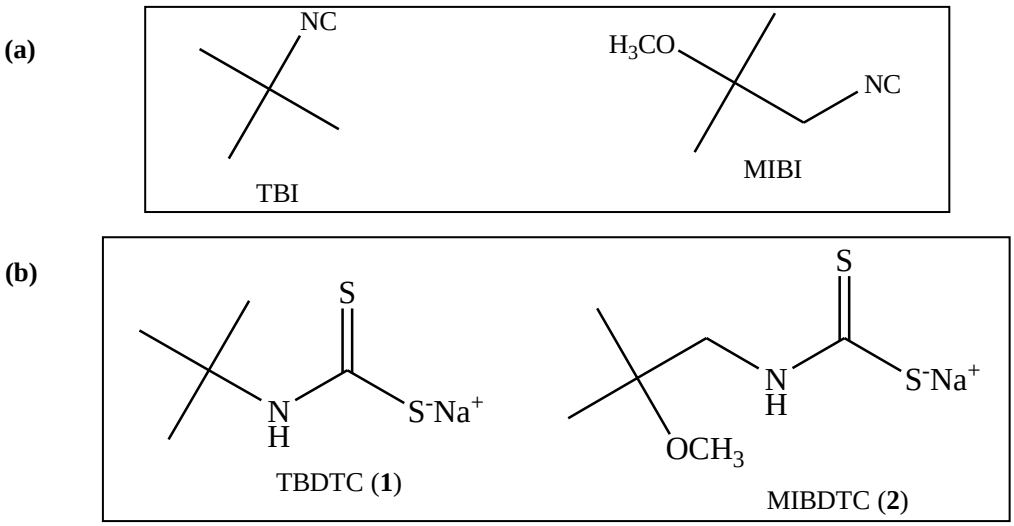

Fig. 2.2 Structural similarity between (a) clinically used ligands and (b) synthesized ligands

their myocardial uptake. The results obtained were compared with that of [^{99m}TcN(NOEt)$_2$] which is now undergoing phase III clinical trials.

2.2.2 Experimental

2.2.2.1 *Materials and methods*

2-methylpropan-2-amine and 2-hydroxy-2-methylpropanenitrile were purchased from M/s Lancaster, England. Sodium N-ethoxy, N-ethyl dithiocarbamate (NOEt), dimethyl cyclodextrin (DMC) and [^{99m}TcN]$^{2+}$ intermediate kit vial were obtained as a gift from Schering Cis Bio International, France through an IAEA coordinated research project. Lithium aluminium hydride (LAH), 15-hydroxypentadecanoic acid, methyl chloroethanamine hydrochloride, 2-bromoethyl methyl ether, ethyl p-toluene sulphonate, n-butyl lithium (2.5 M in hexane), *S*-trityl cysteine, hexadecanedioic acid, 11-amino undecanoic acid, 16-bromo hexadecanoic acid, triethyl silane, succinic dihyhdrazide, stannous chloride and cannula (two tips flexible steel needle) were obtained from M/s Aldrich, USA. Potassium diphenyl phosphide solution in THF (0.5 M), 12-amino dodecanoic acid, 15-bromo pentadecanoic acid, *N*-Boc, *S*-trityl cysteine, anhydrous K_2CO_3 and 1-(3-dimethylaminopropyl)-3-carbodiimide (EDCI) were purchased from M/s Fluka, Germany. Hydrazine hydrate (80%) was purchased from M/s Riedel-de-Haën, Germany. Phthalimide was obtained from M/s Loba Chemicals, India. Sodium hydroxide, anhydrous zinc chloride, carbon disulphide, diethanolamine and thionyl chloride were purchased from M/s S.D. Fine chemicals, Mumbai, India. Iodophenyl pentadecanoic acid (IPPA) was purchased from Emka Chemicals, Germany. All other reagents used were of analytical or HPLC grade. All the organic extracts were dried over anhydrous Na_2SO_4. The solvents were dried following standard protocols. The solvents used for HPLC were filtered through 0.22 μm Millipore filter paper. Bis[(diethoxypropylphosphanyl)ethyl]ethoxyethylamine was obtained as a gift from Prof.

Adriano Duatti, Italy. $Na^{125}I$ was obtained from Radiochemicals section, Radiopharmaceuticals Division, BARC, India. Sodium pertechnetate ($Na^{99m}TcO_4$) was eluted with saline just before use from a ^{99}Mo-^{99m}Tc gel generator supplied by Board of Radiation and Isotope Technology, India. Silica gel plates (Silica Gel 60 F_{254}) were obtained from M/s Merck, India. Whatman chromatography paper (Whatman 3 mm Chr, 20 mm width, Maidstone, England) was used for paper electrophoresis.

Instrumentation methods

The radioactivity profile of TLC and Paper electrophoresis strips were determined using GINA-Star TLC chromatography evaluation system, Germany. Chromatograms of the prepared complexes were obtained with either a JASCO PU 1580 or JASCO PU 2080 Plus dual pump HPLC system, with a JASCO 1575 or JASCO 2075 Plus tunable absorption detector and a radiometric detector system, using a C18 reversed phase HiQ Sil (5 µm, 4 × 250 mm) column. Elemental analyses were performed with a C, H, N, S elemental analyzer, Thermofinnigan, Flash EA 1112 series, Italy. The IR spectra of the compounds were recorded with a JASCO FT-IT/420 spectrophotometer, Japan. The ^1H NMR spectra were recorded with either 200 or 300 MHz Bruker spectrophotometer or 300 MHz Varian spectrophotometer, USA. ^{31}P NMR spectra were recorded with a 300 MHz Bruker spectrophotometer. Mass spectra were recorded with either QTOF micromass instrument using electron spray ionization (ESI) in positive mode or Varian Prostar mass spectrometer using ESI in negative mode.

2.2.2.2 *Synthesis*

2.2.2.2.1 *Synthesis of sodium tert-butylcarbamodithioate (TBDTC)* (**1**)

In a typical procedure, 2-methylpropan-2-amine (0.5 mL, 4.73 mmol) and crushed sodium hydroxide (385 mg, 9.6 mmol) were stirred vigorously in diethyl ether (15 mL) cooled in an ice bath. To the stirred solution, carbon disulphide (0.3 mL, 4.73 mmol) was

added dropwise and stirring continued for 30 min. The reaction mixture was brought to room temperature, stirring continued for another 2 h, the white precipitate was collected by filtration, washed with dry ether and dried under vacuum.

Yield: quantitative (808 mg).

Elemental analysis (C,H,N,S): Observed (Calculated) 35.10 (35.07), 6.23 (5.89), 8.05 (8.18), 37.33 (37.45).

2.2.2.2.2 *Synthesis of sodium 2-methoxy-2-methylpropylcarbamodithioate (MIBDTC)* (**2**)

2-methoxy-2-methylpropanenitrile (**2a**)

2-hydroxy-2-methylpropanenitrile (1 mL, 11 mmol) was added to a solution of freshly fused zinc chloride (1.47 g, 11 mmol) in excess of anhydrous methanol.[228] The reaction mixture was refluxed overnight in an oil bath. After cooling to room temperature, the reaction mixture was poured into ice water and extracted with ether. The ether layer was washed with brine (saturated NaCl solution) and dried. Ether was removed by simple distillation and the pure product was collected by distilling at 120 °C.

Yield: 96% (1.04 g).

^{1}H NMR ($CDCl_3$, δ ppm): 3.25 (s, 3H, -OC$\underline{H}_3$); 1.31 (s, 6H, (C$\underline{H}_3$)$_2$C-) [Fig. 2.3].

2-methoxy-2-methylpropan-1-amine (**2b**)

In a three-necked flask, fitted with a nitrogen inlet, dropping funnel and reflux condenser, LAH (0.8 g, 20 mmols) was taken and suspended in dry diethyl ether (25 mL). The mixture was kept under nitrogen and cooled in an ice bath. Compound **2a** (1 g, 10 mmol) dissolved in dry ether (2 mL), was added dropwise to the well stirred reaction mixture. After 30 min, the reaction mixture was brought to room temperature and stirred overnight. The unreacted LAH was quenched by dropwise addition of aqueous saturated Na_2SO_4 solution. The precipitate formed was filtered through a sintered funnel and washed with ether (2 × 15

mL). The ether layer was washed with brine and dried. The ether was removed by distillation and the pure compound **2b** isolated by distillation at 110 °C.

Yield: 80% (824 mg).

^{1}H NMR ($CDCl_3$, δ ppm): 3.26 (s, 3H, -OC$\underline{H}_3$); 2.65 (s, 2H, -C$\underline{H}_2$); 1.6 (s, 2H, -N$\underline{H}_2$); 1.16 (s, 6H, (C$\underline{H}_3$)$_2$C-) [Fig. 2.4].

Sodium 2-methoxy-2-methylpropylcarbamodithioate (MIBDTC) (**2**)

The procedure followed for the synthesis of **2** was similar to that followed for the synthesis of **1** using **2b** as the starting material.

Yield: 95% (800 mg).

Elemental analysis (C,H,N,S): Observed (Calculated) 34.90 (35.80), 6.50 (6.01), 6.80 (6.96), 31.50 (31.86).

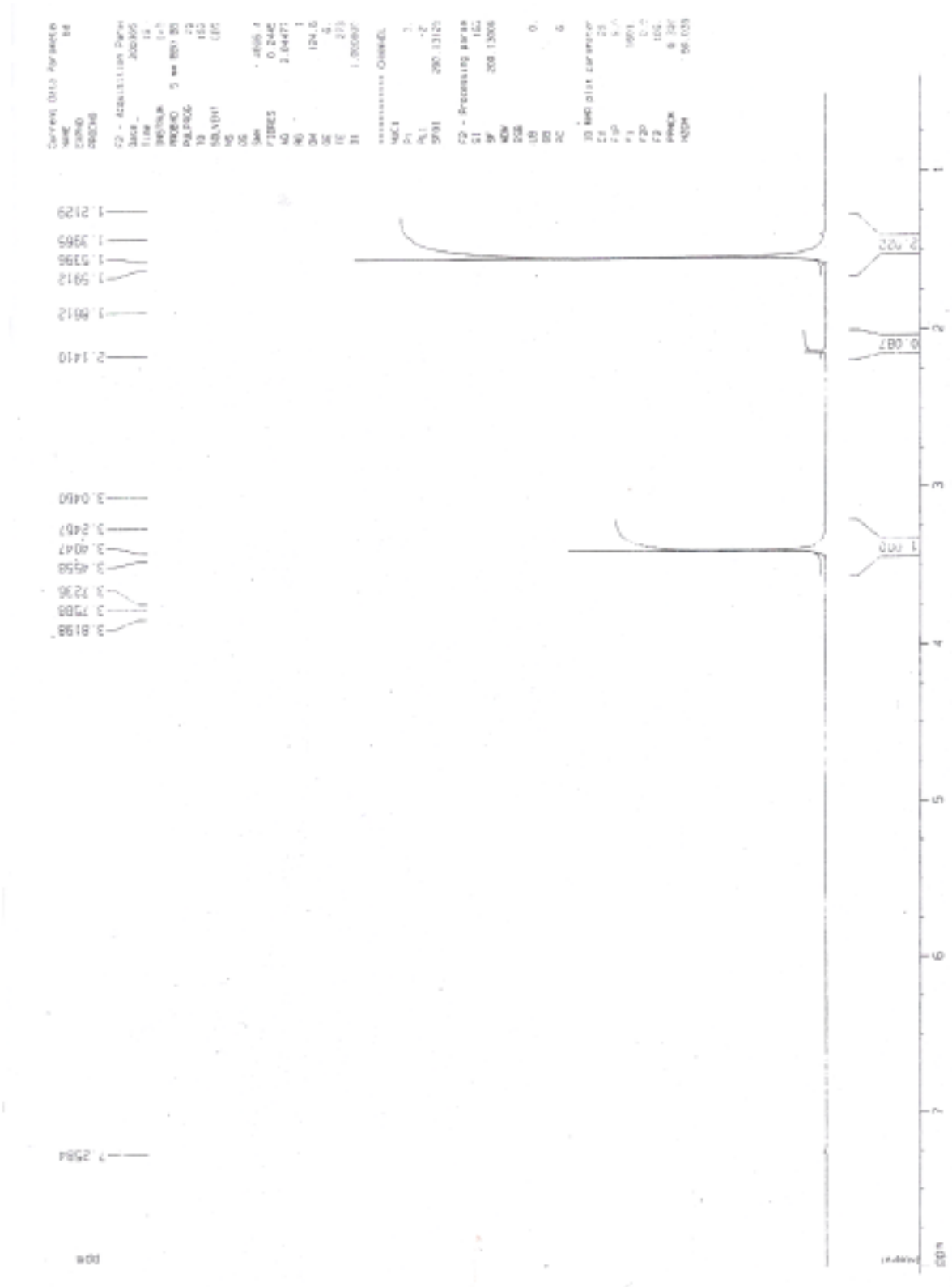

Fig. 2.3 ^{1}H NMR spectrum of compound **2a**

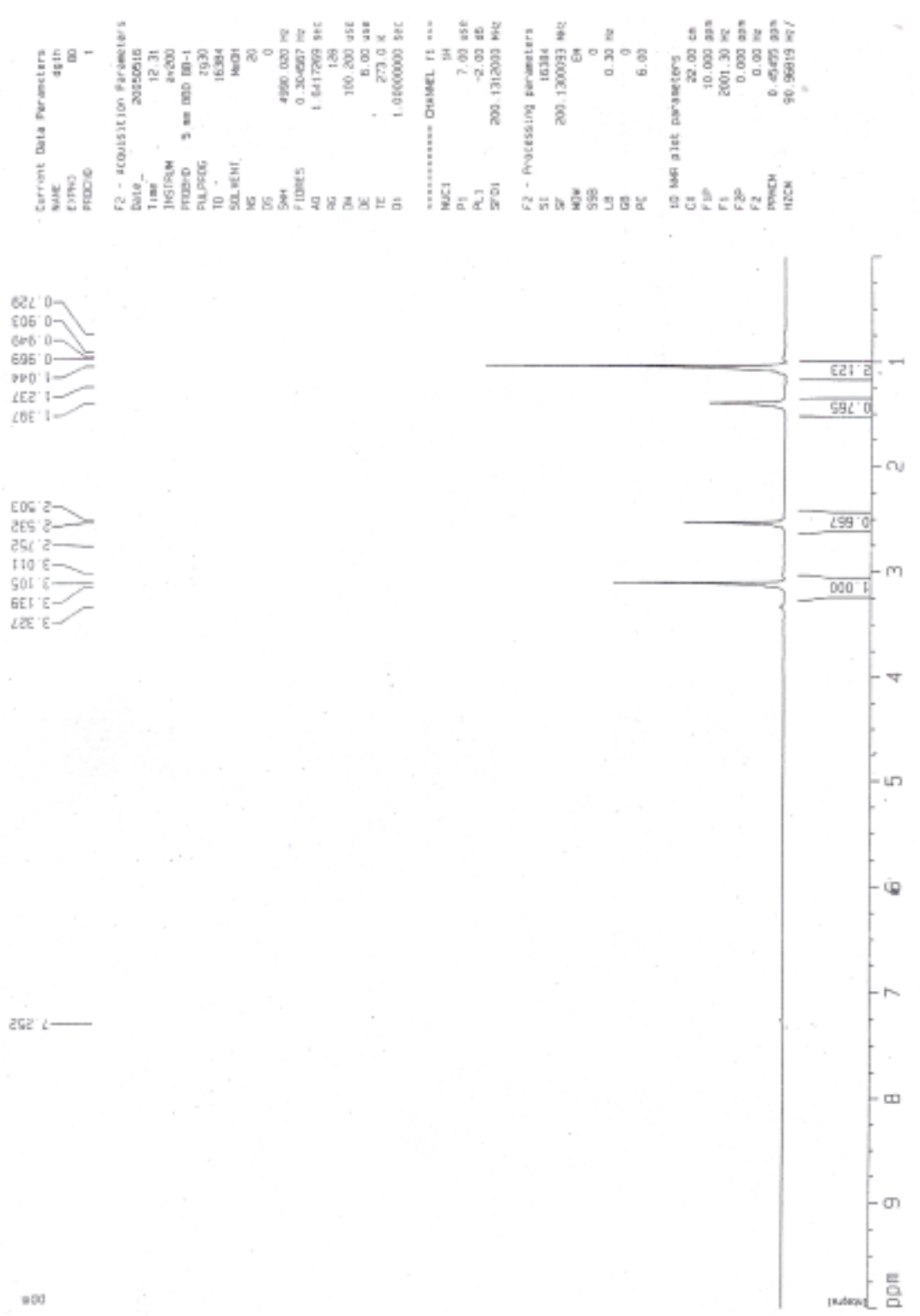

Fig. 2.4 ^{1}H NMR spectrum of compound **2b**

2.2.2.3 *Radiolabeling*

2.2.2.3.1 *Preparation of $[^{99m}TcN]^{+2}$core*

The kit vial for the preparation of $[^{99m}TcN]^{+2}$ core stored at 4 °C was allowed to attain ambient temperature. To this kit vial containing succinic dihydrazide (5 mg) and stannous chloride (0.1 mg), freshly eluted $^{99m}TcO_4^-$ (1 mL, 37 MBq or 1 mCi) was added, vortexed for 1 min and allowed to stand at room temperature for 20 min. The ^{99m}Tc-nitrido core, thus prepared was characterized by TLC, paper electrophoresis and HPLC.

2.2.2.3.2 *Preparation of ^{99m}TcN-Dithiocarbamate complexes*

The synthesized dithiocarbamate ligand (**1** or **2**, 0.1-1 mg) was dissolved in saline (0.5 mL). To this, freshly prepared $[^{99m}TcN]^{+2}$ core (0.5 mL) was added, vortexed for 1 min and the reaction vial incubated for 10 min at room temperature to give desired complexes **1C** and **2C** respectively. The complexes formed were characterized by paper electrophoresis and HPLC.

2.2.2.3.3 *Preparation of $^{99m}TcN(NOEt)_2$*

The $[^{99m}TcN]^{+2}$ core (0.5 mL) was added to a vial, containing NOEt (10 mg) and DMC (10 mg) ligands dissolved in saline (0.5 mL), and vortexed for 1 min and incubated at room temperature (~25 °C) for 10 min. The complex formed was characterized by TLC.

2.2.2.4.4 *Optimization studies*

Parameters such as ligand concentration and reaction time were optimized to obtain maximum complexation yield. Variation in complexation yield was studied by changing the ligand concentration from 0.001 mg/mL to 1 mg/mL.

2.2.2.4 *Quality control techniques*

2.2.2.4.1 *Thin layer chromatography (TLC)*

TLC was carried out using 11 cm long flexible silica gel plates. About, 1-2 µL of the test solution was spotted at 1.5 cm from the bottom of the TLC strip. The TLC strip was

developed in a suitable solvent, dried, cut into 1 cm segments and the radioactivity associated with each segment was measured using a well-type NaI(Tl) detector. For the characterization of ^{99m}Tc-nitrido intermediate species, the plates were developed in ethanol: chloroform: toluene: 0.5M ammonium acetate (6:3:3:0.5 v/v) as well as in saline. The analysis of $^{99m}TcN(NOEt)_2$ complex was carried out using ethyl acetate as the developing solvent.

2.2.2.4.2 *Paper electrophoresis*

Paper electrophoresis was done using a Whatman No.3 chromatography paper and 0.05 M phosphate buffer (pH 7.4). About 2 µL of the test solution was applied at the middle of the strip and the strip was developed under a potential gradient of 10 V/cm for 1 h. The strip was dried, cut into 1 cm segments and the radioactivity associated with these was determined using a well-type NaI(Tl) detector.

2.2.2.4.3 *High performance liquid chromatography (HPLC)*

The $[^{99m}TcN]^{+2}$ core and the labeled complexes were analyzed by HPLC using about 25 µL (925 KBq or 25 µCi) of the test solution. Acetonitrile: water (80:20 v/v) mixture was used as the mobile phase, under isocratic condition, at a flow rate of 1 mL/ min.

2.2.2.4.4 *Partition coefficient*

Lipophilicity (LogP) of the complexes was determined from octanol/ saline partition coefficient (P) following a reported procedure.[229] For the assay, solvent extraction was performed by mixing 1 mL of the reaction mixture with 1 mL of octanol on a vortex mixer for about a minute. The two phases were allowed to separate. Equal aliquots of the organic and aqueous layers were withdrawn and measured for the radioactivity. The organic extract was back-extracted repeatedly with saline to estimate the distribution ratio.

2.2.2.4.5 *Bio-distribution studies*

Normal adult Swiss mice (20-25g body weight) were used for the bio-distribution studies. The radiolabeled preparation (3.7 MBq or 0.1 mCi in 100µL) was injected

intravenously via the tail vein. Individual sets of animals (n = 3) were utilized for studying the bio-distribution at different time points (5 min, 10 min, 30 min and 60 min). The animals were sacrificed immediately at the end of the respective time point and the relevant organs and tissue were excised. The organs were weighed and the radioactivity associated with each was measured with a flat-bed type NaI (Tl) counter using a suitable energy window for ^{99m}Tc (140 keV ± 10%). For the sake of comparison, the activity retained in each organ/ tissue was expressed as percent value of the injected dose per gram (% ID/ g). All procedures performed herein were in strict compliance with the national laws governing conduct of animal experiments.

2.2.3 Results and Discussion

2.2.3.1 *Synthesis of the ligands*

The literature procedure was followed for the preparation of **1** and **2**.[181] The general scheme for the synthesis of dithiocarbamate ligand is shown in Fig. 2.5. The sodium salt of dithiocabamate was precipitated on reaction of CS_2 with respective amines in presence of sodium hydroxide base. The amine precursor **2b** used for the synthesis of **2** was synthesized following the reaction scheme shown in Fig. 2.6. The intermediate **2b** was obtained on *O*-methylation of acetone cyanohydrin using anhydrous zinc chloride and MeOH followed by reduction of the intermediate **2a** using LAH. Both the intermediates, compound **2a** and **2b**, were characterized by ^{1}H NMR spectroscopy. The final dithiocarbamate ligands (**1** and **2**) were characterized by elemental analyses.

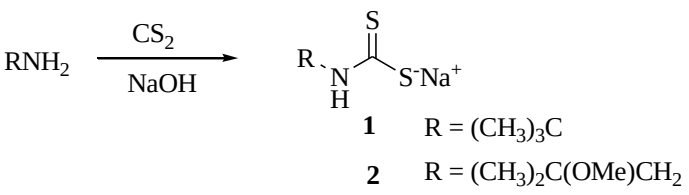

Fig. 2.5 General scheme for the synthesis of dithiocarbamate ligands

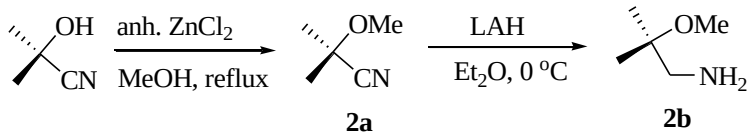

Fig. 2.6 Scheme for the synthesis of methoxyisobutyl amine

2.2.3.2 *Radiolabeling*

The two synthesized dithiocarbamate derivatives act as bi-dentate ligands to co-ordinate with ^{99m}Tc via the $[^{99m}TcN]^{2+}$ intermediate core. The scheme for the formation of $[^{99m}TcN]^{2+}$ intermediate core is shown in Fig. 2.7(a). The radiolabeling strategy involved prior preparation of $[^{99m}TcN]^{2+}$ intermediate using a kit vial containing succinic dihydrazide (SDH) which acts as a nitride donor (N^{3-}) and stannous chloride as reducing agent. To the freshly prepared $[^{99m}TcN]^{2+}$ intermediate, the respective dithiocarbamate ligand (**1** or **2**) was added to obtain the desired complexes [**1C** or **2C,** Fig. 2.7(b)].

The ^{99m}Tc-nitrido intermediate was characterized by TLC and paper electrophoresis. The TLC was carried out using ethanol: chloroform: toluene: 0.5M ammonium acetate mixture (6:3:3:0.5 v/v) as well as saline as developing solvents. In the former solvent system, ^{99m}Tc-nitrido intermediate species remained at the point of application (R_f = 0–0.1) with

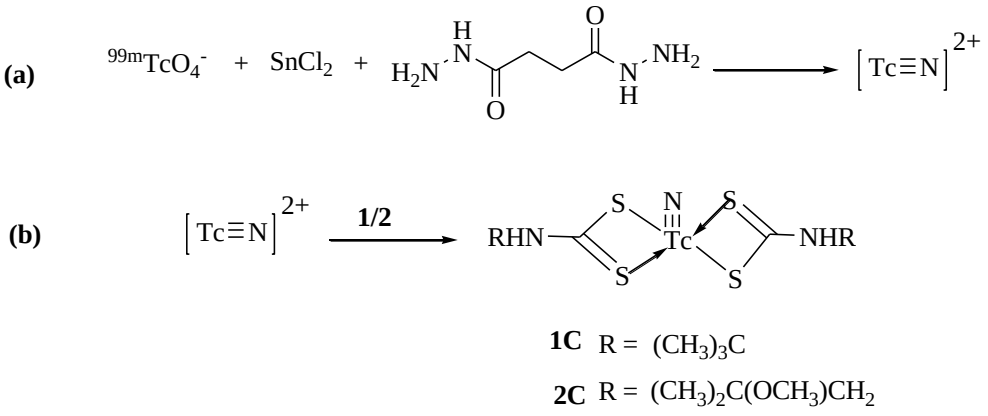

Fig. 2.7 Syntheses of (a) $[^{99m}TcN]^{2+}$ intermediate and (b) $[^{99m}TcN]$-dithiocarbamate complexes

insignificant activity corresponding to $^{99m}TcO_4^-$ (R_f = 0.4-0.6). In the latter solvent system, most of the activity moved with the solvent front (R_f = 0.8-1). The small amount of activity, observed at the point of sample application was attributable to the possible presence of reduced technetium, which does not move in any solvent. Thus, knowing the percentage of unreacted pertechnetate remaining in the reaction mixture from the former solvent system and percentage of reduced technetium in the reaction mixture from the latter solvent system, the extent of formation of ^{99m}Tc-nitrido intermediate was determined and found to be >98%. In paper electrophoresis, the ^{99m}Tc-nitrido intermediate showed a movement of 5 cm/ h towards the anode, thus, confirming the negative charge on the technetium nitrido intermediate [Fig. 2.8(a)].

Both the ^{99m}TcN-dithiocarbamate complexes **1C** and **2C** were prepared in >95% yield at a low ligand concentration of 0.01 mg/mL [$5.8x10^{-5}$ M] for **1** and 1 mg/mL [$4.8x10^{-3}$ M] for **2**. The complexes **1C** and **2C** were characterized by paper electrophoresis and HPLC. In paper electrophoresis almost all the activity was found at the point of application indicating the formation of neutral complexes [Fig. 2.8(b) & 2.8(c)]. The HPLC chromatograms of the ^{99m}TcN-intermediate species, **1C** and **2C** are shown in Fig. 2.9. It was observed that the retention time of ^{99m}TcN-intermediate species was 2.9 ± 0.2 min, while that of radiolabeled complexes **1C** and **2C** were 4.5 ± 0.2 min and 4.1 ± 0.1 min respectively.

The procedure followed for the synthesis of ^{99m}TcN-(NOEt) complex was similar to that of the other two dithiocarbamate complexes. The formation of the complex was confirmed by TLC analysis using EtOAc as the mobile phase. The complex was formed in >98% yield and showed a movement of R_f = 0.7-0.8, whereas the nitrido intermediate remained at the point of spotting (R_f = 0-0.1).

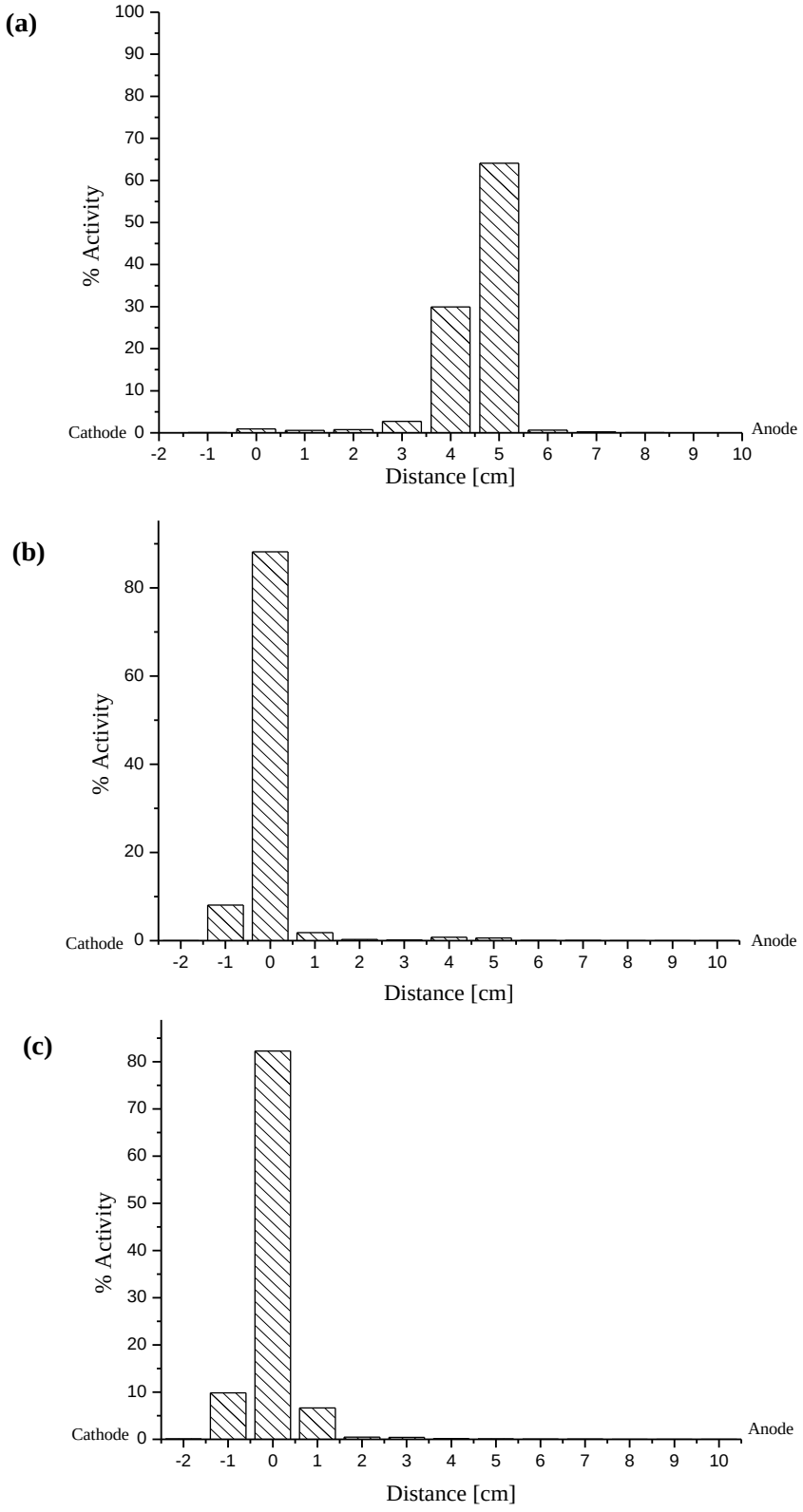

Fig. 2.8 Electrophoresis patterns of (a) ^{99m}TcN intermediate, (b) complex **1C** and (c) complex **2C**

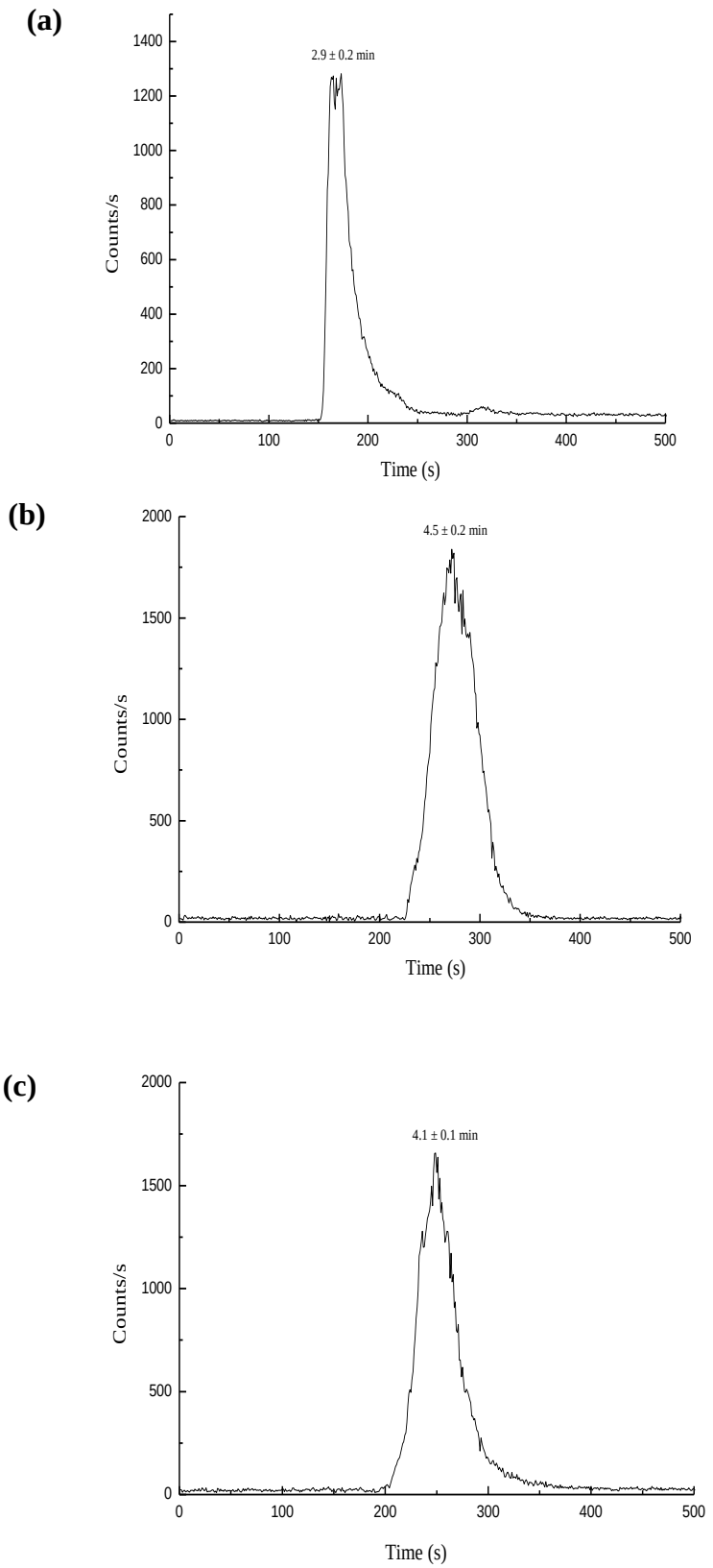

Fig. 2.9 HPLC profiles of (a) ^{99m}TcN intermediate, (b) complex **1C** and (c) complex **2C**

Dithiocarbamates are known to complex with $[^{99m}TcN]^{2+}$core leading to neutral complexes of $^{99m}TcNL_2$ type[171] having square pyramidal geometry with an apical $^{99m}Tc{\equiv}N$ bond and four sulphur atoms spanning the basal plane. Since the two ligands (**1** and **2**) used for complexation via $[^{99m}TcN]^{2+}$core belongs to the same class of dithiocarbamates, the two neutral complexes formed could be envisaged to possess the formula $^{99m}TcN(TBDTC)_2$ and $^{99m}TcN(MIBDTC)_2$ respectively and form square pyramidal complexes.

In the case of complex **1C**, more than 95% complexation yield was observed at a concentration as low as 0.01 mg/mL, whereas in the case of complex **2C**, the yield was more than 90% at 0.1 mg/mL concentration. The formations of the two ^{99m}TcN-complexes **1C** and **2C** were instantaneous at room temperature and the preparations were stable for over a period of 20 h at room temperature with ~90% retention of radiochemical purity.

2.2.3.3 ***Biological studies***

The prepared complexes **1C** and **2C** were bio-evaluated, to evaluate their potential as myocardial agent. Some of the essential characteristics of a ^{99m}Tc formulation as myocardial agent are

(i) *in-vivo* kinetic inertness, so that it does not get degraded inside the body by potential chelates present, such as cysteine, glutathione, serum proteins, etc.

(ii) lipohpilic nature, so as to cross the lipid bi-layer membrane of the cell

(iii) high uptake in the normal myocardium with a long enough retention to carry out SPECT imaging

(iv) rapid clearance from background tissue/ organs such as blood, liver and lungs so as to get a clear image of the target organ. Hence, target/ non-target ratios such as heart/ blood, heart/ liver and heart/ lungs are critical in evaluating the final quality of the image obtained by a myocardial agent.

For the complexes **1C** and **2C,** *in-vitro* challenge experiments, to determine the kinetic stability were not carried out due to the known stability of such category of complexes from the literature.[181] In view of the other parameters, the lipophilicity of the prepared complexes was determined. The Log P values of **1C**, **2C** and $^{99m}TcN(NOEt)_2$ complexes in octanol/ saline partition system were found to be 1.7, 1.9 and 1.98 respectively indicating their high lipophilicity.

To evaluate the other characteristics, *in-vivo* bio-distribution of **1C** and **2C** were carried out with normal Swiss mice and the results are shown in Tables 2.1 and 2.2 respectively. The bio-evaluation of the complex **1C** and **2C** warranted comparison with a known standard agent, hence, $^{99m}TcN(NOEt)_2$ which belongs to similar category of complexes and is currently in phase III clinical trials was taken as a standard. Table 2.3 shows the bio-distribution results of the standard agent $^{99m}TcN(NOEt)_2$ in Swiss mice. Fig. 2.10 shows the myocardial uptake and clearance pattern of **1C**, **2C** and the standard agent. The two complexes showed significant uptake in the myocardium. Among the two, **1C** showed high initial myocardial uptake [8.97 ± 0.51% ID/g at 5 min post injection (p.i.)],

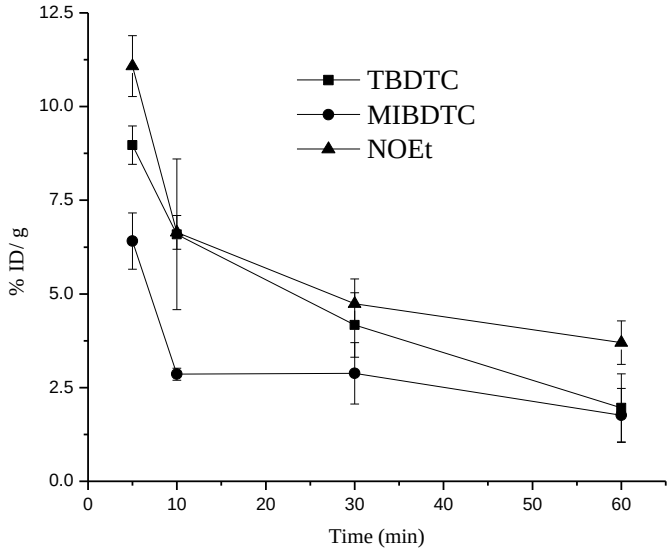

Fig. 2.10 Myocardial uptake pattern of complexes **1C** and **2C** in comparison with $^{99m}TcN(NOEt)_2$

Table 2.1 Bio-distribution pattern of $^{99m}TcN(TBDTC)_2$ in Swiss mice [% ID/g (1SD), n=3]

Organ	*5 min*	*10 min*	*30 min*	*60 min*
Liver	14.43 (1.97)	13.86 (1.00)	16.52 (0.95)	18.91 (4.71)
Heart	8.97 (0.51)	6.59 (2.01)	4.17 (0.86)	1.96 (0.91)
Lungs	9.87 (1.75)	6.5 (0.86)	5.5 (0.9)	5.68 (1.85)
Kidney	8.33 (2.57)	7.7 (3.51)	5.56 (0.68)	4.64 (1.12)
Blood	1.51 (0.09)	1.36 (0.11)	0.82 (0.09)	0.94 (0.32)
Heart/ blood	5.92	5.35	5.11	2.01
Heart/ liver	0.63	0.47	0.25	0.1
Heart/ lung	0.92	1.0	0.75	0.34

Table 2.2 Bio-distribution pattern of $^{99m}TcN(MIBDTC)_2$ in Swiss mice [% ID/g (1SD), n=3]

Organ	*5 min*	*10 min*	*30 min*	*60 min*
Liver	11.41 (2.24)	25.13 (1.65)	33.86 (6.14)	25.15 (1.73)
Heart	6.41 (0.75)	2.86 (0.16)	2.88 (0.82)	1.76 (0.72)
Lungs	7.69 (2.56)	4.24 (0.37)	3.97 (0.36)	3.25 (0.17)
Kidney	9.49 (0.23)	4.75 (0.22)	4.94 (0.68)	3.83 (0.21)
Blood	2.67 (0.46)	1.73 (0.03)	2.13 (0.23)	2.07 (0.77)
Heart/ blood	2.4	1.63	1.35	0.85
Heart/ liver	0.56	0.11	0.09	0.07
Heart/ lung	0.83	0.67	0.73	0.54

Table 2.3 Bio-distribution pattern of $^{99m}TcN(NOEt)_2$ in Swiss mice [% ID/g (1SD), n=3]

Organ	*5 min*	*10 min*	*30 min*	*60 min*
Liver	11.30 (1.96)	9.52 (0.89)	10.22 (0.62)	12.63 (1.86)
Heart	11.08 (0.81)	6.64 (0.45)	4.74 (0.66)	3.7 (0.58)
Lungs	21.48 (3.08)	14.87 (0.89)	14.21 (1.99)	14.18 (0.35)
Kidney	25.97 (2.21)	22.36 (0.35)	18.23 (2.11)	17.08 (1.19)
Blood	2.05 (0.34)	1.25 (0.12)	1.05 (0.13)	0.83 (0.1)
Heart/ blood	5.56	5.36	4.52	4.51
Heart/ liver	1.03	0.71	0.46	0.3
Heart/ lung	0.52	0.45	0.34	0.26

which was slightly lower than that of $^{99m}TcN(NOEt)_2$ (11.41 ± 2.24% ID/g) at the same time point. Similar to the standard agent, the initial accumulated activity for the two complexes in the myocardium was not retained and cleared off with time. The washout kinetics of **1C** was observed to be similar to that $^{99m}TcN(NOEt)_2$, but was significantly different when compared to **2C** complex. The latter complex showed a delayed clearance from the myocardium between 10 and 30 min which may be due to slow washout of the radioactivity from the blood pool (Fig. 2.11).

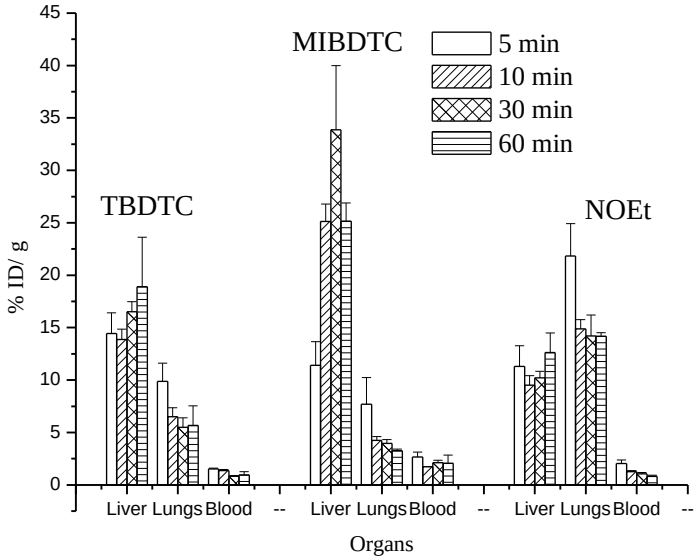

Fig. 2.11 Clearance pattern of complexes **1C**, **2C** and $^{99m}TcN(NOEt)_2$ from the non-target organs

The heart/ blood, heart/ lung and heart/ liver ratios of the two complexes **1C**, **2C** and the standard agent $^{99m}TcN(NOEt)_2$ are shown in Tables 2.1-2.3. The heart/ lung ratios of the two complexes were better than that of the standard agent at all the time points of the study. Similarly, heart/ blood ratio of **1C** was found to be better than that of $^{99m}TcN(NOEt)_2$ up to 30 min p.i. thereafter there was a sharp decline, leading to a lower value at 60 min p.i. The heart/ liver ratios of the two complexes remained below 1 throughout the period of study, and were lower than that of $^{99m}TcN(NOEt)_2$.

The clearance of activity from different organs exhibited by the two radiolabeled compounds **1C**, **2C** and the standard agent $^{99m}TcN(NOEt)_2$ is shown in Fig. 2.11. The two ^{99m}Tc-complexes showed significant liver accumulation with increase in liver activity up to 30 min, after which a definite decline was observed. This may be due to the lipophilic nature of the two complexes which showed clearance via the hepatobiliary system. The clearance of activity from the liver was faster with **2C**, possibly due to the presence of metabolizable ether linkage. The lung uptake observed with both the synthesized ^{99m}TcN-complexes was lower than that of $^{99m}TcN(NOEt)_2$ throughout the period of study, with faster clearance in the case of **2C**. The latter complex however showed significant blood pool activity, which may be due to association of the complex with the serum proteins.

Although the *in-vivo* behavior of the currently studied ^{99m}Tc complexes showed promising myocardial uptake, their rapid myocardial washout and high liver activity, in comparison to the standard agent $^{99m}TcN(NOEt)_2$, limited their potential for the aforementioned application.

2.2.4 Conclusion

The dithiocarbamate ligand analogues of 2-methylpropan-2-amine (TBI) and 2-hydroxy-2-methylpropanenitrile (MIBI) were synthesized and labeled with $[^{99m}TcN]^{2+}$ core to give high specific activity complexes. The bio-distribution studies, carried out in Swiss mice, showed reasonable myocardial uptake and better heart/ lung ratios compared to $^{99m}TcN(NOEt)_2$. Also, the heart/ blood ratio of $^{99m}TcN(TBDTC)_2$ was better than the standard agent. But poor myocardial retention of the complexes and slow liver clearance limited their potential for myocardial perfusion imaging. Nevertheless, this study has given an insight into the easy derivatization of carrier molecules in the form of dithiocarbamate desired for the incorporation of ^{99m}Tc activity via $[^{99m}TcN]^{2+}$ core and their general *in-vivo* behavior.

2.3 A ^{99m}TcN-fatty acid xanthate symmetric [2+2] complex as a myocardial metabolic tracer

2.3.1 Introduction

Fatty acids are taken up in the myocardium and form the source of energy for normoxic cells. With the carboxylic acid termini free to retain the biochemical properties of the molecule, the fatty acid chain length is the major governing determinant for its uptake in the myocardium.[216] Once inside the normoxic cells, fatty acids are rapidly metabolized by β-oxidation. The differential fatty acid metabolism in normal and ischemic cells becomes a tool for detection of cardiovascular diseases using Single Photon Emission Computed Tomography (SPECT) imaging. Several ^{123}I-labeled straight chain fatty acid derivatives have been prepared earlier, and tested *in-vivo*.[230,231] However, *in-vivo* instability and rapid metabolic washout were the limiting factors rendering it unsuitable for SPECT imaging, which is the preferred modality for clear delineation of the myocardium. To overcome the above shortcomings, ^{123}I labeled iodophenylpentadecanoic acid (IPPA) and beta-methyl iodo phenyl pentadecanoic acid (BMIPP)[210,217-218,232-233] were introduced. These agents showed good myocardial uptake with slow clearance making them suitable for SPECT imaging and convenient for use in patients who cannot undergo stress studies using ^{201}TlCl and ^{99m}Tc-MIBI.[234] These two ^{123}I radiolabeled fatty acids have therefore served as gold standards in myocardial functional imaging. However, the inherent drawbacks in the use of cyclotron-produced ^{123}I (limited availability and short half-life) restrict their clinical use. Hence, intense efforts are on to develop suitable ^{99m}Tc-based agents for SPECT imaging. In this regard, a number of ^{99m}Tc-labeled fatty acid derivatives have been prepared, but all of these exhibited poor myocardial extraction. This could be attributed to improper chemical modification in the parent molecule leading to altered biological behavior. The earlier reported ^{99m}Tc-fatty acid

derivatives used the common $[^{99m}Tc=O]^{3+}$ core with N_2S_2 as the chelating atoms that were incorporated into the fatty acid chain. But these complexes showed poor myocardial extraction.[235-237] A modified "3+1" approach[216] using the same core was followed but the product lacked *in-vivo* stability. Also, $[^{99m}Tc(CO)_3(H_2O)_3]^+$ core[238] has been used for labeling a fatty acid derivative via histidine moiety. But, this also did not improved myocardial extraction, due to the stereochemical changes in the molecule.

In the present work, a xanthate derivative of 15-hydroxy pentadecanoic acid (HPDA) (Fig. 2.12) was prepared and labeled using the $[^{99m}TcN]^{2+}$ core. The prepared complex was evaluated in Swiss mice for its biological behavior.

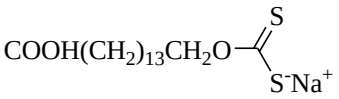

3

Fig. 2.12 Stucture of synthesized fatty acid xanthate

2.3.2 Experimental

2.3.2.1 *Materials and Methods*

The general experimental details are given in section 2.2.2.1.

2.3.2.2 *Synthesis of 15-HPDA xanthate ligand* (3)

In a typical procedure, a mixture of 15-HPDA (0.5 g, 1.94 mmol) and crushed sodium hydroxide (0.78 g, 5.81 mmol) were stirred vigorously in THF (20 mL) for 5 min at room temperature. To the stirred solution, carbon disulphide (0.14 mL, 2.13 mmol) was added. Stirring was continued overnight at room temperature. After completion of the reaction THF was removed under vacuum, the residue was washed with ether and re-crystallized from methanol-ether to obtain the product **3** as a yellow solid.

Yield: 30% (220 mg)

C, H, N, S: Observed (Calculated) 43.96 (44.06), 4.30 (4.52), 5.66 (5.71), 26.45 (26.14).

MS (ESI, +ve mode): Mass (M) (calculated) $C_{16}H_{28}O_3S_2Na_2$ 378.1275; m/z (observed) (M-2Na) 333.1656 [Fig. 2.13].

2.3.2.3 ***Radiolabeling***

To a solution of ligand **3** (~5 mg) in saline (0.5 mL), freshly prepared $[^{99m}TcN]^{2+}$ intermediate (0.5 mL) (as reported in Section 2.2.2.4.1) was added and the pH of the resultant mixture kept around 7-8. The reaction mixture was vortexed for 1 min and incubated at room temperature for 30 min to give the desired complex **3C**.

2.3.2.4 ***Quality Control techniques***

The radiochemical purity of the $[^{99m}TcN]^{2+}$ intermediate was checked by TLC, while that of **3C** by paper electrophoresis and HPLC.

2.3.2.4.1 *TLC*

The $[^{99m}TcN]^{2+}$ intermediate was characterized by TLC using ethanol: chloroform: toluene: 0.5M ammonium acetate (6:3:3:0.5 v/v) as the developing solvent.

2.3.2.4.2 *Paper electrophoresis*

Paper electrophoresis was done using a 37 cm long strip of Whatman No.3 chromatography paper and 0.05 M phosphate buffer (pH 7.4). About 2 μL of the test solution was spotted at the middle of the strip and the electrophoresis was carried out for 1 h under a potential gradient of ~10 V/cm. The strip was dried and the radioactivity profile determined using a TLC chromatography evaluation system.

2.3.2.4.3 *HPLC*

About 25 μL of the test solution was injected into the column and elution was monitored by observing the radioactivity profile. Water (A) and acetonitrile (B) each containing 0.1% trifluoroacetic acid were used as the mobile phase and the following gradient elution technique was adopted for the separation (0 min 98% A, 2 min 98% A, 3 min 2% A, 10 min 2% A).

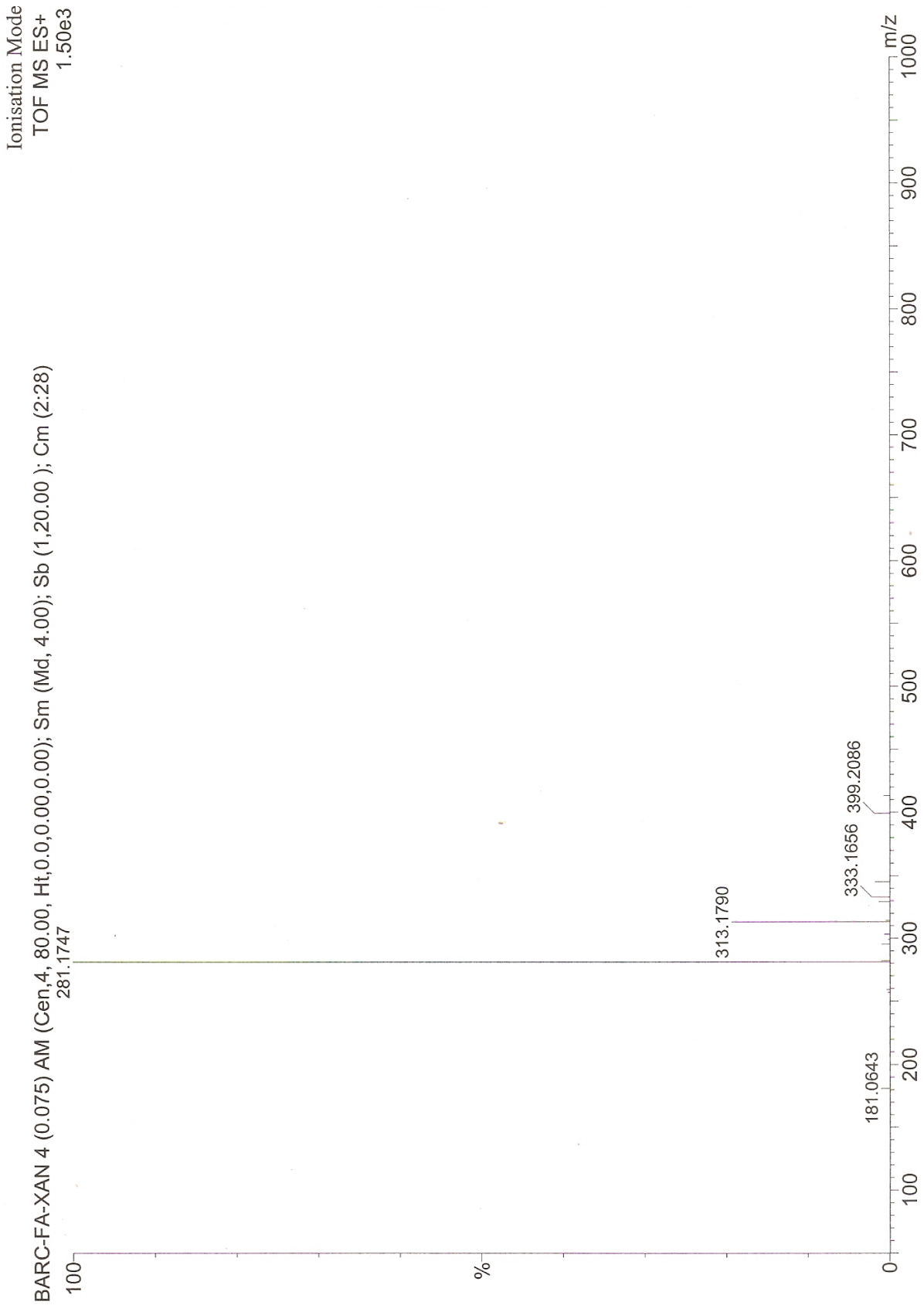

Fig. 2.13 Mass spectrum of compound **3**

2.3.2.4.4 *Biological studies*

2.3.2.4.4.1 Serum stability studies

Stability of the complex **3C** was assessed *in-vitro* in human serum. About 50 μL of the radiolabeled preparation was added to 500 μL serum and the mixture was incubated at 37 °C. Aliquots were taken at the intervals of 30 and 60 min. The serum proteins were precipitated with equal volume of cold ethanol, and the precipitate was removed after centrifugation at 10000 g for 20 min. The respective supernatants were subjected to HPLC as above to quantitate the protein unbound complex.

2.3.2.4.4.2 Bio-distribution studies

Normal Swiss mice (20-25g body weight) were used for the bio-distribution studies. Each animal was intravenously injected with complex **3C** (~2.5 MBq, 0.1 mL) via the tail vein. Four different sets (3 each) of animals were kept under normal conditions for various time periods (5, 10, 30 and 60 min). The animals were sacrificed immediately after the respective incubation periods and the relevant organs and tissues were excised for measuring the associated radioactivity, using a flat-bed type NaI(Tl) scintillation counter with a suitable energy window for ^{99m}Tc. The accumulated activity per gram of the specific organ/tissue was expressed in terms of percentage of the total injected dose. All the procedures were performed in accordance with the national laws pertaining to the conduct of animal experiments.

2.3.3 Results and discussion

2.3.3.1 *Synthesis of 15-HPDA xanthate*

The fatty acid-xanthate (**3**) was synthesized in a single step (Fig. 2.14) by reacting 15-HPDA with CS_2 in presence of sodium hydroxide as the base. The product was obtained in moderate yield and was characterized by elemental and mass spectral analyses.

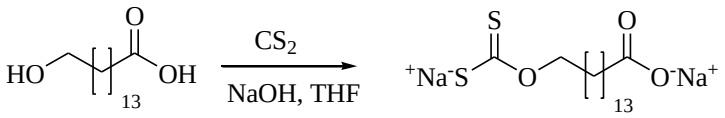

3

Fig. 2.14 Synthesis of xanthate derivative of 15-HPDA

2.3.3.2 *Radiolabeling*

2.3.3.2.1 *[^{99m}TcN]$^{2+}$ intermediate core*

The schematic representation for the formation of [^{99m}TcN]$^{2+}$ core is shown in Fig. 2.7(a). The distinction between the [^{99m}TcN]$^{2+}$ core and its precursor $^{99m}TcO_4^-$ was achieved by TLC, using EtOH/ $CHCl_3$/ toluene/ 0.5M NH_4Ac (6:3:3:0.5 v/v) as the solvent system. The ^{99m}TcN-core (~99%) was found to be concentrated near the point of application (R_f = 0-0.25), while $^{99m}TcO_4^-$ in the same solvent system showed a R_f = 0.4-0.6.

2.3.3.2.2 *[^{99m}TcN]-15-HPDA xanthate complex* (**3C**)

The synthetic scheme of **3C** is shown in Fig. 2.15. The desired complex was obtained on adding freshly prepared [^{99m}TcN]$^{2+}$ core to the synthesized ligand **3**. The final complex **3C** was characterized by paper electrophoresis and HPLC. Electrophoresis pattern of the nitrido intermediate and the complex **3C**, visualised using a radioactive scanner is shown in Fig. 2.16. More than 95% of the radioactivity corresponding to **3C** was seen with the band having an R_f = 0.26. Under identical conditions, the ^{9m}TcN-core had ~98% activity at R_f = 0.62. The HPLC chromatograms of ^{99m}TcN-intermediate and **3C** are shown in Fig. 2.17. The retention times of the complex **3C** was found to be 7.5 ± 0.1 min while that of ^{99m}TcN-core was 2.8 ± 0.1 min.

Xanthates are known to complex with [^{99m}TcN]$^{2+}$ core leading to neutral complexes of $^{99m}TcNL_2$ type[239] having square pyramidal geometry with an apical ^{99m}Tc≡N bond and four sulphur atoms occupying the basal plane. It may be presumed that the neutral fatty acid xanthate complex prepared above would have a similar structure.

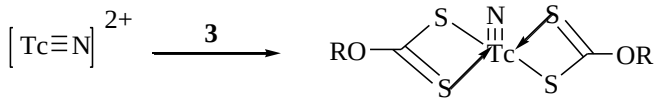

3C R = $COOH(CH_2)_{13}CH_2$

Fig. 2.15 Synthesis of ^{99m}TcN- 15-HPDA xanthate complex

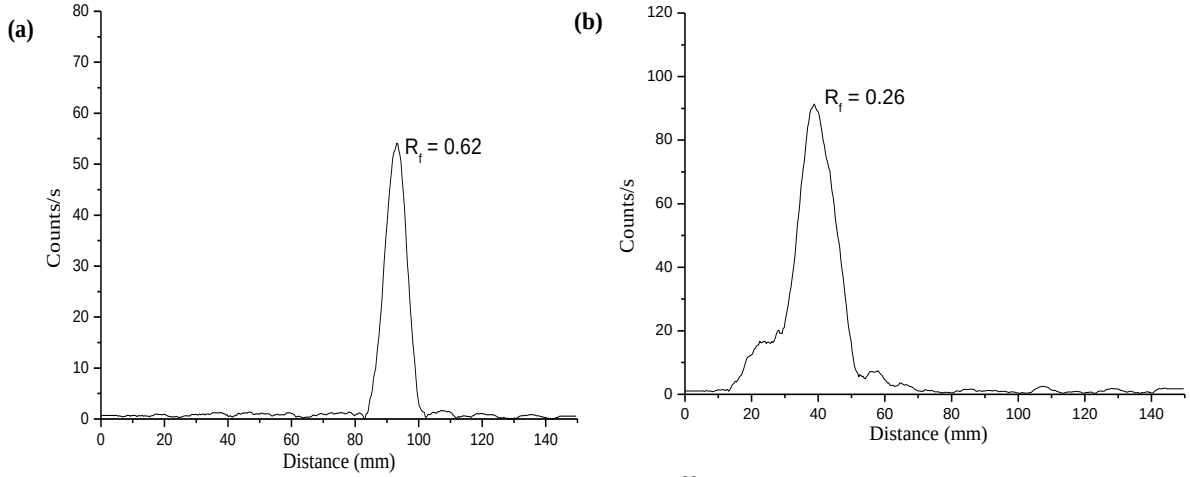

Fig. 2.16 Paper electrophoresis patterns of (a) ^{99m}TcN-intermediate and (b) complex **3C**

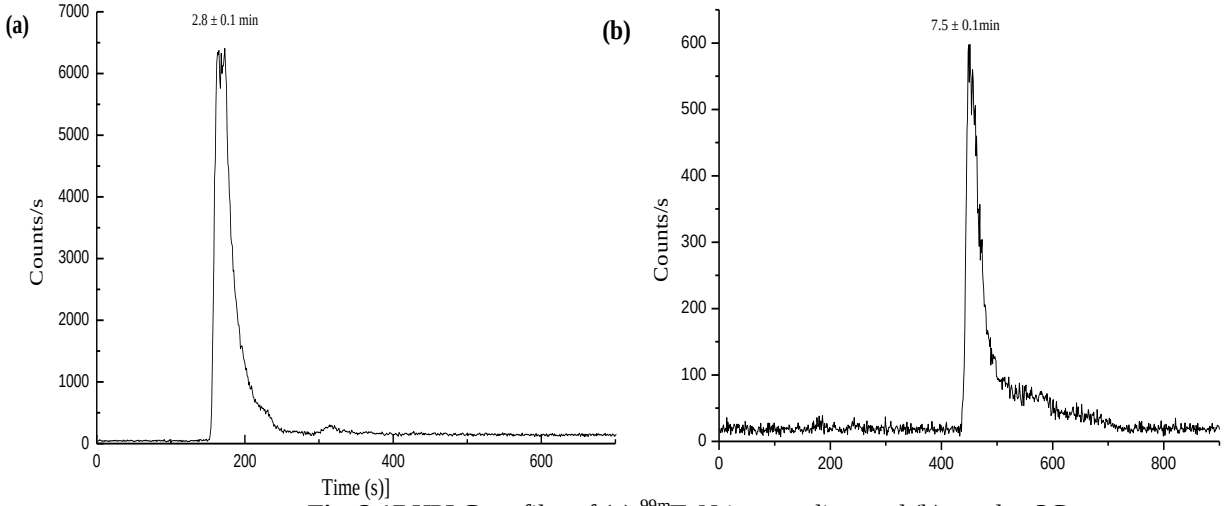

Fig. 2.17 HPLC profiles of (a) ^{99m}TcN-intermediate and (b) comlex **3C**

2.3.3.3 *Biological studies*

In view of the essential parameters (i-iv) required for a myocardial agent as mentioned in section 2.2.3.3, the *in-vitro* stability of the complex was carried out to determine the kinetic inertness of the complex **3C**. The complex was found to be stable in serum up to 1 h as confirmed by HPLC wherein the retention of radioactive peak was observed.

To evaluate the complex **3C** as a potential myocardial agent in terms of its *in-vivo* parameters, bio-distribution studies were carried in Swiss mice. From the bio-distribution studies (Table 2.4) it was observed that the maximum myocardial uptake of this preparation was 3.10 ± 0.08% ID/g at 5 min p.i., with a rapid wash out leading to a meagre 0.79 ± 0.18% ID/g of the activity remaining in the heart at 60 min p.i. The blood pool activity was initially high (8.21 ± 1.10% ID/g at 5 min p.i.), but declined with time. The heart/ blood ratio remained low within a reasonably narrow range throughout the period of the study. The complex showed high liver and lung uptake with slow clearance. Marginal hepatic clearance of the complex was evident from the gradually increased radioactivity in the intestinal region. An appreciable fraction of activity was seen in the kidneys, which could be possibly due to metabolism of the complex **3C** in the liver.

As is well known from the literature,[215] straight chain fatty acids having 15-21 carbon show maximum extraction in the myocardium. But the present complex **3C**, being a symmetric complex may behave as a straight chain of 30 carbon acid and thus have an altered *in-vivo* pharmacokinetic behavior. However, it was thought that the fatty acid (<15 carbon) on complexation with $[^{99m}TcN]^{2+}$ core may not behave as a single straight chain, and subsequently affect the myocardial uptake. Thus, it was decided to use a 15 carbon acid, the minimum chain for favorable myocardial extraction,[210] for the preparation of the complex.

However, as the experiments show, the proposed molecule exhibited limited uptake with rapid clearance from myocardium, decreasing its utility for the intended application.

Table 2.4 Bio-distribution pattern of complex **3C** in Swiss mice [% ID/g (1SD), (n =3)]

Organs	*5 min*	*10 min*	*30 min*	*60 min*
Liver	48.16 (0.02)	29.02 (2.57)	27.07 (1.03)	29.69 (5.67)
Intestine + GB	1.23 (0.08)	0.83 (0.13)	3.66 (0.31)	5.23 (0.64)
Kidney	21.57 (3.89)	17.06 (1.60)	16.29 (1.38)	16.89 (4.29)
Heart	3.10 (0.08)	1.38 (0.19)	0.92 (0.06)	0.79 (0.18)
Lungs	5.84 (0.28)	2.99 (0.67)	2.03 (0.05)	2.96 (1.14)
Blood	8.21 (1.10)	3.06 (0.38)	1.96 (0.23)	1.85 (0.28)
Heart/ blood	0.38	0.45	0.43	0.47
Heart/ lung	0.53	0.46	0.45	0.27
Heart/ liver	0.06	0.05	0.03	0.03

2.3.4 Conclusion

The xanthate derivative of 15-HPDA could be synthesized and labeled with the $[^{99m}TcN]^{2+}$ core yielding more than 95% complexation. Neutral ^{99m}Tc complex could be obtained in high yields and adequate stability. The study indicated that a xanthate derivative of a fatty acid makes a feasible route for labeling biomolecules with ^{99m}Tc tracer via $[^{99m}TcN]^{2+}$ core under mild conditions. Bio-distribution study carried out in Swiss mice showed desirable extent of uptake in myocardium, albeit with significant uptake in the surrounding organs leading to unfavorable target to non-target ratios, which would affect the quality of the images. However, these studies have opened a new route for radiolabeling fatty acids via $[^{99m}TcN]^{2+}$ core.

2.4 Conclusion

The present chapter evaluates the usefulness of $[^{99m}TcN]^{2+}$ core in terms of its ease of preparation and the stability of the intermediate core. Also, it highlights the simple derivatization, in the form of dithiocarbamates and xanthates, required in the lead molecule for the easy incorporation of ^{99m}Tc metal via $[^{99m}TcN]^{2+}$ core. The suitability of this core for the attachment of biomolecules, has been represented by taking an example of fatty acid. Apart from this, the chapter also presents the mild reaction conditions required for final complex formation and *in-vivo* inertness of the final $[^{99m}TcN]$-complexes, which are desirable parameters for final radiopharmaceutical preparations.

CHAPTER 3

Asymmetric [2+2] Neutral Complex

3.1 Introduction

As discussed in the previous chapter, the $[^{99m}TcN]^{2+}$ core co-ordinates symmetrically with bi-dentate ligands, such as dithiocarbamates and xanthates, forming square pyramidal complexes of type $[^{99m}TcNL_2]$[181] (L = bi-dentate ligand). Molecules with potential for targeting the desired organ/ lesion can often be derivatized to dithiocarbamates or xanthates [240-241] making them amenable for labeling with ^{99m}Tc via ^{99m}Tc-nitrido core. The symmetric labeling approach is well suited for small non-specific molecules such as TBDTC and MIBDTC ligands. However, for molecules such as peptides, antibodies, etc. which bind specifically to the target cells, such a symmetric labeling approach is unsuitable, as two of the same carrier molecules in the radiolabeled complex may affect the target binding due to steric factor and also affect the bio-distribution characteristics of the carrier molecule.[242] Also, the symmetric labeling approach for large molecules such as 15-HPDA would furnish bulky complexes, which may affect their uptake and retention characteristics in the target organ leading to undesirable *in-vivo* pharmacokinetics.[243] These factors prompted the search for asymmetric [^{99m}TcNLL'] chemistry, where two different bi-dentate ligands (L and L') can be linked to the ^{99m}Tc-metal centre resulting in complexes that contain a single bioactive moiety per ^{99m}Tc metal (Fig. 3.1).

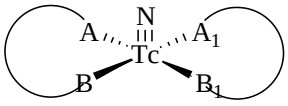

$[^{99m}TcNLL']$

L = Bi-dentate ligand (AB donor)
L'= Bi-dentate ligand (A_1B_1 donor)

Fig. 3.1 General structure of asymmetric [2+2] complexes

The chemistry of asymmetric [^{99m}TcN] complexes evolved from the high stability observed with [^{99m}TcNL$_2$] complexes, where L is a bi-dentate ligand having phosphorus and thiol (PS^-) donor groups.[176,189] The affinity of bi-dentate PS^- donor groups for [^{99m}TcN]$^{2+}$ core is so high that even the kinetically stable [^{99m}TcN]- dithiocarbamate and xanthate complexes reported in the earlier chapter, undergo quantitative degradation in presence of these ligands forming [^{99m}TcN(PS)$_2$] complex.[176] Unlike the square pyramidal geometry formed in the symmetric [2+2] [^{99m}TcN] complexes, the [^{99m}TcN(PS)$_2$] complex follows trigonal bi-pyramidal geometry. Here, the Tc≡N moiety along with two S atoms is along the trigonal plane with two P donor groups occupying the *trans*-axial positions. This observation led to the generalization that [^{99m}TcN]$^{2+}$ core has a strong affinity for bi-dentate ligands containing a combination of π-acceptor (phosphorus donor) and π-donor (S^- donor) groups. The high stability of [^{99m}TcN(PS)$_2$] complexes infused interest in exploring [^{99m}TcN]-complexes formed by mixed bi-dentate P⌒P and S⌒S ligands,[189] for their possible application in radiopharmaceuticals.

In this respect, diphosphines having short spacers between the two P atoms were found to be inappropriate as they furnish unstable complexes. On the other hand diphosphines containing 4 and 6 methylene units as the spacers produced [^{99m}TcN]-complexes that could not be isolated in high purity.[243] In view of these, another set of long chain bi-dentate phosphorus ligands containing a heteroatom X (X = N, S, O) in between the terminal phosphorus ends were evaluated.[244-246] These formed intermediate [^{99m}TcN(PXP)]$^{2+}$ complexes with a single molecule of bi-dentate phosphorus ligand bound to the metal centre and could be isolated in high purity. The final geometry of the intermediate in these ligands is square pyramidal with two P donors occupying the *trans* positions in square basal plane and the other two positions occupied by labile groups. However, the isolated intermediate complexes for diphosphines with more than five spacer including heteroatom were found to

be inert towards π-donor bi-dentate S⌒S type ligands. This was probably due to the steric repulsion arising from the *trans,mer* orientation of the long chain bi-dentate phosphorus ligand to the incoming S⌒S ligand. However, the intermediate $[^{99m}TcN(PXP)]^{2+}$ complex formed using five membered bi-dentate PXP ligands showed reactivity towards the bi-dentate π donor groups.[189] This intermediate $[^{99m}TcN(PXP)]^{2+}$ complex (PXP = five member bi-dentate phosphorus ligand) exists in three different isomeric forms *viz. mer,cis*; *mer,trans* and *fac,cis* (Fig. 3.2).[195] However, when bi-dentate ligands bearing soft π-donor SS, OS, NS coordinating atoms are used only the *fac,cis* form is observed with all types of PXP bis-phosphines. The reason for this is that when a PPSS/ PPSO/ PPSN coordination system is set around a TcN core the trigonal bipyramidal geometry is highly preferred with the two P atoms in *trans* position to each other and the two π-donor atoms on the trigonal plane along with the nitride nitrogen atom. This preference is key to explain the reactivity of TcN(PXP) intermediate when X = NR (R = organic functional group). The very weak *trans* interaction of the NR group with the TcN core (a few kcalories) does not allow the corresponding $TcN(PXP)Cl_2$ complex achieving a full octahedral structure as it happens when X = O, S. Thus, the structure remains 'open' to react with an incoming bi-dentate soft π-donor ligand and finally stabilizes in a highly distorted pseudo-octahedral structure.

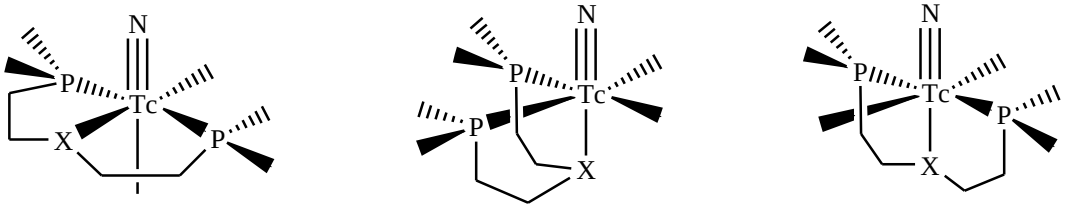

mer, cis *fac, cis* *mer, trans*

Fig. 3.2 Possible isomers of $[^{99m}TcN(PXP)]^{2+}$ intermediate

The $[^{99m}TcN(PXP)]^{2+}$ (X = O, S) intermediate complex predominantly leads to the formation of non reactive *mer* isomers, which yield [2+2] $[^{99m}TcN]$-complexes in poor yield. However, bis (phosphines) having N heteroatom predominantly yield the reactive isomer, where the two P atoms are oriented in the *cis* positions (*fac,cis* isomer) in the square basal plane leaving the other two *cis* positions occupied by labile groups, which can be suitably exchanged with bi-dentate π-donor ligands.[195] Thus, a mixed donor set comprising of π-donor and π-acceptor groups around the $[^{99m}Tc{\equiv}N]^{2+}$core yielded stable bi-substituted complexes.[186,189,195]

The π-donor bi-dentate ligand, suitable for complexation with the intermediate $[^{99m}TcN(PNP)]^{2+}$ were found to possess a combination of SS (dithiols, dithiocarbamates, xanthates)/ SN (SH and NH_2) / SO (SH and COOH) donor groups.[187,190,191,196,247] The intermediate $[^{99m}TcN(PNP)]^{2+}$ has an overall charge of +2 (Fig. 3.3). The nature of charge on the π-donor ligand, whether anionic or di-anionic, decides the overall charge of the final complex. Complexes prepared using $[^{99m}TcN(PNP)]^{2+}$ core and bi-dentate ligands with donor groups S^-, S^- (dithiols)[196] or S^-, COO^- (cysteine)[190] leads to '*asymmetric [2+2] neutral complex*'.

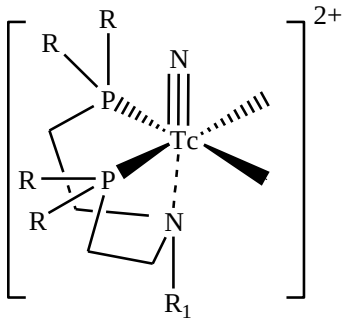

Fig. 3.3 General structure of asymmetric $[^{99m}TcN(PNP)]^{2+}$ intermediate

In the present chapter, an asymmetric [2+2] neutral complex was synthesized, characterized and subsequently bio-evaluated in small animal model. The bi-dentate π

acceptor P⌒P ligand, bis[(diethoxypropylphosphanyl)ethyl]ethoxyethylamine (**6**) ligand used for the formation of asymmetric [2+2] neutral complex was a gift from Prof. Adriano Duatti, Italy. The π-donor ligand **7** was synthesized by modifying the thapsic acid (hexadecanedioic acid), a long chain fatty acid (Fig. 3.4) which is known to go to the myocardium. The synthetic strategy involved mono-amidation of one of the carboxylic acid groups of thapsic acid with cysteine so that the carboxylic acid and thiol moieties (S^-, COO^-) of the cysteine residue are available to form a neutral heterocomplex with the $[^{99m}TcN(PNP)]^{2+}$ core. The asymmetric [2+2] complex, thus, obtained was characterized and evaluated as a potential radiopharmaceutical for myocardial imaging. The results of its bio-distribution were compared with ^{125}I labeled standard agent iodophenylpentadecanoic acid (IPPA).

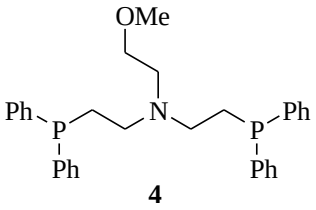

4

Bis[(diphenylphosphanyl)ethyl]methoxyethylamine

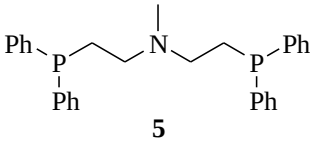

5

Bis[(diphenylphosphanyl)ethyl]methylamine

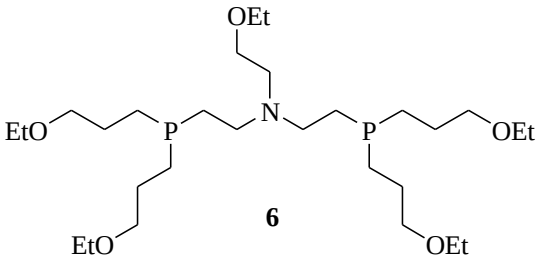

6

Bis[(diethoxypropylphosphanyl)ethyl]ethoxyethylamine

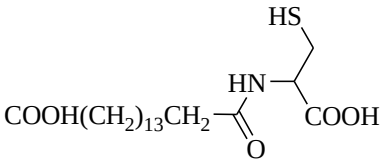

7

Fatty acid-cysteine conjugate

Fig. 3.4 π-acceptor and π-donor ligands used in the present study

This chapter also includes synthesis of two other π-acceptor PNP ligands, namely, bis[(diphenylphosphanyl)ethyl]methoxyethylamine (**4**) and bis[(diphenylphosphanyl)ethyl] methylamine (**5)** (Fig. 3.4) which were also radiolabeled with $[^{99m}TcN]^{2+}$ core to form the

respective intermediate $[^{99m}TcN(PNP)]^{2+}$ complexes. However, these were not used for the preparation of final asymmetric [2+2] complex and subsequent bio-evaluation, due to the poor *in-vivo* pharmacokinetic behavior of such complexes, reported in the literature.[190] This work was undertaken to establish the synthetic steps for preparation of such complexes, as the PNP ligands form stable complexes with $[^{99m}TcN]^{2+}$ and hold promise for preparation of successful radiopharmaceuticals.

3.2 Experimental

3.2.1 Materials and Methods

The general experimental details are given in chapter 2, section 2.2.2.1.

3.2.2 Synthesis of Ligands

3.2.2.1 *π-acceptor ligands*

3.2.2.1.1 *Synthesis of bis[(2-diphenylphosphino)ethyl]methoxyethylamine* (**4**)

The synthesis of this ligand was carried following a literature procedure.[189, 244, 248]

Bis[2-hydroxyethyl]methoxyethylamine (**4a**)

In a 100 mL two necked round bottom flask, equipped with a 100 mL pressure equalizing dropping funnel and a reflux condenser, diethanolamine (6.4 g, 0.061 mol) and anhydrous K_2CO_3 (8.4 g, 0.061 mol) were added to acetonitrile (40 ml) and stirred vigorously. To this, 2-bromoethyl methyl ether (8.5 g, 5.8 mL, 0.061 mol) was added slowly over a period of 1 h at room temperature. After the addition, the reaction mixture was refluxed for 2 days. The progress of the reaction was monitored by TLC. After completion of the reaction, the crude reaction mixture was filtered to remove excess K_2CO_3 and KCl formed during the reaction. The solvent was removed under vacuum to give the crude product as oil. Pure **4a** was obtained after silica gel column chromatography, using 1% NH_3/ MeOH as the eluting solvent.

Yield: 80 % (8 g), R_f = 0.66 (1% NH_3/ MeOH).

^{1}H NMR ($CDCI_3$, δ ppm): 3.60 (t, 4H, $(OHC\underline{H}_2CH_2)_2N$-, *J = 5.1 Hz*); 3.47 (t, 2H, -$C\underline{H}_2OCH_3$, *J = 5.4 Hz*); 3.38 (s, 3H, -$OC\underline{H}_3$); 2.76 (t, 2H, -$NC\underline{H}_2CH_2O$-, *J = 5.1 Hz*); 2.70 (m, 4H, $(OHCH_2C\underline{H}_2)_2N$-) [Fig. 3.5].

Bis[2-chloroethyl]methoxyethylamine (**4b**)

In a 3 necked round bottom flask, equipped with a dropping funnel, nitrogen inlet and a bubble trap containing 20% KOH solution, compound **4a** (7.5 g, 0.046 mol) and pyridine (7.3 mL, 0.092 mol) were added. To the cooled (0 °C) reaction mixture, was slowly added $SOCl_2$ (20.1 mL, 0.276 moles) under vigorous stirring. The solution darkened considerably with evolution of sulphur dioxide. The reaction mixture was then allowed to reach room temperature and stirred overnight. The mixture was refluxed for 3 h on water bath and left to attain room temperature. An ice bath was again placed under the flask and water was dropwise added to the reaction mixture to quench excess thionyl chloride. The reaction mixture was treated with aqueous 30% Na_2CO_3 to bring the pH of the solution to 9 and extracted with diethyl ether (3 × 25 mL). The combined organic extracts were dried and concentrated under vacuum to give the crude dichloride **4b**. This was purified by silica gel column chromatography using $CHCl_3$/ EtOAc (9:1) as the eluting solvent.

Yield: 54% (5 g), R_f = 0.8 [$CHCl_3$/ EtOAc (9:1 v/v)].

^{1}H NMR ($CDCl_3$, δ ppm): 3.53 (t, 4H, -$N(CH_2C\underline{H}_2Cl)_2$, *J = 7.2 Hz*); 3.46 (t, 2H, $CH_3OC\underline{H}_2$-, *J = 5.4 Hz*); 3.35 (s, 3H, $C\underline{H}_3OCH_2$-); 2.96 (m, 4H, -$N(C\underline{H}_2CH_2Cl)_2$); 2.82 (t, 2H, -$NC\underline{H}_2CH_2O$-, *J = 5.7 Hz*) [Fig. 3.6].

Bis[(2-diphenylphosphino)ethyl]methoxyethylamine **(4)**

In a 100 ml 2 necked round bottom flask, fitted with a dropping funnel and a nitrogen inlet, orange-red colored potassium diphenylphosphide solution (0.5 M, 56 mL, 0.028 mol)

was taken. The flask was cooled to -78 °C in a dry ice-acetone bath and compound **2** (2.8 g, 0.014 mol) in THF (20 mL) was added dropwise through the dropping funnel under nitrogen atmosphere. During the addition the orange red colour vanished. The reaction mixture was left to attain room temperature and stirring continued overnight. The flask was cooled to 0 °C and degassed water (10 min) was dropwise added until a clear solution was obtained. The solution was transferred (still under N_2) into a separating funnel by a cannula. Degassed water (30 mL) along with degassed diethyl ether (30 mL) was added to the separating funnel. After thorough mixing, the two phases were separated and the organic layer was collected avoiding contact with air. The aqueous layer was extracted again with degassed diethyl ether (2 × 30 mL), the organic extracts were pooled together and dried. The mixture was filtered avoiding contact with air and the solvent evaporated to obtain a thick yellow colored oil, which was treated with degassed ethanol (10 mL) and left in the fridge at -18 °C overnight. After refrigeration for 1-3 days, compound **4** was obtained as a white precipitate, which was filtered and dried under vacuum.

Yield: 93% (4 g).

^{1}H NMR ($CDCl_3$, δppm): 7.31 (m, 20H, $C_6\underline{H}_5$); 3.32 (t, 2H, $CH_3OC\underline{H}_2CH_2$, *J = 6.0 Hz*); 3.23 (s, 3H, -$OC\underline{H}_3$); 2.66 (m, 6H, -$C\underline{H}_2N(C\underline{H}_2CH_2PPh_2)_2$); 2.14 (m, 4H, $(Ph_2PC\underline{H}_2CH_2)_2N$-) [Fig. 3.7].

^{31}P NMR ($CDCl_3$,δppm): -19.6 [Fig. 3.8]

3.2.2.1.2 *Synthesis of bis[(2-diphenylphosphino)ethyl]methylamine* (**5**)

In a 100 mL three necked round bottom flask, fitted with dropping funnel and nitrogen inlet, potassium diphenylphosphide solution (10.4 mL, 0.5 M) was taken. This was cooled to -78 °C on a acetone-liquid nitrogen bath. In a separate flask, *N*-methyl bis(2-chloroethyl)amine hydrochloride (500 mg, 2.597 mmol) was added to dry THF (15 mL) to make a suspension. This was neutralized by adding n-butyl lithium (2.5 M, 1 mL, 5.97 mmol)

to generate the free amine leading to a clear THF solution. This was transferred into a pressure equalizing dropping funnel and added dropwise to the potassium diphenyl phosphide solution and stirred at -78 °C for 2 h. The reaction mixture was brought to room temperature and stirred overnight. After the reaction, usual isolation as that followed for the PNP ligand **4** afforded the compound **5**.

^{1}H NMR ($CDCl_3$, δppm): 7.25-7.74 (m, 20H, -PPh_2,); 2.65-2.76 (m, 4H, -$N(CH_2C\underline{H}_2PPh_2)_2$); 2.30-2.38 (m, 4H, -$N(C\underline{H}_2CH_2PPh_2)_2$); 2.22 (s, 3H, -$NC\underline{H}_3$) [Fig. 3.9].

^{31}P NMR ($CDCl_3$, δppm): -20.1 [Fig. 3.10].

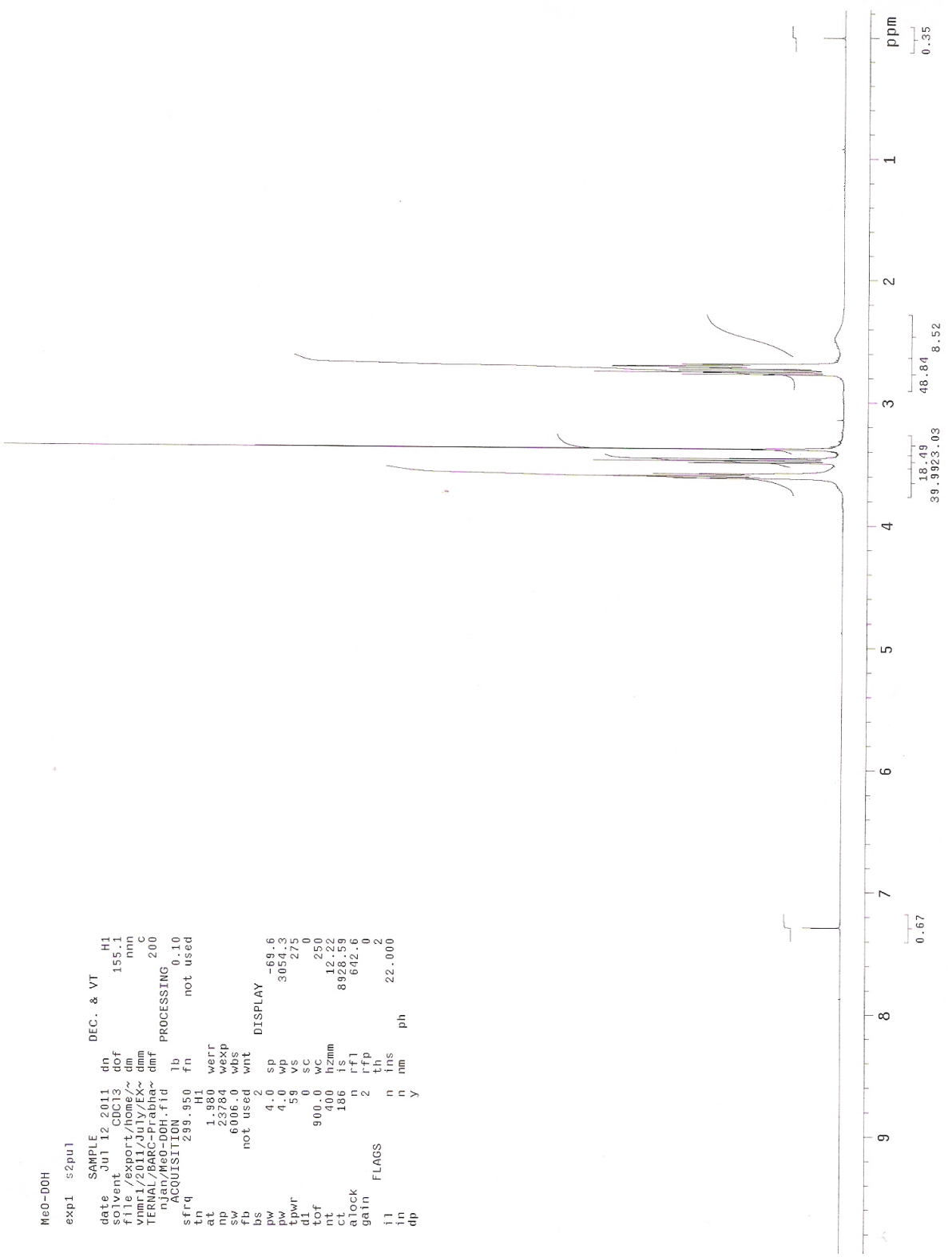

Fig. 3.5 ^{1}H NMR spectrum of compound **4a**

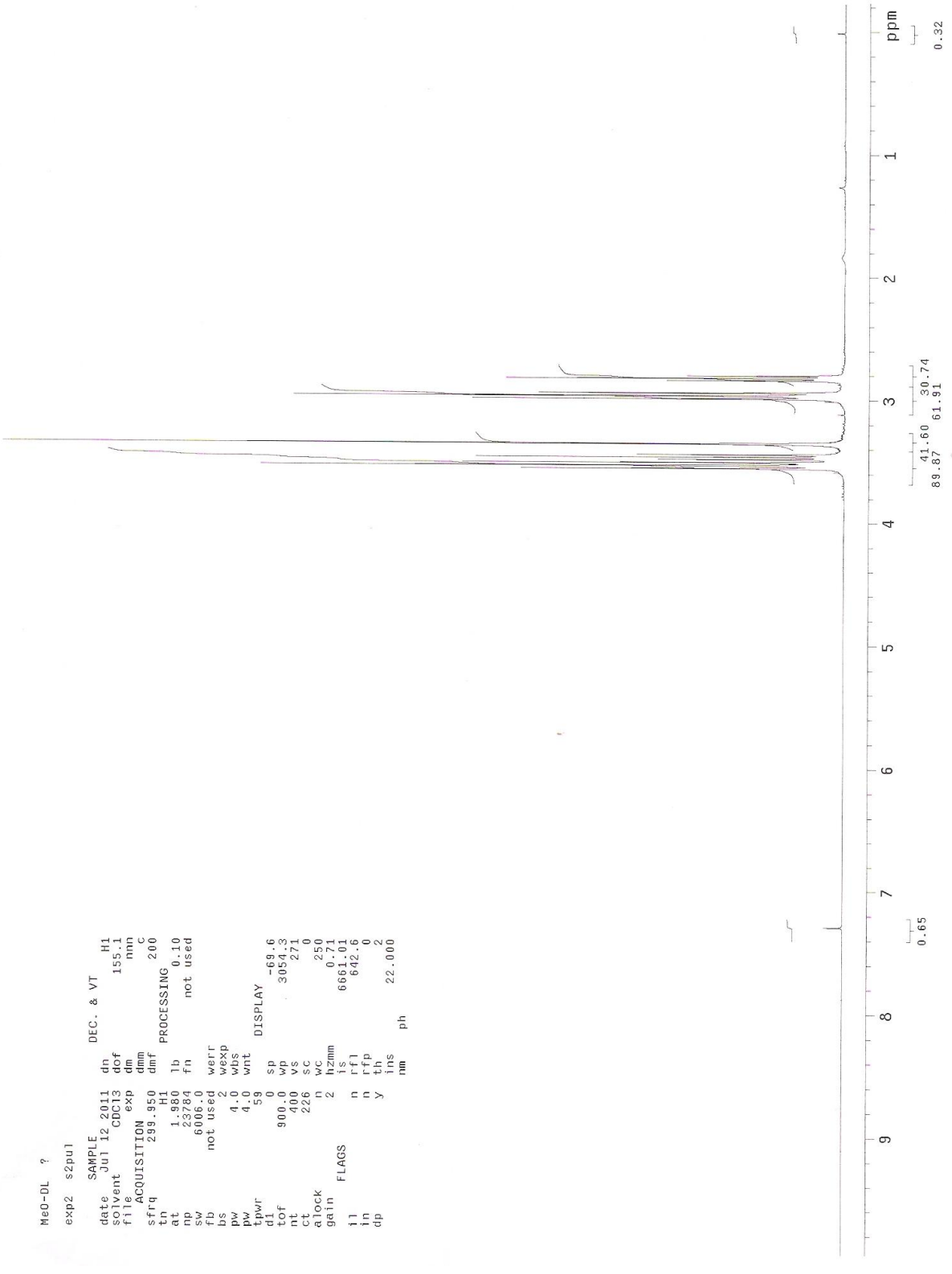

Fig. 3.6 ^{1}H NMR spectrum of compound **4b**

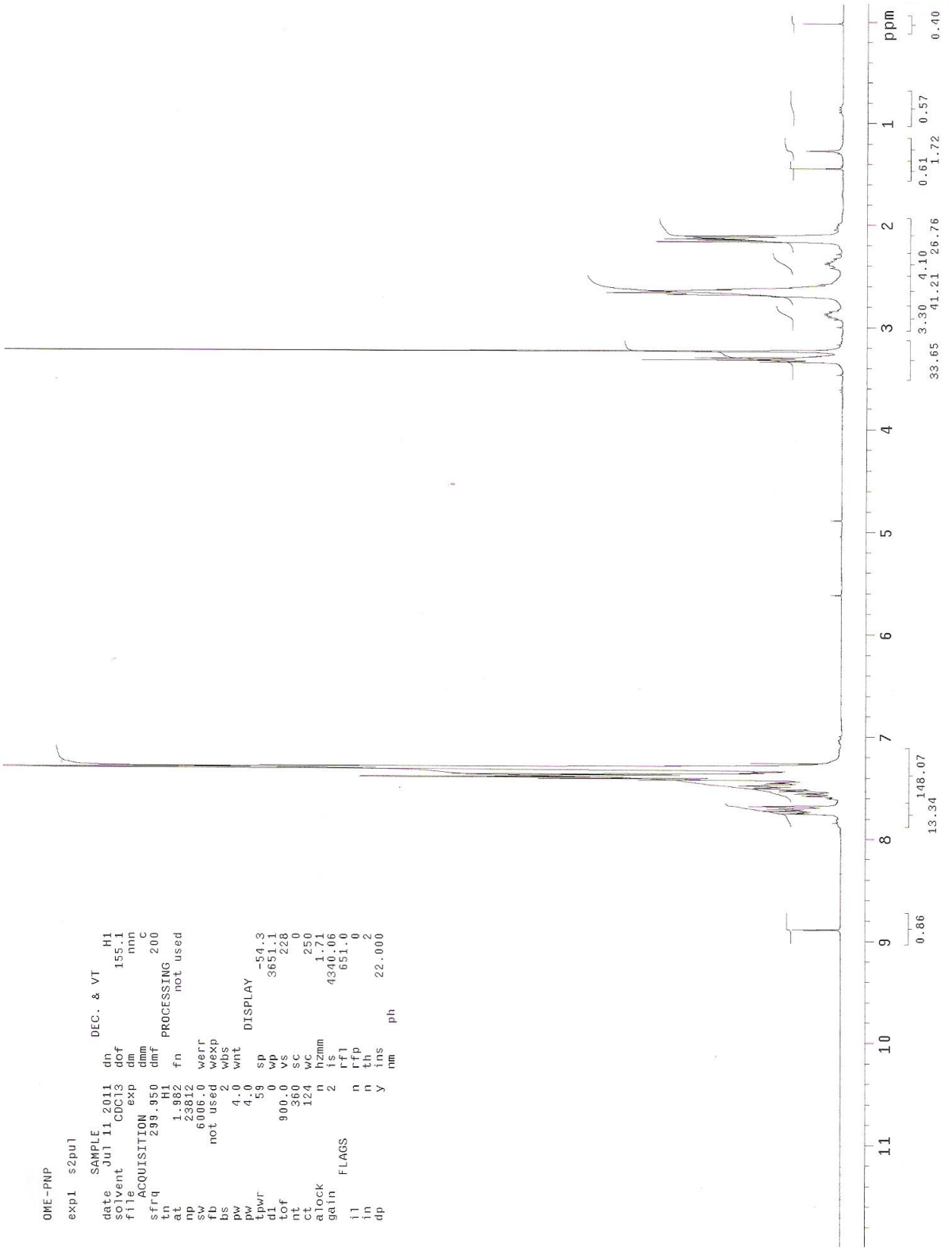

Fig. 3.7 ^{1}H NMR spectrum of compound **4**

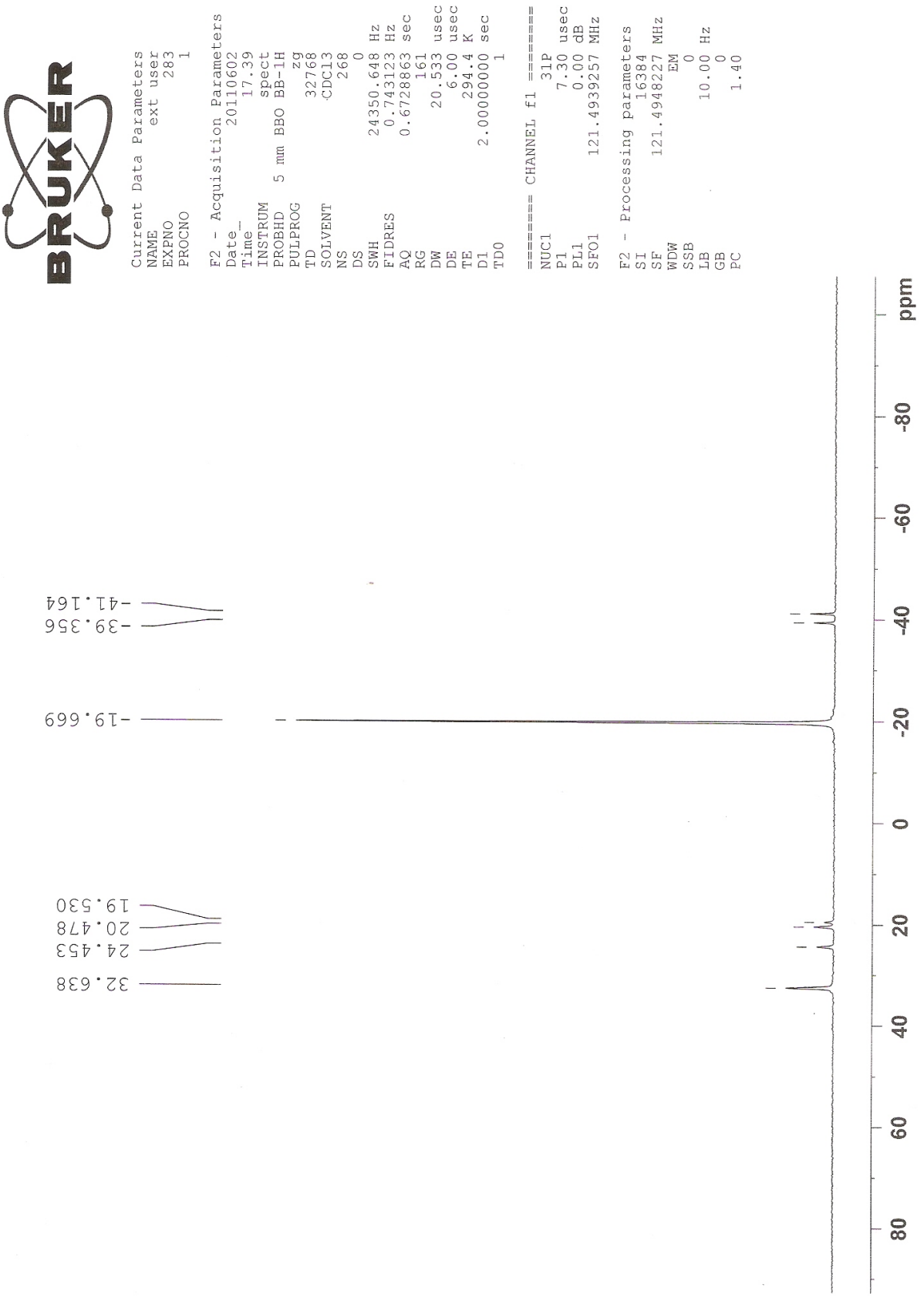

Fig. 3.8 ^{31}P NMR spectrum of compound **4**

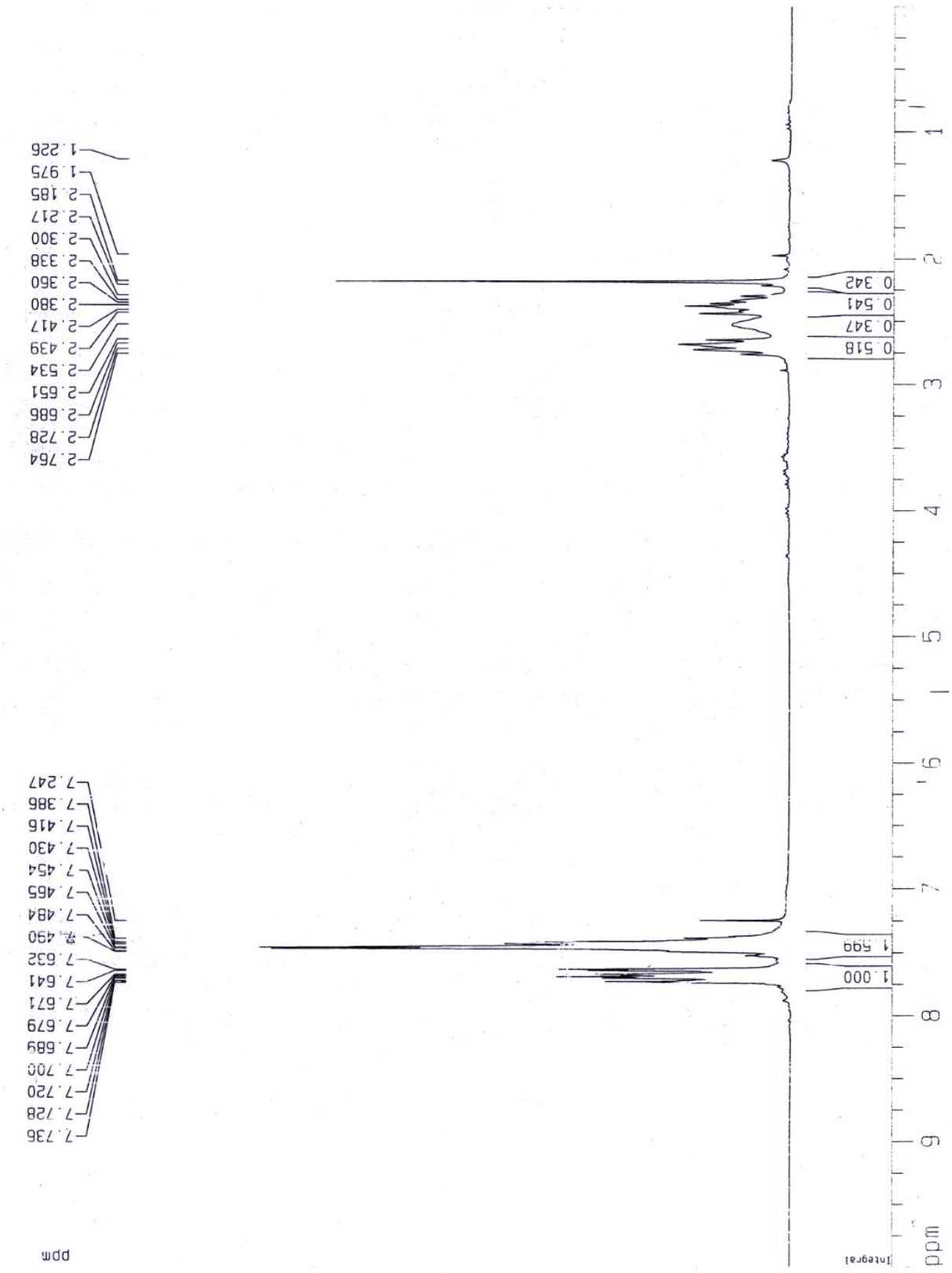

Fig. 3.9 ^{1}H NMR spectrum of compound **5**

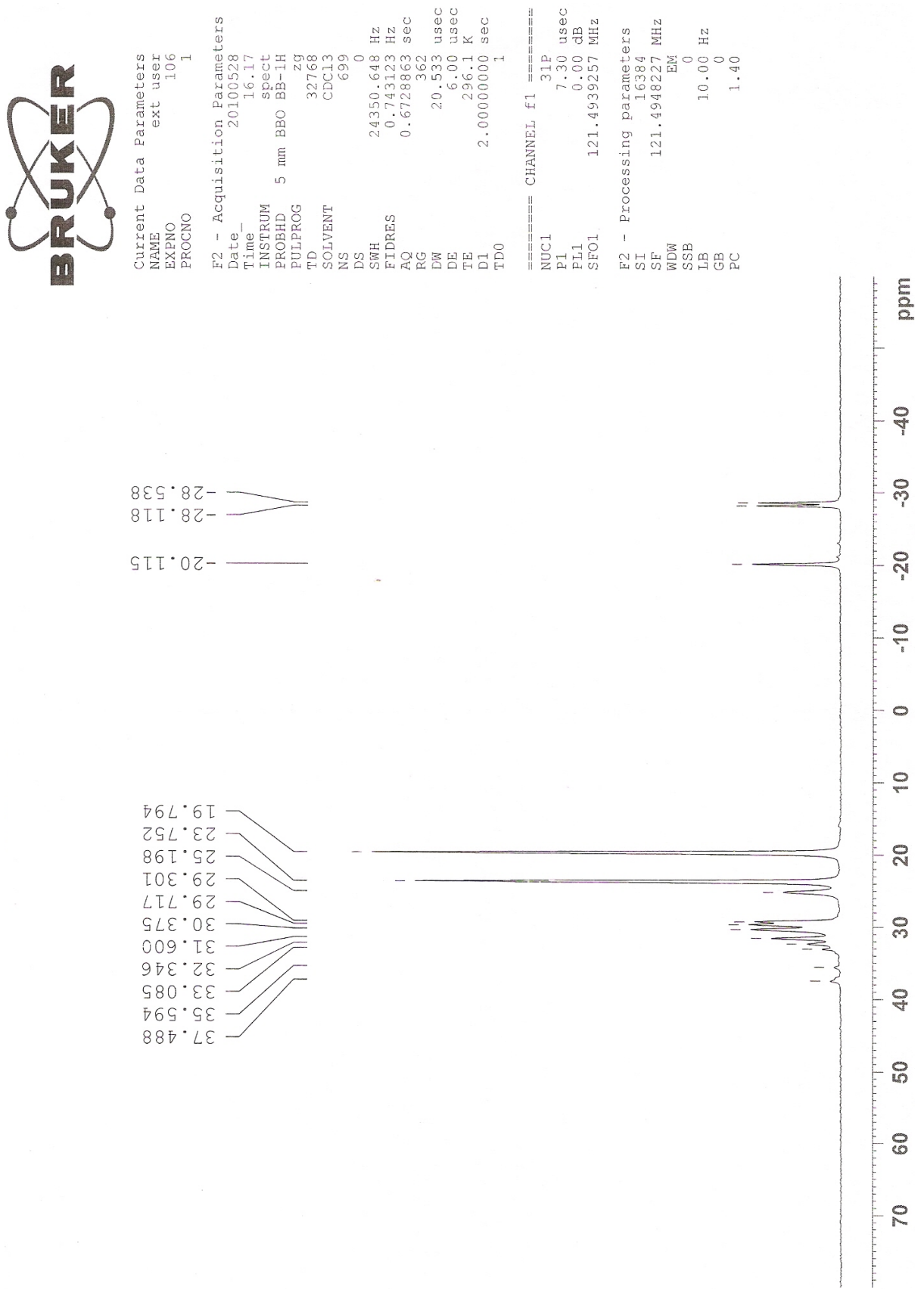

Fig. 3.10 ^{31}P NMR spectrum of compound **5**

3.2.2.2 π-donor ligand

3.2.2.2.1 *Synthesis of a fatty acid-cysteine conjugate* (**7**)

2-Amino-3-tritylsulfanyl-propionic acid ethyl ester (**7a**)

The cysteine derivative was prepared following a reported procedure.[247] In a 100 mL two necked round bottom flask, fitted with a nitrogen inlet and reflux condenser, *S*-trityl-L-cysteine (1.12 g, 3.1 mmol) was suspended in dry ethanol (20 mL). To the stirred solution was added ethyl *p*-toluenesulfonate (1.24 g, 6.2 mmol) and the mixture refluxed. After completion of the reaction (*cf.* TLC, ~48 h), the solvent was removed under vacuum, the residue dissolved in an aqueous solution of $KHCO_3$ (30 mL, pH 8) and extracted with dichloromethane (3 × 15 mL). The combined organic extracts were dried and evaporated under vacuum to obtain the crude ester **7a**, which was purified by silica gel column chromatography, using EtOAc/ $CHCl_3$ (1:19 v/v) mixture as the eluant.

Yield: 80% (0.97 g), R_f ~ 0.4 [EtOAc/ $CHCl_3$ (1:19 v/v)].

^{1}H NMR ($CDCl_3$, δppm): 7.21-7.51 (m, 15H, Ar); 4.15 (q, 2H, $CH_3C\underline{H}_2O$-, *J = 7.1 Hz*); 3.22 (m, 1H, -$CH_2C\underline{H}NH_2$); 2.49-2.68 (m, 2H, -$C\underline{H}_2S$-); 1.26 (t, 3H, -$CH_2C\underline{H}_3$, *J = 7.1 Hz*) [Fig. 3.11].

HRMS (ESI, +ve mode): Mass (calculated) $C_{24}H_{25}NO_2S$ 391.1606; *m/z* (observed) 392.1628 [Fig. 3.12].

16-(ethyl, *S*-trityl cysteinyl amido) hexadecanoic acid (**7b**)

A 100 mL two necked round bottom flask kept under nitrogen was charged with hexadecanedioic acid (100 mg, 0.35 mmol) and compound **7a** (136 mg, 0.35 mmol) in CH_2Cl_2 (15 mL). The reaction mixture was cooled to 0 °C and a solution of EDCI (75 mg, 0.38 mmol) in dimethyl formamide (100 μL) was added. The mixture was stirred at 0 °C for 1 h, brought to room temperature and stirred overnight. Upon completion of the reaction (*cf.* TLC), the solvent was removed under vacuum. Water was added to the residue and the

mixture extracted with CH_2Cl_2 (3 × 10 mL). The combined organic extracts were dried and evaporated to get the crude coupled product, which was purified by silica gel column chromatography using EtOAc/ $CHCl_3$ (1:9 v/v) mixture to obtain **7b**.

Yield: 55% (126 mg), R_f = 0.3 [EtOAc/ $CHCl_3$ (1:9 v/v)]

IR (neat, cm^{-1}): 3056 (w); 2919 (s); 2849 (m); 1740 (s); 1651 (s).

^{1}H NMR ($CDCl_3$, δppm): 7.20-7.39 (m, 15H, $(C_6\underline{H}_5)_3C$-); 5.98 (d, 1H, -CON<u>H</u>-, *J = 7.8 Hz*); 4.58-4.62 (m, 1H, -NHC<u>H</u>CH_2S-); 4.15 (q, 2H, -COOC<u>H_2</u>CH_3, *J = 7.0 Hz*); 2.59-2.63 (m, 2H, -CHC<u>H_2</u>S-); 2.32 (t, 2H, -CH_2C<u>H_2</u>CONH-, *J = 7.4 Hz*); 2.15 (t, 2H, -CH_2C<u>H_2</u>COOH, *J = 7.4 Hz*); 1.58 (bs, 4H, -C<u>H_2</u>CH_2COOH & -C<u>H_2</u>CH_2CONH-); 1.20-1.24 (bs, 23H, $(C\underline{H}_2)_{10}$ & -$COOCH_2C\underline{H}_3$) [Fig. 3.13].

16-(*S*-trityl cysteinyl amido) hexadecanoic acid **(7c)**

A mixture of compound **7b** (98 mg, 0.15 mmol) and aqueous 1M KOH solution (300 µL, 0.3 mmol) in MeOH (600 µL) was stirred at room temperature for 2 days. Upon completion of the reaction (*cf.* TLC), MeOH was removed under vacuum, water (5 mL) added and the pH of the mixture was adjusted to 3 using aqueous 2N HCl to get compound **7c** as a white precipitate. This was filtered and dried under vacuum.

Yield: 80% (75 mg), R_f = 0 [EtOAc/ $CHCl_3$, (1:9 v/v)].

^{1}H NMR ($CDCl_3$, δppm): 7.26-7.32 (m, 15H, $(C_6\underline{H}_5)_3C$-); 5.74-5.90 (m, 1H, -CON<u>H</u>-); 4.9-5.04 (m, 1H, -NHC<u>H</u>CH_2S-); 2.24-2.40 (m, 2H, -CHC<u>H_2</u>S-,); 2.00-2.18 (m, 4H, -CH_2C<u>H_2</u>COOH & -CH_2C<u>H_2</u>CONH-); 1.43-1.67 (m, 4H, -C<u>H_2</u>CH_2COOH & -C<u>H_2</u>CH_2CONH-); 1.26-1.42 (bs, 20H, $(C\underline{H}_2)_{10}$) [Fig. 3.14].

MS (ESI, -ve mode): Mass (calculated) $C_{38}H_{49}NO_5S$ 631.3; *m/z* (observed) 630.8 [Fig. 3.15].

16-(cysteinyl amido) hexadecanoic acid (**7**)

The compound **7** (50 mg, 0.08 mmol) was stirred with trifluoroacetic acid (TFA) (2 mL) for 10 min at room temperature. To the resultant yellow solution, triethylsilane was

added dropwise until the solution turned colorless. Stirring was continued for another 15 min. The solvent was removed under vacuum to obtain the desired product **7** which was dried under vacuum and used as such for radiolabeling without further characterization.

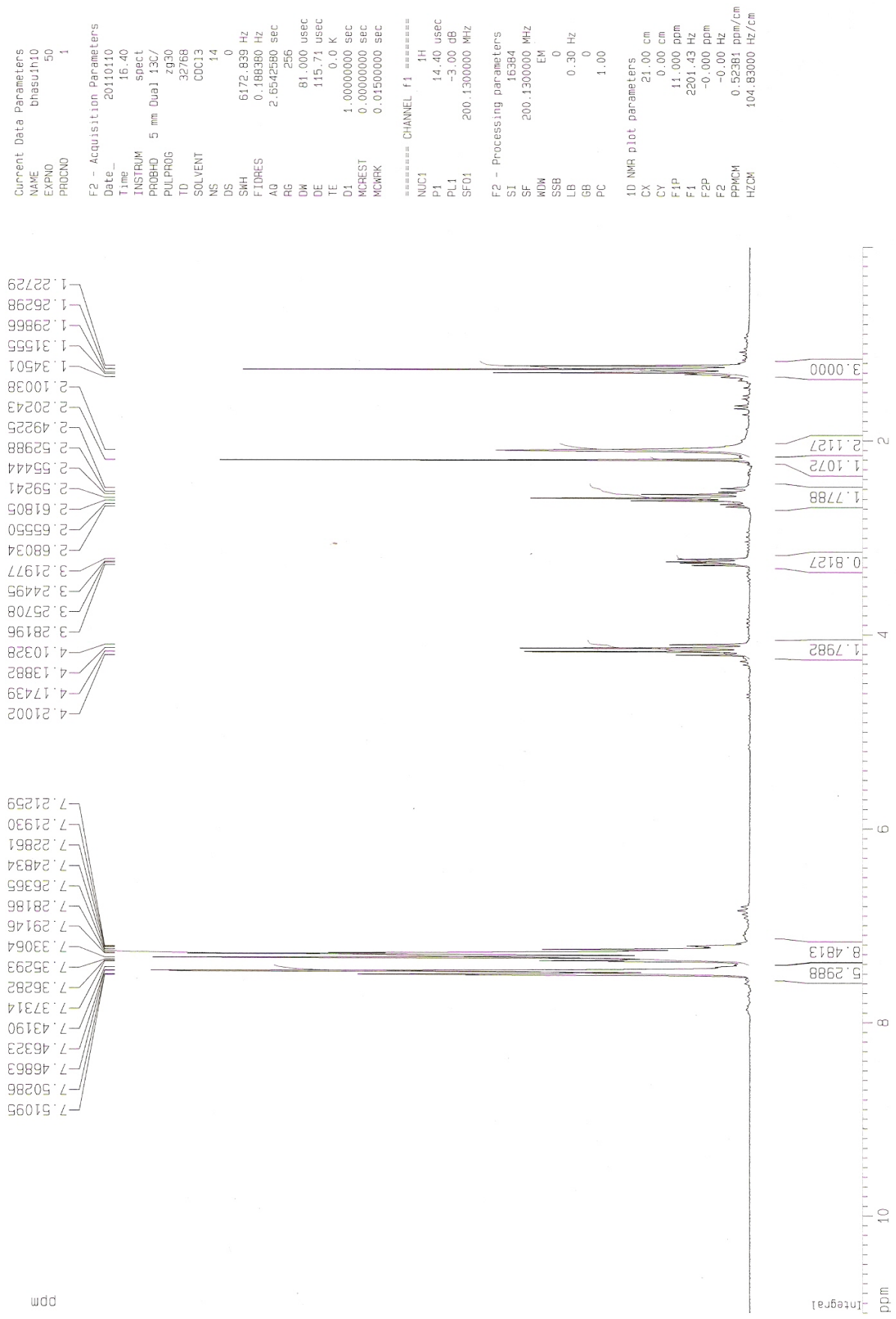

Fig. 3.11 ^{1}H NMR spectrum of compound **7a**

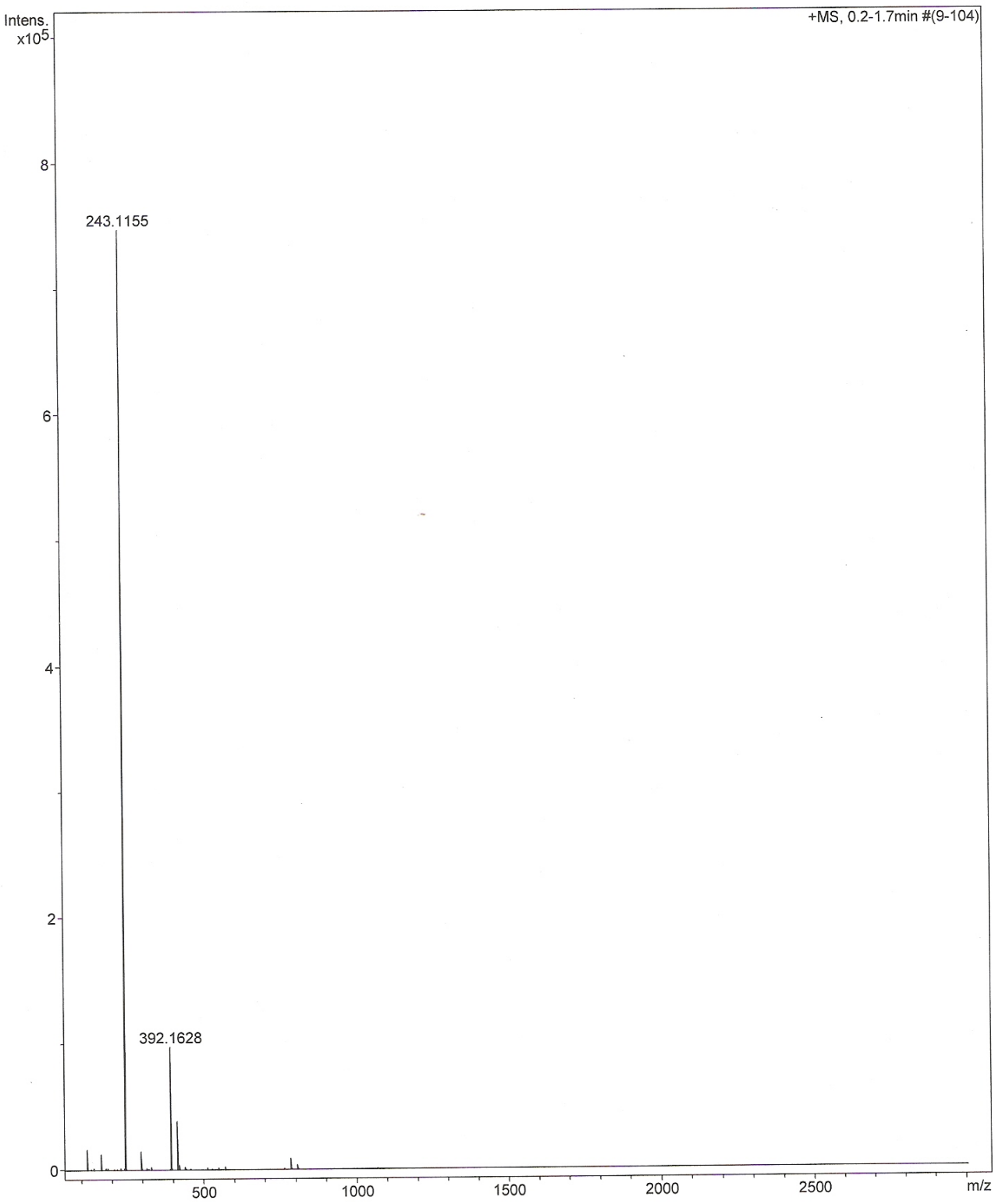

Fig. 3.12 Mass spectrum of compound **7a**

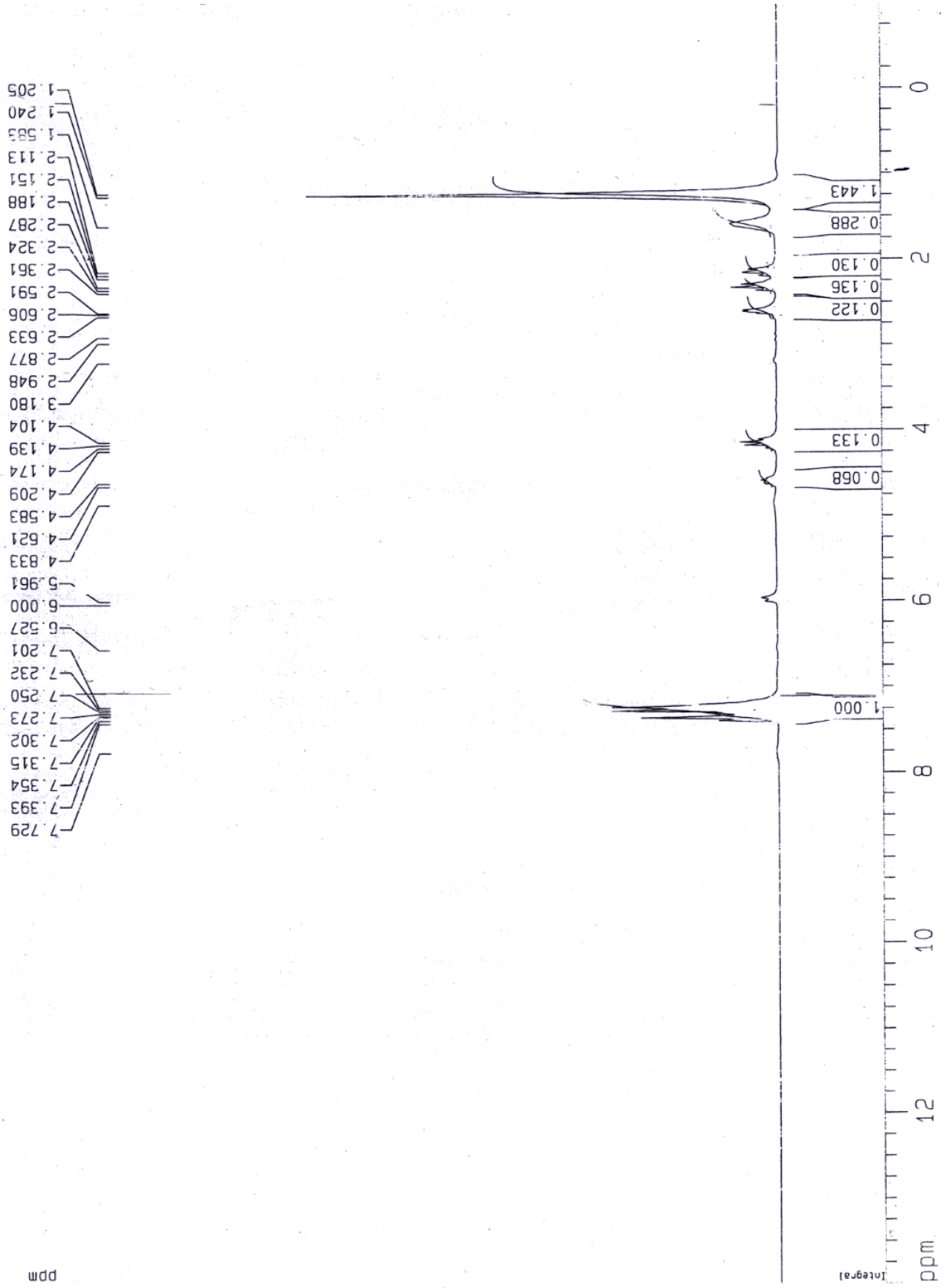

Fig. 3.13 ^{1}H NMR spectrum of compound **7b**

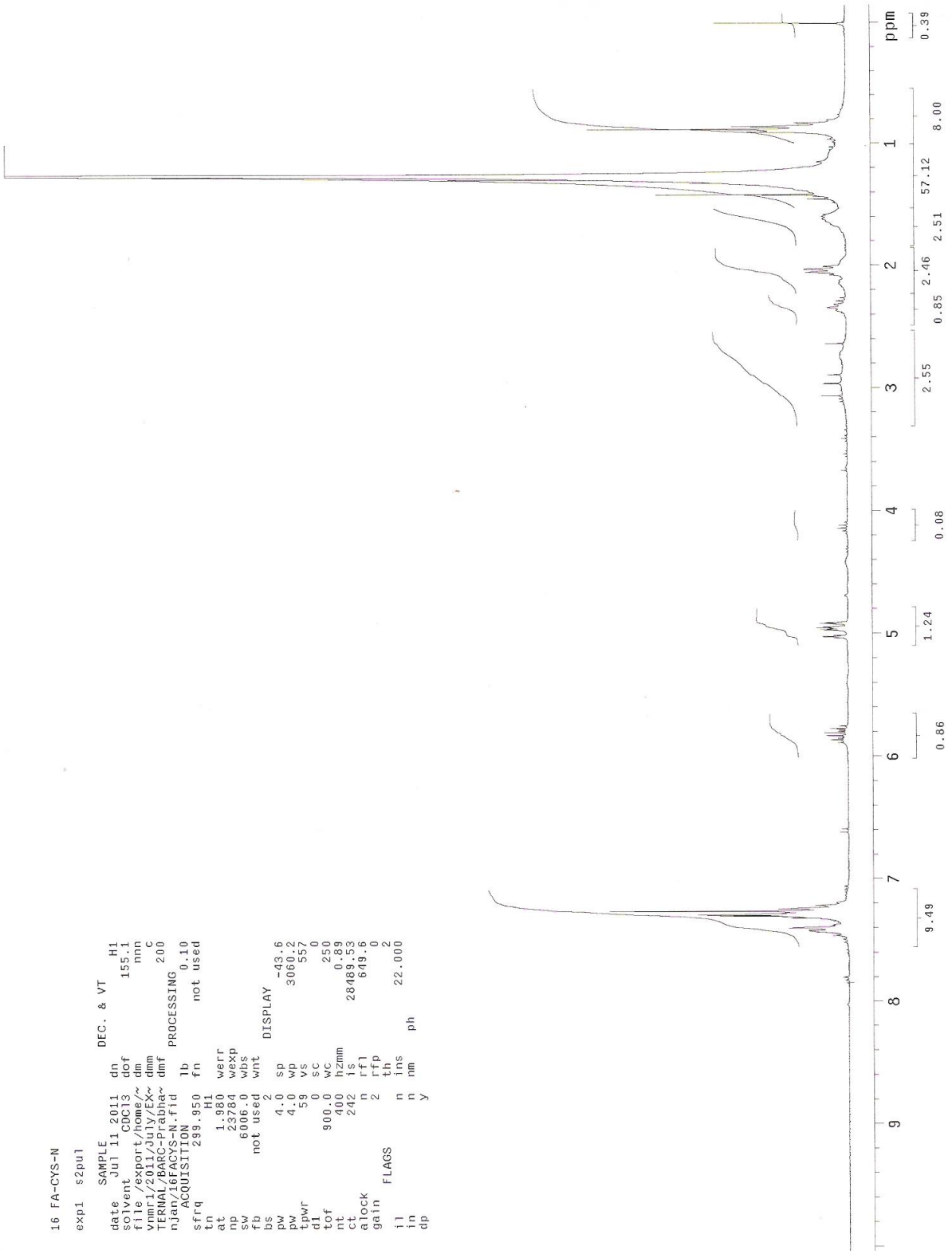

Fig. 3.14 ^{1}H NMR spectrum of compound **7c**

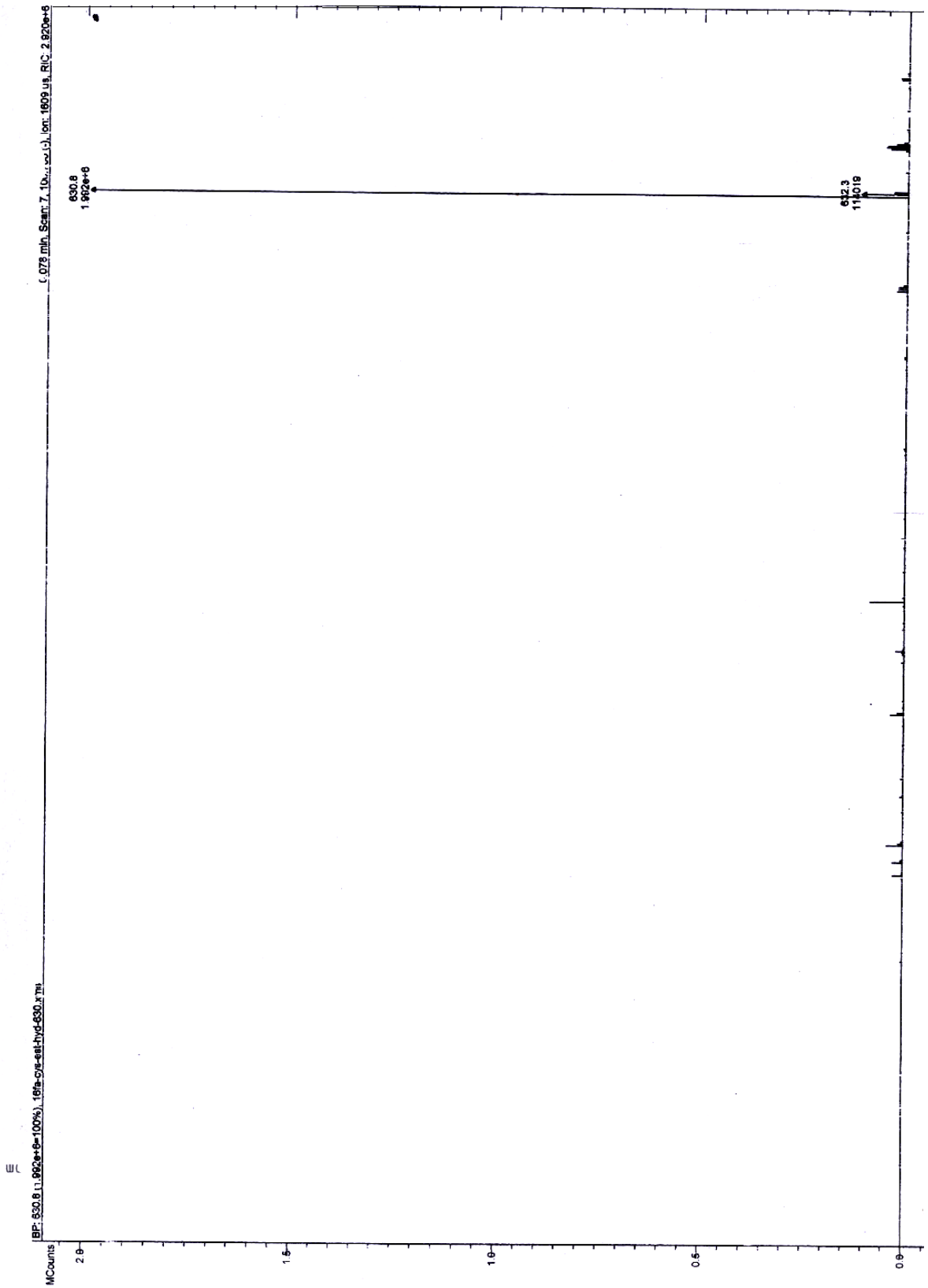

Fig. 3.15 Mass spectrum of compound **7c**

3.2.3 Radiolabeling

3.2.3.1 *Preparation of $[^{99m}TcN]^{2+}$ core*

The formation of this core was carried following a literature procedure.[187] Succinic dihydrazide (5 mg), stannous chloride (0.1 mg dissolved in 100 µL water) and ethanol (250 µL) were taken in a vial to which $Na^{99m}TcO_4$ (750 µL, 37 MBq or 1.85 GBq) was added. The reaction mixture was kept at room temperature for 20 min for the formation of the $[^{99m}TcN]^{2+}$ intermediate.

3.2.3.2 *Preparation of $[^{99m}TcN(PNP)]^{2+}$ intermediate complexes* (**4C**-**6C**)

The PNP ligands **4**, **5** and **6** (3-5 mg) in ethanol (500 µL) were added to three 10 mL glass vials, each containing the $[^{99m}TcN]^{2+}$ core (500 µL). The capped vials were heated on a water bath at 90 °C for 30 min. The vials were brought to room temperature and the products **4C**, **5C** and **6C** characterized by HPLC.

3.2.3.3 *Preparation of $^{99m}TcN(PNP)$ fatty acid complex* (**7C**)

The procedure followed for the formation of asymmetric complex **7C** is as reported by Boschi *et al.*[187] To the prepared $[^{99m}TcN]^{2+}$ core (750 µL, 1.85 GBq or 50 mCi) was added the PNP ligand **6** (~3 µL) alongwith compound **7** (~5 mg), each dissolved in ethanol (250 µL, purged with nitrogen for 15 min) and the reaction mixture heated at 90 °C for 30 min. The final complex **7C** was characterized by HPLC.

3.2.3.4 *Preparation of ^{125}I-p-iodophenylpentadecanoic acid (IPPA)*

The labeling of IPPA with ^{125}I was carried out by a reported isotope exchange method.[62] IPPA (2-3 mg), $CuSO_4.5H_2O$ (68 µg in 20 µL water), sodium metabisulfite (4 mg) and glacial acetic acid (50 µL) were taken in a 10 mL vial to which was added $Na^{125}I$ (50 µL, 185 MBq or 5 mCi). The capped vial was heated at 160 °C for 35-40 min in an oil bath. The vial was cooled and aqueous CH_3COONa solution (2 mL, 0.76 M) was added to the reaction mixture. The labeling yield was ascertained by paper electrophoresis and HPLC. The labeled

product was separated from the unreacted iodide by solvent extraction using CH_2Cl_2. The organic extract was flushed with nitrogen to remove dichloromethane and reformulated in aqueous 10% ethanol. The pure product was characterized by paper electrophoresis and HPLC.

3.2.4 Quality control techniques

3.2.4.1 *Electrophoresis*

Paper electrophoresis was done using a 37 cm long strip of Whatman No.3 chromatography paper and 0.05 M sodium acetate solution. About 2 µL of the test solution was spotted at the middle of the strip and the electrophoresis was carried out for 30 min at a potential gradient of 10 V/cm. The strip was dried and the radioactivity profile determined using a TLC chromatography evaluation system.

3.2.4.2 *HPLC*

The radiochemical purities of the three $[^{99m}TcN(PNP)]^{+2}$ intermediate complexes **4C**-**6C** and the asymmetric complex **7C** were assessed by HPLC using a C18 reversed phase column. Water (A) and acetonitrile (B) were used as the mobile phase with the following gradient elution (0 min 90% A, 28 min 10% A, 50 min 10% A). The radiolabeling yield and radiochemical purity of ^{125}I-IPPA was carried out under isocratic condition using acetonitrile (0.1% TFA): water (0.1% TFA) (90:10) mixture as the mobile phase. Flow rate was maintained at 1 mL/ min. About 25 µL of the test solution was injected into the column and elution was monitored by observing the radioactivity profile.

The same C18 reversed phase analytical column was used for the purification of complex. This could be possible by taking high radioactive concentrations of initial ^{99m}Tc activity. The initial amount of ^{99m}Tc radioactive concentration used for the radiolabeling was 1.85 GBq (50 mCi)/ mL. On purification through HPLC, around 18.5 MBq (500 µCi) of the radiolabeled fatty acid product was obtained in acetonitrile-water medium which was

removed under vacuum and reformulated in aqueous 10% ethanol solution. This was used for carrying out the *in-vivo* evaluation studies.

3.2.4.3 ***Partition coefficient (Log$P_{o/w}$)***

The HPLC purified labeled compound (0.1 mL, 185 KBq or 5 μCi) was mixed with water (0.9 mL) and octanol (1 mL) on a vortex mixer for about 1 min and then centrifuged for 5 min to effect the separation of the two layers. Equal aliquots of the two layers were withdrawn and measured for the radioactivity. The readings thus obtained were used to calculate the Log $P_{o/w}$ value of the complex.

3.2.4.4 ***Stability studies***

3.2.4.4.1 *Ligand exchange studies*

The stability of the complex towards ligand exchange was studied using cysteine as the challenging ligand. For this, [^{99m}TcN(PNP6)] fatty acid complex (~100 μL) was added to 900 μL of phosphate buffered saline containing 10-500 fold molar excess of cysteine over that of the ligand. The samples were incubated at 37 °C for 1 h and then analyzed by HPLC.

3.2.4.4.2 *Serum stability*

Stability of the complex **7C** in serum was tested *in-vitro*. About 50 μL of the radiolabeled preparation was added to 450 μL serum and the mixture was incubated at 37 ºC for 1 h. To this mixture, equal volume of cold ethanol was added to precipitate the serum proteins and centrifuged at 10000 g (4 °C, 20 min). The supernatant was analyzed by HPLC to assess stability of the complex in serum. The precipitate was washed twice with ethanol and counted in the NaI (Tl) scintillation detector to determine the activity associated with serum proteins.

3.2.4.5 ***Bio-distribution studies***

All procedures performed herein were in accordance with the national laws pertaining to the conduct of animal experiments. Normal Swiss mice (20–25 g body weight) were used

for the *in-vivo* distribution assays of the prepared fatty acid complexes. All the mice involved in the study were kept under fasting for 6-7 h prior to the experiment, while water was given *ad libitum*. The HPLC purified radiolabeled preparation (100 μL, 740 kBq or 20 μCi) was administered intravenously through tail vein of each animal. Individual sets of animals (n=3) were utilized for studying the bio-distribution at different time points (2 min, 5 min, 10 min and 30 min). The animals were sacrificed immediately at the end of the respective time point and the relevant organs and tissue were excised for measurement of associated activity. The organs were weighed and the activity associated with each was measured in a flat-bed type NaI (Tl) counter with suitable energy window for ^{99m}Tc (140 keV ± 10%). For the sake of comparison, the activity retained in each organ/tissue was expressed as a percent value of the injected dose per gram (% ID/g).

3.3 Results and discussion

3.3.1 Synthesis of ligands

3.3.1.1 *π-acceptor ligands*

The synthetic schemes for the preparation of the PNP ligands **4** and **5** are shown in Fig. 3.16 and Fig. 3.17, respectively. The synthesis of **4** involved alkylation of diethanolamine with methoxyethyl bromide in acetonitrile in the presence of anhydrous K_2CO_3 as the base to give the *N*-alkylated diethanolamine derivative **4a**. This was then transformed into the corresponding dichloride **4b** using freshly distilled $SOCl_2$. Compound **4b** was subsequently reacted with two equivalents of 0.5 M potassium diphenyl phosphide solution to give the desired PNP ligand **4**.

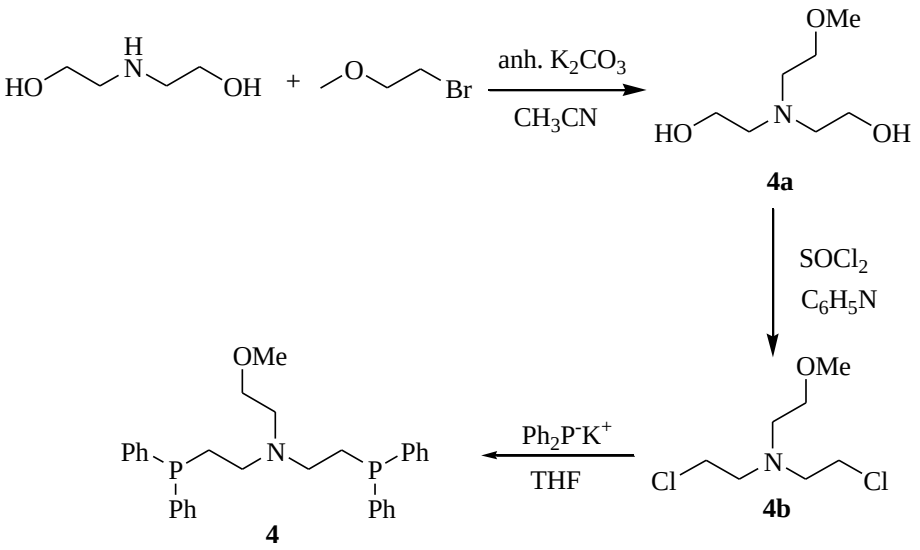

Fig. 3.16 Synthesis of PNP ligand **4**

The PNP ligand **5** was prepared in a single step by *P*-alkylation with *N*-methyl bis(2-chloroethyl) amine hydrochloride at -78 ^{o}C using n-BuLi as the base. The low temperature conditions were desired to prevent the degradation of amine dichloride compound. The ^{31}P NMR spectrum of **5** showed the presence of impurities which could not be removed completely. However, the ligand labeled efficiently with $[^{99m}TcN]^{2+}$ core indicating the nature of impurities did not interfered with the labeling.

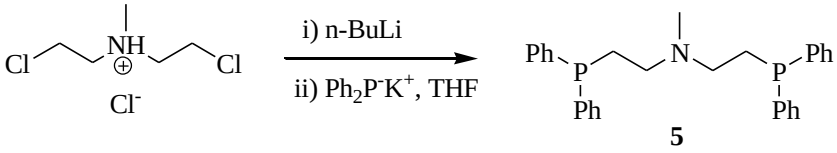

Fig. 3.17 Synthesis of PNP Ligand **5**

3.3.1.2 *π-donor ligand*

The π-donor ligand **7** was designed to contain a carrier biomolecule that shows good target organ specificity inside the body. For this, we chose thapsic acid, a fatty acid as the biomolecule, because of its affinity for the myocardium. Thus, radiolabeled fatty acids have potential for use as tracers to image myocardial metabolism. In order to retain its biological behavior inside the body, the fatty acid should be radiolabeled without synthetically

modifying the carboxylic acid group.[216] In view of this, we derivatized only one of the acid groups of the biomolecule by attaching a cysteine moiety as the bi-functional chelator, while the other acid group was kept intact.

The synthetic scheme for the formation of π-donor ligand is shown in Fig. 3.18. Thus, the acid group of *S*-trityl cysteine was converted to the corresponding ethyl ester **7a**. For this, ethyl p-toluene sulphonate was used as a mild alkylating agent so that the esterification could be carried out under neutral conditions. The amino group of **7a** was then conjugated to one of the carboxylic acid groups of hexadecanedioic acid using 1:1 molar equivalent of reagents and EDCI as the activating agent. The ethyl ester group of the coupled fatty acid derivative **7b** was hydrolyzed under alkaline conditions to give the coupled tritylated fatty acid derivative **7c**. Finally, the target ligand **7** was obtained by removing the trityl protecting group of **7c** with TFA. The deprotection of trityl group generates the stable triphenylcarbonium ion (Ph_3C^+), which can react with the free thiol group. Hence, a hydride donor Et_3SiH was added in the reaction mixture to neutralize the Ph_3C^+ ion and prevent the back reaction. The target ligand **7** contained free SH, COOH groups of the cysteine residue in suitable stereochemical orientations for labeling with the $[^{99m}TcN(PNP)]^{2+}$ core.

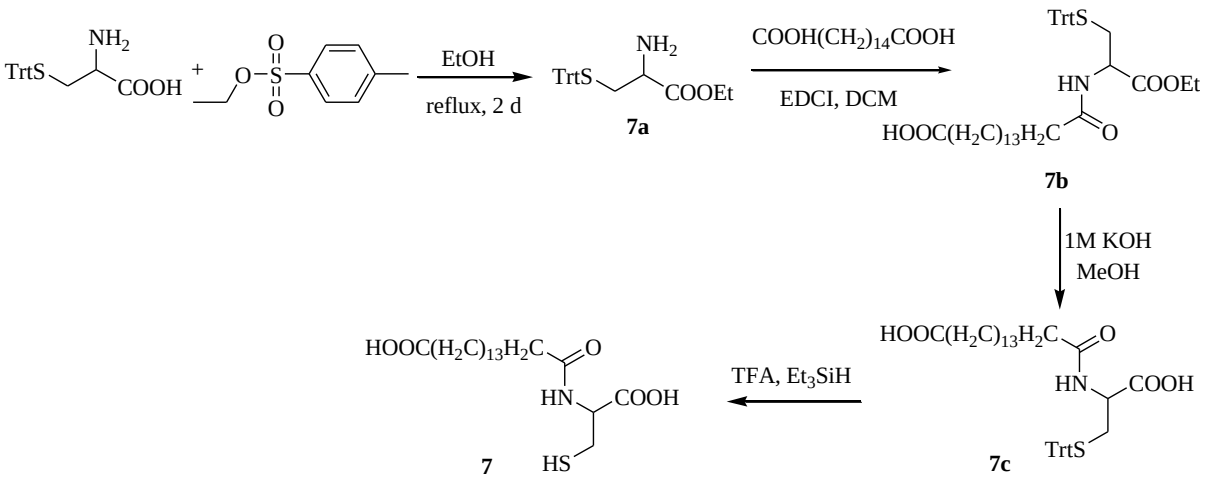

Fig. 3.18 Synthesis of fatty acid-cysteine conjugate **7**

3.3.2 Radiolabeling

The [^{99m}TcN(PNP)]$^{2+}$ intermediate complexes **4C**, **5C** and **6C** were prepared by reacting the [^{99m}TcN]$^{2+}$ core with the three PNP ligands (**4**, **5** and **6**) [Fig. 3.19(a)]. The formation of the [^{99m}TcN(PNP)]$^{2+}$ intermediate complex was characterized by HPLC (Fig. 3.20). The HPLC patterns of the three intermediate [^{99m}TcN(PNP)]$^{2+}$ complexes were observed to have multiple peaks which may be due to the presence of several labile intermediate complexes arising from weak co-ordination of anions present in the medium with the vacant *cis* positions in [^{99m}TcN(PNP)]$^{2+}$ intermediate.

The final [^{99m}TcN(PNP)] fatty acid complex **7C** was prepared by reacting the [^{99m}TcN]$^{2+}$ core alongwith PNP ligand **6** and fatty acid derivative **7** [Fig. 3.19 (b)]. The ^{99m}Tc complex **7C** was prepared using **6**, as it has several *in-vivo* metabolizable ether groups in the alkyl chain, which facilitate fast non-target clearance of the complex **7C** inside the body.

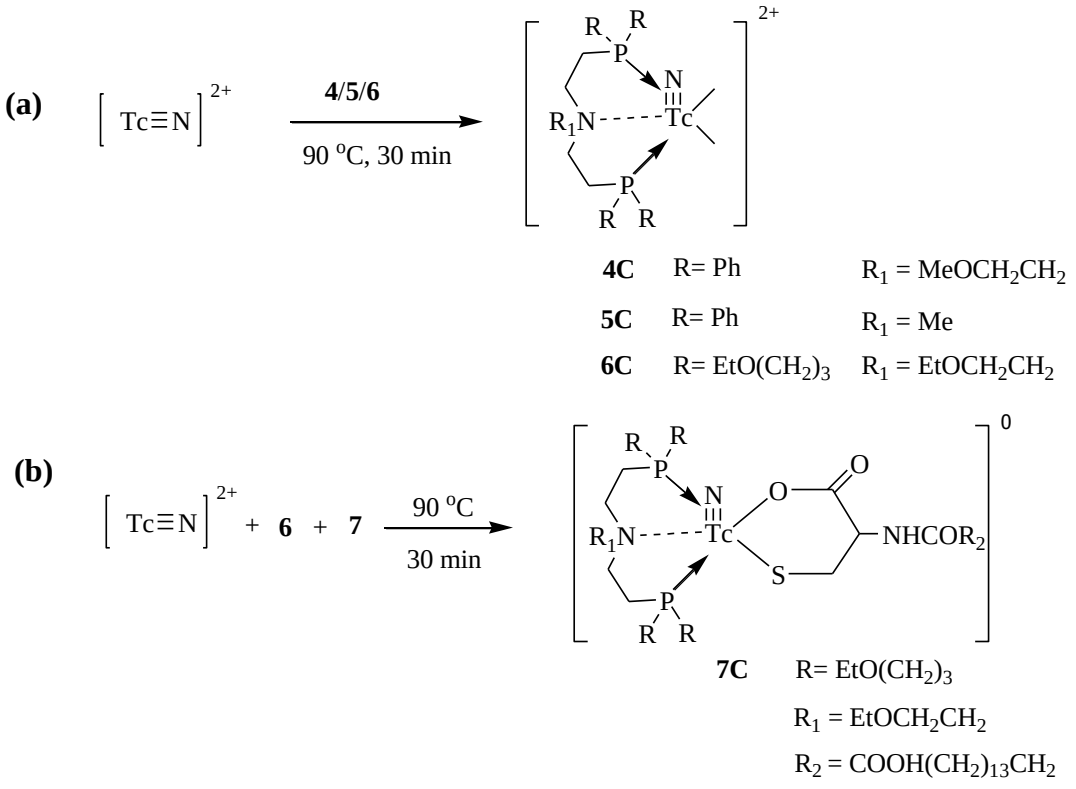

Fig. 3.19 Syntheses of (a) [^{99m}TcN(PNP)]$^{2+}$ intermediate complexes and (b) complex **7C**

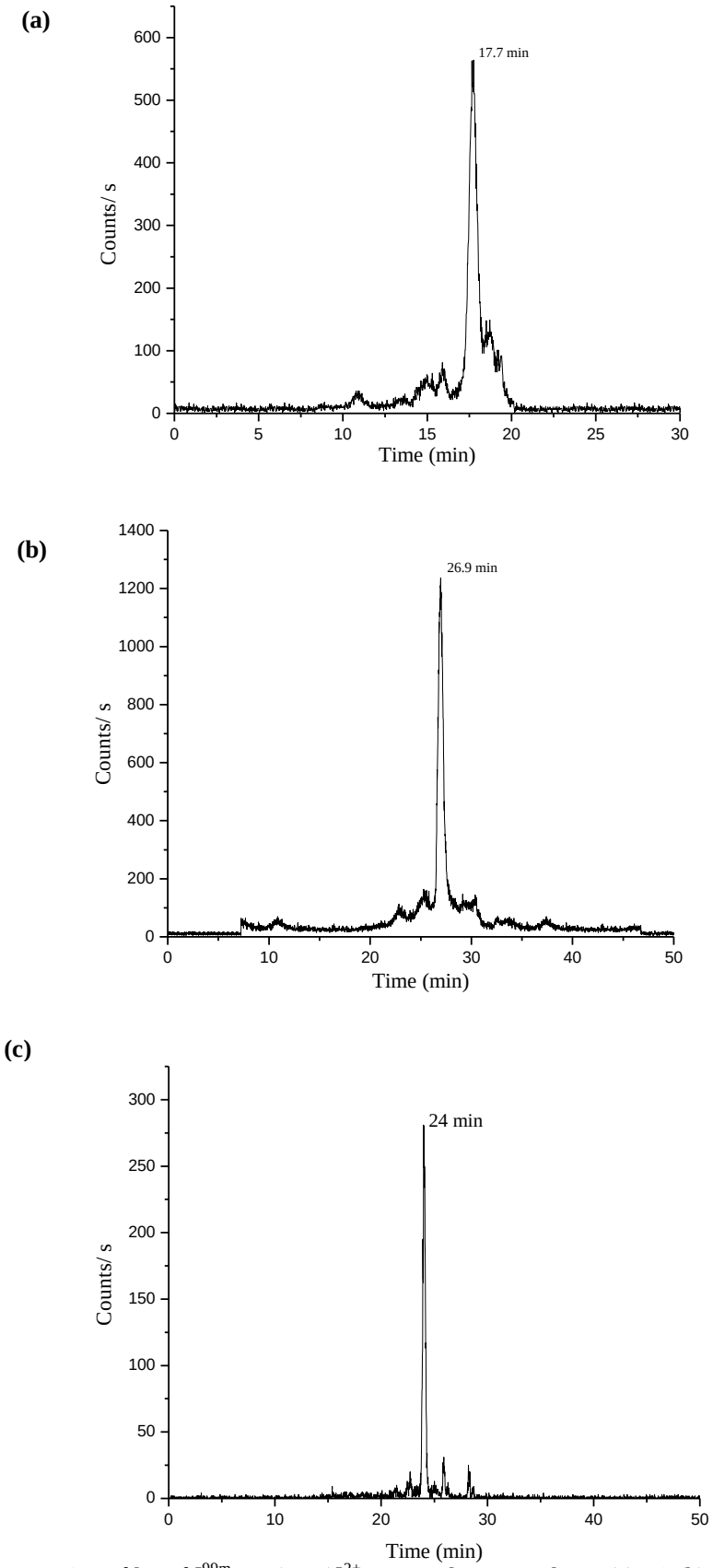

Fig. 3.20 HPLC profiles of $[^{99m}TcN(PNP)]^{2+}$ intermediate complexes (a) **4C** (b) **5C** and (c) **6C**

In the present study, fatty acid derivative **7** has been prepared with the cysteine residue having free thiol and acid groups. It is therefore logical to presume that the structure of the final complex **7C** formed is similar to the square pyramidal neutral [^{99m}TcN(PNP)] complex reported earlier.[187,247] The final complex **7C** was obtained in more than 80% radiolabeling yield as characterized by HPLC (Fig. 3.21). The asymmetric centre in the cysteine residue leads to the formation of a mixture of *syn* and *anti* isomers of the **7C** complex.[190] The HPLC chromatography of the complex revealed two closely spaced peaks accounting for the diastereomeric pair with the predominance of one diastereomer. Stereochemistry of the isomers can be unambiguously ascertained only after preparing the complex in macroscopic level using the long lived ^{99}Tc or inactive rhenium analogue and subsequent characterization. However, this was not attempted considering our major objective to examine the bio-distribution of the complex for its potential application as a myocardial agent. The biological studies were carried out with the major isomer (61%) which was isolated using HPLC.

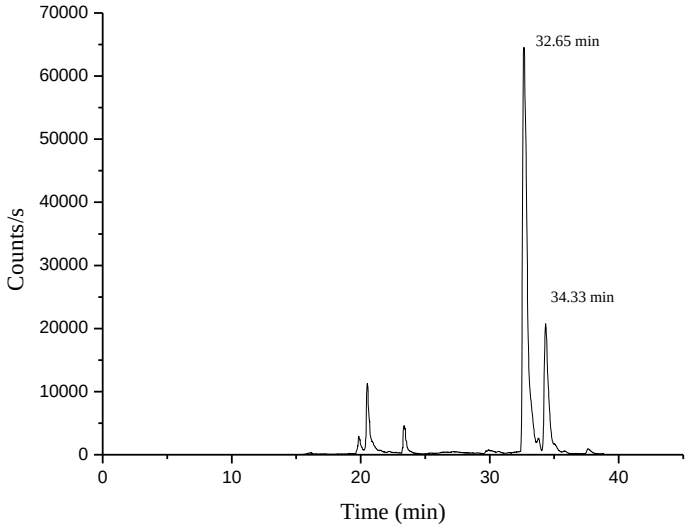

Fig. 3.21 HPLC profile of complex **7C**

3.3.3 Biological studies

3.3.3.1 Stability and hydrophobicity of the complex **7C**

The desirable attributes of a myocardial imaging agent are (i)-(iv) as discussed in chapter 2 (section 2.2.3.3). Hence, for the present work, we have first examined the *in-vitro* behavior of complex **7C** to assess the *in-vivo* kinetic inertness of the final complex. In this view, as the first step of bio-evaluation, the *in-vitro* stability of the complex **7C** was studied in presence of challenging ligand cysteine. Even in the presence of a large excess (up to 50 fold) cysteine, no transchelation of the complex with free cysteine was noticed. This was confirmed by HPLC wherein the retention of radioactive peak was observed. However, at 500-fold excess of cysteine, appreciable exchange (~28 %) was observed. Subsequently, the stability of the complex in serum was assessed. Incubation of the complex in serum up to 1 h did not show appreciable degradation. An insignificant amount of activity (<4%) was found to be associated with the precipitated serum proteins. To assess the hydrophobic nature of the complex, the Log $P_{o/w}$ value of the present complex was carried using octanol-water system and was found to be 1.8.

The bio-evaluation of the complex **7C** warranted comparison with a known standard agent. ^{123}I labeled IPPA is a known radiopharmaceutical for metabolic cardiac imaging and is routinely used clinically, worldwide. However, ^{123}I-IPPA is not available in India. Hence, we synthesized ^{125}I-IPPA as a substitute and used it as the standard. For this, IPPA was labeled with ^{125}I via a Cu(I)- assisted nucleophilic isotopic exchange reaction. ^{125}I-IPPA could be obtained in 57% radiolabeling yield, as ascertained by paper electrophoresis (R_f = 0) and HPLC. The HPLC elution profile of ^{125}I-IPPA showed $^{125}I^-$ peak at 3 min and the labeled product appeared as a sharp peak at 19 min. The labeled product was purified by extraction in CH_2Cl_2. The radiochemical purity of purified ^{125}I-IPPA was found to be more than 98% by paper electrophoresis.

3.3.3.2 Bio-distribution of 7C

In order to evaluate the potential of complex **7C** as myocardial agent, in terms of *in-vivo* parameters, the bio-distribution studies were carried in Swiss mice and compared with the standard agent. The bio-distribution results of **7C** isomer and ^{125}I-IPPA in Swiss mice are shown in Tables 3.1 and 3.2 respectively. Fig. 3.22 shows the myocardial uptake and clearance pattern of the complex **7C** as well as ^{125}I-IPPA. It was observed that the initial uptake of the complex **7C** (3.75 ± 0.28% ID/g) at 2 min post-injection (p.i.) was significantly less than 9.51 ± 1.61% ID/g that of ^{125}I-IPPA. In contrast to ^{125}I-IPPA, the initially accumulated activity of **7C**, was not retained as indicated by the quick clearance from the myocardium. After 30 min p.i., the residual activity of **7C** in the myocardium was 0.39 ± 0.05% ID/g.

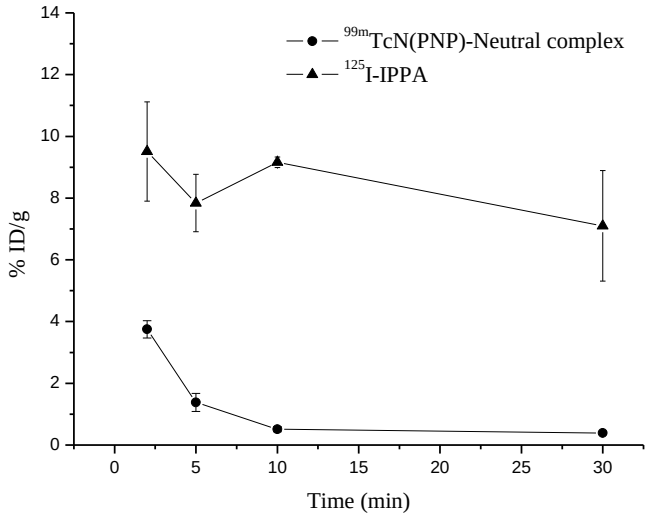

Fig. 3.22 Myocardial uptake pattern of the complex **7C** in comparison with ^{125}I-IPPA

Table 3.1 Bio-distribution of complex **7C** in Swiss mice [% ID/g (1SD), (n=3)]

Organs	*2 min*	*5 min*	*10 min*	*30 min*
Liver	38.80 (2.88)	29.88 (5.62)	24.01 (2.49)	5.98 (1.55)
Intestine	5.84 (1.53)	17.05 (3.20)	17.52 (0.24)	38.91 (4.10)
Kidney	23.48 (5.88)	12.94 (1.18)	5.75 (1.02)	5.38 (2.53)
Heart	3.75 (0.28)	1.38 (0.29)	0.51 (0.08)	0.39 (0.05)
Lungs	5.44 (0.66)	2.70 (0.54)	1.18 (0.15)	1.14 (0.22)
Muscle	0.95 (0.06)	0.86 (0.07)	0.32 (0.04)	0.23 (0.05)
Blood	12.18 (1.54)	3.20 (0.36)	1.52 (0.26)	0.89 (0.06)
Heart/Blood	0.31 (0.03)	0.43 (0.05)	0.34 (0.02)	0.44 (0.05)
Heart/Lungs	0.69 (0.07)	0.52 (0.12)	0.43 (0.04)	0.35 (0.04)
Heart/Liver	0.10 (0.01)	0.05 (0.01)	0.02 (0)	0.07 (0.02)

Table 3.2 Bio-distribution of ^{125}I-IPPA in Swiss mice [% ID/g (1SD), (n=3)]

Organs	*2 min*	*5 min*	*10 min*	*30 min*
Liver	49.39 (6.67)	34.03 (3.45)	47.94 (10.04)	30.40 (6.82)
Intestine	2.09 (0.62)	2.65 (0.46)	2.73 (0.24)	4.81 (1.52)
Kidney	9.96 (2.58)	11.02 (0.1)	15.11 (0.04)	11.25 (1.18)
Heart	9.51 (1.61)	7.84 (0.93)	9.16 (0.17)	7.10 (1.79)
Lungs	23.93 (5.26)	14.47 (3.34)	12.23 (2.39)	11.39 (2.55)
Muscle	1.57 (0.23)	1.91 (0.16)	2.06 (0.01)	1.94 (0.34)
Blood	5.12 (0.52)	5.53 (0.57)	6.36 (1.12)	6.42 (1.59)
Heart/Blood	1.86 (0.24)	1.43 (0.25)	1.46 (0.29)	1.11 (0.07)
Heart/Lungs	0.4 (0.05)	0.56 (0.13)	0.77 (0.16)	0.62 (0.02)
Heart/Liver	0.2 (0.06)	0.23 (0.05)	0.20 (0.04)	0.23 (0.01)

The time dependent changes in the heart/ blood, heart/ lung and heart/ liver ratios with the neutral complex **7C** and ^{125}I-IPPA are shown in Fig. 3.23(a-c). Very little differences in the heart/ lung and heart/ liver ratios were seen among the two labeled fatty acids. However, ^{125}I-IPPA showed better heart/ blood ratio compared to the ^{99m}Tc complex.

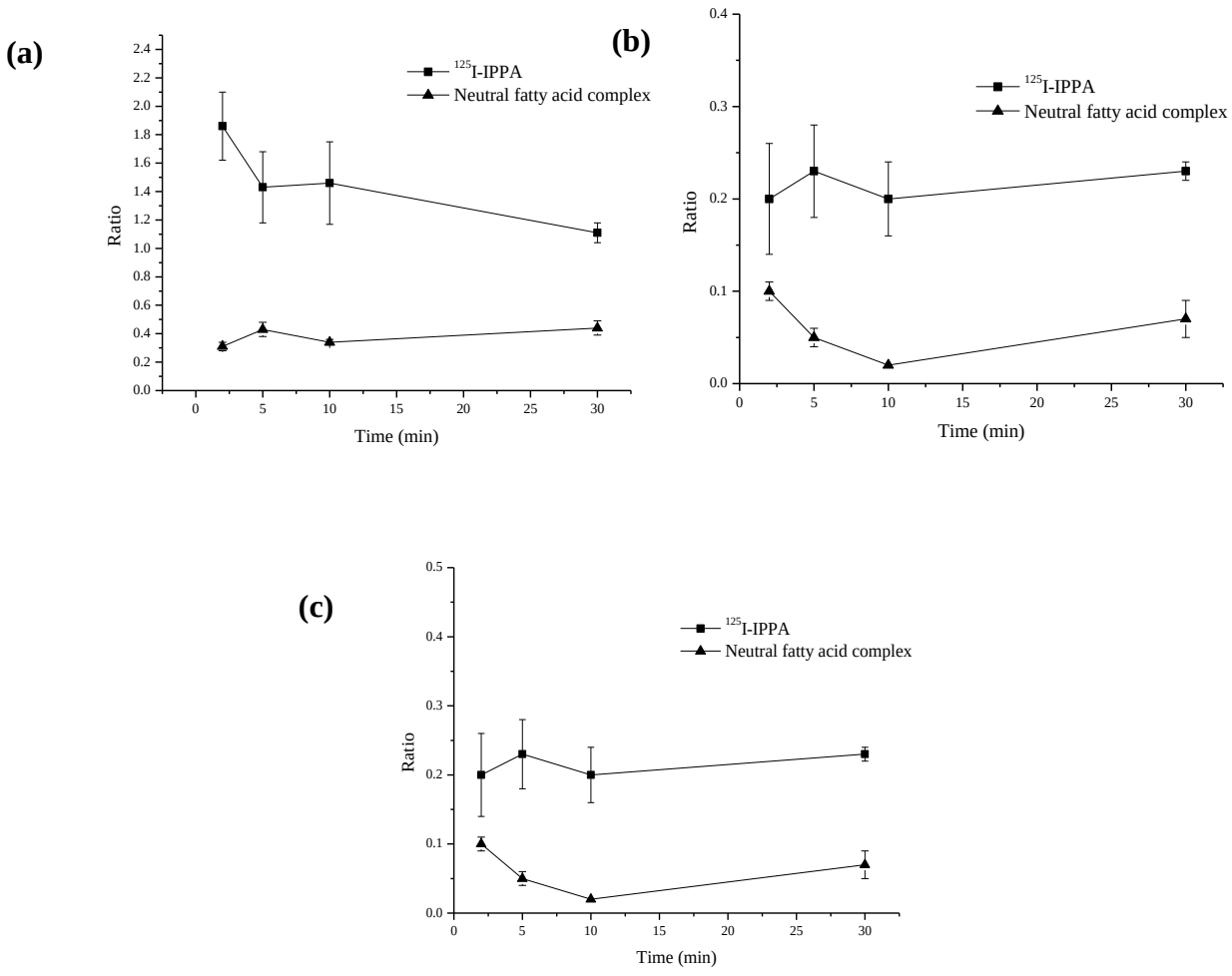

Fig. 3.23 Time dependent changes in the (a) heart/ blood (b) heart/ lung (c) heart/ liver ratios of the complex **7C** and ^{125}I-IPPA

The clearance of activity from different organs exhibited by the two radiolabeled compounds is shown in Fig. 3.24. The complex **7C** showed high initial uptake in liver, lungs and blood, but cleared faster. However, the critical ratios *viz.* heart/ liver, heart/ lung and heart/ blood remained sub-optimal, due to rapid washout of the activity from the target organ as well. The [^{99m}TcN(PNP**6**)]-fatty acid complex cleared mostly through hepatic route as evident from the increase in the radioactivity in intestine. The high rise in intestinal radioactivity with time indicated fast clearance of **7C** from liver which may be due to the

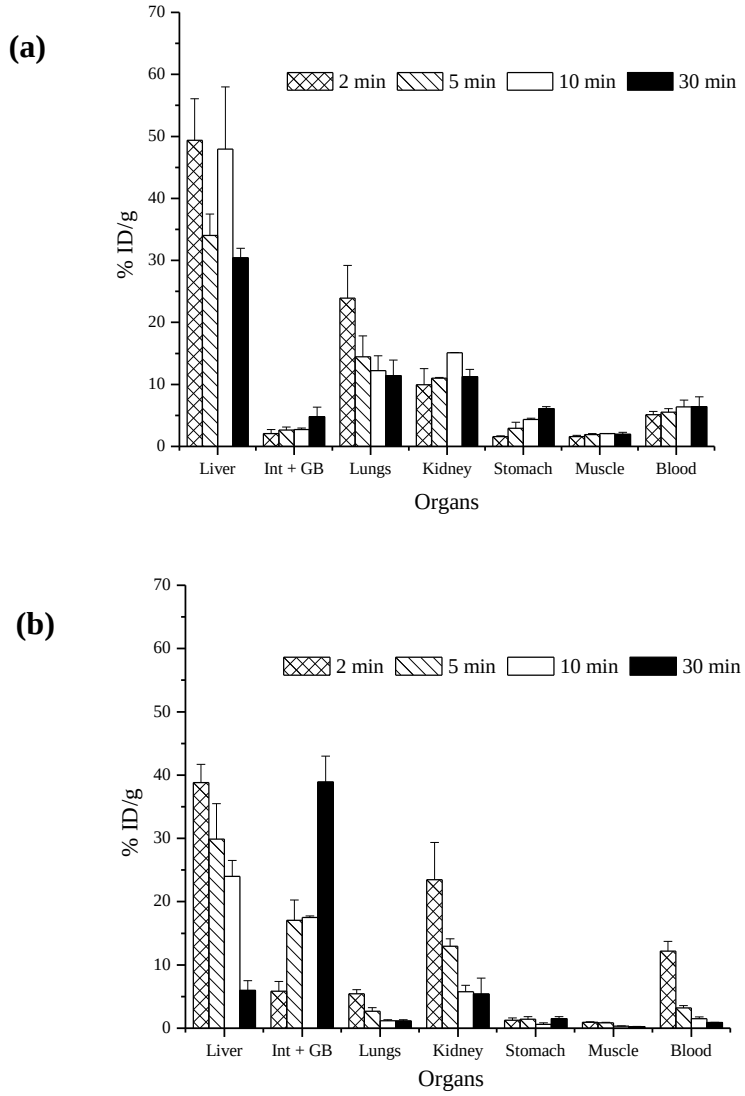

Fig. 3.24 Clearance patterns of (a) ^{125}I-IPPA and (b) complex **7C** from non-target organs

metabolism of ether groups of its constituent PNP ligand in the liver. This would furnish a more hydrophilic species which would get cleared rapidly. P-glycoproteins (Pgp) or multidrug resistance-associated protein (MDR)-Pgp may also be responsible for rapid elimination of lipophilic compounds such as [^{99m}TcN(PNP)] from the tissues.[249] Although the *in-vivo* behavior of the ^{99m}Tc labeled fatty acid currently studied was not good enough for use in myocardial imaging, these studies have provided an insight into preparation and behavior of ^{99m}Tc labeled fatty acids using [^{99m}TcN(PNP)]$^{2+}$ core.

3.4 Conclusion

The present chapter evaluates the usefulness of the [^{99m}TcN]$^{2+}$ core, for labeling bio-molecules for specific *in-vivo* target imaging. In this respect, an asymmetric [2+2] [^{99m}TcN]-fatty acid complex was synthesized and biologically evaluated in mice. The work involved synthesis of two categories of ligand: π-acceptor (PNP ligands **4** and **5**) and π-donor ligand (**7**). The π-donor ligand contained the fatty acid biomolecule, which together with PNP ligand **6** and [^{99m}TcN]$^{2+}$ core, yielded the final complex **7C** in over 80% radiolabeling yield. The complex was obtained as a mixture of two isomers and the major isomer (61%) was isolated by HPLC and bio-evaluated. Bio-distribution studies in Swiss mice, in distinction to ^{125}I-IPPA, showed low myocardial uptake with rapid washout kinetics. An interesting observation found was rapid washout of the [^{99m}TcN(PNP**6**)]$^{2+}$ fatty acid complex from the non-target organs, such as lungs, liver and blood, an important factor that could lead to significant improvement in the quality of the image. The results indicate the need for synthetic modification of the parent fatty acid molecule with a view to increasing its residence time in the myocardium, with retention of its other favorable features**.**

CHAPTER 4

Asymmetric [2+2] Charged complexes

4.1 Introduction

$[^{99m}Tc{\equiv}N]^{2+}$ core, as discussed previously, forms kinetically inert and thermodynamically stable complexes with a combination of π-donor and π-acceptor ligands.[186,189,195] The addition of a long chain π-acceptor bi-dentate PNP ligand to the $[^{99m}Tc{\equiv}N]^{2+}$ core, generates a new versatile intermediate $[^{99m}TcN(PNP)]^{2+}$, that leads to complexes with varied biological characteristics. The *in-vivo* pharmacokinetics of $[^{99m}TcN(PNP)]$ complexes for the same carrier biomolecule can be suitably altered by changing the lipophilicity and the overall charge of the final complex. The lipophilicity of $[^{99m}TcN(PNP)]$ complexes can be tailored by changing the alkyl substituents present on the phosphorus and nitrogen atoms in the PNP ligand. For example, the presence of phenyl substituent in the PNP ligand increases the lipophilicity leading to delayed clearance of the activity from the background organs. Also, the alkyl ether linkages present on the heteroatoms (P and N) increases the *in-vivo* metabolic clearance from the non-target organs. Apart from this, by using different bi-dentate π-donor chelates such as dithiocarbamates, cysteine, etc. and introducing a hydrophilic or hydrophobic linker between the bi-functional chelating agent (BFCA) and the bio-molecule, the *in-vivo* pharmacokinetic behavior of the complexes can be varied to a great extent.

In addition to lipophilicity, the charge on the final complex is another important parameter for determining the pharmacokinetic behavior of the final complexes inside the body. For example, the negatively charged complexes are known to clear rapidly from the

blood pool via the renal pathway[250] whereas the positively charged lipophilic complexes accumulate in the myocardium for prolonged period due to coulombic attraction with the negatively charged mitochondrial membrane.[201] Also, neutral complexes are desired for crossing the blood brain barrier.[251]

In the case of $[^{99m}TcN(PNP)]^{2+}$ complexes the overall charge can be varied by changing the nature of bi-dentate π-donor groups (Fig. 4.1).[187,190,247] A di-anionic ligand (S^-, COO^-), as reported in the previous chapter, leads to neutral complexes whereas uni-positively '*charged asymmetric [2+2] complexes*' are formed if the π-donor ligand is mono-anionic (NH_2, S^- or S, S^-) in nature. The present chapter deals with the investigation on the effect of both charge and lipophilicity on the overall pharmacological behavior of the $[^{99m}TcN(PNP)]^{2+}$ complexes.

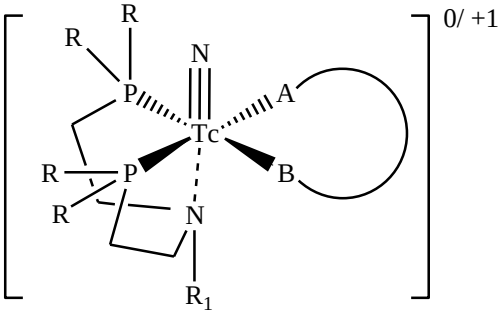

$[^{99m}TcN(PNP)L]$

L= bi-dentate ligand [AB donor =(S,S^-) or (S^-, NH_2) ----Charged complex
(S^-S^-) or (S^-, COO^-)----Neutral complex]

Fig. 4.1 General structure of neutral or charged asymmetric $[^{99m}TcN(PNP)L]$ complex

The amino acid cysteine is a useful BFCA for $[^{99m}TcN(PNP)]^{2+}$ intermediate, where a biomolecule, like fatty acid can be attached either at the -COOH or $-NH_2$ group, and the other two groups, SH and NH_2/ COOH, can be used for labeling with $[^{99m}TcN(PNP)]^{2+}$ core.[187,190,247] The overall charge of the complex depends on the groups in cysteine that are co-ordinated to the $[^{99m}TcN(PNP)]^{2+}$ core. The overall charge will be uni-positive, if -SH and $-NH_2$ groups of cysteine are involved in co-ordination, or neutral, if -SH and -COOH groups are co-ordinated to the $[^{99m}TcN(PNP)]^{2+}$ core.

In the previous chapter, a 16 carbon diacid was derivatized with a cysteine residue, leaving the cysteine SH and COOH groups available for complexation with the $[^{99m}TcN(PNP)]^{2+}$ intermediate to give a neutral complex **7C** [Fig. 4.2(a)]. This chapter presents the synthesis of a uni-positively charged structural analogue **9C** [Fig. 4.2(b)] of the neutral complex and evaluation of its bio-distribution in a mice model. The complex was prepared by coupling a 16 carbon fatty acid to the cysteine residue leaving SH and NH_2 groups free (Fig. 4.3) for co-ordination with the same $[^{99m}TcN(PNP\mathbf{6})]^{2+}$ intermediate. This complex **9C** was evaluated and the bio-distribution results were compared with the neutral analogue to evaluate the effect of charge. The results were also compared with the ^{125}I labeled standard agent IPPA to assess the potential of the prepared complex for use as a radiopharmaceutical to evaluate cardiac function.

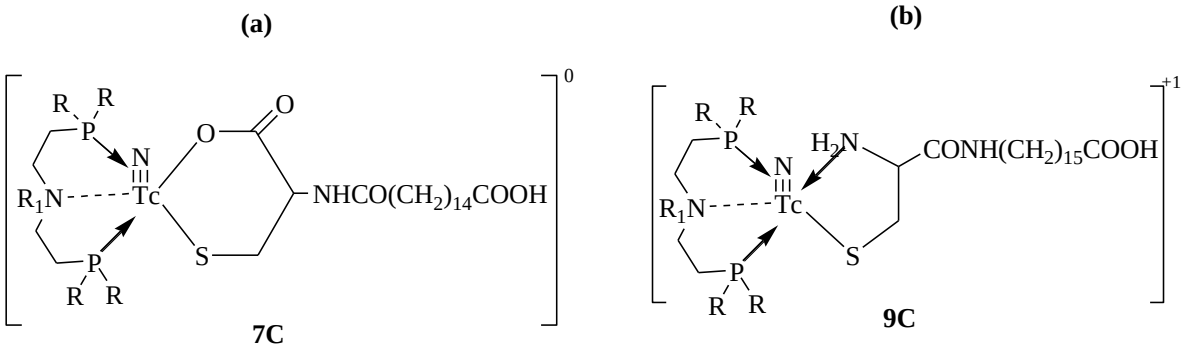

Fig. 4.2 Structural analogues (a) neutral **7C** and (b) charged **9C** 16 carbon fatty acid complexes

The promising *in-vivo* biological results of the 16 carbon uni-positively charged complex **9C** (as discussed later), infused interest in evaluating the other uni-positively charged complexes with different lipophilicities. The lipophilicity was varied by varying the carbon chain lengths of the long chain fatty acid. In this regard, three more fatty acid-cysteine conjugates (**8**, **10** and **11**) were synthesized (Fig. 4.3) and used for the formation of $[^{99m}TcN(PNP)]^{2+}$ fatty acid complexes, keeping the other chemical environment of the final complex *viz.* PNP ligand **6** and BFCA (cysteine) same. These complexes were then evaluated

in mice and the bio-distribution results compared together with the **9C**, to assess the effect of lipophilicity on the target uptake and non-target clearance characteristics.

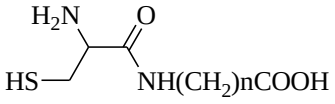

8-11

n = 10 ----Undecanoic acid derivative (**10**)
11----Dodecanoic acid derivative (**11**)
14----Pentadecanoic acid derivative (**8**)
15----Hexadecanoic acid derivative (**9**)

Fig. 4.3 Structure of synthesized fatty acid cysteine conjugates

4.2. Experimental

4.2.1 Materials and Methods

The general experimental details are given in chapter 2, section 2.2.2.1.

4.2.2 Synthesis of fatty acid-cysteine conjugates (8-11)

Ethyl ester of ω-bromo fatty acids **(8b/ 9b)**

A solution of the ω-bromo fatty acid **8a** or **9a** (1.5 mmol) in EtOH (20 mL) and conc. H_2SO_4 (0.1 mL) was refluxed overnight. After cooling, EtOH was removed under vacuum, ice cold water (20 mL) was added to the oily residue and mixture extracted with chloroform (3 × 10 mL). The chloroform extracts were pooled, dried and evaporated to obtain the target compounds **8b** and **9b** respectively.

Ethyl 15-bromopentadecanoate **(8b)**

Yield: 95% (518 mg).

IR (neat, cm^{-1}): 2918 (s); 2850 (m); 1734 (s).

Ethyl 16-bromohexadecanoate **(9b)**

Yield: 97% (525 mg).

IR (neat, cm^{-1}): 2919 (s); 2849 (m); 1740 (s).

ω-phthalimido fatty esters (**8c**/ **9c**)

A mixture of compound **8b**/ **9b** (1.37 mmol), phthalimide (203 mg, 1.37 mmol) and anhydrous potassium carbonate (209 mg, 1.5 mmol) in CH_3CN (15 mL) was refluxed overnight. Upon completion of the reaction (*cf.* TLC), the reaction mixture was cooled, filtered and concentrated under vacuum to obtain the crude product, which on silica gel column chromatography [EtOAc/ hexane (1:9 v/v)] furnished the pure compounds **8c** and **9c** respectively.

Ethyl 15-phthalimidopentadecanoate (**8c**)

Yield: 56% (318 mg), R_f = 0.7 [EtOAc/ hexane (1:9 v/v)].

IR (neat, cm^{-1}): 2918 (s); 2850 (m); 1734 (s); 1702 (s); 1462 (m); 1405 (m); 1170 (m); 1060 (m); 712 (s).

^{1}H NMR ($CDCl_3$, δ ppm): 7.83-7.86 (m , 2H, $C_6\underline{H}_4C$-); 7.69-7.72 (m, 2H, $C_6\underline{H}_4C$-); 4.12 (q, 2H,-$COOC\underline{H}_2CH_3$, *J = 7.2 Hz*); 3.67 (t, 2H, -$CH_2C\underline{H}_2N(CO)_2$, *J = 7.2 Hz*); 2.28 (t, 2H, -$CH_2C\underline{H}_2COOEt$, *J = 7.5 Hz*); 1.59-1.67 (m, 4H,-$C\underline{H}_2CH_2COOEt$ & -$C\underline{H}_2CH_2N(CO)_2$); 1.18-1.32 (m, 23H, $(C\underline{H}_2)_{10}$ & -$COOCH_2C\underline{H}_3$) [Fig. 4.4].

Ethyl 16-phthalimidohexadecanoate (**9c**)

Yield: 87% (511 mg), R_f = 0.8 [EtOAc/ hexane (1:9 v/v)].

IR (neat, cm^{-1}): 2919 (s); 2849 (m); 1740 (s); 1704 (s); 1464 (m); 1406 (m); 1174 (m); 1064 (m); 714 (s).

^{1}H NMR ($CDCl_3$, δ ppm): 7.79-7.85 (m, 2H, $C_6\underline{H}_4C$-); 7.67-7.73 (m, 2H, $C_6\underline{H}_4C$-); 4.11 (q, 2H, -$COOC\underline{H}_2CH_3$, *J = 7.2 Hz*); 3.66 (t, 2H, -$CH_2C\underline{H}_2N(CO)_2$-, *J = 7.0 Hz*); 2.27 (t, 2H, -$CH_2C\underline{H}_2COOEt$, *J = 7.4 Hz*); 1.62 (m, 4H, -$C\underline{H}_2CH_2COOEt$ & -$C\underline{H}_2CH_2N(CO)_2$-); 1.20-1.27 (m, 25H, $(C\underline{H}_2)_{11}$ & -$COOCH_2C\underline{H}_3$) [Fig. 4.5].

Ethyl esters of ω-amino acid **(8d/ 9d/ 10b/ 11b)**

8d/ 9d

A mixture of compound **8c**/ **9c** (0.69 mmol), 80% hydrazine hydrate (219 µL, 3.49 mmol) in EtOH (15 mL) was refluxed for 3 h. The reaction mixture was brought to room temperature, and excess hydrazine hydrate and EtOH were removed under vacuum. The precipitate obtained was re-dissolved in EtOH (15 mL), treated with aqueous 2N HCl (5 mL) and the mixture refluxed overnight. On cooling, solvent was removed under vacuum to obtain white residue, which was re-dissolved in EtOH (15 mL) and conc. H_2SO_4 (0.1 mL) and refluxed overnight. The reaction mixture was cooled to room temperature to obtain a white precipitate (phthalhydrazide) and filtered. The filtrate was evaporated under vacuum to obtain oily residue, to which cold water was added and the pH of the resulting solution adjusted above 7 with aqueous 5% $NaHCO_3$. The aqueous solution was extracted with chloroform (3 × 10 mL), pooled, dried and concentrated under vacuum to give the pure products **8d** and **9d** respectively.

Ethyl 15-aminopentadecanoate (**8d**)

Yield: 97% (191 mg).

IR (neat, cm^{-1}): 3370 (w); 2918 (s); 2850 (s); 1734 (s); 1656 (w); 1599 (w); 1466 (s); 1375 (m); 1180 (s); 1114 (w); 1034 (w); 736 (m).

Ethyl 16-aminohexadecanoate **(9d)**

Yield: quantitative (230 mg).

IR (neat, cm^{-1}): 3197 (w); 2916 (s); 2848 (m); 1738 (s); 1577 (m); 1518 (s); 1463 (m); 1182 (s); 721 (m).

^{1}H NMR ($CDCl_3$, δ ppm): 4.05-4.16 (q, 2H, -COOC$\underline{H}_2$$CH_3$, *J = 7.0 Hz*); 3.00 (m, 2H, -$CH_2C\underline{H}_2NH_2$); 2.27 (t, 2H, -$CH_2C\underline{H}_2$COOEt, *J = 7.4 Hz*); 1.89 (m, 4H, -$C\underline{H}_2CH_2NH_2$ and -

$CH_2CH_2N\underline{H}_2$,); 1.60 (m, 2H, $C\underline{H}_2CH_2COOEt$); 1.24-1.27 (m, 25H, $(C\underline{H}_2)_{11}$ & $-COOCH_2C\underline{H}_3$) [Fig. 4.6].

10b/**11b**

A solution of *ω*-amino fatty acid **10a**/ **11a** (2.3 mmol) in EtOH (20 mL) and conc. H_2SO_4 (0.1 mL) was refluxed overnight. After cooling, solvent was removed under vacuum, ice cold water (20 mL) added and the pH of the solution was brought to 8 using aqueous 5% $NaHCO_3$. The resultant solution was extracted with $CHCl_3$ (3 × 10 mL), dried and evaporated under vacuum to give the products **10b** and **11b** respectively.

11-amino fatty acid ester (**10b**)

Yield: Quantitative (525 mg).

IR (neat, cm^{-1}): 3370 (b); 2918 (s); 2850 (s); 1735 (s); 1599 (w); 1466 (m); 1375 (m); 1180 (s); 1114 (m); 1034 (m); 917 (w); 859 (w); 726 (m).

12-amino fatty acid ester (**11b**)

Yield: 96% (540 mg).

IR (neat, cm^{-1}): 3365 (b); 2922 (s); 2851 (s); 1737 (s); 1594 (m); 1466 (m); 1373 (m); 1181 (s); 1113 (m); 1034 (m); 917 (w); 860 (w); 722 (m).

ω-(N-Boc, S-trityl cysteinyl amido) fatty ester (**8e**/ **9e** /**10c**/ **11c**)

A mixture of *ω*-amino ester **8d**/ **9d**/ **10b**/ **11b** (0.5 mmol) and *N*-Boc, *S*-trityl cysteine (233 mg, 0.5 mmol) in CH_2Cl_2 (15 mL) was cooled to 0 °C in an ice bath. To this, EDCI (106 mg, 0.55 mmol) was added and the mixture stirred at 0°C for 1 h, after which it was brought to room temperature and stirred overnight. Upon completion of the reaction (*cf.* TLC), the reaction mixture was washed with water (3 × 10 mL), dried and concentrated to yield the crude product, which was purified by silica gel column chromatography [EtOAc/ $CHCl_3$ (1:19 v/v)] to give pure **8e**, **9e**, **10c** and **11c** respectively.

11-(N-Boc, S-trityl cysteinyl amido) undecanoic ester (**10c**)

Yield: 88% (297 mg), R_f = 0.6 [EtOAc/ $CHCl_3$ (1:19 v/v)].

IR (neat, cm^{-1}): 3313 (b); 3057 (w); 2924 (s); 2852 (s); 1734 (s); 1713 (s); 1656 (s); 1530 (b); 1491 (m); 1444 (m); 1366 (m); 1248 (w); 1167 (s); 1033 (w); 742 (s); 699 (s).

^{1}H NMR ($CDCl_3$, δ ppm): 7.14-7.41 (m, 15H, $(C_6\underline{H}_5)_3C$-); 6.12 (s, 1H, -CHCON$\underline{H}$$CH_2$-); 4.92-4.96 (m, 1H, -N$\underline{H}$$CHCH_2S$-); 4.09 (q, 2H, -COOC$\underline{H}_2CH_3$, *J = 7.2 Hz*); 3.80-3.83 (m, 1H, -NHC$\underline{H}$$CH_2S$-); 3.09-3.15 (m, 2H, -$CH_2C\underline{H}_2$NHCO-); 2.62-2.68 (m, 1H, -CHC$\underline{H}_A$$CH_B$S-); 2.44-2.54 (m, 1H, -$CHCH_AC\underline{H}_B$S-); 2.26 (t, 2H, -$CH_2C\underline{H}_2$COOEt, *J = 7.4 Hz*); 1.49-1.55 (m, 4H, -C$\underline{H}_2CH_2$COOEt & -C$\underline{H}_2CH_2$NHCO-,); 1.39 (s, 9H, $(C\underline{H}_3)_3$C-); 1.19-1.26 (m, 15H, $(C\underline{H}_2)_6$ & -$COOCH_2C\underline{H}_3$) [Fig. 4.7].

12-(N-Boc, S-trityl cysteinyl amido) dodecanoic ester (**11c**)

Yield: 82% (282 mg), R_f = 0.6 [EtOAc/ $CHCl_3$ (1:19 v/v)].

IR (neat, cm^{-1}): 3309 (b); 3057 (w); 2925 (s); 2852 (s); 1736 (s); 1713 (s); 1656 (s); 1530 (b); 1494 (m); 1444 (m); 1366 (m); 1167 (s); 1033 (w); 742 (s); 699 (s).

^{1}H NMR ($CDCl_3$, δ ppm): 7.14-7.41 (m,15H, $(C_6\underline{H}_5)_3C$-); 6.09 (s, 1H, -CHCON$\underline{H}$$CH_2$-); 4.89-4.93 (m, 1H, -N$\underline{H}$$CHCH_2S$-); 4.09 (q, 2H, -COOC$\underline{H}_2CH_3$, *J = 7.2 Hz*); 3.80-3.83 (m, 1H,-NHC$\underline{H}$$CH_2S$-); 3.09-3.18 (m, 2H,$CH_2C\underline{H}_2$NHCO-); 2.62-2.65 (m, 1H, -CHC$\underline{H}_A$$CH_B$S-); 2.44-2.53 (m, 1H, -$CHCH_AC\underline{H}_B$S-); 2.22-2.29 (t, 2H, $CH_2C\underline{H}_2$COOEt, *J = 7.6 Hz*); 1.49-1.59 (m, 4H, -C$\underline{H}_2CH_2$COOEt & -C$\underline{H}_2CH_2$NHCO-); 1.39 (s, 9H, $(C\underline{H}_3)_3$C-); 1.12-1.26 (m, 17H, $(C\underline{H}_2)_7$ & $COOCH_2C\underline{H}_3$) [Fig. 4.8].

Ethyl 15-(N-Boc, S-trityl cysteinyl amido)pentadecanoate **(8e)**

Yield: 68% (248 mg), R_f = 0.6 [EtOAc/ $CHCl_3$ (1:19 v/v)].

IR (neat, cm^{-1}): 3314 (b); 3054 (w); 2972 (w); 2920 (s); 2848 (s); 1711 (bs); 1680 (m); 1489 (m); 1362 (m); 1162 (s); 1030 (w); 742 (s); 698 (s).

^{1}H NMR ($CDCl_3$, δ ppm): 7.21-7.43 (m, 15H, $(C_6\underline{H}_5)_3C$-); 6.02 (s, 1H,-CHCON$\underline{H}CH_2$-); 4.84 (m, 1H, -N$\underline{H}$CHCH_2S-); 4.12 (q, 2H, -COOC$\underline{H}_2$CH_3, *J = 7.2 Hz*); 3.81 (m, 1H, -NHC$\underline{H}$CH_2S-); 3.15-3.17 (m, 2H, -CH_2C$\underline{H}_2$NHCO-); 2.68-2.70 (m, 1H, -CHC$\underline{H}_A$$H_B$S-); 2.48-2.52 (m, 1H, -CHC$H_A$$\underline{H}_B$S-); 2.29 (t, 2H, -C$H_2C\underline{H}_2$COOEt, *J = 7.5 Hz*); 1.61 (m, 4H, -C$\underline{H}_2$CH_2COOEt & -C$\underline{H}_2$CH_2NHCO-); 1.41 (s, 9H, -C$(CH_3)_3$); 1.23-1.25 (m, 23H, $(C\underline{H}_2)_{10}$ & -COOCH_2C$\underline{H}_3$) [Fig. 4.9].

Ethyl 16-(N-Boc, S-trityl cysteinyl amido)hexadecanoate **(9e)**

Yield: 72% (267 mg), R_f = 0.6 [EtOAc/ $CHCl_3$ (1:19 v/v)].

IR (neat, cm^{-1}): 3316 (b); 3057 (w); 2975 (w); 2925 (s); 2853 (s); 1713 (bs); 1681 (m); 1488 (m); 1366 (m); 1168 (s); 1032 (w); 743 (s); 700 (s).

^{1}H NMR ($CDCl_3$, δ ppm): 7.22-7.43 (m, 15H, $(C_6\underline{H}_5)_3C$-); 5.99 (m, 1H, -CHCON$\underline{H}CH_2$-); 4.82 (m, 1H, -N$\underline{H}$CHCH_2S-); 4.11 (q, 2H, -COOC$\underline{H}_2$CH_3, *J = 7.2 Hz*); 3.81 (m, 1H, -NHC$\underline{H}$CH_2S-); 3.14-3.19 (m, 2H, -CH_2C$\underline{H}_2$NHCO-); 2.67-2.74 (m, 1H, -CHC$\underline{H}_A$$H_B$S-); 2.45-2.53 (m, 1H, -CHC$H_A$$\underline{H}_B$S-); 2.29 (t, 2H, -C$H_2C\underline{H}_2$COOEt, *J = 7.5 Hz*); 1.61 (m, 4H, -C$\underline{H}_2$CH_2COOEt & -C$\underline{H}_2$CH_2NHCO-); 1.41 (s, 9H, $(CH_3)_3$C-); 1.15-1.35 (m, 25H, $(C\underline{H}_2)_{11}$ & -COOCH_2C$\underline{H}_3$) [Fig. 4.10].

ω-(N-Boc, S-trityl cysteinyl amido) fatty acid (**8f**/ **9f**/ **10d**/ **11d**)

A mixture of **8e**/ **9e**/ **10c**/ **11c** (0.15 mmol) and aqueous 1M KOH solution (300 µL, 0.3 mmoles) in MeOH (600 µL) was stirred at room temperature for 2 d. Upon completion of the reaction (*cf*. TLC), MeOH was removed under vacuum, water (5 mL) was added and the pH of the reaction mixture was adjusted to 3 using aqueous 2N HCl to give compound **8f**, **9f**, **10d** and **11d** respectively as white precipitate which was filtered and dried under vacuum.

11-(N-Boc, S-trityl cysteinyl amido) undecanoic acid (**10d**)

Yield: 80% (78 mg), R_f = 0.2 [EtOAc/ $CHCl_3$ (1:9 v/v)].

IR (neat, cm^{-1}): 3313 (b); 3057 (w); 2924 (s); 2852 (s); 1685 (s); 1656 (s); 1530 (b); 1491 (m); 1444 (m); 1366 (m); 1248 (w); 1167 (s); 1033 (w); 742 (s); 699 (s).

^1H NMR ($CDCl_3$, δ ppm): 7.14-7.41 (m, 15H, $(C_6\underline{H}_5)_3C$-); 6.32 (s, 1H, -CHCON$\underline{H}$$CH_2$-); 5.22 (bs, 1H, -N$\underline{H}$$CHCH_2S$-); 3.80-3.83 (m, 1H, -NHC$\underline{H}$$CH_2S$-); 3.09-3.15 (m, 2H, -$CH_2C\underline{H}_2NHCO$-); 2.62-2.68 (m, 1H, -$CHC\underline{H}_ACH_BS$-); 2.44-2.54 (m, 1H, -$CHCH_AC\underline{H}_BS$-); 2.22-2.29 (m, 2H,-$CH_2C\underline{H}_2COOH$); 1.49-1.55 (m, 4H, -$C\underline{H}_2CH_2COOH$ & -$C\underline{H}_2CH_2NHCO$-); 1.39 (s, 9H, -$C(C\underline{H}_3)_3$); 1.23 (s, 12H, $(C\underline{H}_2)_6$) [Fig. 4.11].

MS (ESI, -ve mode): Mass (calculated) $C_{38}H_{50}N_2O_5S$ 646.8; *m/z* (observed) 645.5 [Fig. 4.12].

12-(N-Boc, S-trityl cysteinyl amido) dodecanoic acid (**11d**)

Yield: 75% (74 mg), R_f = 0.2 [EtOAc/ $CHCl_3$ (1:9 v/v)].

IR (neat, cm^{-1}): 3309 (b); 3057 (w); 2925 (s); 2852 (s); 1685 (s); 1656 (s); 1530 (b); 1494 (m); 1444 (m); 1366 (m); 1167 (s); 1033 (w); 742 (s); 699 (s).

^1H NMR ($CDCl_3$, δ ppm): 7.14-7.42 (m, 15H, $(C_6\underline{H}_5)_3C$-); 6.22 (bs, 1H, -CHCON$\underline{H}$$CH_2$-); 5.12 (bs, 1H, -N$\underline{H}$$CHCH_2S$-); 3.80-3.83 (m, 1H, -NHC$\underline{H}$$CH_2S$-); 3.09-3.18 (m, 2H, -$CH_2C\underline{H}_2NHCO$-); 2.62-2.65 (m, 1H, -$CHC\underline{H}_ACH_BS$-); 2.44-2.53 (m, 1H, -$CHCH_AC\underline{H}_BS$-); 2.22-2.29 (m, 2H, -$CH_2C\underline{H}_2COOH$); 1.49-1.59 (m, 4H, -$C\underline{H}_2CH_2COOH$ & -$C\underline{H}_2CH_2NHCO$-); 1.39 (s, 9H, -$C(C\underline{H}_3)_3$); 1.19 (s, 14H, $(C\underline{H}_2)_7$) [Fig. 4.13].

MS (ESI, -ve mode): Mass (calculated) $C_{39}H_{52}N_2O_5S$ 660.9; *m/z* (observed) 659.5 [Fig. 4.14].

15-(N-Boc, S-trityl cysteinyl amido) pentadecanoic acid (**8f**)

Yield: 80% (84 mg), R_f = 0.2 [EtOAc/ $CHCl_3$ (1:9 v/v)].

IR (neat, cm^{-1}): 3312 (b); 3053 (w); 2923 (s); 2850 (s); 1681 (s); 1655 (s); 1528 (b); 1488 (m); 1443 (m); 1366 (m); 1247 (w); 1167 (s); 1032 (w); 740 (s); 696 (s).

^1H NMR ($CDCl_3$, δ ppm): 7.18-7.42 (m, 15H, $(C_6\underline{H}_5)_3C$-), 6.16 (m, 1H, -CHCON$\underline{H}$$CH_2$-); 5.06 (m, 1H, -N$\underline{H}$$CHCH_2S$-); 3.82 (m, 1H, -NHC$\underline{H}$$CH_2S$-); 3.14-3.16 (m, 2H,-$CH_2C\underline{H}_2NHCO$-); 2.64-2.70 (m, 1H, -$CHC\underline{H}_AH_BS$-); 2.47-2.52 (m, 1H, -$CHCH_A\underline{H}_BS$-); 2.31

(m, 2H, -$CH_2C\underline{H}_2COOH$); 1.59-1.60 (m, 4H,-$C\underline{H}_2CH_2COOH$ & -$C\underline{H}_2CH_2NHCO$-); 1.40 (s, 9H, -$C(CH_3)_3$); 1.25 (s, 20H, $(C\underline{H}_2)_{10}$) [Fig. 4.15].

MS (ESI, -ve mode): Mass (calculated) $C_{42}H_{58}N_2O_5S$ 702.4; *m/z* (observed) 701.7 [Fig. 4.16].

16-(N-Boc, S-trityl cysteinyl amido) hexadecanoic acid (**9f**)

Yield: 80% (86 mg). R_f = 0.2 [EtOAc/ $CHCl_3$ (1:9 v/v)].

IR (neat, cm^{-1}): 3313 (b); 3057 (w); 2924 (s); 2852 (s); 1685 (s); 1656 (s); 1530 (b); 1491 (m); 1444 (m); 1366 (m); 1248 (w); 1167 (s); 1033 (w); 742 (s); 699 (s).

^{1}H NMR ($CDCl_3$, δ ppm): 7.21-7.43 (m, 15H, $(C_6\underline{H}_5)_3C$-); 6.18 (s, 1H,-CHCON$\underline{H}CH_2$-); 5.09 (m, 1H, -N$\underline{H}CHCH_2S$-); 3.85 (m, 1H, -NHC$\underline{H}CH_2S$-); 3.08-3.17 (m, 2H, -$CH_2C\underline{H}_2NHCO$-); 2.67 (m, 1H, -$CHC\underline{H}_AH_BS$-); 2.52 (m, 1H, -$CHCH_A\underline{H}_BS$-); 2.32-2.34 (m, 2H, -$CH_2C\underline{H}_2COOH$); 1.62 (m, 4H, -$C\underline{H}_2CH_2COOH$ & -$C\underline{H}_2CH_2NHCO$-); 1.40 (s, 9H, $(C\underline{H}_3)_3C$-); 1.26 (s, 22H, $(C\underline{H}_2)_{11}$) [Fig. 4.17].

MS (ESI, -ve mode): Mass (calculated) $C_{43}H_{60}N_2O_5S$ 716.4; *m/z* (observed) 715.6 [Fig. 4.18].

ω- (cysteinyl amido) fatty acid (**8**/ **9**/ **10**/ **11**)

The compound **8f**/ **9f**/ **10d**/ **11d** (0.08 mmoles) was stirred with TFA (2 mL) for 2 h at room temperature. To the resultant yellow solution, Et_3SiH was added dropwise until the solution turned colorless. Stirring was continued for another 15 min. The solvent was removed under vacuum to give the desired products **8**, **9**, **10** and **11** respectively and used as such for radiolabeling without further characterization.

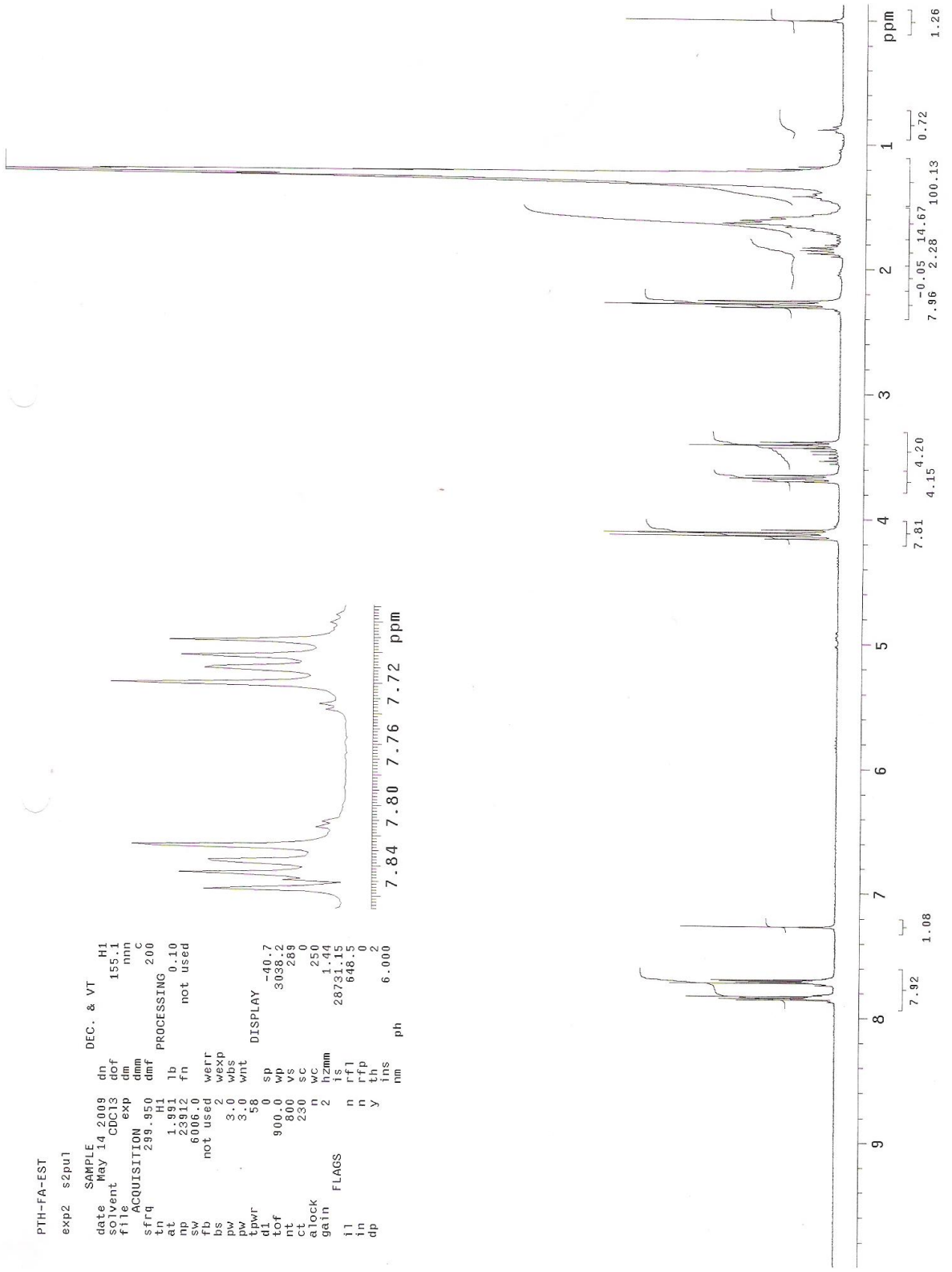

Fig. 4.4 ^{1}H NMR spectrum of compound **8c**

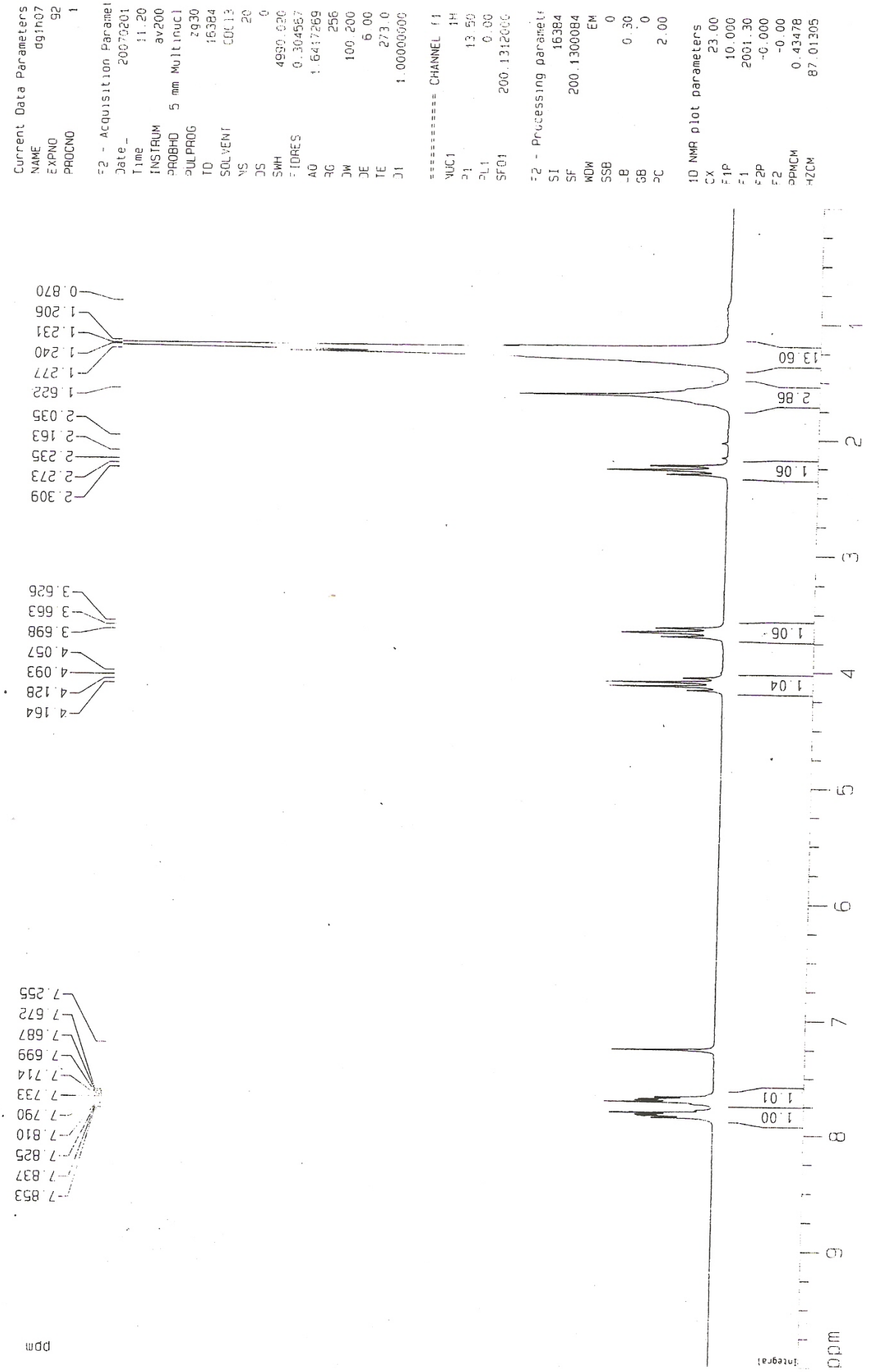

Fig. 4.5 ^{1}H NMR spectrum of compound **9c**

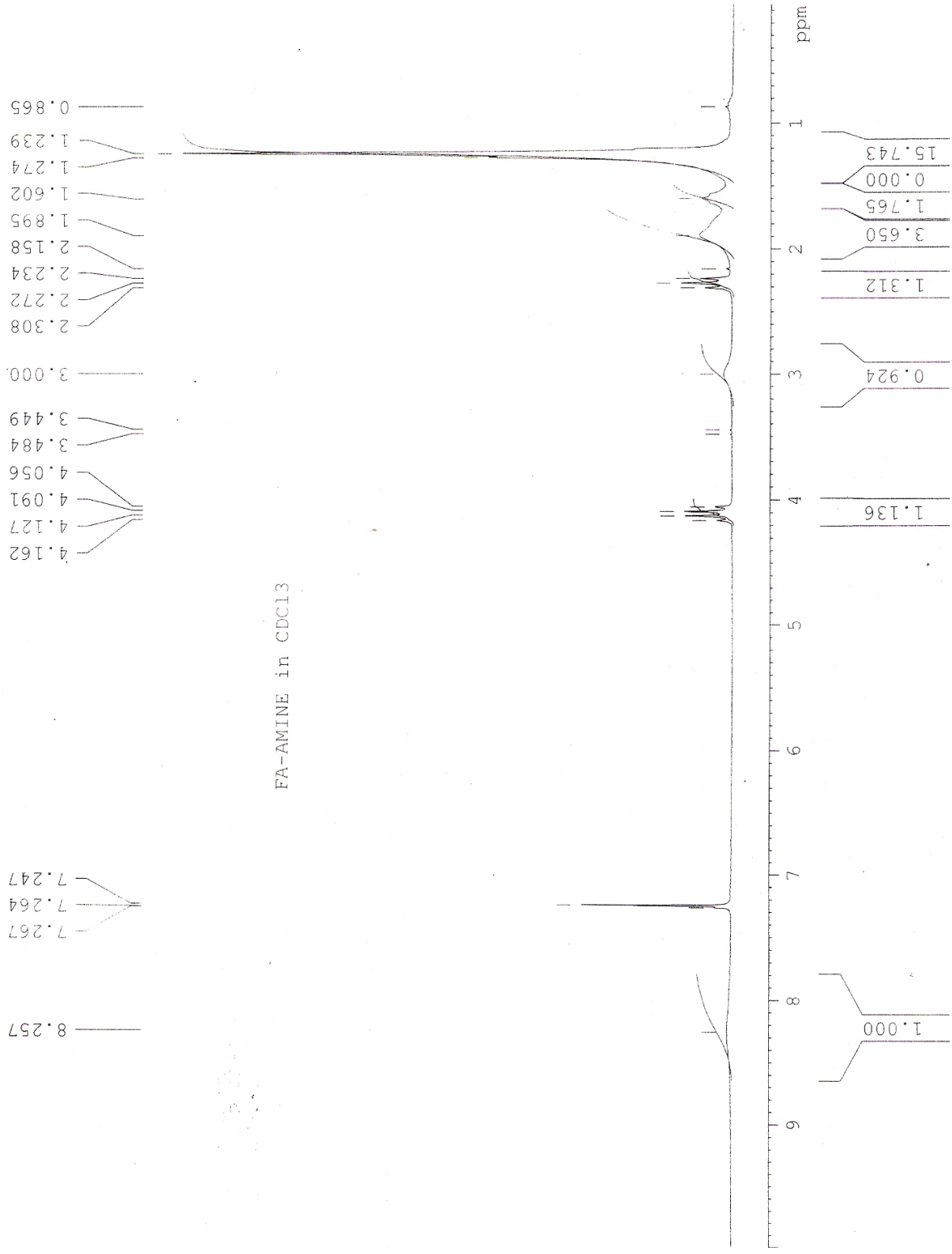

Fig. 4.6 ^{1}H NMR spectrum of compound **9d**

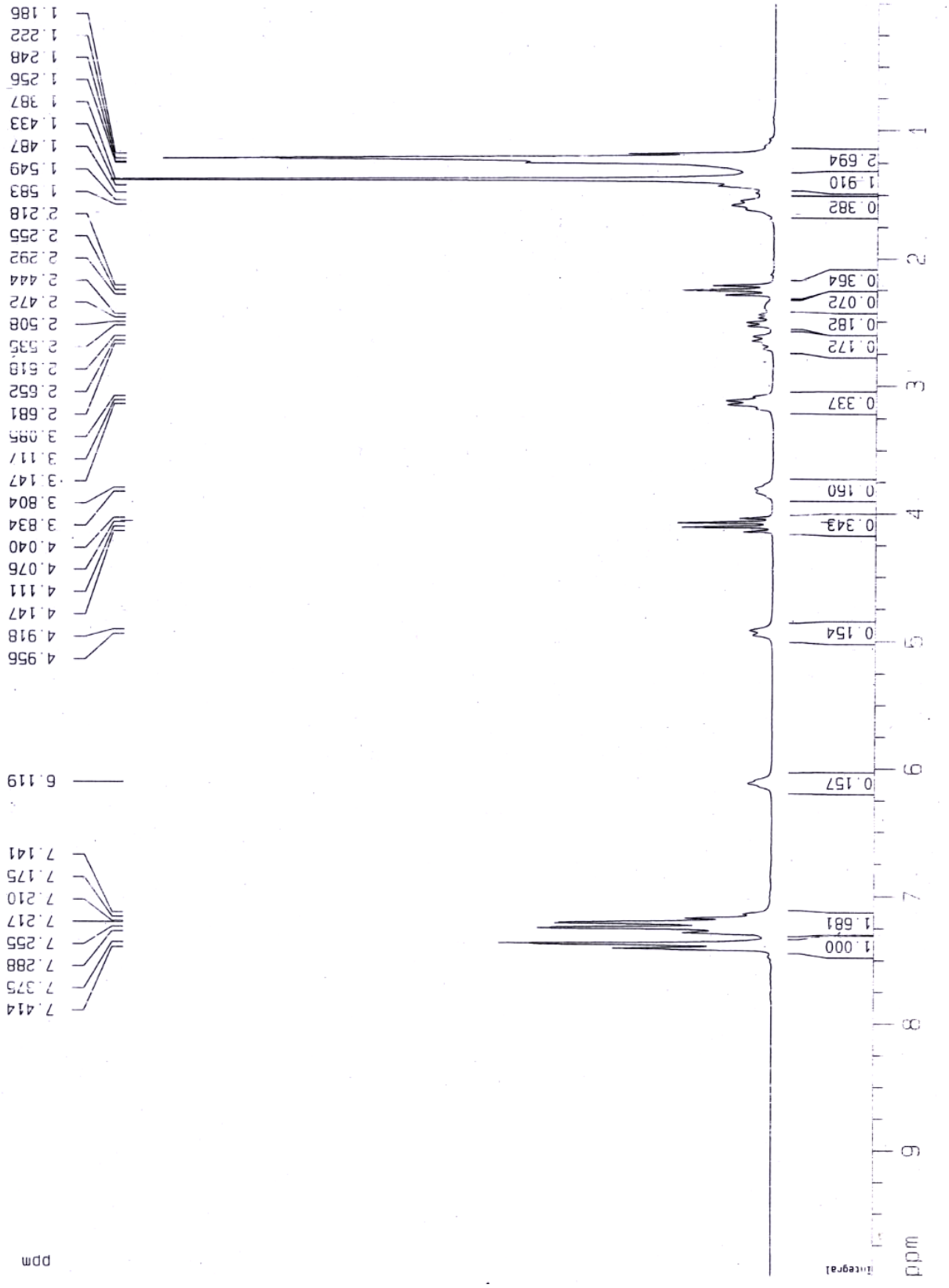

Fig. 4.7 ^{1}H NMR spectrum of compound **10c**

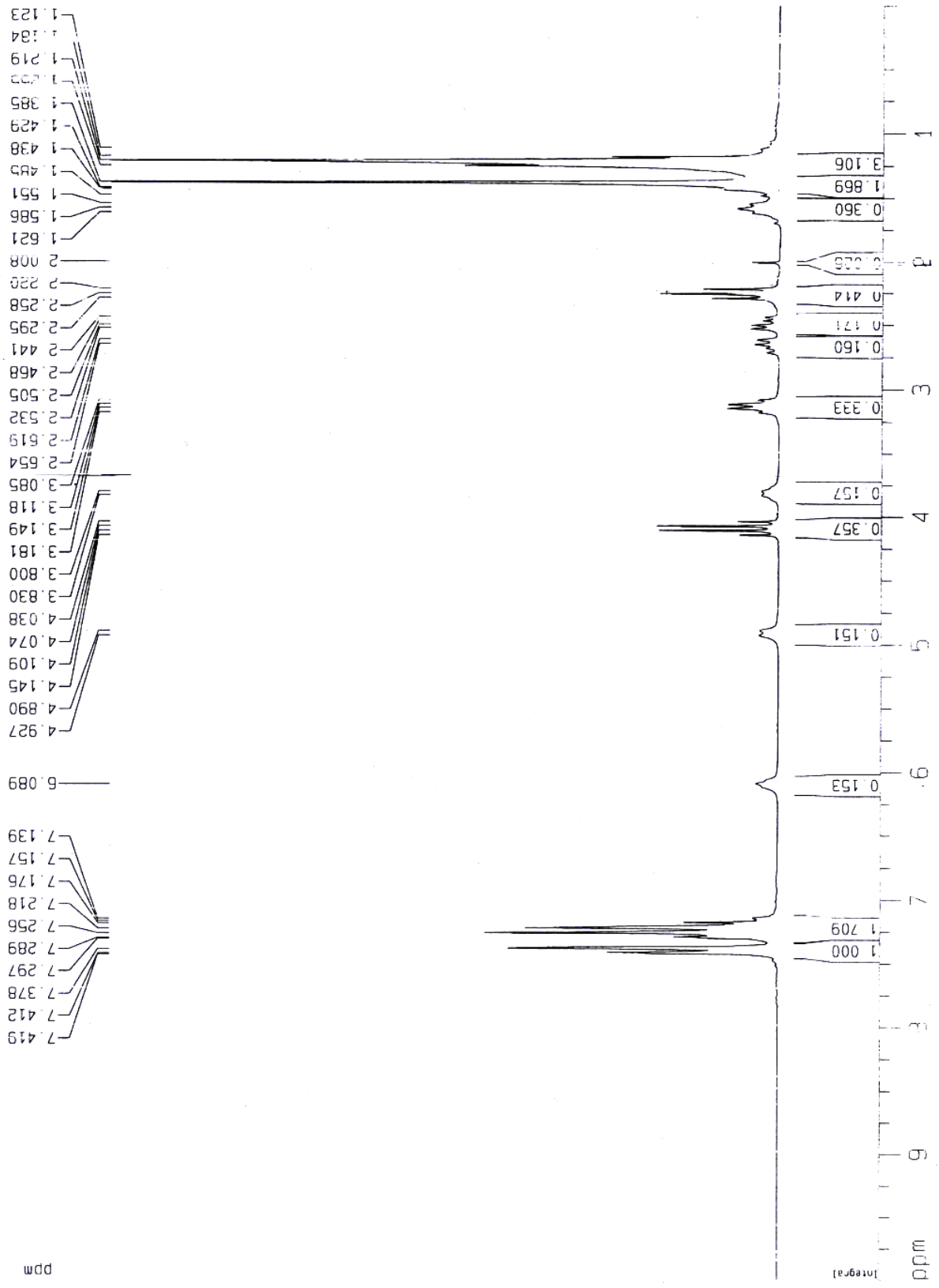

Fig. 4.8 ^{1}H NMR spectrum of compound **11c**

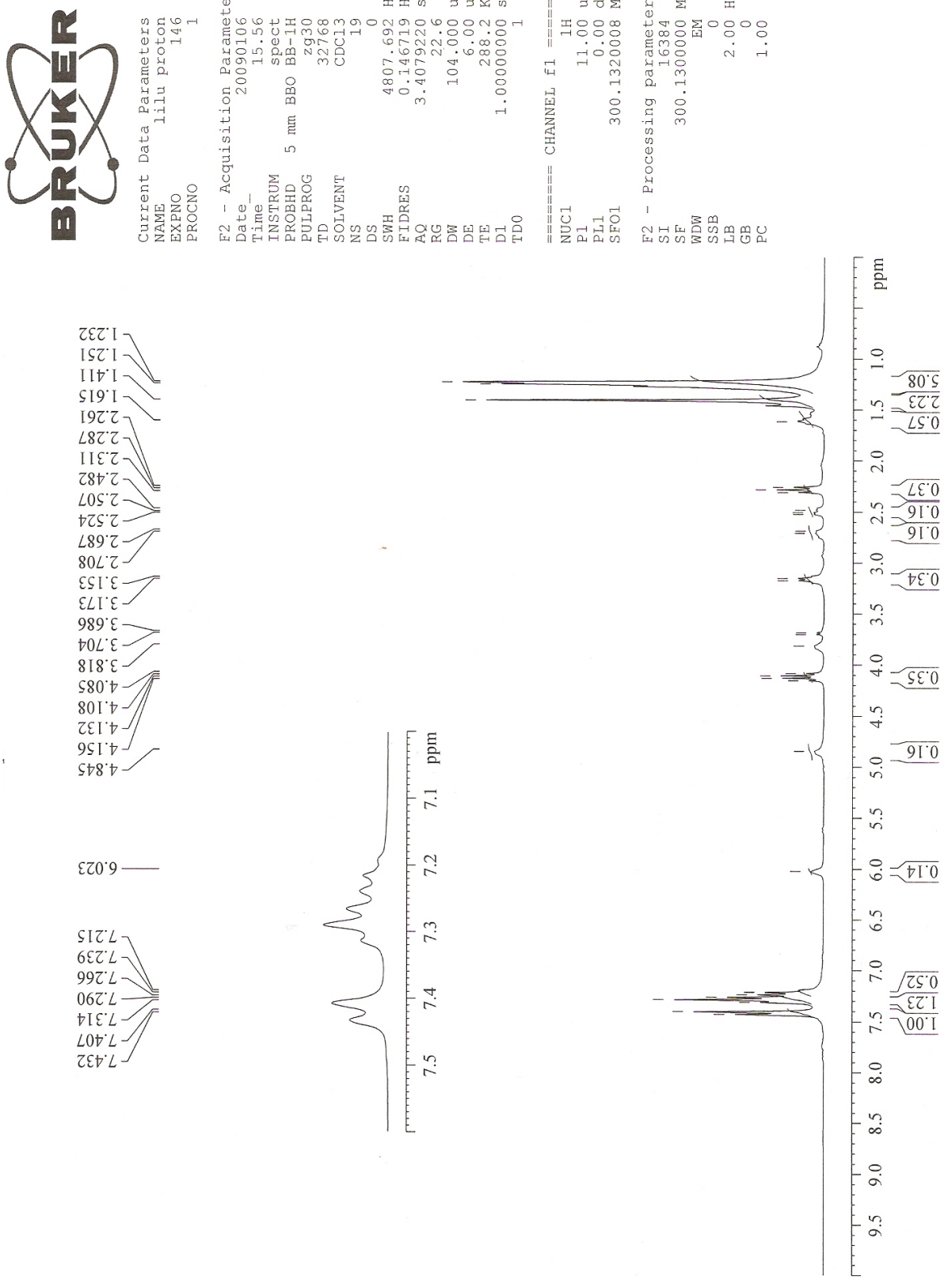

Fig. 4.9 ^{1}H NMR spectrum of compound **8e**

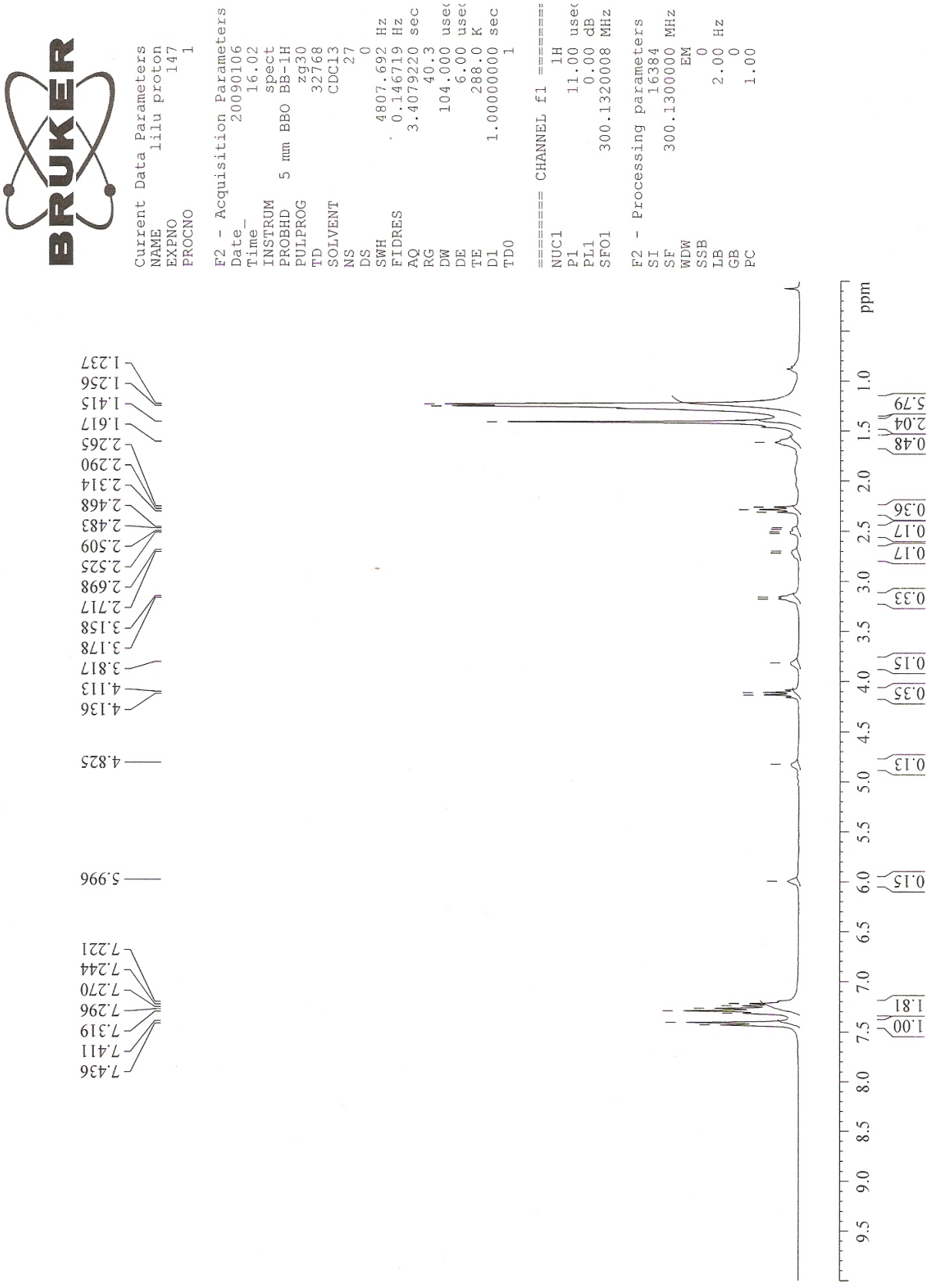

Fig. 4.10 ^{1}H NMR spectrum of compound **9e**

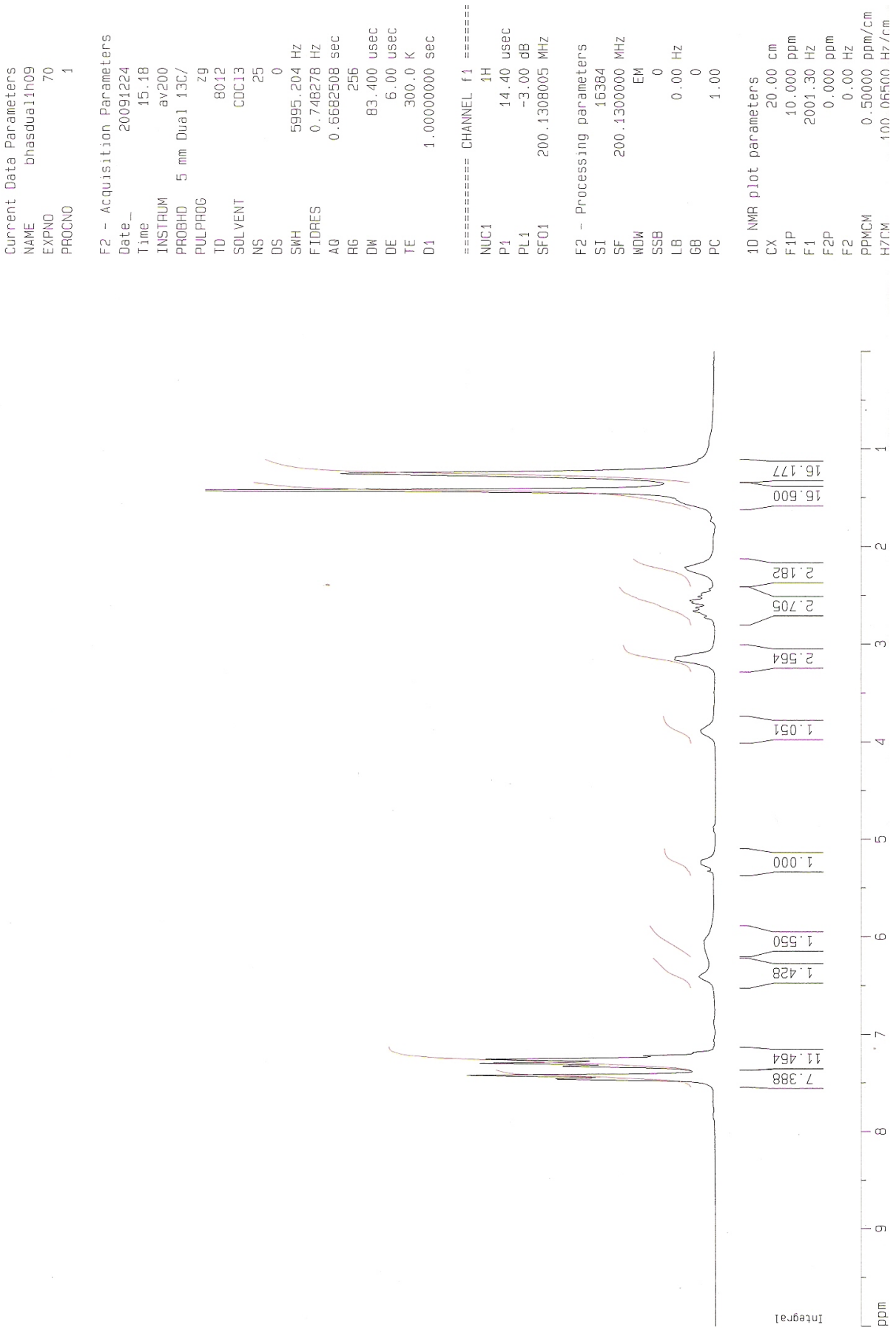

Fig. 4.11 ^{1}H NMR spectrum of compound **10d**

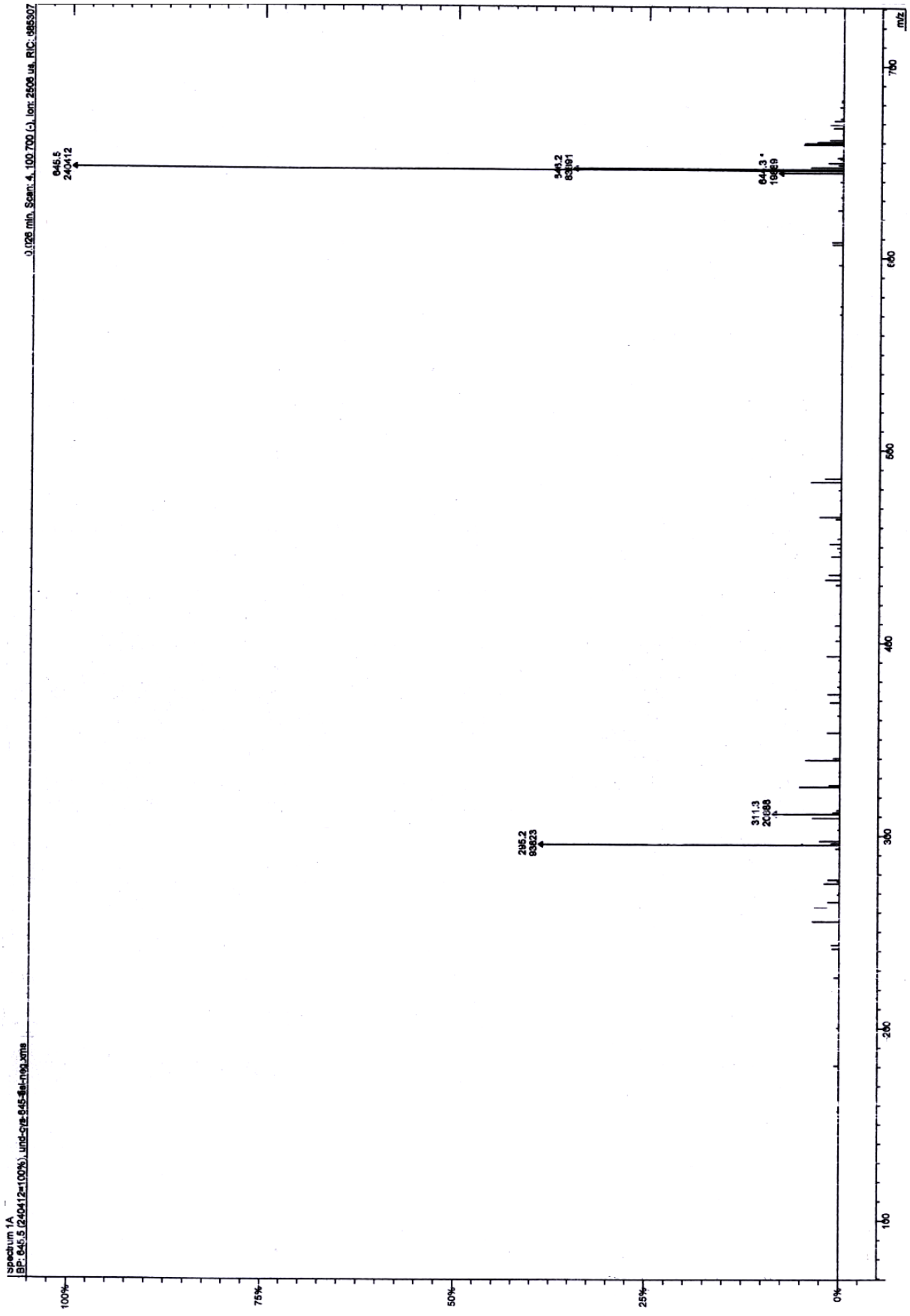

Fig. 4.12 Mass spectrum of compound **10d**

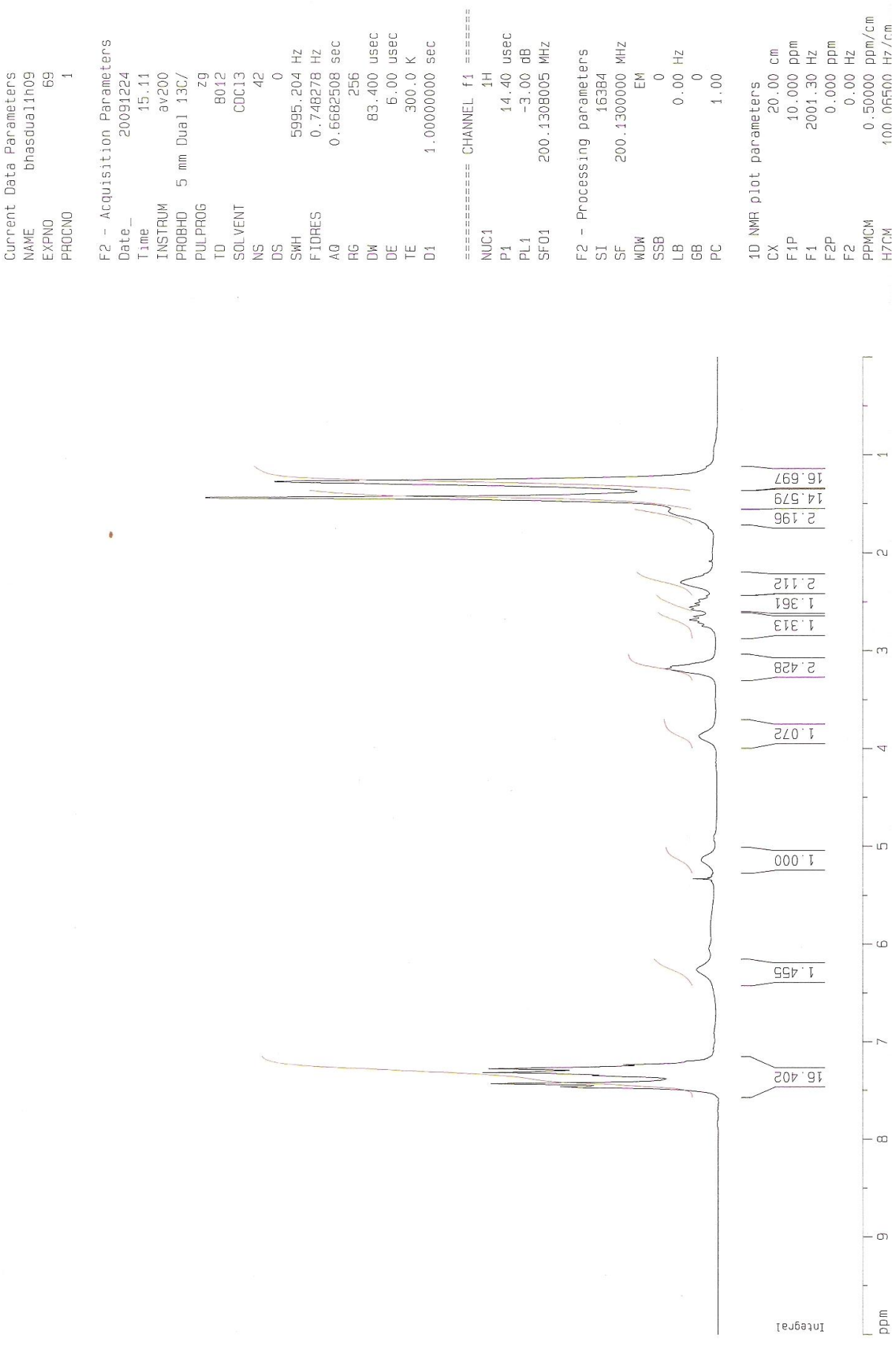

Fig. 4.13 ^{1}H NMR spectrum of compound **11d**

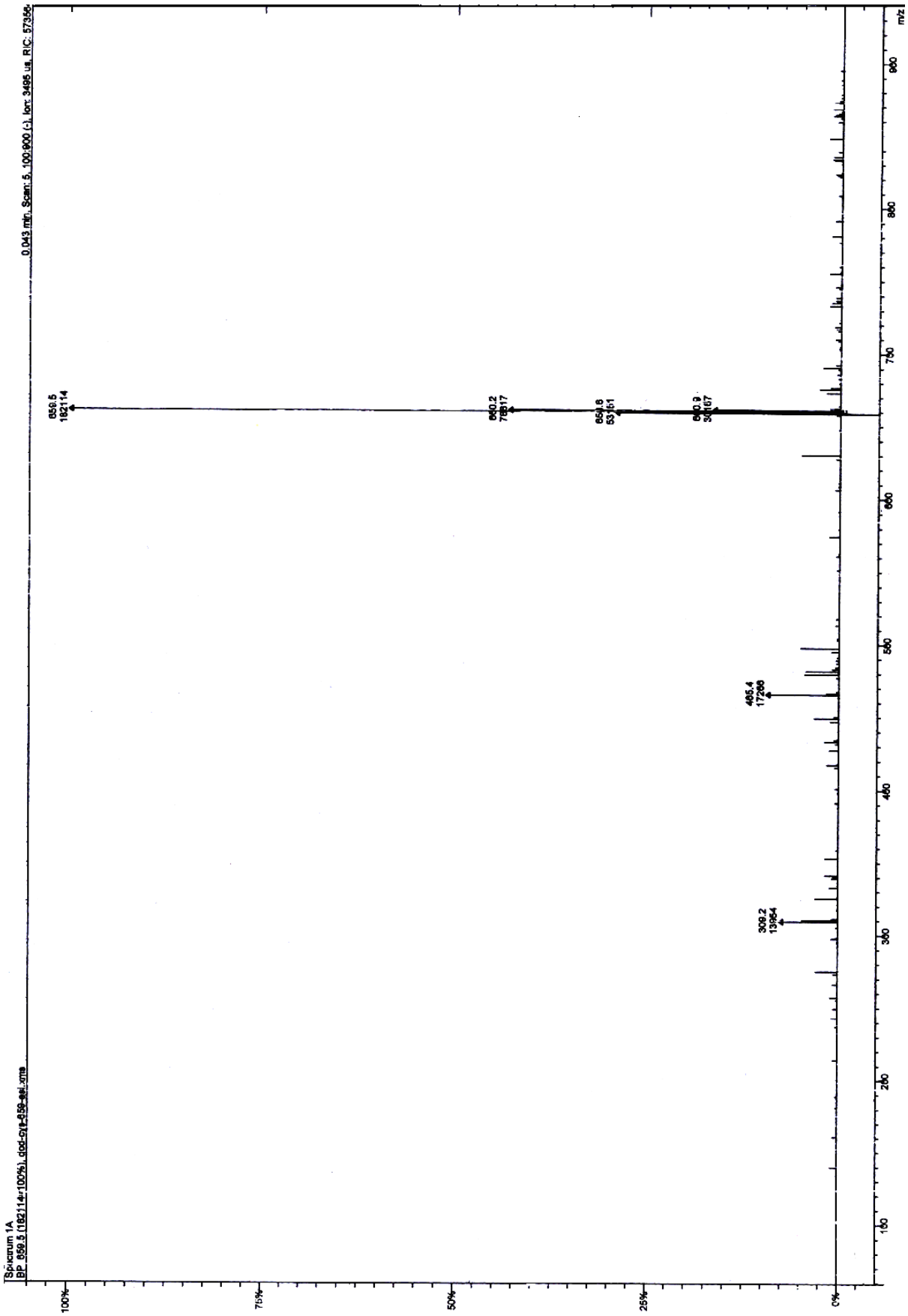

Fig. 4.14 Mass spectrum of compound **11d**

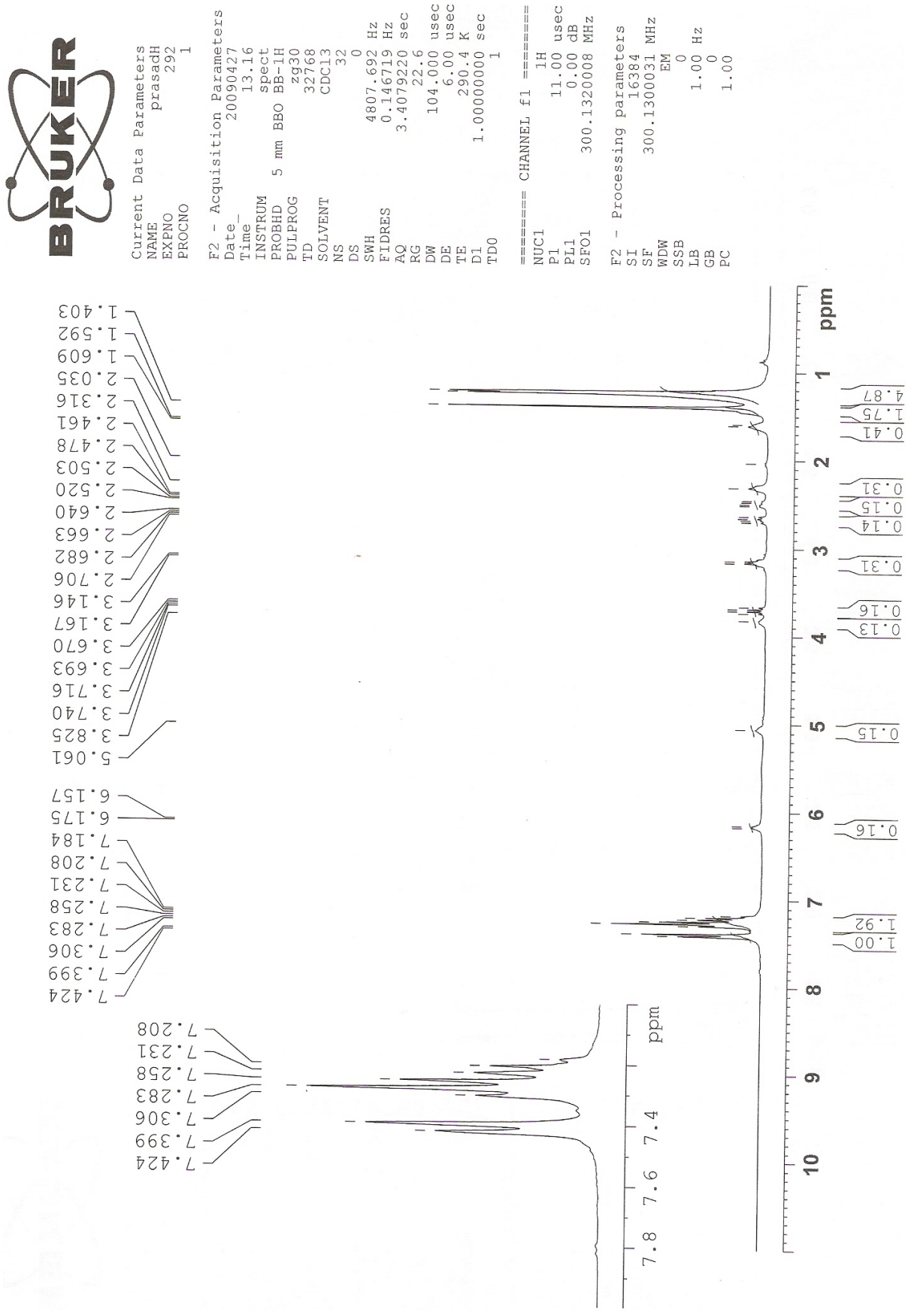

Fig. 4.15 ^{1}H NMR spectrum of compound **8f**

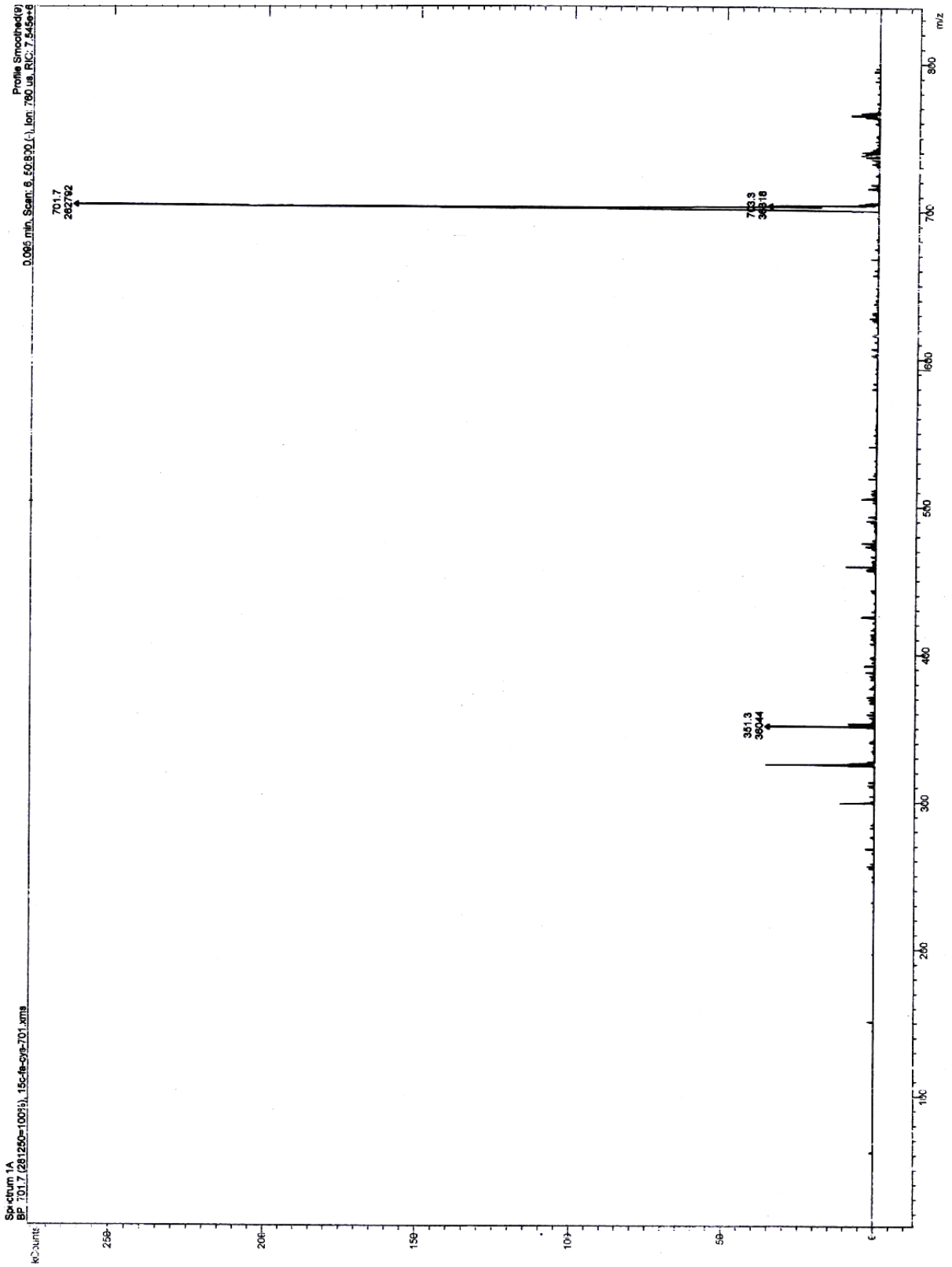

Fig. 4.16 Mass spectrum of compound **8f**

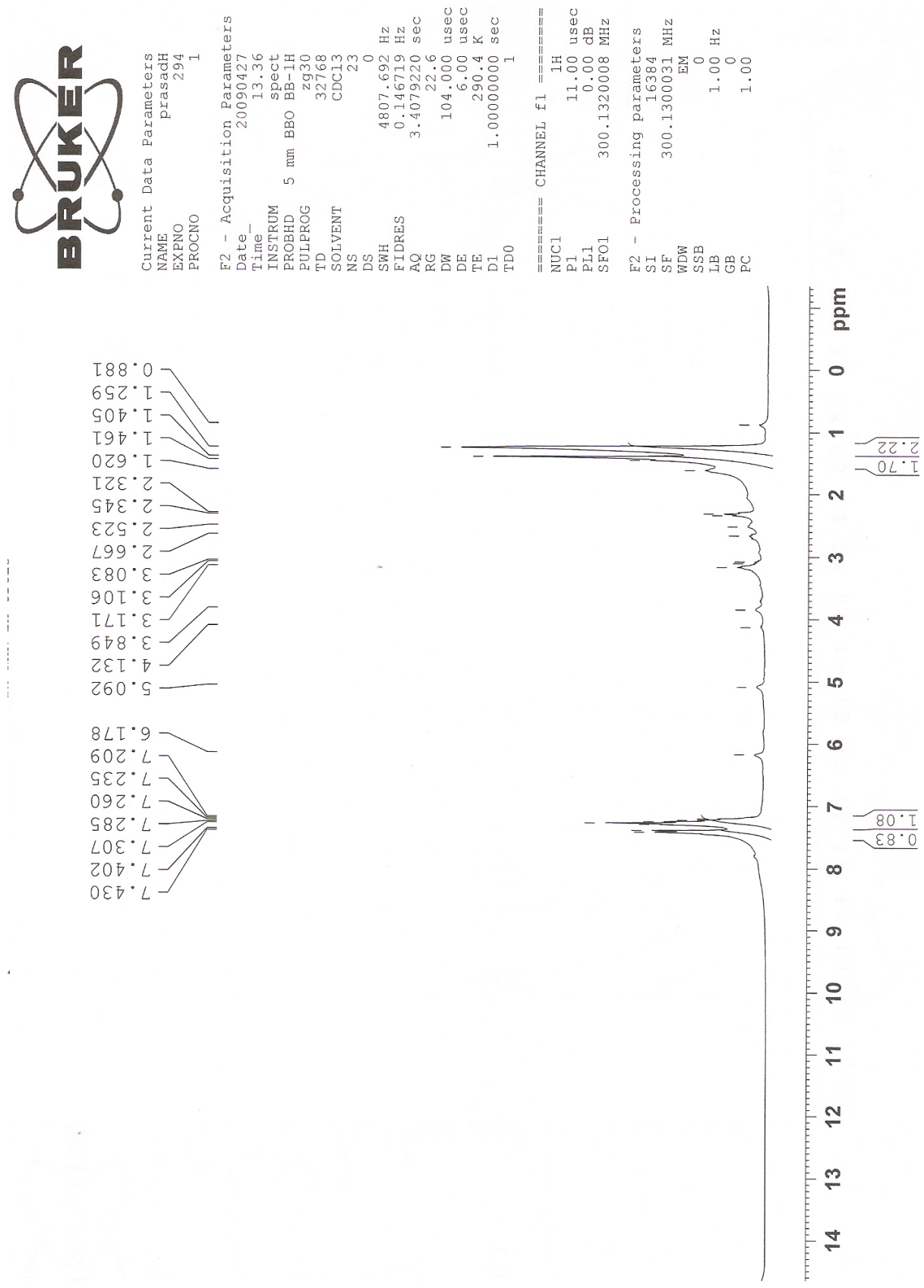

Fig. 4.17 ^{1}H NMR spectrum of compound **9f**

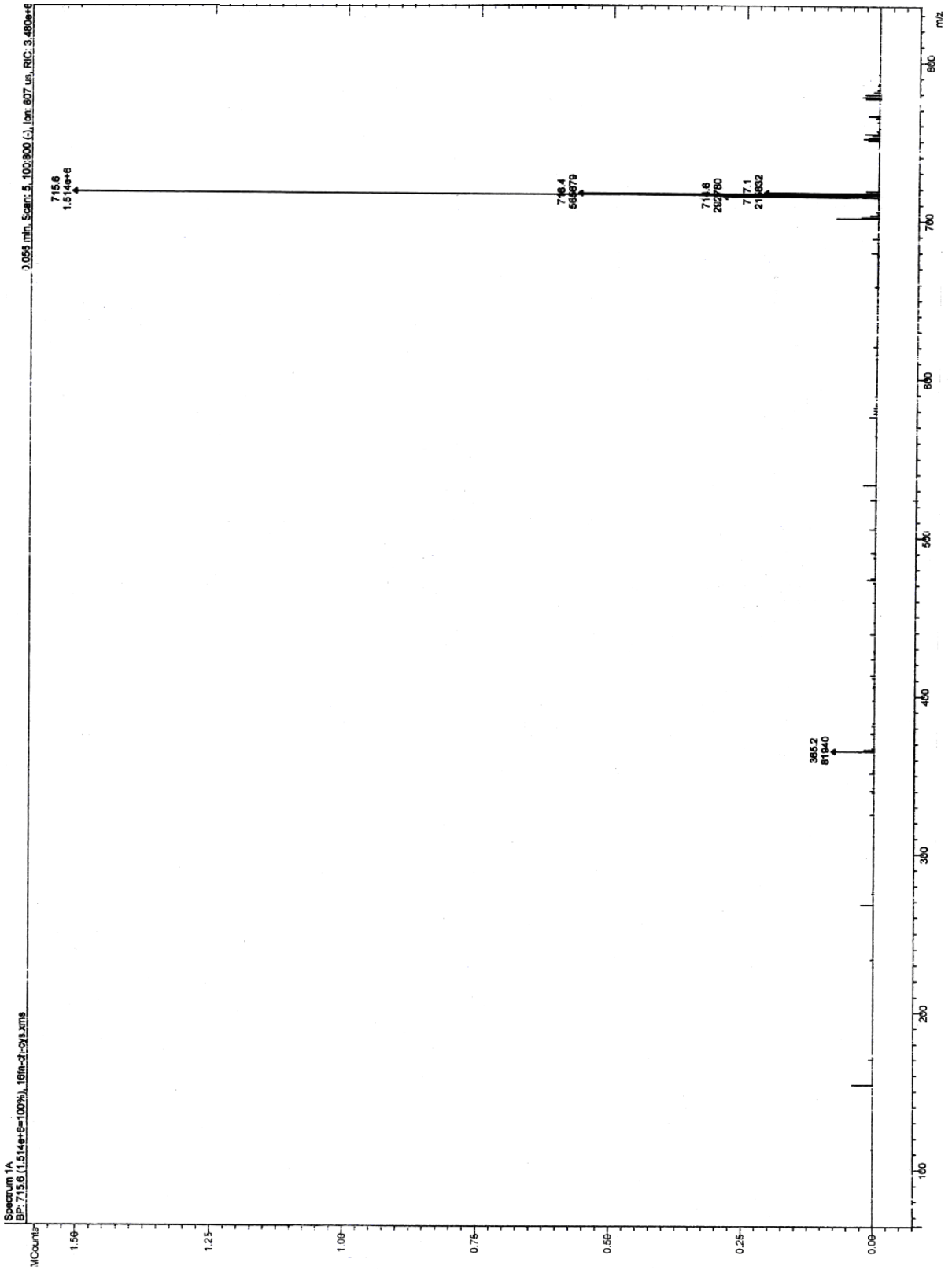

Fig. 4.18 Mass spectrum of compound **9f**

4.2.3 Radiolabeling

To the freshly prepared $[^{99m}TcN]^{2+}$ intermediate core (750 µL, 1.85 GBq or 50 mCi), was added PNP ligand **6** (~2.5 mg) alongwith compound **8**/ **9**/ **10**/ **11** (~5 mg) each dissolved in nitrogen-purged ethanol (250 µL) and the reaction mixture heated at 90 °C for 30 min. The prepared final complexes **8C**, **9C**, **10C** and **11C** respectively were characterized by HPLC.

4.2.4 Quality control techniques

4.2.4.1 *HPLC*

The radiochemical purities of the $[^{99m}TcN(PNP)]^{+2}$ complexes were assessed by HPLC using a C18 reversed phase column. Water (A) and methanol (B) were used as the mobile phase and the following gradient elution technique was adopted for the separation (0 min 50% A, 15 min 0% A, 50 min 0% A). Flow rate was maintained at 1 mL/ min. The test solution (25 µL) was injected into the column and elution was monitored by observing the radioactivity profile.

The same C18 reversed phase analytical column was used for the purification of complexes. On purification through HPLC, around 18.5 MBq (500 µCi) of the radiolabeled fatty acid product was obtained in MeOH-water medium which was removed under vacuum and reformulated in aqueous 10% ethanol solution. This was used for carrying out the *in-vitro* and *in-vivo* evaluation studies.

4.2.4.2 *Partition coefficient ($LogP_{o/w}$)*

The HPLC purified labeled compound (0.1 mL, 185 KBq or 5 µCi) was mixed with water (0.9 mL) and octanol (1 mL) on a vortex mixer for about 1 min and then centrifuged for 5 min to effect the separation of the two layers. Equal aliquots of the two layers were withdrawn and measured for the radioactivity. The readings thus obtained were used to calculate the Log $P_{o/w}$ value of the complex.

4.2.4.3 *Stability studies*

4.2.4.3.1 *Cysteine challenge*

A mixture of purified fatty acid complex **8C**/ **9C**/ **10C**/ **11C** (50 μL, 370 KBq or 10 μCi) and aqueous 10 mM cysteine solution (50 μL) in saline (400 μL) was incubated at 37 °C for 30 min. Thereafter, the respective samples were analyzed by TLC to determine the radiochemical integrity of the complexes [**8C**: R_f = 0.0-0.1, **9C**: R_f = 0.0-0.1, **10C**: R_f = 0.1-0.2, **11C**: R_f = 0.1-0.2 [EtOH/ $CHCl_3$/ C_6H_6/ 0.5 M CH_3COONH_4 (1.5:2:1.5:0.5 v/v)].

4.2.4.3.2 *Serum stability*

The purified fatty acid complex **8C**/ **9C**/ **10C**/ **11C** (50 μL, 370 KBq or10 μCi) was incubated with human serum (450 μL) at 37 °C for 30 min. Thereafter, the serum proteins were precipitated by addition of EtOH (500 μL), the solution centrifuged and the supernatant analyzed by TLC.

4.2.4.3 *Bio-distribution studies*

All procedures performed herein were in accordance with the national laws pertaining to the conduct of animal experiments. Normal Swiss mice (20–25 g body weight) were used for the *in-vivo* distribution studies. All the mice involved in the study were kept under fasting condition for 6-7 h prior to the experiment, with water given *ad libitum*. The HPLC purified radiolabeled preparation (100 μL, 740 Kbq or 20 μCi) was administered intravenously through tail vein of each animal. Individual sets of animals (n=3) were utilized for studying the bio-distribution at different time points (2 min, 5 min, 10 min and 30 min). The animals were sacrificed immediately at the end of the respective time point and the relevant organs and tissue were excised for measurement of associated activity. The organs were weighed and the activity associated with each was measured in a flat-bed type NaI(Tl) counter with suitable energy window for ^{99m}Tc (140keV ± 10%). For the sake of comparison, the activity

retained in each organ/tissue was expressed as a per cent value of the injected dose per gram (% ID/g).

4.3 Results and discussion

4.3.1 Synthesis

Four fatty acids, having chain lengths of 11, 12, 15 and 16 carbon atoms respectively, were modified with cysteine at ω-position following a four (**10** and **11**) and six (**8** and **9**) step synthetic procedures respectively (Fig. 4.19 and Fig. 4.20). All the derivatives **8-11** were prepared after attaching ω-amino group of long chain fatty acid to acid residue of cysteine. The ω-amino esters **8d** and **9d** were prepared from ω-bromo acids in additional three steps. The first step involved the acid group protection of **8a** and **9a** followed by conversion of the bromo group to amine via the Gabriel phthalimide synthesis to yield **8d** and **9d** respectively. The other two amino esters **10b** and **11b** were directly obtained upon acid protection of **10a** and **11a** respectively. The free amino group of **8d/ 9d/ 10b/ 11b** was coupled with *N*-Boc, *S*-trityl cysteine using EDCI as a coupling agent. The ethyl ester group of the coupled derivative **8e/ 9e/ 10c**/ **11c** was hydrolyzed under alkaline conditions to give **8f/ 9f/ 10d**/ **11d**. The intermediates were characterized using FT-IR, ^{1}H NMR and Mass spectroscopies. Finally, the target compounds, **8-11** were obtained respectively by simultaneous deprotection of Boc and trityl groups using TFA-Et_3SiH. The compounds **8-11** contained free SH, NH_2 groups of the cysteine residue in suitable stereochemical orientations for labeling with the $[^{99m}TcN(PNP)]^{2+}$ core.

4.3.2 Radiolabeling

The radiolabeling strategy involved prior preparation of $[^{99m}TcN]^{2+}$ intermediate, to which PNP ligand **6** and respective fatty acid derivative **8-11** were added, to yield the desired

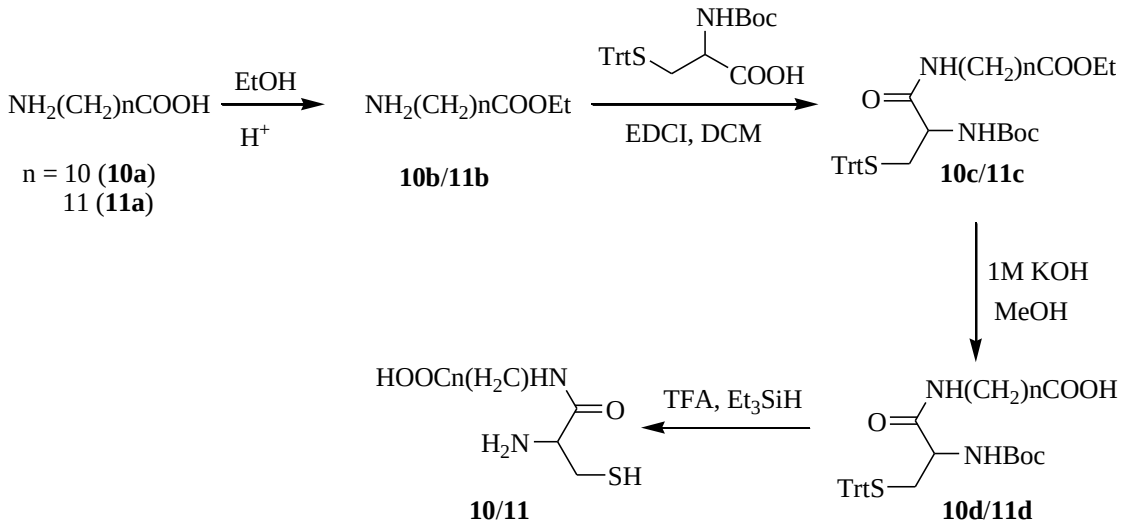

Fig. 4.19 Synthesis of 11 and 12 carbon fatty acid-cysteine conjugates

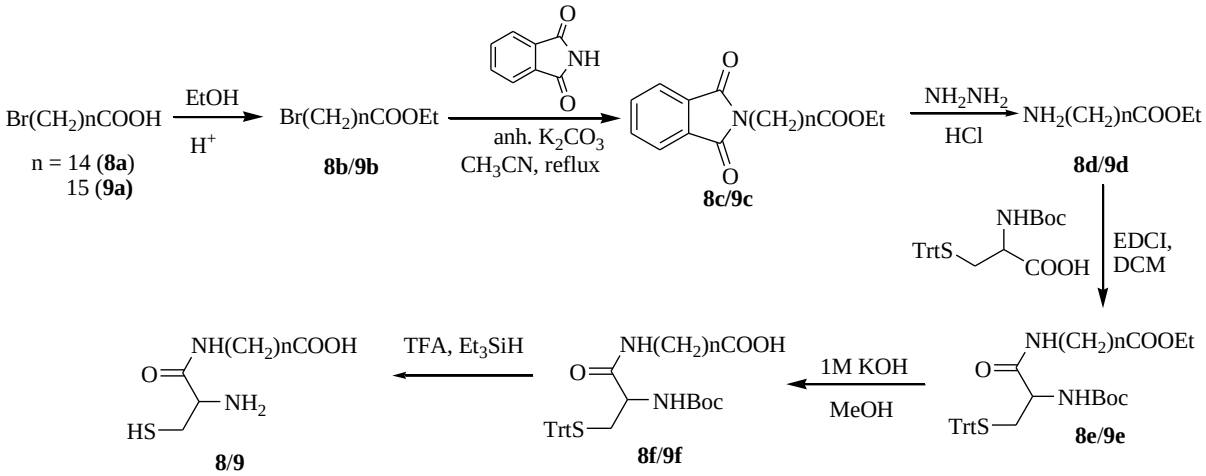

Fig. 4.20 Synthesis of 15 and 16 carbon fatty acid-cysteine conjugates

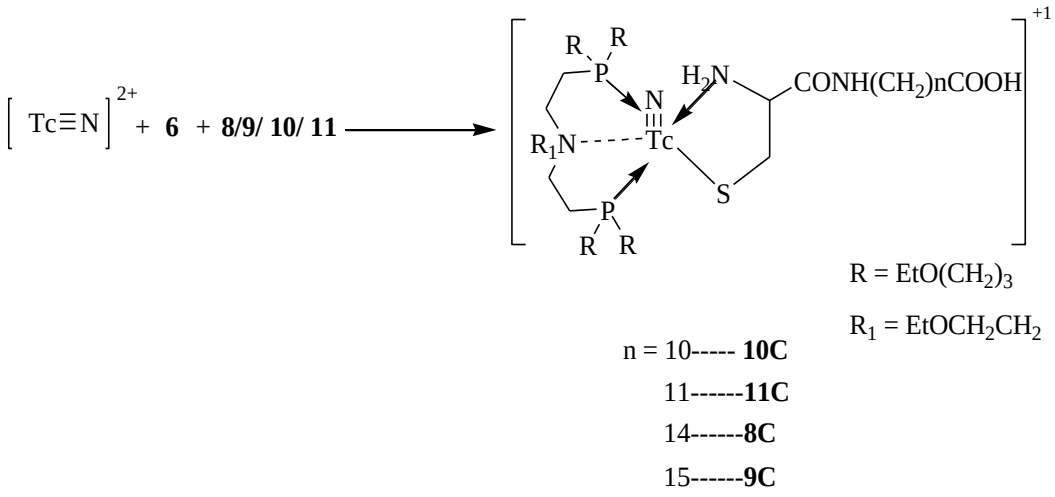

Fig. 4.21 Synthesis of fatty acid complexes **8C**-**11C**

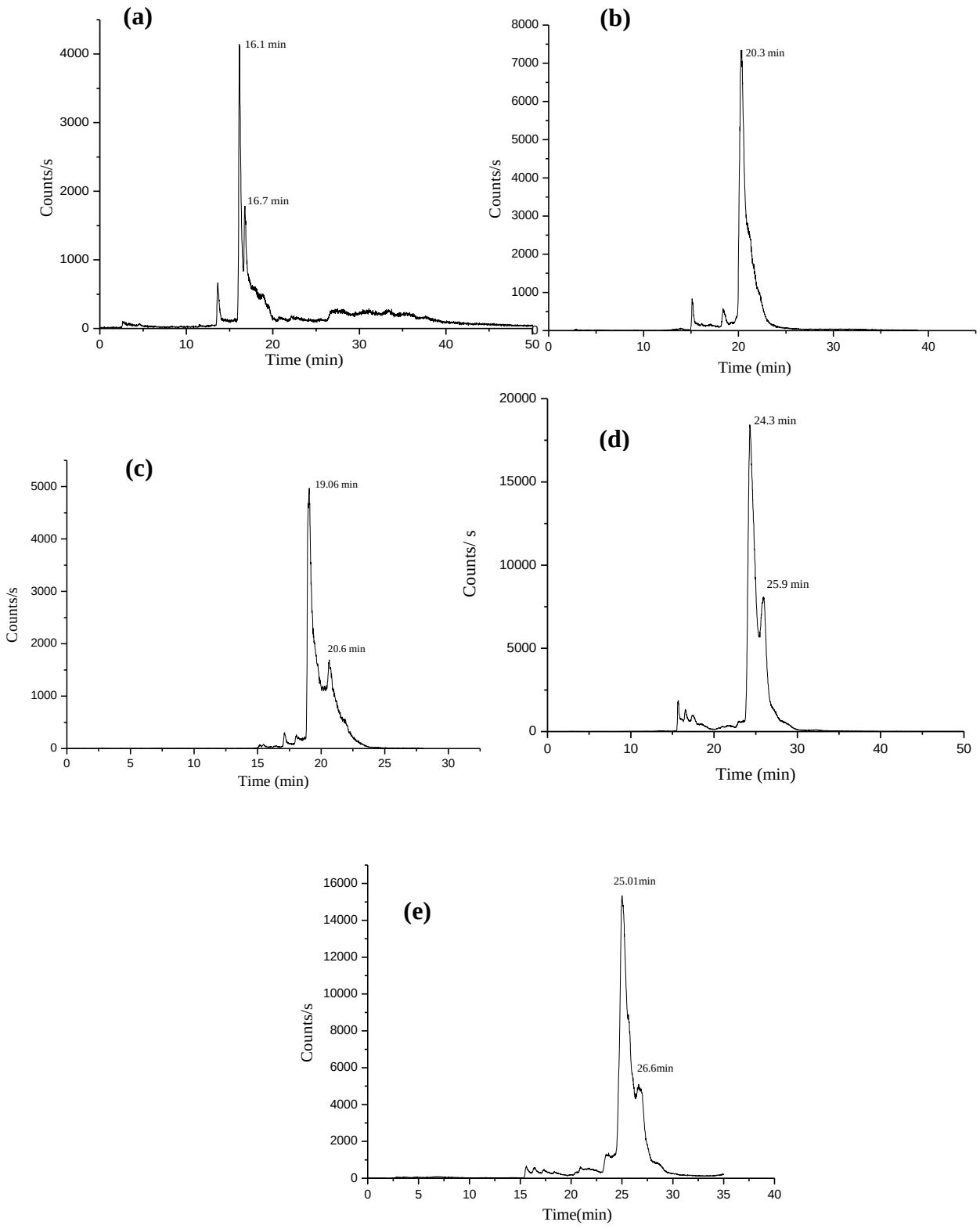

Fig. 4.22 HPLC profiles of (a) [^{99m}TcN(PNP**6**)] core and complexes (b) **10C** (c) **11C** (d) **8C** (e) **9C**

complexes **8C-11C** (Fig. 4.21). These were characterized by HPLC [Fig. 4.22(b)-(e)] and the peak area measurements indicated the radiolabeling yields >80%.

The *syn* and *anti* isomers of the complexes **8C-11C** are possible due to the presence of chiral carbon in cysteine residue.[191] However, the two isomers could be observed only if they are sufficiently resolved in the HPLC column. Thus, while two closely spaced peaks, accounting for the diastereomeric pair with the predominance of one diastereomer, could be observed in the HPLC elution profile of **8C**, **9C** and **11C** complex, such a pattern was not visible in the case of complex **10C**. Stereochemistry of the isomers can be unambiguously ascertained only after preparing the complex in macroscopic level using the long lived ^{99}Tc or inactive rhenium analogue and subsequent characterization. However, this was not attempted considering our major objective to examine the potential of the radiolabeled complexes as a myocardial agent. The major isomer was isolated by HPLC and used for bio-evaluation studies.

In the present study, fatty acid derivatives **8-11** have been prepared with the cysteine residue having free thiol and amino groups. The respective addition of these ligands to the intermediate $[^{99m}TcN(PNP)]^{2+}$ yields a uni-positively charged [2+2] asymmetric *pseudo*-octahedral complex. Since the complexes **8C-11C** are similar to the complexes reported earlier,[187,190,191,247] therefore these were envisaged to exhibit similar geometry with an overall uni-positive charge.

4.3.3 Biological studies

4.3.3.1 *Stability and hydrophobicity of the complexes* 8C-11C

As the first step of bio-evaluation, the *in-vitro* stability of the HPLC purified complexes **8C-11C** was studied in presence of challenging ligand cysteine.The complexes upon incubation with excess of cysteine were found to be stable and showed no transchelation as analyzed by TLC. Also, the stability of the complexes in serum was

assessed. The complexes **10C** and **11C** were found to be stable in serum, however, complexes **8C** and **9C** showed degradation to an extent of 20% and 10% respectively. The Log $P_{o/w}$ values of the four complexes **8C-11C** as determined using octanol-water system were found to be 0.80, 0.83, 1.13 and 1.20 respectively.

4.3.3.2 *Bio-distibution studies*

4.3.4.1 *Charged complex* 9C in c*omparison with neutral analogue* 7C *and* ^{125}*I-IPPA*

To evaluate the effect of charge on the *in-vivo* pharmacokinetic behavior, in terms of target uptake and non-target clearance characteristics, the bio-distribution results of charged **9C** and its neutral analogue **7C** compared. Also, to evaluate the potential of charged complex **9C** as myocardial agent, its bio-distribution results were compared with the standard agent ^{125}I-IPPA. The Fig. 4.23 shows the myocardial uptake and clearance pattern of the charged complex **9C** under evaluation. The results obtained with ^{125}I-IPPA as well as earlier reported neutral analogue **7C** are also shown for comparison. The initial uptake shown by **9C** (9.88 ± 2.99% ID/g) in the myocardium at 2 min p.i. is similar to that of ^{125}I-IPPA. However, initially accumulated activity was not retained and gets cleared from the myocardium. This shows that the [^{99m}TcN(PNP)]-cysteine moiety is not functioning like the ^{125}I-iodophenyl ring in ^{125}I-IPPA. Though the initial myocardial uptake value of neutral complex **7C** was far below **9C**, however, the washout kinetics from the myocardium was similar.

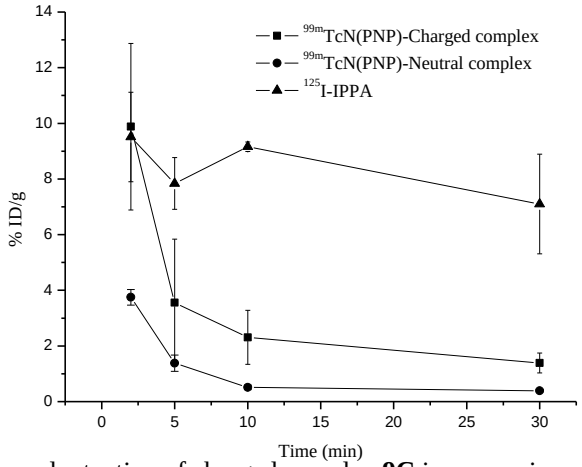

Fig. 4.23 Myocardial uptake and retention of charged complex **9C** in comparison with ^{125}I-IPPA and neutral complex **7C**

The time dependent variation in heart/ blood, heart/ lung and heart/ liver ratios of **9C**, **7C** and ^{125}I-IPPA are shown in Fig. 4.24(a)-(c). There is no significant difference in heart/ lung and heart/ liver ratios among the three radiolabeled compounds. ^{125}I-IPPA, however, showed better heart/ blood ratio compared to the other two complexes **9C** and **7C**. Unlike the neutral complex **7C**, charged analogue **9C** showed increased radioactivity uptake in non-target organs with slow washout, accounting for the similarity in the heart/ liver, heart/ lung and heart/ blood ratios of the two complexes.

The clearance of activity from different organs exhibited by **9C**, **7C** and ^{125}I-IPPA is shown in Fig. 4.25. Both **9C** and **7C** cleared via the hepatobiliary route. The rapid increase in the intestinal radioactivity with time indicates fast clearance of the radioactivity from liver. This may be due to metabolizable ether residues present on the final [^{99m}TcN(PNP)] complex which facilitates early clearance of the radioactivity from the liver. Also, a different

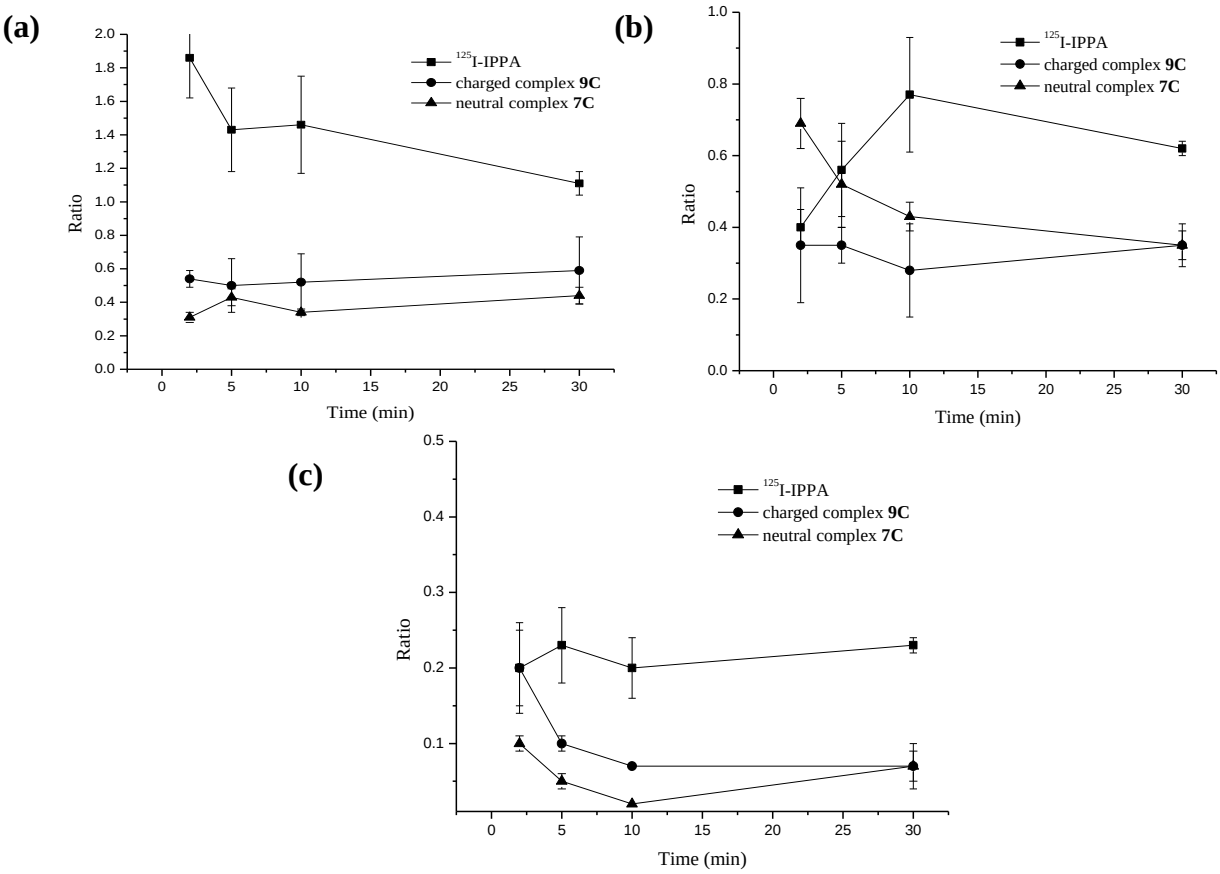

Fig. 4.24 Time dependent changes in the (a) heart/ blood (b) heart/ lung (c) heart/ liver ratios of the charged complex **9C,** ^{125}I-IPPA and neutral complex **7C**

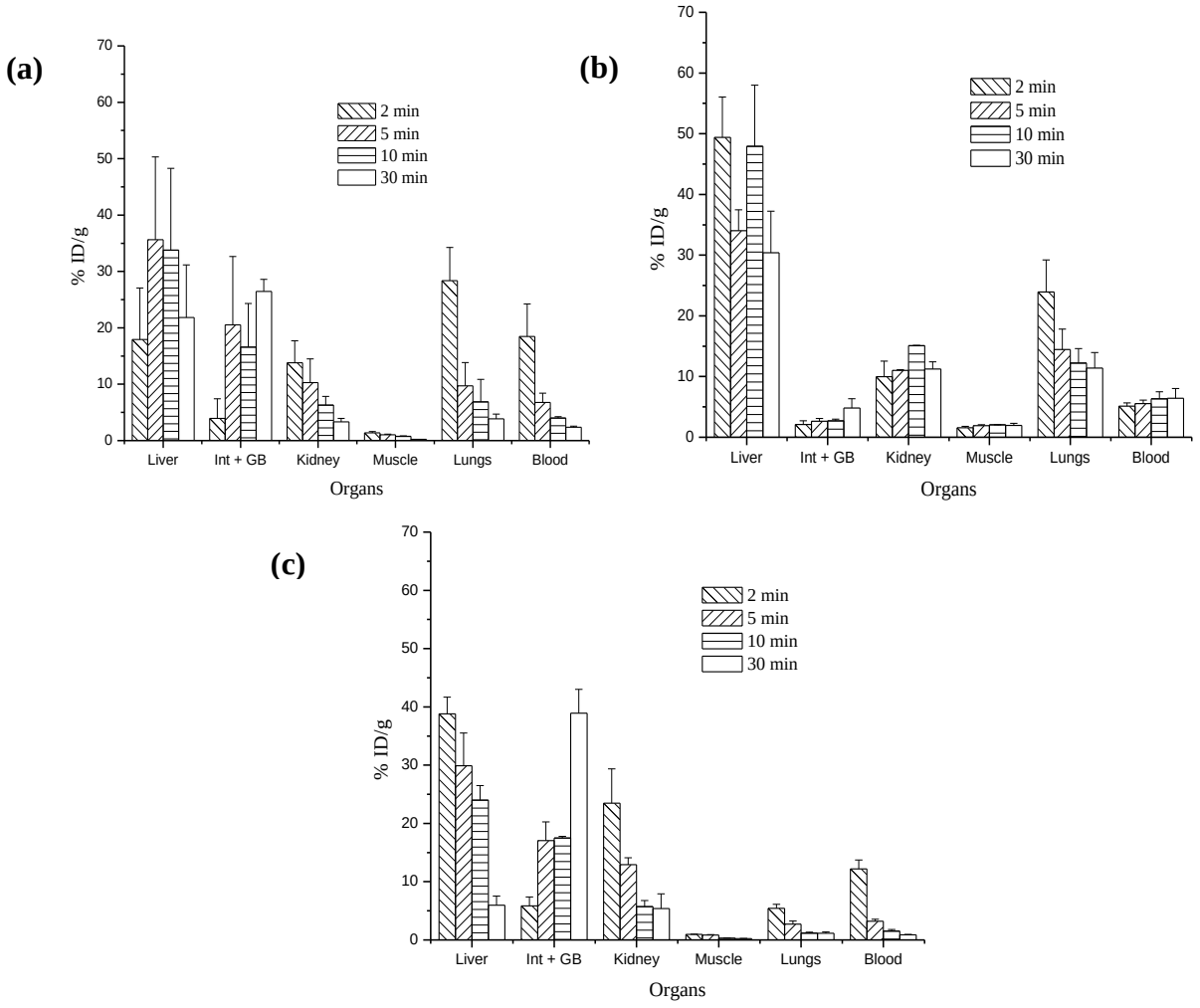

Fig. 4.25 Activity distribution pattern of (a) charged complex **9C** (b) ^{125}I-IPPA and (c) neutral complex **7C** in different organs in Swiss mice

mechanism based on P-glycoproteins (Pgp) or multidrug resistance-associated protein (MDR)-Pgp may also be responsible for rapid elimination of [^{99m}TcN(PNP)] complex from the tissues.[249] Contrary to **9C** and **7C**, ^{125}I-IPPA shows slow clearance of liver activity which results in low heart/ liver ratios. The effectiveness of [^{99m}TcN(PNP)]$^{2+}$ intermediate in achieving good *in-vivo* pharmacokinetic behavior is evident from the rapid non-target clearance pattern of [^{99m}TcN(PNP)]$^{2+}$ complexes compared to ^{125}I-IPPA.

Thus, charged complexes seem to be better molecules than their neutral counterparts in terms of target uptake (initial value similar to the standard agent), however, show inferior

behavior in terms of non-target clearance kinetics. Both the complexes show identical behavior in terms of washout kinetics of the radioactivity from the myocardium and in target/ non-target ratios.

4.3.4.2 *Other fatty acid complexes*

The superior target uptake pattern of charged complex over its neutral analogue infused interest in exploring the different charged complexes of varying chain lengths. In this view, the bio-distribution of purified complexes **8C**, **10C** and **11C** were carried in Swiss mice and their results compared alongwith **9C**. Also, to evaluate their potential as myocardial agent, the comparison with ^{125}I-IPPA has been carried out. The bio-distribution results of **8C-11C** are shown in Tables 4.1-4.4. All four complexes showed uptake in the myocardium (Fig. 4.26). A steady rise in the myocardial uptake values was observed on increasing the fatty acid chain length (lipophilicity), however, the initial uptake was not retained. The clearance of radioactivity from the myocardium was non-uniform with the initial rapid clearance phase up to 10 min p.i. was followed by slow phase upto 30 min p.i.

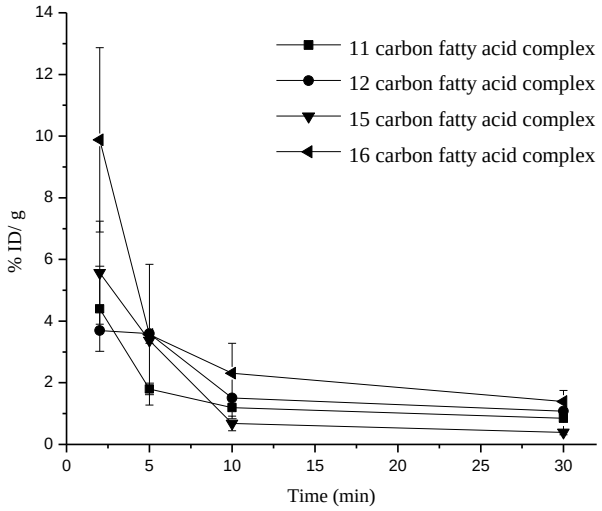

Fig. 4.26 Uptake and retention characteristics of different fatty acid complexes (**8C-11C**) in the myocardium of Swiss mice

Table 4.1 Bio-distribution of complex **10C** in Swiss mice [% ID/ g (1SD), (n=3)]

Organs	*2 min*	*5 min*	*10 min*	*30 min*
Liver	84.03 (11.46)	73.78 (10.72)	63.23 (19.69)	23.87 (3.68)
Int + GB	5.10 (1.63)	16.99 (6.35)	34.01 (5.14)	55.82 (10.22)
Kidney	9.83 (0.75)	5.95 (1.48)	3.17 (0.40)	2.38 (0.93)
Heart	4.40 (1.38)	1.80 (0.19)	1.19 (0.36)	0.85 (0.12)
Lungs	12.24 (4.68)	4.40 (0.76)	1.89 (0.70)	1.15 (0.31)
Muscles	0.67 (0.05)	0.60 (0.09)	0.46 (0.02)	0.22 (0.05)
Blood	6.77 (3.07)	1.22 (0.16)	0.85 (0.16)	0.25 (0.01)
Heart/ blood	0.8(0.3)	1.48(0.12)	1.36(0.18)	3.44 (0.76)
Heart/ liver	0.06 (0.02)	0.02 (0.00)	0.02 (0.00)	0.04 (0.01)
Heart/ lungs	0.4 (0.15)	0.42 (0.07)	0.69 (0.18)	0.8 (0.2)

Table 4.2 Bio-distribution of complex **11C** in Swiss mice [% ID/ g (1SD), (n=3)]

Organs	*2 min*	*5 min*	*10 min*	*30 min*
Liver	35.71 (5.24)	38.94 (4.09)	30.04 (4.24)	15.57 (3.03)
Int + GB	7.65 (3.05)	20.33 (2.93)	15.44 (1.59)	33.10 (6.10)
Kidney	12.06 (0.69)	9.39 (1.15)	6.02 (1.26)	4.91 (0.57)
Heart	3.65 (0.74)	3.59 (0.23)	1.51 (0.27)	1.08 (0.08)
Lungs	8.66 (1.75)	2.67 (1.56)	2.02 (1.12)	1.09 (0.46)
Muscles	0.96 (0.05)	0.98 (0.07)	0.55 (0.15)	0.50 (0.15)
Blood	10.40 (1.29)	7.34 (1.65)	3.98 (0.52)	2.64 (0.24)
Heart/ blood	0.35(0.08)	0.52 (0.12)	0.38 (0.03)	0.41 (0.00)
Heart/ liver	0.1 (0.03)	0.09 (0.01)	0.05 (0.00)	0.07 (0.02)
Heart/ lungs	0.42 (0.02)	0.33 (0.03)	0.33 (0.03)	0.3 (0.09)

Table 4.3 Bio-distribution of complex **8C** in Swiss mice [% ID/ g (1SD), (n=3)]

Organs	*2 min*	*5 min*	*10 min*	*30 min*
Liver	33.97 (14.45)	26.48 (8.03)	29.43 (4.58)	17.73 (5.13)
Int + GB	3.10 (1.66)	4.30 (2.19)	8.12 (2.10)	15.57 (3.23)
Kidney	9.75 (3.50)	6.85 (0.74)	4.73 (2.96)	2.62 (1.10)
Heart	5.57 (1.67)	3.37 (0.09)	0.68 (0.24)	0.39 (0.08)
Lungs	16.84 (2.88)	8.12 (1.92)	2.11 (0.28)	1.09 (0.36)
Muscles	0.97 (0.3)	0.58 (0.12)	0.32 (0.10)	0.14 (0.08)
Blood	16.83 (3.00)	10.94 (3.74)	2.11 (0.93)	1.09 (0.36)
Heart/ blood	0.36 (0.18)	0.32 (0.06)	0.35 (0.12)	0.38 (0.05)
Heart/ liver	0.18 (0.08)	0.13 (0.02)	0.03 (0.00)	0.02 (0.00)
Heart/ lungs	0.34 (0.1)	0.42 (0.05)	0.42 (0.13)	0.21 (0.05)

Table 4.4 Bio-distribution of complex **9C** in Swiss mice [% ID/ g (1SD), (n=3)]

Organs	*2 min*	*5 min*	*10 min*	*30 min*
Liver	17.92(9.15)	35.63 (14.71)	33.80 (14.53)	21.82 (9.34)
Int + GB	3.92 (3.49)	20.53 (12.16)	16.60 (7.73)	26.46 (2.12)
Kidney	13.81 (3.90)	10.27 (4.21)	6.32 (1.52)	3.33 (0.60)
Heart	9.88 (2.99)	3.56 (2.28)	2.31 (0.97)	1.39 (0.36)
Lungs	28.38 (5.89)	9.70 (4.13)	6.87 (3.98)	3.87 (0.84)
Muscles	1.36 (0.24)	1.03 (0.11)	0.76 (0.08)	0.24 (0.00)
Blood	18.46 (5.77)	6.77 (1.63)	4.00 (0.23)	2.37 (0.18)
Heart/ blood	0.54 (0.05)	0.5 (0.16)	0.52 (0.17)	0.59 (0.2)
Heart/ liver	0.90 (0.75)	0.1(0.01)	0.07(0.00)	0.07(0.03)
Heart/ lungs	0.35 (0.16)	0.35 (0.06)	0.28 (0.13)	0.35 (0.05)

For the complex **10C**, the heart/ blood ratio improved with time attaining a maximum of 3.44 ± 0.76 at 30 min p.i., which was observed to be better than the value obtained with ^{125}I-IPPA [Fig. 4.27 (a)] at same interval of time. However, for complexes **8C**, **9C** and **11C** the ratio did not improve above 1 throughout the period of study. The heart/ lung and heart/ liver ratios also did not exceed 1 and similar trend was obtained with ^{125}I-IPPA [Fig. 4.27 (b) & 4.27 (c)].

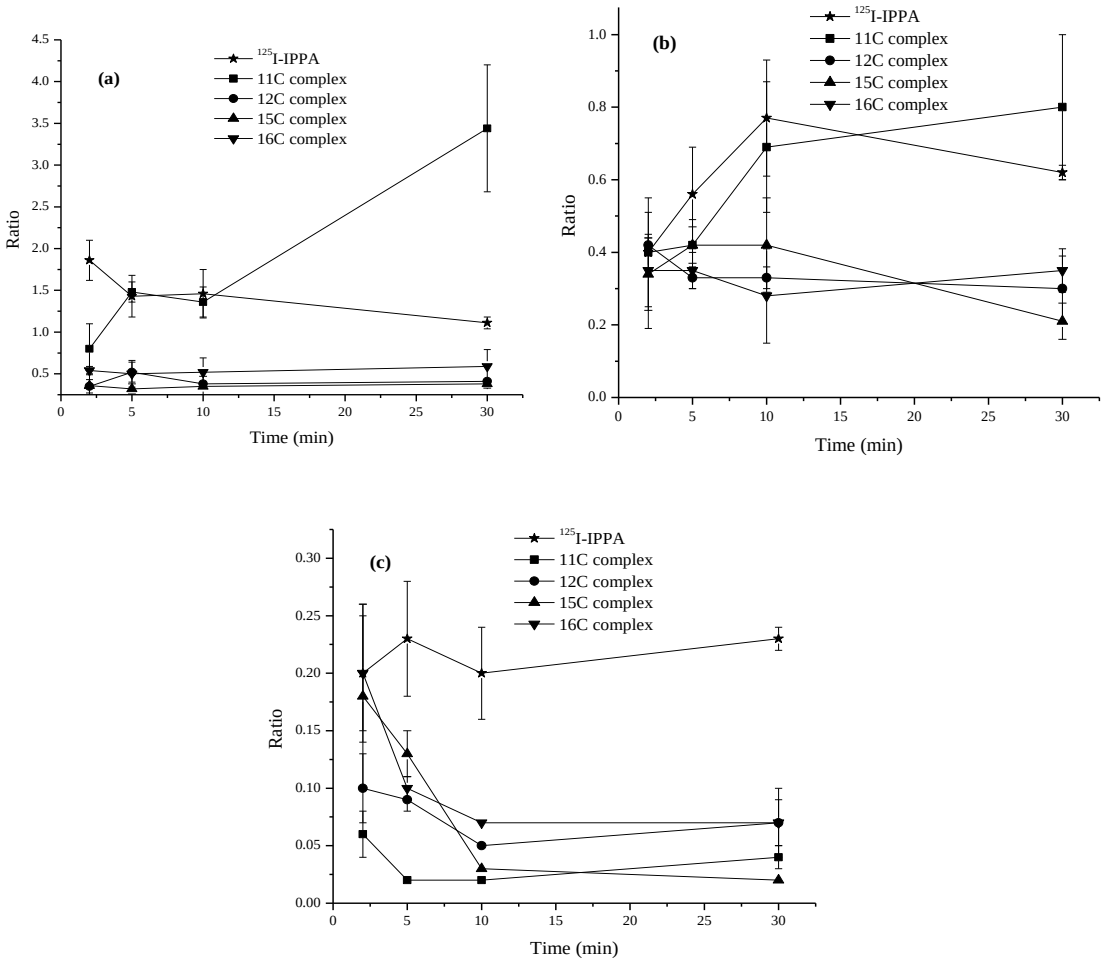

Fig. 4.27 Time dependent changes in the (a) heart/ blood (b) heart/ lung (c) heart/ liver ratios of different radiolabeled fatty acids (**8C-11C** and ^{125}I-IPPA)

The time dependent radioactivity profile of the complexes **8C**, **10C** and **11C** in other non-target organs is shown in Fig. 4.28. The washout pattern of radioactivity from blood, liver and lungs shows a decreasing trend with increase in the fatty acid chain length (lipophilicity). The complexes cleared mainly via the hepatobiliary route. The radioactivity from other non-target organs was also found to clear with time.

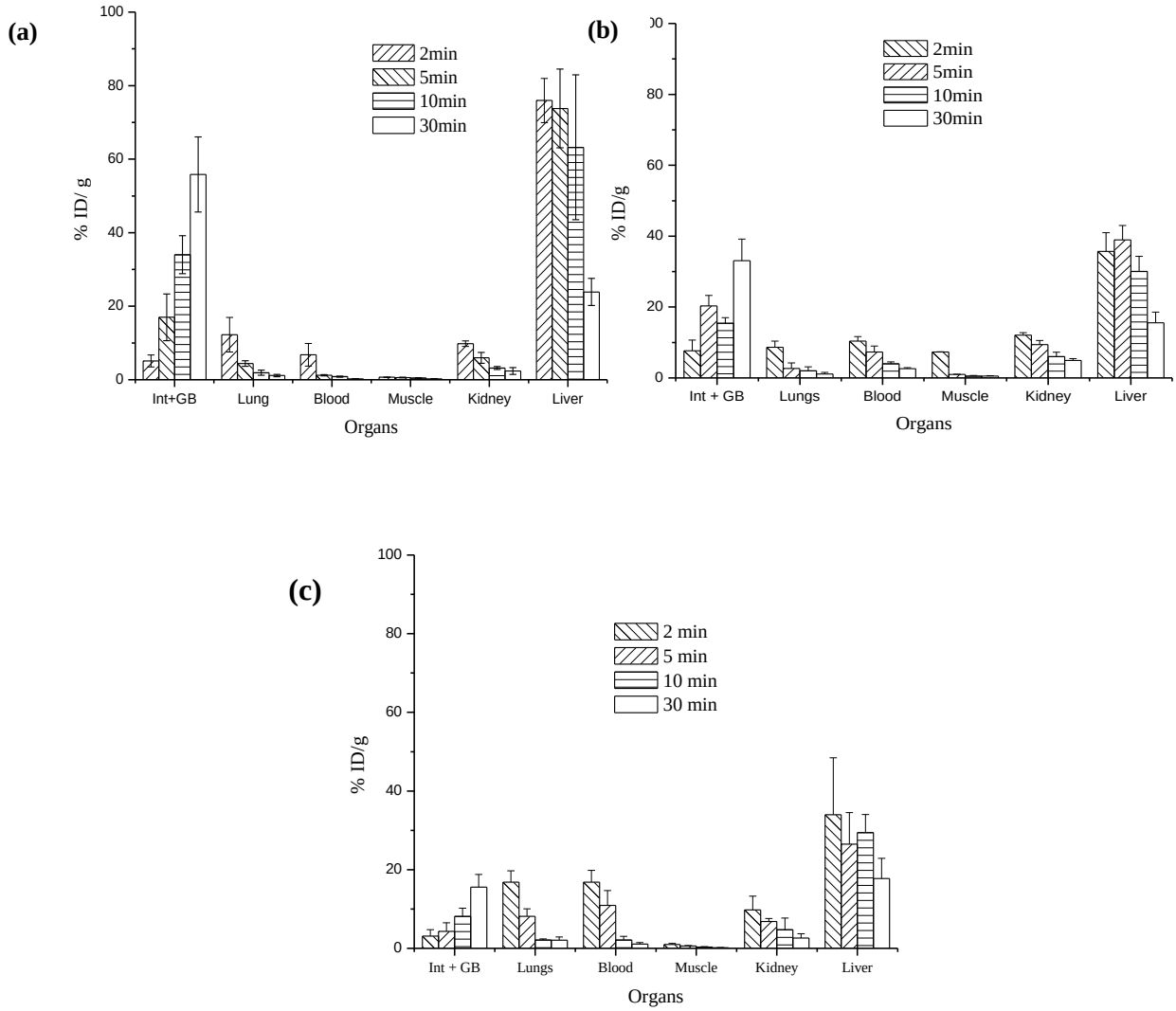

Fig. 4.28 Activity distribution pattern of complexes (a) **10C** (b) **11C** and (c) **8C** in different organs in Swiss mice

4.4 Conclusion

The present chapter is aimed at depicting the versatility of $[^{99m}TcN(PNP)]^{2+}$ intermediate by varying the charge and lipophilicity of $[^{99m}TcN(PNP)]^{2+}$ complexes. In this regard, a series of four uni-positively charged fatty acid complexes of varying chain lengths (11, 12, 15 and 16 carbon) were synthesized. The bio-distribution studies of uni-positively charged 16 carbon fatty acid complex in Swiss mice showed high initial myocardial extraction similar to the standard agent ^{125}I-IPPA at 2 min p.i., however with poor retention subsequently. The complex showed better uptake characteristics than the neutral analogue. Thus, positively charged fatty acid derivatives, prepared using $[^{99m}TcN(PNP)]^{2+}$ core seem to be better candidates for the development of myocardial metabolic tracers than their neutral counterparts reported in the previous chapter.

The increase in the fatty acid chain length from 11 to16 showed steady improvement in the myocardial uptake values. However, all the complexes showed rapid washout from the myocardium limiting their utility for external imaging. The effect of lipophilicity increase on the clearance pattern from the non-target organs, on the contrary, showed a decreasing trend. Thus, a proper balance of chain length, which shows an optimum uptake and clearance from the non-target organs so as to maximize target/ non-target ratio, and a modification in the lead molecule to affect prolonged retention in the myocardium, is desired for the development of a new myocardial metabolic tracer.

CHAPTER 5

$[^{99m}TcN]^{2+}$ core for other imaging applications

5.1 Introduction

$[^{99m}TcN]^{2+}$ core, explored in the previous chapters for developing a myocardial imaging radiopharmaceutical agent has potential for use in other diagnostic applications as well.[240-241] The attachment of core to different carrier biomolecules could lead to preparations with varied biological applications. The radiolabeling of target specific molecules requires a prior knowledge of biomolecule-target site interaction. The structure-activity relationship provides information about the active part of the biomolecule responsible for its specificity towards a particular target site. The biologically less active part of the molecule is then identified and the necessary chemical modification, if required, is carried in that region to introduce the radioactive label.

The introduction of $[^{99m}TcN]^{2+}$ core to a biomolecule requires use of either symmetric [2+2] or asymmetric [2+2] labeling approach, as discussed previously.[181,189] The desired use of the radiopharmaceutical and the choice of carrier molecule, govern the mode of labeling technique to be followed for the preparation of ^{99m}TcN-labeled molecule. The charge and lipophilicity of the $[^{99m}TcN]$-radiolabeled biomolecule, can be varied over a broad range by changing the labeling approach. Thus, this $[^{99m}TcN]^{2+}$ core has all the attributes for its varied use, in wide range of diagnostic imaging applications. In the present work, $[^{99m}TcN]^{2+}$ core has been used for the labeling of a hypoxia targeting molecule, nitrotriazole.

Hypoxia as the term suggests is a situation where there is oxygen deficiency, which could result from reduced or improper blood supply or poisoning with gases such as carbon

monoxide, in a tissue or an organ. Such hypoxic conditions can be observed in oncology, cardiovascular disease, cerebrovascular disease, diabetes, infection, during wound healing, joint hypoxia etc.[252]

Hypoxic regions in tumors result when tumor growth exceeds the capacity of accompanying blood vasculature to deliver adequate quantity of oxygen to the growing mass of tumor cells.[253] In cancers which manifest as large tumors, hypoxia is fairly common and this severely affects the treatment, be it chemotherapy or radiation therapy,[254-255] leading to ineffective therapy and poor prognosis. Hence the knowledge about the occurrence of hypoxia and its delineation is very important in such cancers for proper treatment planning. The inherent drawbacks of invasive techniques to detect hypoxia[256] have provided an impetus for the development of suitable radiopharmaceuticals that can be utilized for imaging tumor hypoxia. Imaging hypoxic regions non-invasively would be a great tool for the oncologists who treat patients with hypoxic tumors. Thus developing a suitable radiopharmaceutical that can image hypoxic tissues has been pursued avidly, with some success with a ^{18}F based molecule. However, no promising ^{99m}Tc based molecule has reached the clinics, although there have been efforts towards this goal. In the present chapter, an attempt has been made to develop a radiopharmaceutical agent based on ^{99m}Tc useful for imaging tumor hypoxia.

Nitro heterocyclics (imidazoles and triazoles) have shown a tendency to accumulate in the hypoxic regions of tumors, providing the attractive possibility of employing these molecules as carriers for targeting hypoxic tissues.[256-259] The mechanism of reduction of nitro-heterocycles, is well documented by Nunn et al.[253] These compounds enter the cells non-specifically and undergo a one electron reduction. While in normoxic cells, this reduction step is reversible, in hypoxic cells the compounds undergo a series of further reductions till the ring gets fragmented and the reactive fragments finally get irreversibly

bound to the cellular components. This property is exploited to selectively target hypoxic cells.

^{18}F-2-fluoromisonidazole is a known agent for hypoxia targeting.[260] A series of ^{123}I-labeled 2-nitroimidazole derivatives for imaging has been investigated with the more widely available SPECT, culminating with ^{123}I-iodoazomycin arabinoside (IAZA) which is in clinical trials.[261-263] The above agents are based on cyclotron produced radioisotopes, ^{18}F and ^{123}I. Though the number of cyclotrons is increasing every year, cyclotron based isotopes are still not widely available in all parts of the world. Hence, molecules labeled with ^{99m}Tc, which is a more widely available isotope, is preferable for wide use. In this context, several nitro-imidazoles and triazoles, have been suitably modified to hold the ^{99m}Tc metal core and evaluated.[241,264-267] However, none of these exhibited the desired biological characteristics. The search for an ideal hypoxia-imaging agent must take into consideration the factors such as a simple, cost-effective preparation route, stability, rapid accumulation in tumors, sufficient retention times therein, and rapid clearance from other tissues, to provide better contrast between lesion and background.

In the work reported, $[^{99m}TcN]^{2+}$ was explored for developing a hypoxia imaging agent. Among the different strategies to label a molecule using the $[^{99m}TcN]^{2+}$ core, labeling via $[^{99m}TcN(PNP)]^{2+}$ intermediate was deemed as an excellent approach, as the complexes that result exhibit high non-target clearance characteristics. The asymmetric complexes as discussed in the previous chapters were found to clear rapidly from blood, liver and other non-target organs. This is an important consideration in the design of hypoxia imaging agent. Also, the tumors located in the abdominal region can be imaged early, as the final asymmetric complex clears rapidly from spleen, lungs and liver.

Cysteine is an ideal BFCA for $[^{99m}TcN(PNP)]^{2+}$ intermediate where the target molecule can be linked to either an amino or acid residue and complexed via free (COOH,

SH) or (NH_2, SH) of the coupled cysteine conjugate, respectively. In the present work, a 2-(5-nitro-1H-1,2,4-triazol-1-yl) acetic acid or sanazole acid has been linked to an amino group of cysteine (Fig. 5.1) and complexed with $[^{99m}TcN(PNP)]^{2+}$ core yielding [2+2] asymmetric complex which was subsequently bio-evaluated in tumor bearing mice.

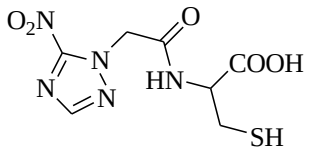

12

Fig. 5.1 Structure of synthesized nitrotriazole-cysteine conjugate

5.2 Experimental

5.2.1 Materials and Methods

The nitrotriazole, 2-(5-nitro-1H-1,2,4-triazol-1-yl) acetic acid (sanazole acid, **12a**) was obtained as a gift from Dr. V.T. Kagia, Health Research Foundation, Kyoto, Japan. The other general experimental details are given in chapter 2, section 2.2.2.1.

5.2.2 Synthesis of 2-(2-(5-nitro-1H-1,2,4-triazol-1-yl)acetamido)-3-mercaptopropanoic acid (12)

2-Amino-3-tritylsulfanyl-propionic acid ethyl ester (**7a**)

The synthesis and characterization of this compound **7a** is mentioned in Chapter 3, section 3.2.2.2.1.

Ethyl 2-(2-(5-nitro-1H-1,2,4-triazol-1-yl)acetamido)-3-(tritylthio)propanoate (**12b**)

A mixture of **12a** (100 mg, 0.58 mmol) and compound **7a** (226 mg, 0.58 mmol) in CH_2Cl_2 (15 mL) was stirred and cooled to 0 °C in an ice bath. To the cooled reaction mixture, EDCI (123 mg, 0.63 mmol) was added and the mixture stirred at 0 °C for 1 h. Thereafter, it was brought to room temperature and stirred overnight. Upon completion of the reaction (*cf.* TLC), the reaction mixture in CH_2Cl_2 was washed with water (3 × 10 mL), dried and

concentrated to give the crude product, which was purified by silica gel chromatography [EtOAc/ $CHCl_3$ (1:9 v/v)] to yield pure **12b** as colorless oil.

Yield: 291mg (92 %), R_f = 0.3 [EtOAc/ $CHCl_3$ (1:9 v/v)].

^{1}H NMR ($CDCl_3$, δ ppm): 8.32 (s, 1H, Triazole); 7.22-7.42 (m, 15H, $(C_6\underline{H}_5)_3C$-); 6.36 (d, 1H, -CON<u>H</u>-, *J = 7.5 Hz*); 4.90 (s, 2H, -NC<u>H</u>$_2$-); 4.48-4.54 (m, 1H, -NHC<u>H</u>COO-); 4.19 (q, 2H, $CH_3C\underline{H}_2O$-, *J = 7.2 Hz*); 2.75-2.81 (m, 1H, -SC<u>H</u>$_A$H$_B$-); 2.60-2.66 (m, 1H, -SCH$_A$<u>H</u>$_B$-); 1.25 (t, 3H, -$CH_2C\underline{H}_3$, *J = 7.2 Hz*) [Fig. 5.2].

MS (ESI, -ve mode): Mass (calculated) $C_{28}H_{27}N_5O_5S$ 545.2; *m/z* (observed) 544.2 [Fig. 5.3].

2-(2-(5-nitro-1H-1,2,4-triazol-1-yl)acetamido)-3-(tritylthio)propanoic acid (**12c**)

To a solution of **12b** (0.18 mmoles, 100 mg) in MeOH (600 µL), aqueous 1M KOH solution (400 µL, 0.4 mmoles) was added and stirred for 48 h at room temperature. Upon completion of the reaction (*cf*. TLC), MeOH was removed under vacuum, water (5 mL) was added and the pH of the reaction mixture was adjusted to 3 using aqueous 2N HCl to give **12b** as white precipitate which was filtered and dried under vacuum.

Yield: 80% (75 mg). R_f = 0 [EtOAc/ $CHCl_3$ (1:9 v/v)].

^{1}H NMR (CD_3OD, δ ppm): 8.63 (s, 1H, Triazole), 7.22-7.42 (m, 15H, $(C_6\underline{H}_5)_3C$-); 5.15 (s, 2H, -NC<u>H</u>$_2$-); 4.26-4.30 (m, 1H, -C<u>H</u>COO-); 2.61-2.66 (m, 2H, -C<u>H</u>$_2$S-) [Fig. 5.4].

2-(2-(5-nitro-1H-1,2,4-triazol-1-yl)acetamido)-3-mercaptopropanoic acid (**12**)

The compound **12c** (0.096 mmoles, 50 mg) was stirred with TFA (2 mL) for 10 min at room temperature. To the resultant yellow solution, Et_3SiH was added dropwise until the solution turned colorless. Stirring was continued for another 15 min. The solvent was removed under vacuum to obtain the desired product **12** which was dried under vacuum and used as such for radiolabeling without further characterization.

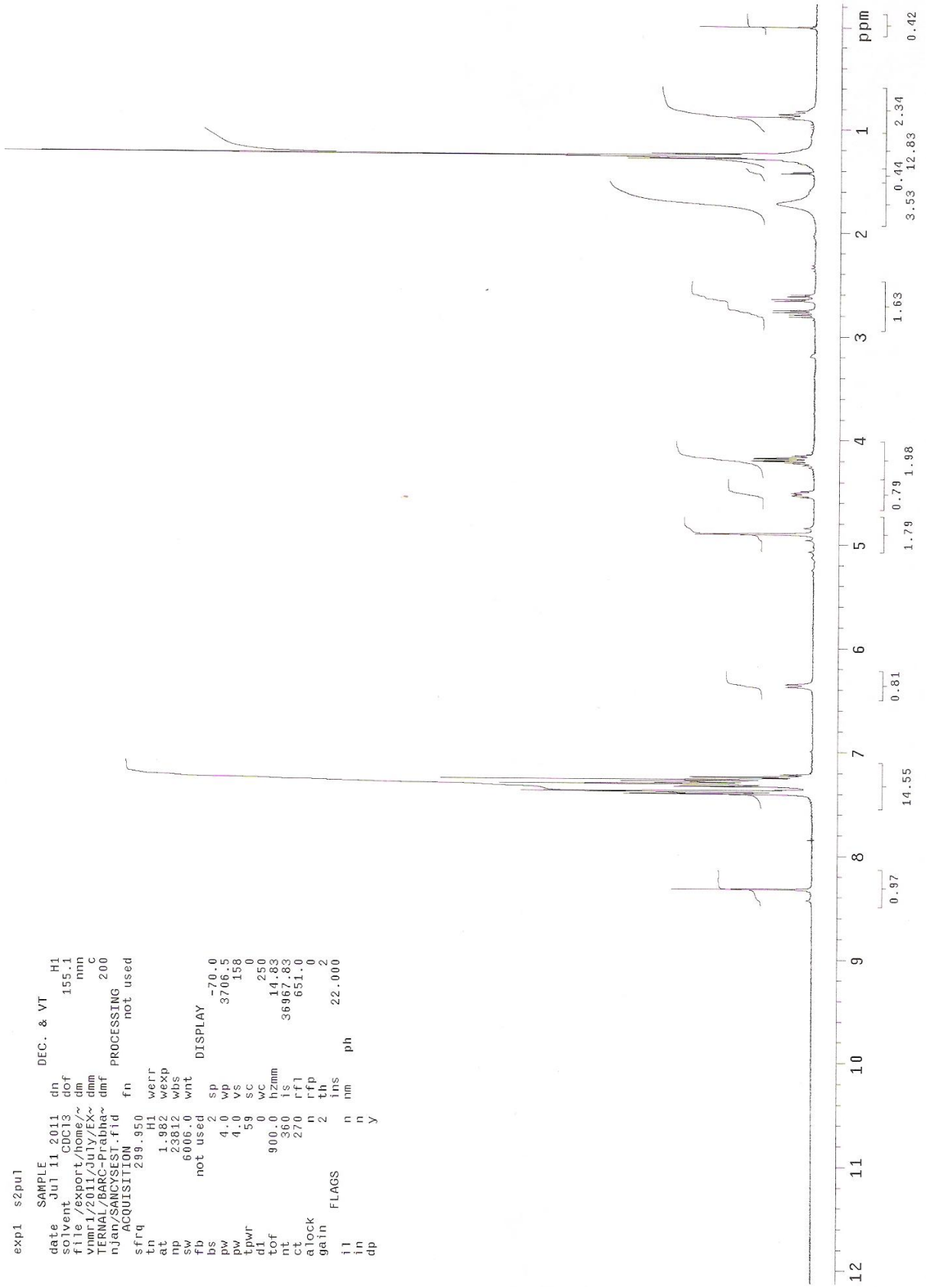

Fig. 5.2 ^{1}H NMR spectrum of compound **12b**

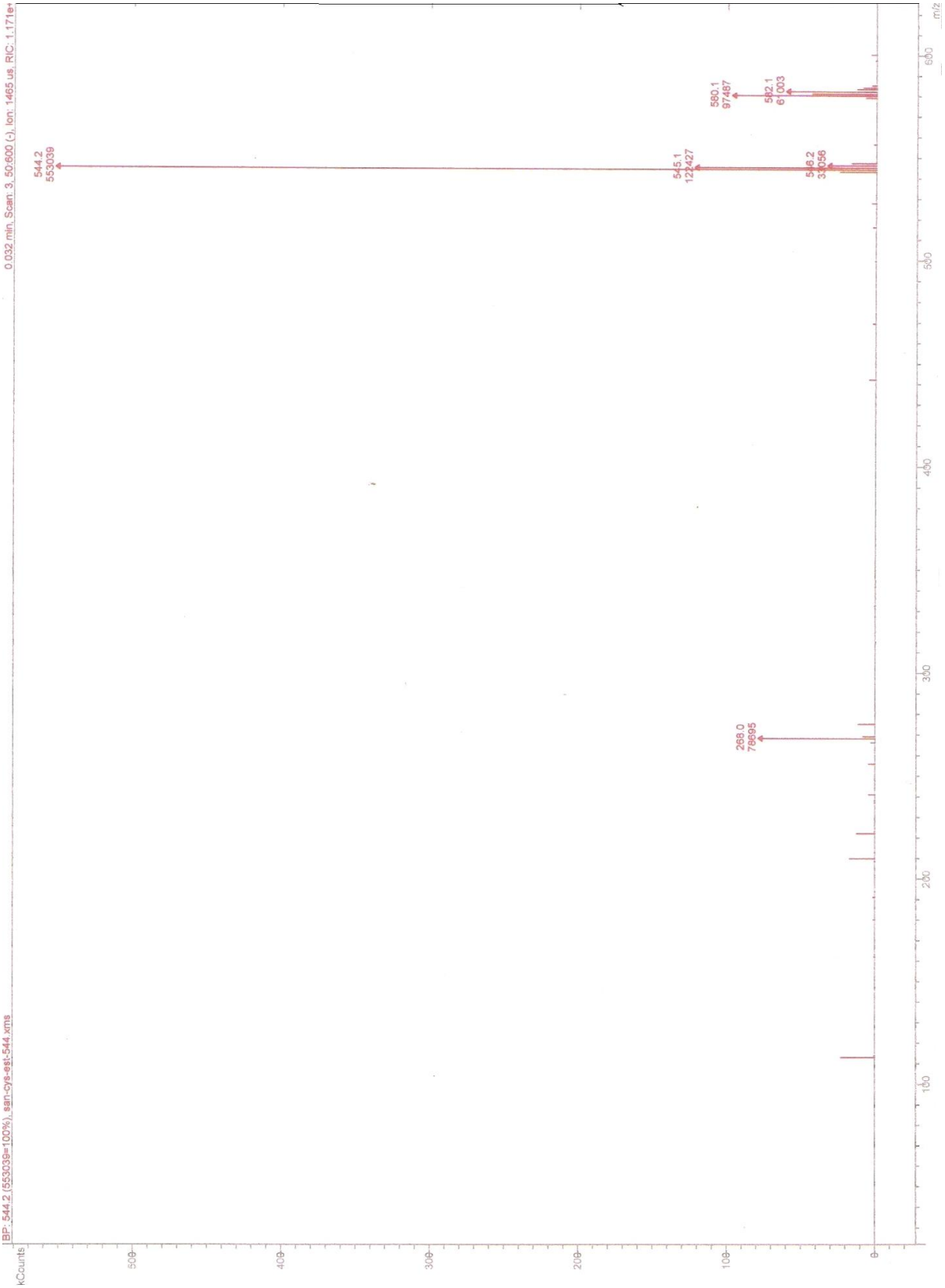

Fig. 5.3 Mass spectrum of compound **12b**

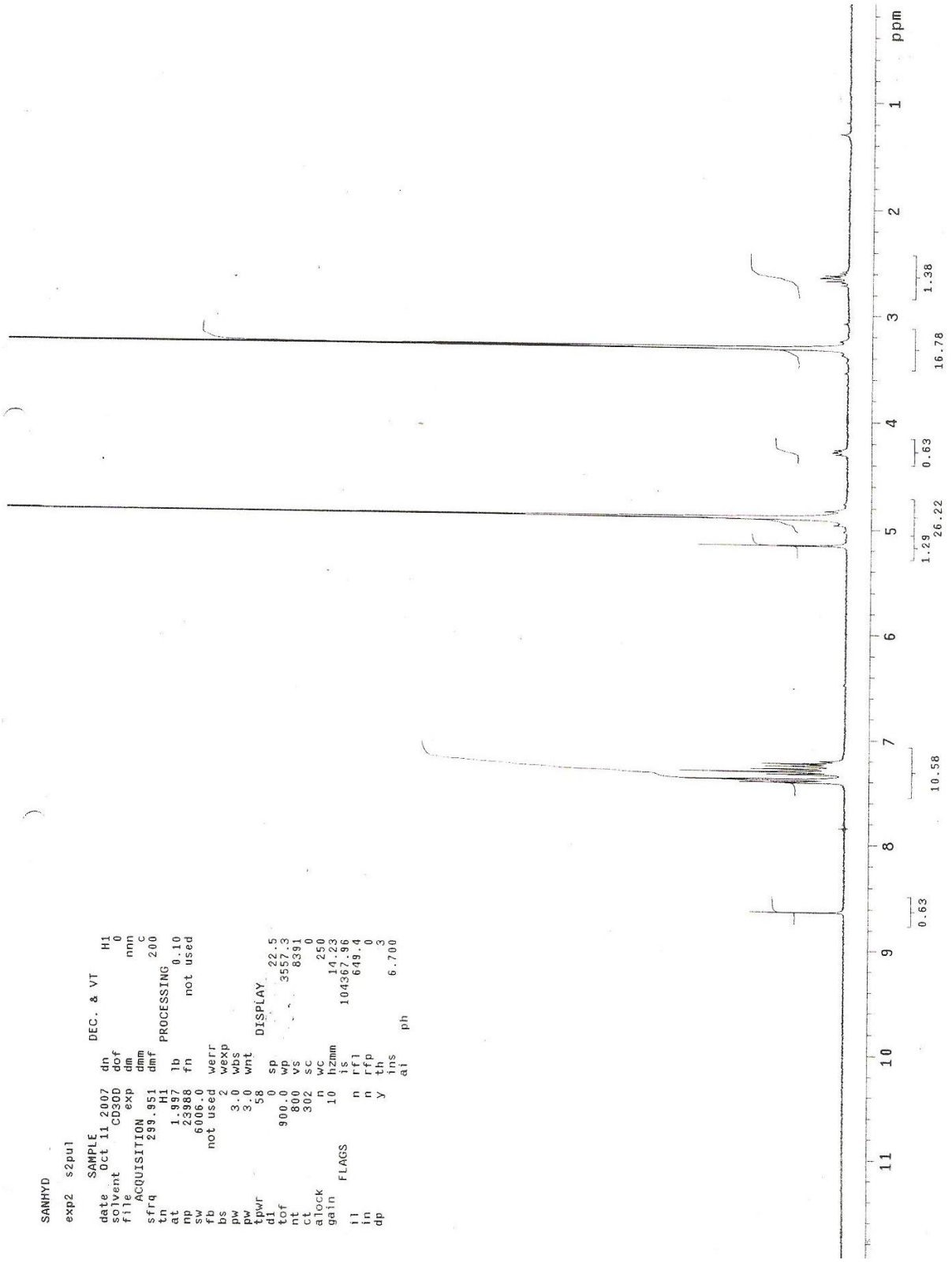

Fig. 5.4 ^{1}H NMR spectrum of compound **12c**

5.2.3 Radiolabeling

5.2.3.1 *Preparation of [^{99m}TcN(PNP)] complex* (**12C**)

In a 10 mL glass vial containing freshly prepared $[^{99m}TcN]^{2+}$ core (750 µL, 1.85 GBq or 50 mCi), PNP ligand **6** (~3 µL) alongwith **12** (~5 mg), both dissolved in EtOH (250 µL, purged with nitrogen for 15 min), were added. The capped vial was heated on a water bath at 90 °C for 30 min. The vial was brought to room temperature and the product **12C** characterized by HPLC.

5.2.4 Quality control techniques

5.2.4.1 *HPLC*

The radiochemical purity of the complex **12C** was assessed by HPLC using a C18 reversed phase column. Water (A) and acetonitrile (B) were used as the mobile phase with the following gradient elution (0 min 90% A, 28 min 10% A, 50 min 10% A). Flow rate was maintained at 1 mL/min. About 25 µL of the test solution was injected into the column and elution was monitored by observing the radioactivity profile.

The same C18 reversed phase analytical column was used for the purification of complex. On purification around 18.5 MBq (500 µCi) of **12C** was obtained in acetonitrile-water mixture which was dried under vacuum and reformulated in aqueous 10% ethanol solution. This was used for carrying out the *in-vivo* evaluation studies.

5.2.4.2 *Partition coefficient (Log$P_{o/w}$)*

The HPLC purified labeled compound (100 µL) was mixed with water (0.9 mL) and octanol (1 mL) on a vortex mixer for about 1 min and then centrifuged for 5 min to effect the separation of the two layers. Equal aliquots of the two layers were withdrawn and measured for the radioactivity. The readings thus obtained were used to calculate the Log $P_{o/w}$ value of the complex.

5.2.4.3 *Stability studies*

5.2.4.3.1 *Ligand exchange studies*

The stability of the complex towards ligand exchange was studied using cysteine as the challenging ligand. For this, complex **12C** (~100 µL) was added to 900 µL of phosphate buffered saline containing 10-50 fold molar excess of cysteine over that of the ligand. The samples were incubated at 37 °C for 1 h and then analyzed by HPLC.

5.2.4.3.2 *Serum stability*

Stability of the complex **12C** in serum was tested *in-vitro*. About 50 µL of the radiolabeled preparation was added to 450 µL serum and the mixture was incubated at 37 ºC for 1 h. To this mixture, an equal volume of cold ethanol was added to precipitate the serum proteins and centrifuged at 10000 g (4 °C, 20 min). The supernatant was analyzed by HPLC to assess the stability of the complex in serum.

5.2.4.4 *Bio-distribution studies*

Swiss mice (20–25 g body weight) bearing fibrosarcoma tumor were used for the bio-distribution studies. The HPLC purified radiolabeled preparation **12C** (100 µL, 740 KBq or 20 µCi) was administered intravenously through the tail vein of each animal. Individual sets of animals (n=3) were utilized for studying the bio-distribution at different time points (30 min, 60 min and 180 min). The animals were sacrificed immediately at the end of the respective time points and the relevant organs and tissues were excised for measurement of associated activity. The organs were weighed and the activity associated with each was measured in a flat-bed type NaI (Tl) counter with suitable energy window for ^{99m}Tc (140 keV ± 10%). Accumulated activity was expressed in terms of percentage of the total injected dose associated with per gram of the specific organ/tissue. All the procedures performed were in accordance with the national laws pertaining to the conduct of animal experiments.

5.3 Results and discussion

5.3.1 Synthesis

The scheme for the synthesis of **12** is shown in Fig. 5.5. The amino group of **7a** was conjugated to the carboxylic acid group of **12a** using EDCI as the coupling agent. The ethyl ester group of **12b** was then hydrolyzed under alkaline conditions to give **12c**. Finally, the target ligand **12** was obtained on trityl deprotection of **12c** using TFA-Et_3SiH. The target ligand **12** contained free SH and COOH groups of cysteine residue to complex with $[^{99m}TcN(PNP)]^{2+}$ core.

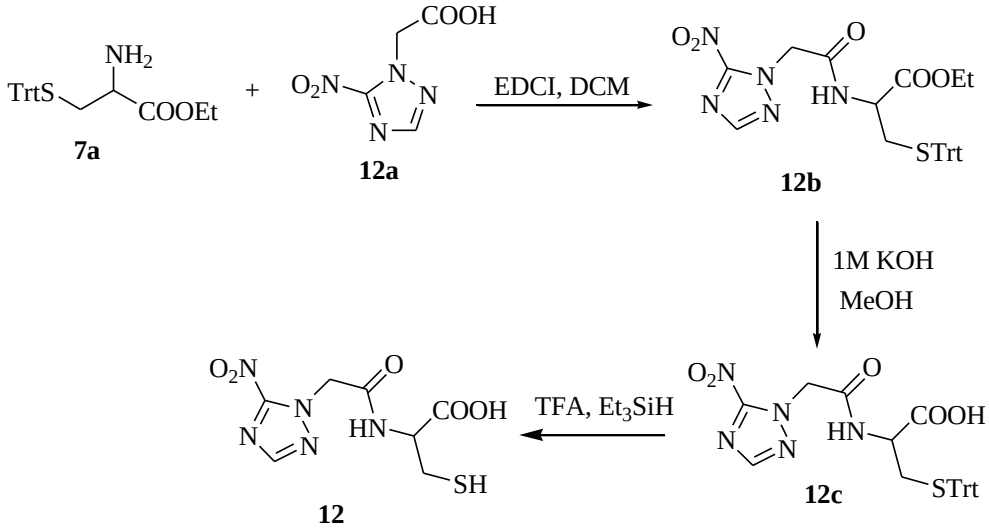

Fig. 5.5 Scheme for the synthesis of nitrotriazole-cysteine conjugate

5.3.2 Radiolabeling

The scheme for the synthesis of complex **12C** is shown in Fig. 5.6. This involved prior preparation of $[^{99m}TcN]^{2+}$ core, using SDH and $SnCl_2$, followed by reaction with PNP ligand **6** and triazole derivative **12** to yield the final complex **12C** (Fig. 5.7).

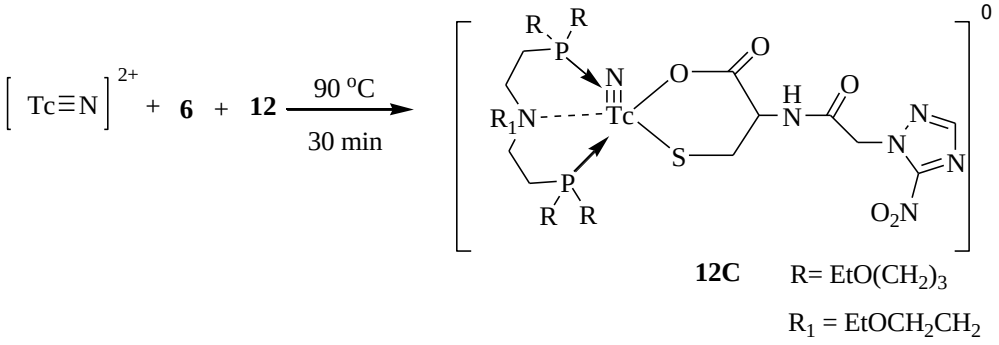

Fig. 5.6 Synthesis of $[^{99m}TcN(PNP\mathbf{6})]$-nitrotriazole complex

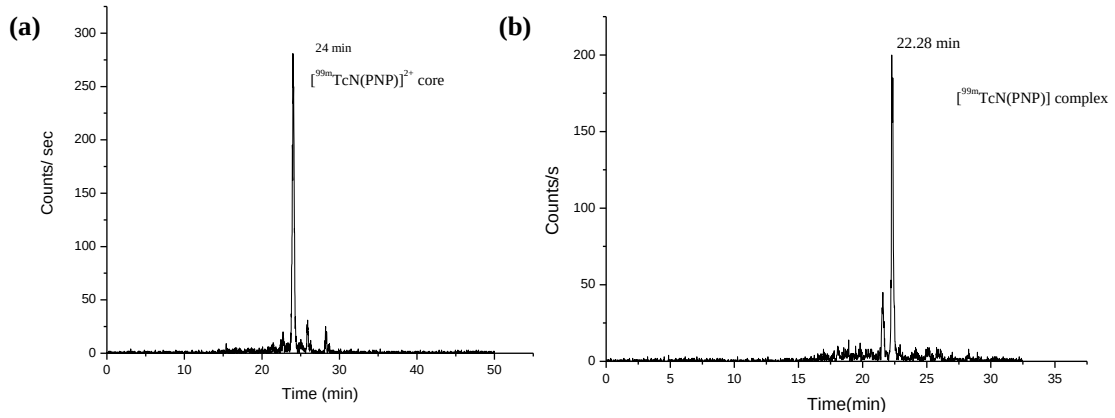

Fig 5.7 HPLC profile of (a) [^{99m}TcN(PNP**6**)] core and (b) complex **12C**

Since the complex **12C** synthesized using **12,** with free SH, COOH of cysteine moiety, is similar to the [^{99m}TcN(PNP)] complex reported earlier[187,190,247], hence it is presumed to have similar square pyramidal geometry. The final complex was obtained in more than 80% radiolabeling yield as characterized by HPLC [Fig. 5.7(b)]. The HPLC of complex **12C** revealed two closely spaced peaks resulting from a *syn-anti* isomeric pair, with one isomer being predominant. The stereochemistry of isomers can be ascertained only after preparing the complex in macroscopic level which was not attempted considering our major objective to examine the bio-distribution of the complex for its potential application as hypoxia marker.

5.3.3 Biological studies

The complex **12C** was bio-evaluated, to assess its potential as a tumor hypoxia marker. Some of the essential characteristics of a radiolabeled hypoxia marker are *in-vivo* stability, adequate lipohpilicity so as to enter the hypoxic cells by passive diffusion, maximal uptake and retention in the hypoxic cells, and rapid clearance from the non-target tissue/ organs such as blood, muscle, etc. so as to obtain a clear image. Thus, tumor/ blood and

tumor/ muscle ratios are critical parameters in evaluating the potential of a radiolabeled hypoxia marker.

In this view, the *in-vitro* experiments involving cysteine challenge and serum stability were carried to assess the kinetic inertness of the complex. Even in the presence of a large excess (up to 100 fold) cysteine, no transchelation of the complex with free cysteine was noticed. Also, the incubation of the complex in serum up to 1 h did not show appreciable degradation. These were confirmed by HPLC wherein the retention of radioactive peak was observed. To assess the lipophilic nature of the complex, the Log $P_{o/w}$ value of the present complex was carried using octanol-water system and was found to be 1.3 which is sufficiently hydrophobic to enter the cell by passive diffusion.

To evaluate the other parameters of the complex **12C** for a hypoxia agent, *in-vivo* experiments were carried out in tumor bearing mice. The bio-distribution results of **12C** are shown in Table 5.1. The tumor uptake pattern of the prepared complex in fibrosarcoma tumor is shown in Fig. 5.8. It was observed that the initial uptake of the complex **12C (**0.34 ± 0.07% ID/g at 30 min p.i.) was significantly low which may be due to short biological half-life of the complex **12C** in blood (0.22 ± 0.13% ID/g at 30 min p.i.), thereby not allowing sufficient

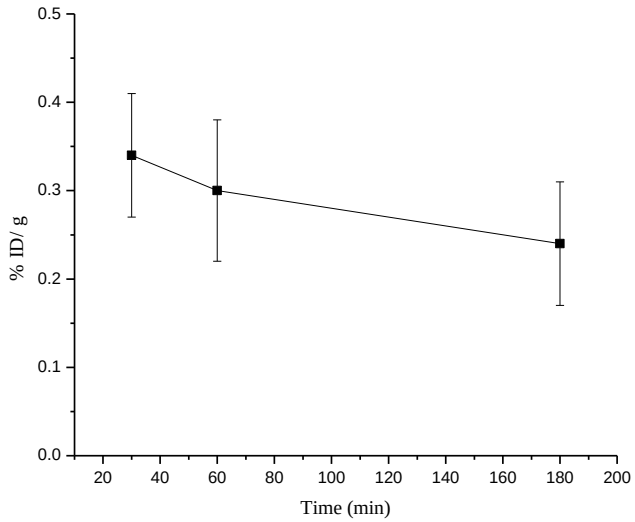

Fig. 5.8 Uptake and retention behavior of complex **12C** in fibrosarcoma tumor

time for equilibration and subsequent uptake in the tumor by passive diffusion. However, the initially accumulated radioactivity of **12C** showed steady retention throughout the period of study up to 3 h as desired for a hypoxic marker.

Table 5.1 Bio-distribution of nitrotriazole complex **12C** in Swiss mice [%ID/g (1SD), (n=3)]

Organs	*30 min*	*60 min*	*180 min*
Blood	0.22 (0.13)	0.23 (0.11)	0.07 (0.06)
Liver	3.67 (1.12)	8.91 (2.88)	6.05 (3.38)
Int+GB	39.3 (9.63)	54.4 (4.52)	60.15 (6.18)
Lung	1.09 (0.58)	0.41 (0.33)	0.39 (0.07)
Spleen	0.31 (0.1)	0.31(0.3)	0.69 (0.3)
Bone	0.7 (0.62)	1.00 (0.38)	0.83 (0.4)
Muscle	1.03 (0.97)	0.26 (0.12)	0.27 (0.17)
Tumor	**0.34 (0.07)**	**0.3 (0.08)**	**0.24 (0.07)**
Kidney	0.7 (0.3)	0.43 (0.24)	0.53 (0.13)
Tumor/ blood	0.98 (0.27)	1.5 (0.51)	0.94 (0.08)
Tumor/ muscle	1.12 (0.31)	1.42 (0.56)	1.1 (0.44)

The time dependent variation of tumor/ blood and tumor/ muscle ratios is shown in Fig. 5.9(a). Both ratios improved steadily up to 1 h p.i., henceforth no significant decrease was observed. This may be due to major clearance of **12C** up to 1 h from the non-target organs after which equilibrium is attained.

The clearance pattern of the activity from different non-target organs/ tissue is shown in Fig 5.9(b). The activity from differnt organs such as liver, blood, muscle, etc seems to clear with time. The increase in the intestinal radioactivity indicates the clearance of **12C** via the hepatobiliary route. This is attributed to ether residues present on the PNP ligand and the MDR-Pgp pump which is responsible for rapid elimination of lipophilic compounds such as [^{99m}TcN(PNP)] from the liver.[249] Thus, though, the synthesized complex **12C** showed steady

retention in tumor, however, the absolute uptake values were sub-optimal and due to the non-availability of any standard agent distribution data for comparison, the efficacy of the complex **12C** could not be ascertained completely.

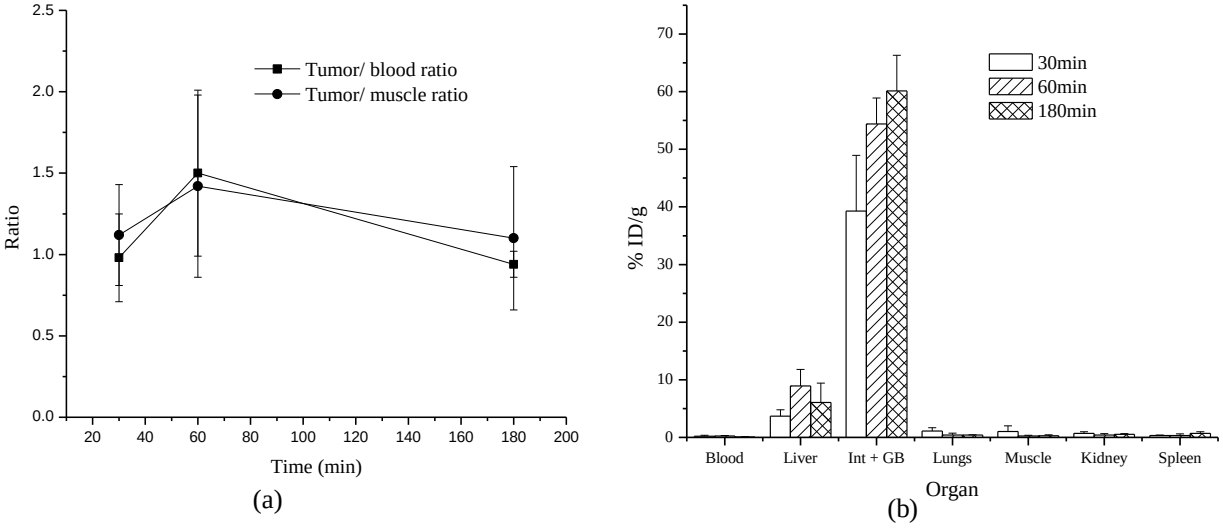

Fig. 5.9 Time dependent variation of (a) tumor/ blood & tumor/ muscle ratios and (b) non-target distribution pattern of complex **12C** in Swiss mice

5.4 Conclusion

The present chapter highlights the usefulness of $[^{99m}TcN]^{2+}$ core for diverse imaging applications, with favorable *in-vivo* characteristics in terms of rapid non-target clearance. In this respect, a hypoxic target molecule, nitro-triazole, was synthetically derivatized with cysteine residue in good yields and labeled with $[^{99m}TcN]^{2+}$ core along with PNP ligand **6** yielding asymmetric [2+2] neutral complex in 80% radiolabeling yield. Bio-distribution studies in fibrosarcoma tumor bearing Swiss mice showed considerable retention of activity in tumor even after 3 h post-injection. Though, retention of radioactivity was observed in tumor, the efficacy could not be ascertained completely due to low initial uptake values. The *in-vivo* pharmacological behavior observed with asymmetric ^{99m}TcN-labeled nitrotriazole complex provides reasonable promise toward the development of a hypoxia-imaging agent and favors the use of $[^{99m}TcN]^{2+}$ core for similar imaging applications.

REFERENCES

1. Weissleder R. *Science,* **2006**, *312*, 1168.

2. Weissleder R. *Nat. Rev. Cancer*, **2002,** *2*, 11.

3. Juweid M.E., Cheson B. D. *N. Engl. J. Med.,* **2006,** *354*, 496

4. Verbruggen A.M. *Eur. J. Nucl. Med.*, 1990, *17*, 346.

5. Jurisson S., Berning D., Jia W., Dangshe M. *Chem. Rev.*, **1993**, *93*, 1137.

6. Jurisson S., Lydon J.D. *Chem. Rev.*, **1999**, *99*, 2205.

7. Banerjee S., Pillai M.R.A., Ramamoorthy N. *Sem. Nucl. Med.*, **2001**, *32*, 260.

8. Liu S. *Chem Soc Rev*. **2004**, *33*, 445.

9. Potamianos B., Varvarigou A. D., Archimandritis S. C. *Anticancer Res.*, **2000**, *20*, 925.

10. Vriesendorp H. M. , Quadri S. M., Borchardt P. E. *BioDrugs,* **1998**, *10*, 275.

11. Wun T., Kwon D. S., J. M. Tuscano. *BioDrugs*, **2001**, *15*, 151.

12. Witzig T. E. *Semin. Oncol,* **2000**, *27(12)*, 74.

13. Culy C. R., Lamb H. M. *BioDrugs*, **2000**, *14*, 195.

14. Lister-James J., Moyer B. R., Dean R. T. Q. *J. Nucl. Med.*, **1997**, *41*, 111.

15. Liu S., Edwards D. S. *Chem. Rev.*, **1999**, *99*, 2235.

16. Volkert W. A., Hoffman T. J. *Chem. Rev*., **1999**, *99*, 2269.

17. Anderson C. J., Welch M. J. *Chem. Rev.*, **1999**, *99*, 2219.

18. Blok D., Feitsma R. I. J., Vermeij P., Pauwel E. J. K. *Eur. J. Nucl. Med*., **1999**, *26*, 1511.

19. Okarvi S. M., *Nucl. Med. Commun.*, **1999**, *20*, 1093.

20. Kwekkeboom D., Krenning E. P., de Jong M. *J. Nucl. Med.*, 2000, *41*, 1704.

21. Boerman O. C., Oyen W. J. G., Corstens F. H. M. *Semin. Nucl. Med*., **2000**, *30*, 195.

22. Signore A. , Annovazzi A., Chianelli M., Coretti F., Van de Wiele C. , Watherhouse R. N., Scopinaro F. *Eur. J. Nucl. Med.*, **2001**, *28*, 1555.

23. Hoffman T. J., Quinn T. P., Volkert W. A. *Nucl. Med. Biol*., **2001**, *28*, 527.

24. Weiner R. E., Thakur M. L. *Appl. Radiat. Isot.*, **2002**, *57*, 749.

25. de Jong M.,Kwekkeboom D.,Valkema R., Krenning E. P. *Eur. J. Nucl. Med.*, **2003**, *30*, 463.

26. Fichna J., Janecka A. *Bioconjug. Chem.*, **2003**, *14*, 3.

27. Liu S., Edwards D. S. *Bioconjug. Chem*, **2001**, *12*, 7.

28. Schubiger P. A., Alberto R., Smith A. *Bioconjug. Chem*.,**1996**, *7*, 165.

29. McDevitt M.R., Sgouros G., Finn R.D., Humm J. L., Jurcic J.G., Larson S.M.,. Scheinberg D. A. *Eur. J. Nucl. Med.*, **1998**, *25*, 1341.

30. Atkins H.L. *Appl. Radiat. Isot.*, **1998**, *49*, 277.

31. Ehrhardt G.J., Ketring A.R., Ayers L.M. *Appl. Radiat. Isot.*, **1998**, *49*, 295.

32. Knapp Jr. F. F., Mirzadeh S., Beets A. L., O'Doherty M., Blower P. J., Verdera E., Gaudiano J. S., Kropp J., Guhlke J., Palmedo H., Biersack H. J. *Appl. Radiat. Isot*., **1998**, *49*, 309

33. Jain D. *Semin. Nucl. Med*., **1999**, *29*, 221.

34. Liu S. *Adv Drug Deliv Rev.*, **2008**, *60(12)*, 1347.

35. *IAEA Technical Report Series*, **1971,** *128*.

36. *IAEA-TECDOC*, **1998,** *1007*.

37. IAEA Training Course Manual for "Research Reactor Utilisation for Production and Applications of Radioisotopes", **1989**.

38. *IAEA-TECDOC*, **1999,** *1065*.

39. Rahmim A., Zaidi H. *Nucl Med Commun*, **2008,** *29*, 193.

40. www.bnl.gov/bnlweb/history/tc99m.asp

41. (a) Anger H. *Biology and Medicine Quarterly Report UCRL*, **1957**, *3653*, 38. (b) Anger H.O. *J. Nucl. Med.*, **1964**, *65*, 515.

42. (a) Husarik D.B., Steinert H.C. *Semin Nucl Med.*, **2007**, *37*, 29.(b) Krausz Y., Israel O. *Semin Nucl Med.*, **2006**,*36*, 267. (c) Schillaci O. *Semin Nucl Med.*, **2006,** *36*, 275.

43. Horger M., Bares R. *Semin Nucl Med.*, **2006**, *36*, 286.

44. Bunyaviroch T., Aggarwal A., Oates M.E. *Semin Nucl Med.*, **2006**, *36*, 295.

45. Sodee D.B., Sodee A.E., Bakale G. *Semin Nucl Med.*, **2007**, *37*, 17.

46. Schillaci O., Filippi L., Manni C., Santoni R. *Semin Nucl Med.*, **2007**, *37*, 34.

47. Hong H., Zhang Y., Sun J., Cai W. *Amino Acids*, **2010,** *39*, 11.

48. Coenen H.H., Elsinga P.H., Iwata R., Kilbourn M.R., Pillai M.R.A., Rajan M.G.R., Wagner Jr. H.N., Zaknun J.J. *Nucl. Med. Biol.*, **2010**, *37*, 727.

49. Miller P.W., Long N.J., Vilar R., Gee A.D. *Angew. Chem. Int. Ed Engl.*, **2008,** *47*, 8998.

50. (a) Kayani I., Groves A.M. *Clin. Med.* **2006,** *6*, 240. (b) Rohren E.M., Turkington T.G., Coleman R.E. *Radiology*, **2004,** *231*, 305.

51. Kelloff G.J., Hoffman J.M., Johnson B., Scher H.I., Siegel B.A., Cheng E.Y., Cheson B.D., O'Shaughnessy J., Guyton K.Z., Mankoff D.A., Shankar L., Larson S.M., Sigman C.C., Schilsky R.L., Sullivan D.C. *Clin. Cancer Res.*, **2005,** *11*, 2785.

52. (a) Antunes P.,Ginj M., Zhang H., etal. *Eur. J. Nucl. Med. Mol. Imag.* **2007**, *34*, 982. (b) AmbrosiniV,et.al. *Eur. J. Radiol.*, **2010**, doi:10.1016/j.ejrad.2010.07.022

53.Volkert W.A., Goeckeler W.F., Ehrhardt G.J., Ketring A.R. *J. Nucl. Med.*, **1991**, *32*, 174.

54. Ehrhardt G.J., Ketring, A.R., Ayers L. M. *Appl. Radiat. Isot.*, **1998**, *49*, 295.

55. Troutner D.E. *Int. J. Radiat. Appl. Inst.*, **1987**, *14*, 171.

56. Wheldon T.E., O'Donoghue J.A. *Int. J. Radiat. Biol.*, **1990**, *58*, 1.

57. O'Donoghue, J.A., Bardies M., Wheldon T.E. *J. Nucl. Med.*, **1995**, *36*, 1902.

58. Eckelman W.C. *Eur. J. Nucl. Med.*, **1995**, *22*, 249.

59. DiZio J.P.; Fiaschi R., Davison A., Jones A.G., Katzenellenbogen J.A. *Bioconjug. Chem.*, **1991**, *2*, 353.

60. Vaidyanathan G. *Q J Nucl Med Mol Imag.*, **2008**, *52*, 351.

61. Stanko V.I., Ironshnikova N.G., Volkov A.F., Klimova A.I. *Appl. Radiat. Isot*., **1984**, *35*, 1129.

62. Neves M., Paulo A., Patricio L., *Appl. Radiat. Isot.*, **1992**, *43*, 737.

63. Samnick S., Bader J.B., Muller M., Chapot C., Richter S., Schaefer A., Sax B., Kirsch C.M. *Nucl Med Commun.*, **1999**, *20*, 537.

64. Vaidyanathan G., Affleck D.J., Alston K.L., Zalutsky M.R. *J Label Compd Radiopharm.*, **2007**, *50*, 177.

65. Roesch F. *Radiochim Acta*, **2007**, *95*, 303.

66. Ehrhardt G.J., Ketring A.R., Ayers L.M. *Appl. Radiat. Isot.*, **1998,** *49*, 295.

67. Karelin Y.A., Toporov Y.G. *Appl. Radiat. Isot.*, **1998**, *49*, 299.

68. Knapp Jr. F.F., Mirzadeh S., Beets A.L., Doherty M.O., Blower P.J., Verdera E.S., Gaudiano J.S., Kropp J., Gihlke J., Palmedo H., Biersack H.J. *Appl. Radiat. Isot.*, **1998**, *49*, 309.

69. Snider S.E., Kilbourn M.R. *Handbook of Radiopharmaceuticals: Radiochemistry and Applications, John Wiley & Sons, New York,* **2003**, 195.

70. Finn R. *Handbook of Radiopharmaceuticals: Radiochemistry and Applications, John Wiley & Sons, New York*, **2003**, 423.

71. Coenen H.H., Moerlein S.M. *J. Fluor. Chem.*, **1987**, *36*, 63.

72. Adam M.J., Jivan S. *Appl. Radiat. Isot.*, **1988**, *39*,1203.

73. Namavari M., Bishop A., Satyamurthy N., Bida G., Barrio J.R. *Appl. Rad. Isot.*, **1992**, *43*, 989.

74. Pearson R.G. *J. Am. Chem. Soc.*, **1963**, *85*, 3533.

75. Bandoli G., Tisato F., Dolmella A., Agostini S. *Coord. Chem. Rev.*, **2006,** *250*, 561.

76. Delmon-moingeon L.I., Mahmood A., Davison A., Jones A.G. *J. Nucl. Biol. Med.*, **1991**, *35*, 47.

77. Rhodes B.A. *Nucl. Med. Biol.*, **1991**, *18*, 667.

78. Eckelman W.C., Steigman J. *Nucl. Med. Biol.*, **1991** *18*, 3.

79. Griffiths G.L., Goldenberg D.M., Jones A.L., Hansen H.J. *Bioconjug. Chem.*, **1992**, *3*, 91.

80. Zamora P.O., Rhodes B.A. *Bioconjug. Chem.*, **1992**, *3*, 493.

81. Eary J.F., Schroff R.W., Abrams P.G., Fritzberg A.R., Morgan A.C., Kasina S., Reno J.M., Srinivasan A., Woodhouse C.S., Wilbur D.S., Natale R.B., Collins C., Stehlin J.S., Mitchell M., Nelp W.B. *J. Nucl. Med.*, **1989**, *30*, 25.

82. Kasina S., Rao T.N., Srinivasan A., Sanderson J.A., Fitzner J.N., Reno J.M., Beaumier P.L., Fritzberg A.R. *J. Nucl. Med.*, **1991**, *32*, 1445.

83. Schwochau K. *Technetium: Chemistry and Radiopharmaceutical Applications. Wiley-VCH Verlag GmbH: Weinheim.* **2000**, 4.

84. *Trends in Radiopharmaceuticals (ISTR-2005), Proceedings of an International Symposium*, **2007**, *1*.

85. *Technical report series*, IAEA. **2007**, *459*.

86. *IAEA-TECDOC*, **2003**, *1340*, 135.

87. (a) Eckelman W.C., Coursey B.M. *Int. J. Appl. Radiat. Isot.*, **1982**, *33(10)*. (b) *Radiochimica Acta*, **1987**, *41(2/3)*.

88. Chattopadhyay S., Das S.S., Das M.K., Goomer N.C. Appl. Rad. Isot., **2008**, *66*,1814.

89. Liu S., Edwards D.S., Barrett J.A.*Bioconjug. Chem.*, **1997**, *8*, 621.

90. Tisato F., Porchia M., Bolzati C., Refoso F., Vittadini A. *Coord. Chem. Rev.*, **2006**, *250*, 2034.

91. Hansen L., Marzilli L.G., Taylor A. *Q. J. Nucl. Med.*, **1998**, *42*, 280.

92. Liu S. *Dalton Trans*., **2007**, 1183.

93. Arano Y. *Annals Nucl. Med.*, **2002**, *16,* 79.

94. Banerjee S.R., Maresca K.P., Francesconi L., Valliant J., Babich J.W., Zubeita J., *Nucl. Med. Biol.*, **2005**, *32*, 1.

95. Alberto R. *Technetium in Comprehensive Co-ordination Chemistry II*, **2004**, *5*, 127.

96. Hom R.K., Katzenellenbogen J.A. *Nuclear Medicine Biol.*, **1997**, *24*, 485.

97. Dilworth J.R., Parrott S.J. *Chemical Soc. Rev.*, **1998**, *27*, 43.

98. Mease R.C., Lambert C. *Sem. Nucl. Med.*, **2001**, *32*, 278.

99. Fichna J., Janecka A. *Bioconjug. Chem.*, **2003**, *14*, 3.

100. Klingensmith W.C.III, Fritzberg A.R., Spitzer V.M., Johnson D.L., Kuni C.C., Williamson M.R., Washer G., Weil R.III. *J. Nucl. Med.*, **1984**, *25*, 42.

101. Rao T.N., Adhikesavalu D., Camerman A., Fritzberg A.R. *J. Am. Chem. Soc.*, **1990**,*112*, 5798.

102. Eshima D., Taylor A. Jr., Fritzberg A.R., Kasina S., Hansen L., Sorenson J.F. *J. Nucl. Med*. **1987**, *28,* 1180.

103. Vanbilloen H.P., De Roo M.J., Verbruggen A.M. *Eur. J. Nucl. Med.*, **1996**, *23,* 40.

104. Liu S., Edwards D.S., Looby R.J., Harris A.R., Poirier M.J., Rajopadhye M., Bourque J.P., Carroll T.R. *Bioconjug. Chem*., **1996**, *7*, 196.

105. Barrett J.A., Damphousse D.J., Heminway S.J., Liu S., Edwards D.S., Looby R.J., Carroll T.R. *Bioconjug. Chem*., **1996**, *7*, 203.

106. Rajopadhye M., Edwards D.S., Bourque P.J., Carroll T.R. *Bioorg. & Med. Chem. Lett*., **1996**, *6*, 1737.

107. Lever S.Z., Baidoo K.E., Mahmood A. *Inorg. Chim. Acta*, **1990**, *176*,183.

108. Harris T.D., Edwards D.S., Platts S.H. *J. Nucl. Med.*, **1992**, *33*, 979.

109. Oya S., Kung M.P., Frederick D., Kung H.F. *Nucl. Med. Biol.*, **1995**, *22*, 749.

110. Kung H.F., Guo Y.Z., Yu C.C., Billings J., Subramanyam V., Calabrese J.C. *J.Med. Chem.*, **1989**, *32*, 433.

111. Francesconi L.C., Graczyk G., Wehrli S., Shaikh S.N., McClinton D., Liu S., Zubieta J., Kung H.F. *Inorg. Chem.*, **1993**, *32*, 3114.

112. Mach R.H., Kung H.F., Guo Y.Z., Yu C.C., Subramanyam V., Calabrese J.C. *Nucl. Med. Biol.*, **1989**, *16*, 829.

113. Baidoo K.E., Lever S.Z. *Bioconjug. Chem.*, **1990**, *1*,132.

114. Eisenhut M., Lehmann W.D., Becker W., Behr T., Elser H., Strittmatter W., Baum R.P. Valerius T., Repp R., Deo Y. *J. Nucl. Med.*, **1996**, *37*, 362.

115. O'Neil J.P., Wilson S.R., Katzenellenbogen J.A. *Inorg. Chem.*, **1994**, *33*, 319.

116. O'Neil J.P., Carlson K.E., Anderson C.J., Welch M.J., Katzenellenbogen J.A. *Bioconjug. Chem.*, **1994**, *5*,182.

117. DiZio J.P., Anderson C.J., Davison A., Ehrhardt G.J., Carlson K.E., Welch M.J., Katzenellenbogen J.A. *J. Nucl. Med.*, **1992**, *33*, 558.

118. Meegalla S., Plüssl K., Kung M.P., Chumpradit S., Stevenson D.A., Frederick D., Kung H.F. *Bioconjug. Chem.*, **1996**, *7*, 421.

119. Rajagopalan R., Grummon G.D., Bugaj J., Hallemann L.S., Webb E.G., Marmion M.E., Vanderheyden J.L., Srinivasan A. *Bioconjug. Chem.*, **1997**, *8*, 407.

120. Wong E., Fauconnier T., Bennett S., Valliant J., Nguyen T., Lau F., Lu L.F.L., Pollak A., Bell R.A., Thornback J.R. *Inorg. Chem.*, **1997**, *36*, 5799.

121. Lister-James J., Knight L.C., Maurer A.H., Bush L.R., Moyer B.R., Dean R.T. *J. Nucl. Med.*, **1996**, *37*, 775.

122. Muto P., Lastoria S., Varrella P., Vergara E., Salvatore M., Morgano G., Lister-James J., Bernardy J.D., Dean R.T., Wencker D., Borer J.S. *J. Nucl. Med.*, **1995**, *36*, 1384.

123. Pearson D.A., Lister-James J., McBride W.J., Wilson D.M., Martel L.J., Civitello E.R.,

Dean R.T. *J. Med. Chem.*, **1996**, *39*, 1372.

124. Lister-James J., Vallabhajosula S., Moyer B.R., Pearson D.A., McBride B.J., De Rosch M.A., Bush L.R., Machac J., Dean R.T. *J. Nucl. Med.*, **1997**, *38*, 105.
125. Alberto R., Schibli R., Egli A., Schubiger P.A., Abram U., Kaden T.A. *J. Am. Chem. Soc.*, **1998**, *120*, 7987.
126. Alberto R., Ortner K, Wheatley N., Schibli R., Schubiger P.A. *J. Am. Chem. Soc.*, **2001**, *123*, 3135.
127. Schibli R., Schwarzbach R., Alberto R., Ortner K., Schmalle H., Dumas C., Egli A., Schubiger P.A. *Bioconjug. Chem.*, **2002**, *13*, 750.
128. Kim Y., He Z., Hsieh W., Liu S. *Inorg. Chim. Acta*, **2006**, *359*, 2479.
129. Stichelberger A., Waibel R., Dumas C., Schubiger P.A., Schibli R. *Nucl. Med. Biol.*, **2003**, *30*, 465.
130. Alberto R., Schibli R., Schubiger P.A., Abram U., Pietzsch H.J., Johannsen B. *J. Am. Chem. Soc.*, **1999**, *121*, 6076.
131. La Bella R., Garcia-Garayoa E., Langer M., Bläuenstein P., Beck-Sickinger A.G., Schubiger P.A. *Nucl. Med. Biol.*, **2002**, *29*, 553.
132. Schibli R., La Bella R., Alberto R., Garcia-Garayoa E., Ortner K., Abram U., Schubiger P.A. *Bioconjug. Chem.*, **2000**, *11*, 345.
133. Zhang X., Chen X. *Appl. Radiat. Isot.*, **2007**, *65*, 70.
134. Alves S., Correia J.D.G., Gano L., Rold T.L., Prasanphanich A., Haubner R., Rupprich M., Alberto R., Decristoforo C., Snatos I., Smith C.J. *Bioconjug. Chem.*, **2007**, *18*, 530.
135. Alberto R., Schibli R., Waibel R., Abram U., Schubiger P.A. *Coord. Chem. Rev.*, **1999**, *190–192*, 901.
136. Schibli R., Schubiger P.A. *Eur. J. Nucl. Med.*, **2002**, *29*, 1529.
137. Abrams M.J., Juweid M., tenKate C.I., Schwartz D.A., Hauser M.M., Gaul F.E.,

Fuccello A.J., Rubin R.H., Strauss H.W., Fischman A.J. *J. Nucl. Med.*, **1990,** *31*, 2022.

138. Schwartz D.A., Abrams M.J., Hauser M.M., Gaul F.E., Larsen S.K., Rauh D., Zubieta J. *Bioconjug. Chem.*, **1991**, *2*, 333.

139. Ultee M.E., Bridger G.J., Abrams M.J., Longley C.B., Burton C.A., Larsen S., Henson G.W., Padmanabhan S., Gaul F.E., Schwartz D.A. *J. Nucl. Med.*, **1997**, *38*, 133.

140. Babich J.W., Solomon H., Pike M.C., Kroon D., Graham W., Abrams M.J., Tompkins R.G., Rubin R.H., Fischman A.J. *J. Nucl. Med.*, **1993**, *34*, 1967.

141. Babich J.W., Fischman A.J. *Nucl. Med. Biol.*, **1995**, *22*, 25.

142. Babich J.W., Graham W., Barrow S.A., Fischman A.J. *Nucl. Med. Biol.*, **1995**, *22*, 643.

143. Babich J.W., Coco W.G., Barrow S.A., Fischman A.J., Femia F.J., Zubieta J. *Inorg. Chim. Acta,* **2000,** *309*, 123.

144. Decristoforo C., Mather S.J. *Bioconjug. Chem.*, **1999**, *10*, 431.

145. Decristoforo C., Melendez L., Sosabowski J.K., Mather S.J. *J. Nucl. Med.*, **2000**, *41*, 1114.

146. Decristoforo C., Mather S.J. *Nucl. Med. Biol.*, **1999**, *26*, 389.

147. Decristoforo C., Mather S.J. *Eur. J. Nucl. Med.*, **1999**, *26*, 869.

148. Bangard M., Béhé M., Guhlke S., Otte R., Bender H., Maecke H.R., Birsack H.J. *Eur. J. Nucl. Med.*, **2000**, *27*, 628.

149. Decristoforo C., Mather S.J., Cholewinski W., Donnemiller E., Riccabona G., Moncayo R. *Eur. J. Nucl. Med.*, **2000**, *27*, 1318.

150. Brouwers A.H., Laverman P., Boerman O.C., Oyen W.J.G., Barrett J.A., Harris T.D., Edwards D.S., Corstens F.H.M. *Nucl. Med. Commun.*, **2000**, *21*, 1043.

151. Liu S., Harris A.R., Ziegler M.C., Edwards D.S., Williams N.E. *Bioconjug. Chem.*, **2002**, *13*, 881.

152. Liu S., Edwards D.S., Ziegler M.C., Harris A.R., Hemingway S.J., Barrett B.A.

Bioconjug. Chem., **2001**, *12*, 624.

153. Liu S., Hsieh W., Jiang Y., Kim Y., Sreerama S.G., Chen X., Jia B., Wang F. *Bioconjug. Chem.*, **2007**, *18*, 438.
154. Jia B., Shi J., Yang Z., Xu B., Liu Z., Zhao H., Liu S., Wang F. *Bioconjug. Chem.*, **2006**, *17*, 1069.
155. Laverman P., Dams E.T.M., Oyen W.J.G., Storm G., Koenders E.B., Prevost R., van der Meer J.W.M., Corstens F.H.M., Boerman O.C. *J. Nucl. Med.*, **1999**, *40*, 192.
156. Zhang Y., Liu N., Zhu Z.H., Rusckowski M., Hnatowich D.J. *Eur. J. Nucl. Med.*, **2000**, *27*, 1700.
157. Hnatowich D.J., Winnard Jr. P., Virzi F., Fogarasi M., Santo T., Smith C.L., Cantor C.R., Rusckowski M. *J. Nucl. Med.*, **1995**, *36*, 2306.
158. Liu S., Edwards D.S., Looby R.J., Harris A.R., Poirier M.J., Barrett J.A., Heminway S.J., Carroll T.R. *Bioconjug. Chem.*, **1996**, *7*, 63.
159. Edwards D.S., Liu S., Ziegler M.C., Harris A.R., Crocker A.C., Heminway S.J., Barrett J.A., Bridger G.J., Abrams M.J., Higgins J.D. *Bioconjug. Chem.*, **1999**, *10*, 884.
160. Edwards D.S., Liu S., Barrett J.A., Harris A.R., Looby R.J., Ziegler M.C., Heminway S.J., Carroll T.R. *Bioconjug. Chem.*, **1997**, *8*, 146.
161. Liu S., Edwards D.S., Harris A.R. *Bioconjug. Chem.*, **1998**, *9*, 583.
162. Seifert S., Drews A., Gupta A., Pietzsch H.J., Spies H., Johannsen B. *Appl. Rad. Isot.*, **2000**, *53*, 431.
163. Pietzch H.J., Tisato F., Refosco F., Leibnitz P., Drews A., Seifert S., Spieset H. *Inorg. Chem.*, **2001**, *40*, 59.
164. Pietzch, H.J., Seifert S., Syhre R., Tisato F., Refosco F., Leibnitz P., Spies H. *Bioconjug. Chem.*, **2003**, *14*, 136.
165. Seifert S., Kunstler J.U., Schiller E., Pietzsch H.J., Pawelke B., Bergmann R., Spies H.

Bioconjug. Chem., **2004**, *15*, 856.

166. Jung C.M., Kraus W., Leibnitz P., Pietzsch H.J., Kropp J., Spies H. *Eur. J. Inorg. Chem.*, **2002**, *7*, 1219.
167. Pietzsch H.J., Gupta A., Syhre R., Leibnitz P., Spies H. *Bioconjug. Chem.*, **2001**, *12*, 538.
168. Heintz A.C., Jung C.M., Stehr S.N., Mirtschink P., Walther M., Pietzsch J., Bergmann R., Pietzsch H.J., Spies H., Wunderlich G., Kropp J., Deussen A. *Nucl. Med. Commun.*, **2007**, *28*, 637.
169. Walther M., Jung C.M., Bergmann R., Pietzsch J., Rode K., Fahmy K., Mirtschink P., Stehr S., Heintz A., Wunderlich G., Kraus W., Pietzsch H.J., Kropp J., Deussen A., Spies H. *Bioconjug. Chem.*, **2007**, *18*, 216.
170. Mirtschink P., Stehr S.N., Pietzsch H.J., Bergmann R., Pietzsch J., Wunderlich G., Heintz A.C., Kropp J., Spies H., Kraus W., Deussen A., Walther M.. *Bioconjug. Chem.*, **2008**, *19*, 389.
171. Baldas J., Bonnyman J., Pojer P.M., Williams G.A., Mackay M.F. *J Chem Soc Dalton Trans.*, **1981**, 1798.
172. Baldas J., Bonnyman J. *Int J Appl Rad Isot.*, **1985**, *36*, 133.
173. Baldas J., Bonnyman J., Williams G.A. *Inorg. Chem.*, **1986**, *25*, 150.
174. Abram U., Lorenz B., Kaden L., Scheller D. *Polyhedron*, **1988**, *7*, 285.
175. Duatti A., Marchi A., Pasqualini R. *J Chem Soc Dalton Trans.*, **1990**, 3729.
176. Bolzati C., Boschi A., Uccelli L., Malago E., Bandoli G., Tisato F., Refosco F., Pasqualini R., Duatti A. *Inorg. Chem.*, **1999**, *38*, 4473.
177. Marchi A., Marvelli L., Rossi R., Magon L., Bertolasi V., Ferretti V., Gilli P. *J. Chem. Soc. Dalton Trans.*, **1992**, 1485.
178. Pasqualini R., Duatti A. *J Chem Soc Chem Commun.*, **1992**,1354.

179. Dehnicke K., Strähle J. *Angew. Chem. Int. Ed. Eng.*, **1992**, *31*, 955.

180. Pasqualini R., Comazzi V., Bellande E., Duatti A., Marchi A. *App. Radiat. Isot.*, **1992**, *43*, 1329.

181. Pasqualini R., Duatti A., Bellande E., Comazzi V., Brucato V., Hoffschir D., Fagret D., Comet M. *J. Nucl. Med.*, **1994**, *35*, 334.

182. Fagret D., Ghezzi C., Vanzetto G. *J. Nucl. Med.*, **2001**, *42*,1395.

183. Zhang J., Wang X., Li C.Y. *Appl. Radiat. Isot.*, **2002**, *56*, 857.

184. Mallia M.B., Mathur A., Subramanian S., Banerjee S., Kothari K., Koiry S.P., Sarma H.D., Venkatesh M. *Appl. Radiat. Isot.*, **2006**, *64*, 361.

185. Refosco R., Bolzati C., Duatti A., Tisato F., Uccelli L. *Recent Rev. Devel. Inorg. Chem.* **2000**, *2*, 89.

186. Bolzati C., Boschi A., Duatti A., Prakash S., Uccelli L., Refosco F., Tisato F., Bandoli G. *J. Am. Chem. Soc.*, **2000**, *122*, 4510.

187. Boschi A., Bolzati C., Benini E., Malago E., Uccelli L., Duatti A., Piffanelli A., Refosco F., Tisato F. *Bioconjug. Chem.*, **2001**, *12*, 1035.

188. Boschi A., Bolzati C., Uccelli L., Duatti A., Benini E., Refosco F., Tisato F., Piffanelli. *Nucl. Med. Commun.*, **2002**, *23*, 689.

189. Bolzati C., Boschi A., Uccelli L., Tisato F., Refosco F., Cagnolini A., Duatti A., Prakash S., Bandoli G., Vittadini A. *J. Am. Chem. Soc.*, **2002**, *124*, 11468.

190. Boschi A., Uccelli L., Duatti A., Bolzati C., Refosco F., Tisato F., Romagnoli R., Baraldi P.G., Varani K., Borea P.A. *Bioconjug. Chem.*, **2003**, *14*, 1279.

191. Boschi A., Uccelli L., Bolzati C., Duatti A., Sabba N., Moretti E., Di Domenico G., Zavattini G., Refosco F., Giganti M. *J. Nucl. Med.*, **2003**, *44*, 806.

192. Boltzati C., Muhmood A., Malago E., Uccelli L., Boschi A., Jones A.G., Refosco F., Duatti A., Tisato F. *Bioconjug. Chem.*, **2003**, *14*, 1231.

193. Bolzati C., Refosco F., Cagnolini A., Tisato F., Boschi A., Duatti A., Uccelli L., Dolmella A., Marotta E., Tubaro M. *Eur. J. Inorg. Chem.*, **2004**, *9*, 1902.

194. Hatada K., Riou L.M., Ruiz M., Yamamichi Y., Duatti A., Lima R.L., Goode A.R., Watson D.D., Beller G.A., Glover D.K. *J. Nucl. Med.*, **2004**, *45*, 2095.

195. Tisato F., Refosco F., Porchia M., Bolzati C., Bandoli G., Dolmella A., Duatti A., Boschi A., Jung C.M., Pietzsch H.J., Kraus W. *Inorg. Chem.*, **2004**, *43*, 8617.

196. Cazzola E., Benini E., Pasquali M., Mirtschink P., Walther M., Pietzsch H.J., Uccelli L., Boschi A., Bolzati C., Duatti A. *Bioconjug. Chem.*, **2008**, *19*, 450.

197. Faintuch B.L., Teodoro R., Duatti A., Muramoto E., Faintuch S., Smith C.J. *Nucl. Med. Biol.*, **2008**, *35*, 401.

198. Decristoforo C., Santos I., Pietzsch H.J., Kuenstler J.U., Duatti A., Smith C.J., Rey A., Alberto R., Guggenberg E.V., Haubner R. *Q J Nucl Med Mol Imag.*, **2007**, *51*, 33.

199. Hatada K., Ruiz M., Riou L.M., Lima R.L., Goode A.R., Watson D.D., Beller G.A., Glover D.K. *J. Nucl. Cardiol.* **2006**, *13*, 779.

200. Liu S., He Z.J., Hsieh W.Y., Kim Y.S. *Nucl. Med. Biol.*, **2006**, *33*, 419.

201. Kim Y.S., Wang J., Broisat A., Glover D.K., Liu S. *J. Nucl. Cardiol.* **2008**, *15*, 535.

202. Hearse D.J. *Cardiovasc. Res.*, **1994**, *28*, 1737.

203. Saha G.B., MacIntyre W.J., Brunken R.C., Go R.T., Raja S., Wong C.O., Chen Q.E. *Semin. Nucl. Med.*, **1996**, *26*, 315.

204. Opie L.H., Hesse B. *Eur. J. Nucl. Med.*, **1997**, *24*, 1183.

205. Acampa W., Di Benedetto C., Cuocolo A. *J. Nucl. Cardiol.*, **2000**, *7*, 701.

206. Kapur A., Latus K.A., Davies G., Dhawan R.T., Eastick S., Jarritt P.H., Roussakis G., Young M.C., Anagnostopoulos C., Bomanji J., Costa D.C., Pennell D.J., Prvulovich E.M., Ell P.J., Underwood S.R. *Eur. J. Nucl. Med.*, **2002**, *29*, 1608.

207. Kailasnath P., Sinusas A.J. *J. Nucl. Cardiol.*, **2001**, *8*, 482**.**

208. Schwaiger M., Melin J. *Lancet*, **1999**, *354*, 661.

209. Giubbini R.M.T. *Trends in Radiopharmaceuticals (ISTR-2005) Proceedings of an International Symposium*, **2007**, *1*, 103**.**

210. Tamaki N., Morita K., Kuge Y., Tsukamoto E. *J. Nucl. Med.*, **2000**, *41*, 1525.

211. Yoshinaga K., Tamaki N. *Curr. Opin. Biotech.*, **2007**, *18*, 52.

212. Milger K., Herrmann T., Becker C., Gotthardt D., Zickwolf J., Ehehalt R., Watkins P.A., Stremmel W., Füllekrug J. *J Cell Sci.*, **2006**, *119*, 4678.

213. Dilsizian V., Bateman T.M., Bergmann S.R., Prez R.D., Magram M.Y., Goodbody A.E., Babich J.W., Udelson J.E. *Circulation*, **2005**, *112*, 2169.

214. Pastore C.J., Babich J.W., Udelson J.E. *J Nucl Cardiol.*, **2007**, *14*, S153.

215. Otto C.A., Brown L.E., Wieland D.M., Beierwaltes W.H. *J Nucl. Med.*, **1981**, *22*, 613.

216. Maresca K.P., Shoup T.M., Femia F.J., Burker M.A., Fischman A., Babich J.W., Zubieta J. *Inorgan. Chim. Acta*, **2002**, *338*, 149.

217. Knapp F.F. Jr., Ambrose K.R., Goodman M.M. *Eur J Nucl Med.*, **1986**, *12*, S539.

218. Knapp F.F. Jr., Kropp J. *Eur J Nucl Med.*, **1995**, *22*, 361.

219. Fitzgerald J., Parker J.A., Danias P.G. *J. Nucl. Cardiol.*, **2000**, *7*, 382.

220. Tillisch J., Brunken R., Marshall R., Schwaiger M., Mandelkern M., Phelps M., Schelbert H. *N Engl J Med.*, **1986**, *314*, 884.

221. Aloj L., Caraco C., Jagoda E., Eckelman W.C., Neumann R.D. *Cancer Res.*, **1999**, *59*, 4709.

222. Torizuka T., Tamaki N., Inokuma T., Magata Y., Sasayama S., Yonekura Y., Tanaka A., Yamaoka Y., Yamamoto K., Konishi J. *J. Nucl. Med.*, **1995**, *36*, 1811.

223. Nunn A.D. *Radiopharmaceuticals: Chemistry and pharmacology. New York: Marcel Decker Inc. (Ed. Nunn A.D.)*, **1992**, 97.

224. Seldin D.W., Johnson L.L., Blood D.K., Muschel M.J., Smith K.F., Wall R.M., Cannon

P.J. *J.Nucl.Med*, **1989**, *30*, 312.

225. Thorley P.J., Ball J., Sheard K.L., Sivananthan U.M. *Nucl. Med. Comm.*, **1995**, *16*, 733.
226. Kronauge J.F. Chiu M.L., Cone J.S., Davison A., Holman B.L., Jones A.G., Piwnica-Worms D. *Nucl. Med. Biol.*, **1992**, *19*, 141.
227. Rumsey W.L., Rosenspire K.C., Nunn A.D. *J. Nucl. Med.*, **1992**, *33*, 94.
228. Navalokina R.A., Zil'berman E.N. *J. Org. Chem. USSR (Engl. Trans.)*, **1980**, *16*, 1382.
229. Kothari K., Banerjee S., Sarma H.D., Pillai M.R.A. *Appl. Rad. Isot.*, **2000**, *52*, 69.
230. Poe N.D., Robinson G.D., Graham S., MacDonald N.S. *J. Nucl. Med.*, **1976**, *17*, 1077.
231. Poe N.D., Robinson D.G. Jr., Zielinski F.W., Cabeen W.R. Jr., Smith J.W., Gomes A.S. *Radiology*, **1977**, *124*, 419.
232. Machulla H.J., Stoecklin G., Kupfernagel C., Freundilieb C., Hock A., Vyska K., Feinendegen L.E. *J. Nucl. Med.*, **1978**, *19*, 298.
233. Goodman M.M., Kirsch G., Knapp F.F.Jr. *J. Nucl. Med.*, **1984**, *27*, 390.
234. Tamaki N. *J. Nucl. Card.*, **2005**, *12*, 148.
235. Jones G.S.Jr., Elmaleh D.R., Strass H.W., Fichman A.J. *Bioorg. Med. Chem. Lett.*, **1996**, *6*, 2399.
236. Mach R.H., Kung H.F., Jungwiwattanaporn P., Guo Y. *Nucl. Med. Biol.*, **1991**, *18*, 215.
237. Jones G.S.Jr., Elmaleh D.R., Strass H.W., Fichman A.J. *Nucl. Med. Biol.*, **1994**, *21*, 117.
238. Chu T., Zhang Y., Liu X., Wang Y., Hu S., Wang X. *Appl. Rad. Isot.*, **2004**, *60*, 845.
239. Abram S., Abram A., Spies H., Munze R. *J. Radioanal. Nucl. Ch. Ar.* IV., **1986**, *102*, 309.
240. Korde A., Satpati D., Mathur A., Mallia M., Banerjee S., Kothari K., Sarma H.D., Choudhari P., Venkatesh M. *Bioorg. Med. Chem.*, **2006**, *14*, 793.
241. Mallia M.B., Mathur A., Subramanian S., Banerjee S., Sarma H.D., Venkatesh M. *Bioorg. Med. Chem. Lett.*, **2005**, *15*, 3398.

242. Tisato F., Bolzati C., Porchia M., Refosco F. *Mass Spectrometry Rev.*, **2004**, *23*, 309.

243. Archer C., Dilworth J., Griffiths D., McPartlin M., Kelly J. *J. Chem.Soc., Dalton Trans*., **1992**, *183*, 1972.

244. Morassi R., Sacconi L. *J. Chem. Soc. A*, **1971**, 492.

245. Bianchini C., Peruzzini M., Romerosa A., Zanobini F. *Organometallics*, **1995**, *14*, 3152.

246. Bianchini C., Casares J.A.C., Peruzzini M., Romerosa A., Zanobini F. *J. Am. Chem. Soc.*, **1996**, *118*, 4585.

247. Bolzati C., Mahmood A., Malago E., Uccelli L., Boschi A., Jones A.G., Refosco F., Duatti A., Tisato F. *Bioconjug. Chem*. **2003**, *14*, 1231.

248. Porchia M., Tisato F., Refosco F., Bolzati C., Cavazza-Ceccato M., Bandoli G., Dolmella A. *Inorg. Chem.*, **2005**, *44*, 4766.

249. Bolzati C., Cavazza-Ceccato M., Agostini S., Tokunaga S., Casara D., Bandoli G. *J. Nucl. Med.*, **2008**, *49*, 1336.

250. Verbruggen A.M., De Roo M.J.K. *Radiopharmaceuticals: Chemistry and pharmacology. New York: Marcel Decker Inc. (Ed. Nunn A.D.)*, **1992**, 365.

251. Nowotnik D.P. *Radiopharmaceuticals: Chemistry and pharmacology. New York: Marcel Decker Inc. (Ed. Nunn A.D.)*, **1992**, 37.

252. Mallia M.B., Banerjee S., Venkatesh M. *Technetium-99m Radiopharmaceuticals: Status and Trends, IAEA*, **2009**, 253.

253. Nunn A., Linder K., Strauss H.W. *Eur. J. Nucl. Med.*, **1995**, *22*, 265.

254. Gary L.H., Conger A.D., Ebert M., Hornsey S., Scott O.C.A. *Br. J. Radiol.*, **1953**, *26*, 638.

255. Moulder J.E., Rockwell S. *Cancer Metastasis Rev.*, **1987**, *5*, 313.

256. Ballinger J. R. *Semin. Nucl. Med.*, **2001**, *31*, 321.

257. Krohn K.A., Link J.M., Mason R.P. *J. Nucl. Med.*, **2008**, *49*, 129S.

258. Höckel M., Vaupel P. *J. National Cancer Institute*, **2001**, *93*, 266.

259. Wiebe L.I., Machulla H.J. Hypoxia: *An Introduction, in: Machulla, H.J. (ed): Imaging Hypoxia, Netherlands, Kluwer Academic Publishers*, **1999**, 1.

260. Koh W. J., Rasey J.S., Evans M.L., Grierson J.R., Lewellen T.K., Graham M.M., Krohn K.A., Griffin T.W. *Int. J. Radiat. Oncol. Biol. Phys.*, **1992**, *22*, 199.

261. Mannan R.H., Somayaji V.V., Lee J., Mercer J.R., Chapman J.D., Wiebe L.I. *J. Nucl. Med.*, **1991**, *32*, 1764.

262. Parliament M.B., Chapman J.D., Urtasun R.C., McEwan A.J., Golberg L., Mercer J.R., Mannan R.H., Wiebe L.I. *Br. J. Cancer*, **1992**, *65*, 90.

263. Groshar D., McEwan A.J.B., Parliament M.B., Urtasun R.C., Golberg L.E., Hoskinson M., Mercer J.R., Mannan R.H., Wiebe L.I., Chapman J.D. *J. Nucl. Med.*, **1993**, *34*, 885.

264. Ballinger J.R., Judy W.M.K., Rauth A.M. *J. Nucl. Med.* **1996**, *37*, 1023.

265. Melo T., Duncan J., Ballinger J.R., Rauth A.M. *J. Nucl. Med.*, **2000**, *41*, 169.

266. Zhang X., Melo T., Ballinger J.R., Raut A.M. *Int. J. Radiat. Oncol. Biol. Phys.*, **1998**, *42*, 737.

267. Mallia M.B., Subramanian S., Mathur A., Sarma H.D., Venkatesh M., Banerjee S. *J. Label Compd. Radiopharm.*, **2008**, *51*, 308.

THESIS PUBLICATIONS

1. "Synthesis, Radiolabeling and Evaluation of a New Positively Charged ^{99m}Tc-labeled Fatty Acid Derivative for Myocardial Imaging"

Anupam Mathur, Madhava B. Mallia, Haladhar D. Sarma, Sharmila Banerjee, Meera Venkatesh

J. Label. Compd. Radiopharm. v.54, p. 150-156, 2011.

2. "Evaluation of New Positively Charged 11- and 12-Carbon ^{99m}Tc-labeled Fatty Acid Derivatives for Myocardial Imaging"

Anupam Mathur, Madhava B. Mallia, Haladhar D. Sarma, Sharmila Banerjee, Meera Venkatesh

J. Label. Compd. Radiopharm. v.53, p. 580-585, 2010.

3. "Synthesis and bio-evaluation of a new fatty acid derivative for myocardial imaging"

Anupam Mathur, Suresh Subramanian, Madhava B.Mallia, Sharmila Banerjee, Grace Samuel, Haladhar D.Sarma, Meera Venkatesh

Bioorg. &Med. Chem. v.16, p. 7927-7931, 2008.

4. "Synthesis and bioevaluation of a new fatty acid derivative labeled with Technetium-99m"

Anupam Mathur, Madhava B Mallia, Suresh Subramanian, Sharmila Banerjee, K. Kothari, H.D. Sarma, Meera Venkatesh.

J. Label. Compd. Radiopharm. v.49, p. 1053-1060, 2006.

5. "^{99m}TcN-complexes of tert-butyl dithiocarbamate (TBDTC) and Methoxyisobutyl dithiocarbamate (MIBDTC) as myocardial and brain imaging agents"

Anupam Mathur, Madhava B. Mallia, Suresh Subramanian, Bhaskar D., Sharmila Banerjee, Kanchan Kothari, H.D. Sarma, Meera Venkatesh.

Nucl. Med. Commun. v.26, p. 1013-1019, 2005.

6. A new fatty acid cysteine conjugate for asymmetric [2+2] [^{99m}TcN(PNP)]$^{2+}$synthon labeling for possible use as metabolic cardiac imaging

Anupam Mathur, Madhava B. Mallia, Sharmila Banerjee, Meera Venkatesh

J. Label. Compd. Radiopharm.(Abstract), v.50, supp.1, S223, 2007.

7. Synthesis of novel 15 and 16 C-fatty acid derivatives labeled with [^{99m}TcN(PNP)]$^{2+}$ for myocardial imaging.

A. Mathur, M.B. Mallia, S.Banerjee, H. Sarma, M.Venkatesh

J. Label. Compd. Radiopharm.(Abstract), v.52, supp.1, S448, 2009.

OTHER PUBLICATIONS*

1. A novel $[^{99m}Tc{\equiv}N]^{+2}$ complex of metronidazole xanthate as a potential agent for targeting hypoxia

Madhava B Mallia, **Anupam Mathur**, Suresh Subramanian, Sharmila Banerjee, H. D. Sarma, Meera Venkatesh

Bioorg. Med. Chem. Lett. v.15, p.3398-3401, 2005.

2. Evaluation of ether containing ^{99m}Tc-nitrido dithiocarbamate complexes as brain perfusion imaging agent

Madhava B Mallia, **Anupam Mathur**, Suresh Subramanian, Sharmila Banerjee, Kanchan Kothari, S. P. Koiry, H. D. Sarma, Meera Venkatesh

Appl. Rad. Isot. v.64, p.361-367, 2006.

3. ^{99m}Tc-labeling of Colchicine using $[^{99m}Tc(CO)_3(H_2O)_3]^+$ and $[^{99m}TcN]^{2+}$ core for the preparation of potential tumor targeting agents.

Aruna Korde, Drishty Satpaty, **Anupam Mathur**, Madhava B Mallia, Sharmila Banerjee, Kanchan Kothari, H. D. Sarma, Meera Venkatesh

Bioorg.Med. Chem. v.14, p.793-799, 2006**.**

4. Preparation and in vivo evaluation of ^{99m}TcN-tertiary butyl xanthate as a potential myocardial agent

Anupam Mathur, Madhava B Mallia, Suresh Subramanian, Sharmila Banerjee, H.D. Sarma, Kanchan Kothari, Meera Venkatesh

Appl. Rad. Isot. v.64, p. 663-667, 2006.

5. Comparing hypoxia targeting potential of $^{99m}Tc(CO)_3$-labeled 2-nitro and 4-nitroimidaole.

Madhava B Mallia, Suresh Subramanian, **Anupam Mathur**, H.D. Sarma, Meera Venkatesh, Sharmila Banerjee.

*J. Label. Compd. Radiopharm.***,** v. 51, p.308-313, 2008**.**

6. On the isolation and evaluation of a novel unsubstituted 5-nitroimidazole derivative as an agent to target tumor hypoxia.

Madhava B Mallia, Suresh Subramanian, **Anupam Mathur**, H.D. Sarma, Meera Venkatesh, Sharmila Banerjee.

Bioorg. Med. Chem. Lett. v.18, p.5233-5237, 2008**.**

7. Synthesis and evaluation of 2-, 4-, 5-substituted nitroimidazole- iminodiacetic acid-99mTc(CO)3 complexes to target hypoxic tumors

Madhava B Mallia, Suresh Subramanian, **Anupam Mathur**, H.D. Sarma, Meera Venkatesh, Sharmila Banerjee.

J. Label. Compd. Radiopharm. v.53, p.535-542, 2010.

8. Synthesis, radiolabeling and evalution of 99mTc(CO)3-labeled misonidazole analogue to target tumor hypoxia

Madhava B. Mallia, **Anupam Mathur**, Sharmila Banerjee, H.D. Sarma, Meera Venkatesh

Nucl. Med. Biol. v.37, p.677–726, 2010.

*Not included in the thesis